Investigation of colloidal, biophysical and liquid crystalline properties of synthetic alkyl glycosides and glycolipids

Dissertation

zur Erlangung des Doktorgrades
des Fachbereiches Chemie
der Universität Hamburg
vorgelegt von

Götz Eckart Milkereit
aus Lübeck

Hamburg 2006

The work in hand was carried out between March 2001 and October 2005 in the Department of Organic Chemistry at the University of Hamburg and the Material Science Department of the GKSS Research Centre, Geesthacht. Followed by participation in a research assignment at the Beiersdorf AG in Hamburg from August 2004 until May 2005.

1st referee: Prof. Dr. Joachim Thiem
2nd referee: PD Dr. Regine Willumeit
Day of the last oral examination: 30.03.2006

March 2006

The publishers own the copyrights for prior publication of the following articles

Chapter 2 previously published in

Elsevier Ireland Ltd.: *Chem. Phys. Lipids*, 131, **2004**, pp.51-61.

Chapter 3 previously published in

Elsevier B.V.: *Chem. Phys. Lett.*, 392, **2004**, pp.105-109.

Chapter 4 previously published in

American Chemical Society: *J. Phys. Chem. B*, 109, **2005**, pp.1599-1608.

Chapter 5 previously published in

Elsevier Inc.: *J. Coll. Interface Sci.*, 284, **2005**, pp.704-713.

Chapter 6 previously published in

Elsevier Ireland Ltd.: *Chem. Phys. Lipids*, 135, **2005**, pp.1-14.

Chapter 7 previously published in

Elsevier Ireland Ltd.: *Chem. Phys. Lipids*, 135, **2005**, pp.15-26.

Chapter 8 previously published in

Springer Science & Business Media B.V.: *J. Therm. Anal. Calorim.*, 82, **2005**, pp. 477-481.

Chapter 9

Elsevier B.V. (Under consideration for publication).

Chapter 10

Taylor & Francis Ltd. (Under consideration for publication).

Parts of this work are protected under German law (Pat. pending).

„Litterarum radices amaras esse, fructus iucundiores.“

(Cato)

Table of contents

Abstract (english)

The form of organisation of amphiphilic compounds is of great importance for several biological and technical applications. Nevertheless the structure-property relationship of these compounds has in many areas not been investigated thoroughly yet. Especially the influence of chirality and complex structures is in many parts still not clear, in particular regarding the difference in energetically comparable structural order. The aim of this work is largely the investigation of the form of organisation of micelles, vesicles and membranes in aqueous media, as well as their interaction and transitions.

Different structures from simple alkyl glycosides, alkyl glycosides with spacers to complex glyco glycero lipids can serve as target compounds for these investigations.

The investigation of these properties requires the use of different characterisation methods and their combinations, as well as theoretical concepts.

Liquid crystalline properties were determined using polarising microscopy. The thermotropic phase behaviour was determined by heating the sample, whereas the lyotropic phase behaviour was determined by the contact of the sample with water. In case of the lyotropic phase behaviour it is possible to observe the complete phase sequence over the whole concentration range. The characterisation of the single phases requires different physical methods. Information about the calorimetric data of the phase transitions determined by differential scanning calorimetry (DSC) accomplish the results from the polarising microscopy, but is restricted to the investigation of defined concentrations.

The aggregation of amphiphiles in solution starts above the critical micelles concentration (*CMC*). The *CMC* was determined from the change of the surface tension in dependence of the concentration of amphiphile in solution, using a tensiometer. Furthermore it is possible to determine the area of an amphiphile molecule at the air-water interface, as well as to predict the possible shape of the micelles formed above the *CMC*.

The aggregate structure of amphiphiles in dilute solution (< 5 wt%) was determined using small-angle neutron scattering (SANS). The micellar form and structure can be determined very exactly due to the different scattering behaviour of neutrons on the nuclei of hydrogen and deuterium. In some cases it was also possible to determine the change of the micellar structure, in dependence of the concentration or temperature. The micellar structures were calculated using two different ways, a model-independent approach and fitting of the scattering data to different models. Comparing the results of both approaches gives concise information on the studied systems.

For the characterisation of the higher ordered lyotropic phases, especially of the biological relevant lamellar and cubic phases, small-angle x-ray scattering (SAXS) experiments where performed. Additional information about the packing order of the hydrophobic alkyl- and acyl

chains was retrieved from the investigation with fourier-transform-infrared-spectroscopy (FTIR).

The foaming properties of amphiphiles are an important technical feature of these compounds. The foaming behaviour was determined using a modification of the standard procedure according to DIN 53902-2, which gave reliable results, but required only very small amounts of amphiphile. The in-vivo characterisation of the foam structure and aging of the foams was made using a modified light microscope. These gave insights into the foam structure and the statistic pore size distribution of the air-bubbles inside of the foam.

The theoretical concept of the hydrophilic-lipophilic balance (*HLBG*) was accomplished by practical tests. The concept of the critical packing parameter (*CPP*), which predicts the possible aggregate form in dilute solution, was compared with the results from the SANS-experiments.

The investigated compounds were synthesised using several synthetic pathways, which gave the target compounds in gram scale and in highest purity. The different structural types covered ranged from alkyl glycosides and alkyl glycosides with different types of spacers to complex glyco glycero lipids. The molecular shape was also varied by the use of different carbohydrates (Glucose, Lactose, Maltose, Melibiose, Gentiobiose, Maltotriose). For some compounds the synthetic pathways were optimised, which gave the compounds in considerable higher yields and, in part, less synthetic steps. It was also observed, that the differences in the physical properties of glyco glycero lipids with the alkyl chain connected via an ether or ester linkage are very small. Moreover the 1,3-ether lipids can be synthesised in a few steps in gram scale, whereas the synthesis of the ester based lipids requires numerous steps. From 49 lipids synthesised in this work, 32 were synthesised for the first time.

The thermotropic liquid crystalline properties of the investigated alkyl glycosides differ mainly in the transition temperatures. High melting points were determined for compounds with linear alkyl chains. The melting point is lower for compounds with unsaturated and with methyl branched alkyl chains compared to the corresponding analogues with linear alkyl chains. In this case most of the compounds are in the liquid crystalline state at room temperature. Exceptions were found for compounds with unsaturated alkyl chains containing amide groups in the hydrophilic or in the spacer part. Here the melting point is above room temperature. Nearly all alkyl glycosides with disaccharide headgroups formed exclusively a smectic A phase. Only for three compounds was a cubic phase observed on cooling.

Glyco glycero lipids with trisaccharide carbohydrate headgroups or with two methyl branched alkyl chains only show smectic A phases, too. Interestingly it was found that 1,3-di-*O*-alkyl-glycero glyco lipids show nearly the same phase behaviour and transition temperatures as the corresponding glycosyl diacyl glycerols. The formation of columnar phases besides the smectic A phase was observed for slightly wedge shaped compounds, whereas Y-shaped

glyco glycero lipids and lipids with tilted headgroups also have the ability to form cubic phases.

Conversely to thermotropism, the lyotropic phase behaviour is already affected by small changes of the molecular structure. Generally it was found that, with the exception of Y-shaped glyco glycero lipids, all compounds investigated in this work show lamellar phases and so have the ability to act as membrane forming or membrane stabilising compounds. In the case of glyco glycero lipids with disaccharide headgroups and linear alkyl chains inverted phases are formed, whereas most of the alkyl glycosides form hexagonal and partly lyotropic cubic phases. An interesting exception was found for compounds with an ethanolamine spacer. Except for one compound it was observed that the spacer allows only the formation of lamellar phases. Investigation of the lyotropic aggregate structure of the lipid 1,3-di-*O*-(*cis*-9-octadecenyl)-2-*O*-β-D-maltopyranosyl-sn-glycerol showed the formation of a well-resolved cubic phase over a broad concentration and temperature range. This result is of high biological relevance as such behaviour has so far only been observed for a few lecithine lipids.

Y-mesogenes exhibit thermotropic and lyotropic cubic phases. The structure enables the formation of cubic structures. Supposably this structure facilitates the formation of cubic phases in biological processes.

The chemical structure of the amphiphiles strongly influences the *CMC*. Additionally it was found that amphiphiles with a Maltose carbohydrate headgroup are more surface-active than amphiphiles bearing Melibiose or Maltotriose headgroups.

Micelle formation was observed for several amphiphilic lipids. A more detailed concept for the formation of micelles by carbohydrate-based amphiphiles could be derived from this data. The change of the micellar structure can be explained using a general structural concept. Compounds of a rod-like molecular shape with n-alkyl chains form large aggregates. Amphiphiles with a wedge-shaped or tilted structure and a n-alkyl chain show a critical chain length above which rod-like micelles are formed and below it spherical micelles. The growth of rod-like micelles of the investigated lipids was determined to follow standard models. Spacers will change the micellar structure. Ethylene glycol spacers increase the hydrophilic part of the molecule and also the flexibility of the alkyl chain. Ethanolamine spacers connected with the fatty acid chain by an amide group also increase the hydrophilic part, but the flexibility is dramatically reduced. In contrast an ethyl branching in the spacer part of ethanolamine increases the hydrophobic part.

Short methyl branched chains, instead of n-alkyl chains, favour the formation of bilayer structures whereas long methyl branched chains will form micellar structures. Large carbohydrate headgroups (trisaccharides) as well as broad hydrophilic headgroups (Y-shaped lipids) can only form spherical micelles. Also bolaamphiphiles with two disaccharide headgroups can form spherical micelles, but only in a very narrow concentration range, most

probably followed by the formation of bilayer structures. This effect shows, that the interaction between membranes formed by the bolaamphiphile and vesicles or micelles is different as it is for non-bola lipids

The interaction of a carbohydrate-based bolaamphiphile with octyl β-D-glucopyranoside was found to be antagonistic, which is confirmed by a higher mixture *CMC* compared to the ideal mixing expectation and a decreasing of length of octyl β-D-glucopyranoside micelles upon addition of a small amount of bolaamphiphile to the solution. These results are unexpected, because the chemical structures of the investigated compounds are very similar and thus an increase in the size of micelles would normally be expected.

Thermotropic properties can be related to the micellar structure in dilute solution. Compounds showing a complex thermotropic phase behaviour due to a labile balance between the hydrophilic and hydrophobic moiety form large aggregate structures already at low concentrations in aqueous solution. A simple thermotropic phase behaviour is connected with the formation of small micelles in dilute solution.

Prediction of the aggregate form above the critical micelle concentration (*CMC*) by the Critical Packing Parameter (*CPP*), derived from the headgroup area at the air-water interface is only of limited use for carbohydrate-based amphiphiles. The micelle shape moreover depends on small changes of the molecular structure not captured by the adsorption at the liquid-air interface.

The relationship between the chemical structure and the micellar forms can be used for the design of micellar solutions in new applications.

The aqueous solubility of the amphiphiles in this thesis follows the general trend expected from their hydrophilic-lipophilic balance according to Griffin (*HLBG*), e.g. good water solubility was found for amphiphiles with a high *HLBG* number and a good emulsification ability was found for lipids with low *HLBG* number.

The method of methylation of the alkyl chain controls the self-assembly and can explain different biological functions for either plants (variable temperature) or animals (constant temperature). The solubility of the melibioside (*2R,4R,6R,8R*)-2,4,6,8-tetramethyldecyl-6-*O*-(α-D-galactopyranosyl)-β-D-glucopyranoside (Mel-β-TMD) was found to be low even above its Krafft-temperature. This is similar to observations made for the (all-*R*) tetramethyldecyl wax esters of the preen gland, which is responsible for the good water protection of the feathers of the domestic goose. The TMD-chains retains this effect even as a part of a more hydrophilic molecule. Additionally a methyl-branched chain favours the formation of membranes. Conversely the formation of cubic and columnar phases is suppressed.

Carbohydrate based amphiphiles are good foaming agents above their Krafft-temperature already at very low concentrations. Foams formed by the investigated compounds are very stable, especially compared to technical surfactants. The foaming ability increases with increasing temperature. The results give new insights in the relationship between the chemical

structure of the amphiphiles and the foaming behaviour, which allows the selection of an appreciable foamer. For use as cosmetic detergent it was found, by foaming microscopy, that these new amphiphilic sugar surfactants have the ability to form very fine structured foams, with a very narrow pore-size distribution of small air-bubbles. Also the stability of the foam is superior compared to standard cosmetic surfactants.

The general concepts, derived from the phase behaviour of the investigated simple lipid structures can be validated in future for its use on more complex and natural structures.

Abstract (german)

Die Organisationsformen amphiphiler Verbindungen sind von zentraler Bedeutung für viele biologische und technische Anwendungen. Die Struktur-Eigenschafts-Beziehungen dieser Verbindungen sind in vielen Bereichen jedoch noch nicht ausreichend erforscht. Besonders der Einfluß von Chiralität und komplexen Strukturen wirft noch viele Fragen auf, insbesondere im Unterschied energetisch vergleichbarer Ordnungsstrukturen. Das Ziel dieser Arbeit ist im wesentlichen die Untersuchung der Organisationsform von Micellen, Vesikeln und Membranen im wässrigen Medium, ihrer Wechselwirkung und Übergänge.

Als Zielstrukturen für diese Untersuchungen kommen Lipide von Alkylglycosiden Alkylglycosiden mit Spacer bis hin zu komplexen Glyco-Glycerolipiden in Betracht.

Die Untersuchung der Eigenschaften erfordert den Einsatz und die Kombination verschiedener Meßmethoden und theoretischer Konzepte, die sich gegenseitig ergänzen.

Die Bestimmung der flüssigkristallinen Eigenschaften erfolgte mittels der Polarisationsmikroskopie. Das thermotrope Phasenverhalten wird durch Aufheizen der Probe bestimmt, das lyotrope hingegen durch Kontakt mit Wasser. Im Fall des lyotropen Phasenverhaltens kann man so über den Konzentrationsgradienten das gesamte Phasendiagramm beobachten. Die Charakterisierung der Strukturen der einzelnen Phasen erfordert verschiedene physikalische Meßmethoden. Die Untersuchung der Proben durch Differential Scanning Calorimetry (*DSC*) gibt ergänzend zur Polarisationsmikroskopie Informationen über kalorimetrische Daten der Phasenumwandlungen, erlaubt aber nur die Untersuchung von definierten Konzentrationen.

Die Aggregation von Amphiphilen in Lösung beginnt im Allgemeinen oberhalb der kritischen Micell Konzentration (*CMC*). Diese Grenze wurde mittels Änderung der Oberflächenspannnung, in Abhängigkeit von der Konzentration mit einem Tensiometer bestimmt. Außer der *CMC* lassen sich aus dem Verlauf der Oberflächenspannnung auch Rückschlüsse auf den beanspruchten Platz eines Moleküls an der Oberfläche, sowie auf die mögliche Form der oberhalb der *CMC* gebildeten Micellen ziehen.

Die Aggregatstrukturen der Amphiphile in verdünnter Lösung (< 5 Gew.%) wurden mit der Neutronenkleinwinkelstreuung (SANS) bestimmt. Durch das unterschiedliche Streuverhalten von Neutronen am Wasserstoff- und Deuteriumkern lassen sich Micellform und -struktur sehr genau bestimmen. Darüberhinaus konnte in einigen Fällen auch die Strukturänderung der Micellen, bedingt durch Änderung der Konzentration oder Temperatur, bestimmt werden. Die Micellstrukturen wurden auf zwei unterschiedlichen Wegen berechnet, modellunabhängig und durch Anfitten unterschiedlicher Modelle. Aus dem Vergleich der Ergebnisse aus beiden Methoden erhält man zuverlässige Informationen über die untersuchten Systeme.

Die Charakterisierung höher geordneter lyotroper Phasen, insbesondere der biologisch relevanten, lamellaren und kubischen Phasen, erfolgte durch Röntgenkleinwinkelstreuung (SAXS). Zusätzliche Informationen über das Packungsverhalten der hydrophoben Alkyl- und Acylketten, wurden durch Fourier-Transform-Infrarot-Spektroskopie (*FTIR*) erhalten.

Eine wichtige technische Kenngröße von Amphiphilen ist ihr Schäumungsverhalten. Für die Bestimmung der Schaumhöhe und Stabilität wurde das Standardverfahren nach DIN 53902-2 vereinfacht, so daß eine repräsentative Untersuchung des Schäumungsverhaltens mit deutlich geringeren Einsatzkonzentrationen an Amphiphil möglich war. Die Charakterisierung der Struktur und des Alterungsverhaltens von in vivo erzeugten Schäumen wurde mit einem modifizierten Lichtmikroskop durchgeführt. Diese Untersuchung liefert Erkenntnisse über die Struktur des Schaums und die statistische Verteilung der Porengröße der Luftblasen innerhalb desselben.

Das theoretische Konzept der Hydrophilic-Lipophilic Balance (*HLBG*), das eine Vorhersage der Tensid/Emulgator Eigenschaften auf Grund theoretischer Berechnungen ermöglicht, wurde durch praktische Tests ergänzt. Das theoretische Konzept des kritischen Packungs-Parameters (*CPP*), der eine Vorhersage der Aggregatform in verdünnter Lösung oberhalb der *CMC* ermöglicht, wurden mit den Ergebnissen der SANS-Experimente verglichen.

Die Herstellung der untersuchten Verbindungen erfolgte auf unterschiedlichen synthetischen Wegen. Die Verbindungen wurden in höchster Reinheit und im Grammmaßstab erhalten. Auf diese Weise wurden Verbindungen von Alkylglycosiden, Alkylglycosiden mit Spacer bis hin zu komplexen Glyco-Glycerolipiden realisiert. Die Molekülstruktur wurde weiterhin durch die Nutzung verschiedener Zuckerkopfgruppen variiert (Glucose, Lactose, Maltose, Melibiose, Gentiobiose, Maltotriose). Durch die Optimierung von Synthesewegen gelang die Synthese von verschiedenen Verbindungen in deutlich höheren Ausbeuten und teilweise weniger Syntheseschritten. Auch zeigte sich, daß der Unterschied zwischen den physikalischen Eigenschaften von Glyco-Glycerolipiden in denen die Kette Ether oder Ester-gebunden vorliegt sehr gering ist. Die Ether-Lipide sind dafür aber leicht in wenigen Stufen und im Grammmaßstab herstellbar, wohingegen die Herstellung der Ester-Lipide eine wesentlich größere Anzahl von Syntheseschritten erfordert. Von den 49 hergestellten Zielverbindungen sind 32 in dieser Arbeit zum ersten Mal beschrieben worden.

Die Untersuchung des thermotropen Phasenverhaltens der Lipide zeigt im Wesentlichen Unterschiede in den Umwandlungstemperaturen und nicht im Phasenverhalten selber. n-Alkylglycoside zeigen einen hohen Schmelzpunkt, der durch den Einsatz ungesättigter oder methylierten Alkylketten gesenkt werden kann. Die meisten Verbindungen mit ungesättigten oder methylierten Alkylketten sind bei Raumtemperatur flüssigkristallin, eine Ausnahme bilden Lipide bei denen die Alkylkette amidisch gebunden ist; diese zeigen einen höheren Schmelzpunkt. Fast alle Alkylglycoside und deren Derivate zeigen nur eine thermotrope

smektisch A Phase, nur für drei Verbindungen wurde beim Abkühlen aus der isotropen Lösung die Bildung einer kubischen Phase beobachtet.

Auch Glyco-Glycerolipide mit Trisaccharid-Kohlenhydratkopfgruppen und Glyco-Glycerolipide mit zwei methylierten Ketten bilden nur eine smektisch A Phase. Interessanterweise ist dabei das Phasenverhalten der hergestellten 1,3-Di-*O*-Alkyl Glyco-Glycerolipide vergleichbar zu dem der entsprechenden Glycosyl-Diacylglycerole. Die Bildung einer columnaren Phase neben der smektischen Phase wurde für leicht gekrümmte Verbindungen beobachtet, wohingegen Y-Mesogene und Verbindungen mit stark gekrümmter Struktur auch kubische Phasen bilden.

Das lyotrope Phasenverhalten wird bereits durch kleine Änderungen der Molekülstruktur beeinflußt. Alle Verbindungen mit Ausnahme der Y-Mesogene bilden lamellare Phasen, und zeigen somit ihre Eigenschaft als Membranbildner oder Stabilisatoren. Glyco-Glycerolipide bilden neben der lamellaren Phase inverse Strukturen, während die meisten Alkylglycoside neben der lamellaren Phase hexagonale und teilweise kubische Phasen bilden. Für Verbindungen mit einem Ethanolaminspacer wurde, mit einer Ausnahme, nur die Bildung von lamellaren Phasen beobachtet. Das synthetische Lipid 1,3-Di-*O*-(*cis*-9-Octadecenyl)-2-*O*-β-D-maltopyransoyl-sn-glycerol hingegen, bildet eine kubische Phase über einen weiten Konzentrations- und Temperaturbereich. Dieses Resultat ist von biologischer Relevanz, da ein solches Phasenverhalten bis jetzt nur für einige biologisch relevante Lecithine beobachtet wurde.

Y-Mesogene zeigen neben thermotrop kubischen, auch lyotrop kubische Phasen. Möglicherweise erleichtert hierbei die Y-förmige Struktur die Bildung kubischer Phasen in biologischen Vorgängen.

Bei den untersuchten Amphiphilen wird die kritische Micellkonzentration (*CMC*) durch die individuelle chemische Struktur stark beeinflußt. Darüberhinaus wurde beobachtet, daß Amphiphile mit einer Maltose-Kohlenhydratkopfgruppe stärker grenzflächenaktiv sind als solche mit Melibiose- oder Maltotriose-Kopfgruppen.

Ein Großteil der untersuchten Lipide bildet Micellen in wässriger Lösung. Daraus konnte ein detailliertes Konzept für die Micellbildung von Kohlenhydratamphiphilen abgeleitet werden. Die Änderung der micellaren Strukturen kann mit folgendem generellen Strukturkonzept erklärt werden. Verbindungen die eine n-Alkylkette tragen, weisen sowohl mit leicht, als auch mit stark gekrümmter Struktur eine kritische Kettenlänge auf. Während oberhalb dieser kritischen Kettenlänge eine zylindrische Micelle gebildet wird, erfolgt unterhalb die Bildung einer kugelförmigen Micelle. Das Micellwachstum der zylindrischen Micellen folgt den bekannten Modellen. Die Micellstruktur wird durch Spacer verändert: Ethylenglycol Spacer vergrößern den hydrophilen Molekülteil und erhöhen die Flexibilität der Kette. Beim Einsatz von Ethanolamin Spacern, bei denen die Fettsäurekette über eine Amidbindung an den Spacer gebunden ist, wird ebenfalls der hydrophile Teil des Moleküls vergrößert, die Flexibilität der

Kette jedoch drastisch reduziert. Eine Ethylgruppe am Ethanolamin Spacer erhöht hingegen den hydrophoben Teil des Moleküls.

Kurze methylierte Ketten an Stelle von n-Alkyl Ketten führen zur Bildung von Doppelschicht-Strukturen, wohingegen lange methylierte Ketten micellare Strukturen bilden. Große voluminöse Kopfgruppen (Trisaccharide) und auch breite Kopfgruppen (Y-Mesogene) können nur kugelförmige Micellen bilden. Auch bilden Bolaamphiphile mit zwei Disaccharid Kopfgruppen kugelförmige Micellen, aber nur in einem schmalen Konzentrationsbereich, nach den dann, bereits in verdünnter Lösung, die Bildung größerer, wahrscheinlich Doppelschichtstrukturen folgt. Dieser Effekt zeigt, daß die Wechselwirkung dieser Membranen mit Vesikeln oder Micellen anders ist als bei Membranen normaler Lipide.

Eine antagonistische Wechselwirkung zwischen einem Bolaamphiphil mit Kohlenhydratkopfgruppen und Octyl-β-D-glucopyranosid wurde durch eine höhere Mischungs-*CMC*, im Vergleich zur idealen Mischung, und eine Verringerung der Micelllänge von Octyl-β-D-glucopyranosid-Micellen nach Bolaamphiphil-Zugabe bestätigt. Dieses Ergebnis ist unerwartet, da die ähnlichen chemischen Strukturen der Kopfgruppen normalerweise einen synergistischen Effekt auf die Micellgröße erwarten lassen.

Ein weiterer, interessanter Zusammenhang kann zwischen den thermotropen Eigenschaften und der Micellstruktur in verdünnter Lösung hergestellt werden. Verbindungen, die auf Grund eines instabilen Gleichgewichts zwischen dem hydrophilen und hydrophoben Molekülteil ein komplexes Phasenverhalten zeigen, neigen bereits in verdünnter Lösung zur Bildung großer Aggregatstrukturen. Ein einfaches thermotropes Phasenverhalten kann mit der Bildung kleiner Micellstrukturen korreliert werden.

Die Vorhersage der Micellstruktur mittels des Kritischen Packungs Parameters (*CPP*), der aus der Adsorption an der Luft-Wasser Grenzfläche berechnet wird, ist nur sehr bedingt tauglich für Kohlenhydratamphiphile. Die Micellstruktur wird bereits von kleinen strukturellen Änderungen beeinflußt, die sich auf das Verhalten an der Grenzfläche aber nicht auswirken.

Der Zusammenhang zwischen der chemischen Struktur und der Micellform kann für die Herstellung micellarer Systeme für neue Anwendungen genutzt werden.

Die Löslichkeit der Amphiphile folgt im Großen und Ganzen dem Konzept der Hydrophilic-Lipophilic Balance nach Griffen (*HLBG*), z.B. wurde eine gute Wasserlöslichkeit für Verbindungen mit hohen *HLBG*-Werten und gute Emulgatoreigenschaften für niedrige *HLBG*-Werte gefunden.

Das Aggregationsverhalten kann durch die Art der Methylierung der Alkylkette kontrolliert und darüberhinaus können damit die unterschiedlichen biologischen Funktionen für Pflanzen (variable Temperatur) oder Tiere (konstante Temperatur) erklärt werden. Die Löslichkeit von (*2R,4R,6R,8R*)-2,4,6,8-Tetramethyldecyl-6-*O*-(α-D-galactopyranosyl)-β-D-glucopyranosid (Mel-β-TMD) ist auch oberhalb der Krafft-Temperatur niedrig. Ein ähnliches Löslichkeitsverhalten wurde bereits für die (all-*R*) Tetramethyldecyl Wachs-Ester aus der

Bürzeldrüse der Hausgans, die für die wasserabweisenden Eigenschaften der Federn verantwortlich sind, beobachtet. Die TMD-Kette behält diesen Einfluß auch als Teil eines wesentlich polareren Moleküls. Darüberhinaus favorisiert eine methylierte Kette die Bildung von Doppelschichten (Membranen), wohingegen die Bildung kubischer und columnarer Phasen unterdrückt wird.

Kohlenhydratamphiphile zeigen oberhalb ihrer jeweiligen Krafft-Temperatur bereits in niedrigen Konzentrationen gute Schäumungseigenschaften. Die Schäume sind sehr stabil, besonders im Vergleich zu industriellen Standardschäumern. Auch erhöht sich die Schaumbildung mit steigender Temperatur. Die Ergebnisse geben einen neuen Einblick in die Beziehung zwischen der chemischen Struktur des Amphiphils und dem Schäumungsverhalten, was eine gezieltere Auswahl eines gewünschten Schäumers ermöglicht. Die in dieser Arbeit untersuchten neuen Kohlenhydratamphiphile bilden sehr feine, kugelörmige Schäume mit einer Größenverteilung hauptsächlich zu schmalen Luftbläschen hin. Auch die Stabilität der Schäume ist, im Vergleich zu Standardschäumern der kosmetischen Industrie, deutlich höher.

Die allgemeinen Konzepte, entwickelt aus dem Phasenverhalten der hier untersuchten einfachen Grundstrukturen, können zukünftig auf ihre Anwendbarkeit auf natürliche, komplexere Strukturen hin untersucht werden.

List of abbreviations

a0	headgroup area at the liquid-air interface
abs.	absolute
APG	alkyl polyglucoside
$BF_3 \cdot Et_2O$	borontrifluoride diethyletherate
b.p.	boiling point
Cbz	carbonylbenzyloxy
$CDCl_3$	chloroform (deuterated)
$C_{12}E_6$	hexaethyleneglycoldodecylether (Laureth-6)
$CHCl_3$	chloroform
CH_2Cl_2	dichloromethane
C_5H_5N	pyridine
CMC	critical micelle concentration
CPP	critical packing parameter
col	columnar mesophase
Conc.	concentration
Cr	crystalline
cub	cubic mesophase
cub_{bi}	bicontinous cubic mesophase
cub_{dis}	discontinous cubic mesophase
d	doublet
dd	double doublet
DIN	Deutsche Industrie Norm
DLS	dynamic light scattering
DMF	N,N-dimethylformamide
DMSO	dimethylsulfoxide
D_2O	deuteriumoxide
DSC	differential scanning calorimetry
dt	double triplet
Et_3N	triethylamine
EO	ethyleneoxide

FeCl$_3$	ferric (III) chloride
FTIR	fourier transform infrared spectroscopy
g	glass state
gal	Galactose
Gen	Gentiobiose (6-O-β-D-glucopyranosyl)-D-glucopyranoside
glc	Glucose
H$_2$	hydrogen
H$_I$	hexagonal phase (lyotropic)
H$_{II}$	inverted hexagonal phase (lyotropic)
HIRES-FAB-MS	high-resolution fast-atom-bombardment mass spectroscopy
HLB	hydrophilic-lipophilic balance
IFT	indirect fourier transform
L	length
L$_\alpha$	lamellar phase (lyotropic)
Lac	Lactose (4-O-β-D-galactopyranosyl)-D-glucopyranoside
L$_\beta$	gel-phase (lyotropic)
M	molar concentration
mM	millimolar concentration
Mal	Maltose (4-O-α-D-glucopyranosyl)-D-glucopyranoside
MALDITOF-MS	matrix assisted laser desorption and ionisation time of flight mass spectroscopy
Maltri	Maltotriose (4-O-(4'-O-α-D-glucopyranosyl)-α-D-glucopyranosyl)-D-glucopyranoside
m$_c$	multiplet centred
Mel	Melibiose (6-O-α-D-galactopyranosyl)-D-glucopyranoside
MeOH	methanol
min.	minute
M$_w$	molecular weight
NaN$_3$	sodium azide
NaOMe	sodium methoxide
NMR	nuclear magnetic resonance spectroscopy

o/w   oil in water

Pd/C   palladium on charcoal
PEO   polyethyleneoxide
Phy   phytol (3,7,11,15-tetramethylhexadecyl)

R   radius
R_{CS} radius of cross section

S_A, SmA   smectic A mesophase
SANS   small-angle neutron scattering
SAXS   small-angle x-ray scattering
SDS   sodium dodecyl sulfate
SLES   sodium laurylether sulfate

t   triplet
T   temperature
T_c chain melting temperature ($L_\beta \leftrightarrow L_\alpha$ transition)
THF   tetrahydrofurane
T_K Krafft-eutectic temperature
TLC   thin layer chromatography
TMD   (*2R,4R,6R,8R*)-2,4,6,8-tetramethyldecyl
TMS   tetramethylsilane

V_I bicontinous cubic phase (lyotropic)
V_{II} inverted bicontinous cubic phase (lyotropic)
v/v%   volume percent

w/o   water in oil
wt%   weight percent
w/v%   weight to volume percent

Chapter 1

Introduction

1.1 Amphiphiles

The great importance of amphiphilic molecules for biological systems and technical applications is their ability to form both thermotropic liquid crystalline phases in their pure state upon heating and lyotropic liquid crystalline phases upon addition of solvent.
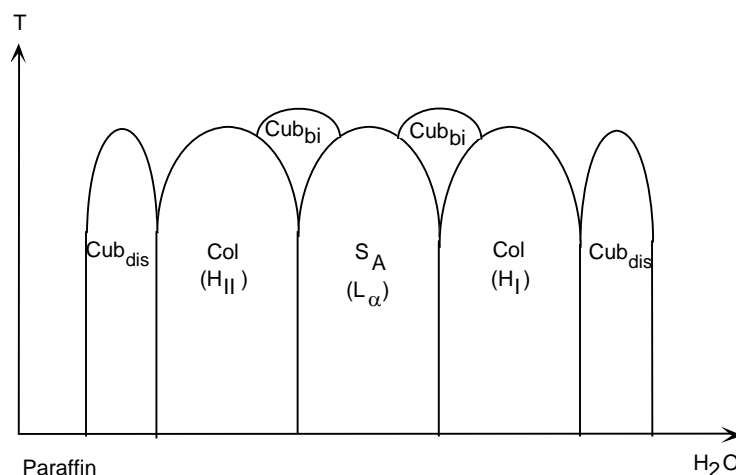

FIGURE 1.1: Phase behaviour of amphiphiles in principle (Prade *et al.*, 1995; Blunk *et al.*, 1998).

The driving force for the mesophase formation is a micro phase separation leading, in the case of amphiphilic molecules, to an aggregate structure with separated regions for the lipophilic and hydrophilic moieties. This enables the maintenance of the van der Waals interaction in the hydrophilic region. The phase behaviour of these compounds in principle is shown in Figure 1.1 (Prade *et al.*, 1995; Blunk *et al.*, 1998). At a fixed amphiphile/water ratio, corresponding to a vertical line in the diagram, amphiphiles normally display the same phase even as the temperature varies, exceptions can be found especially if these compounds have an unusual geometry of the carbohydrate headgroup. In this case cubic phases may also be observed, while simple amphiphiles exhibit only a thermotropic Smectic A phase. Deviation from the phase behaviour of the pure amphiphiles, that is only changed by the temperature, will occur upon the addition of solvents. The lamellar phase consists of planar bilayers, which are built up by rod-like molecules. The bilayers stack on top of the other and each one is separated by a layer of water in aqueous systems. Hence this phase is importance as it corresponds to the cell membrane in biological systems (Rilfors *et al.*, 1984). Whereas small amounts of, for example water, will not change the phase type and transition temperatures, larger amounts will induce new mesophases such as cubic and columnar phases ($H_{I/II}$) besides the lamellar mesophase. The discontinuous cubic phases are based upon varied packing of

spherical or slightly anisotropic micelles, whereas the bicontinous cubic phases with interwoven fluid porous structures are based on underlying infinite periodic minimal surfaces (Fairhurst *et al.*, 1998). Bicontinous cubic phases are of great biological interest as they are supposed to play an important role during the process of cell-fusion or exocytosis (Siegel, 1986; Ellens *et al.*, 1989; Siegel *et al.*, 1989; Nivea *et al.*, 1995), despite that the molecular mechanism behind the fusion process is not yet full understood. It is known that the key step in a fusion process has to be the rearrangement of the lipid molecules of the formerly apposed two bilayers to form a single, continous membrane connecting both cells. Cubic phases can also be induced, by using simple alkyl glycosides as dopants to membrane forming lipids (Minden et al., 2002a).

Besides the homogenous liquid crystalline or single phases (Holmberg *et al.*, 2003a) other heterogeneous systems consisting of two or more phases can be formed by amphiphiles (see Table 1.1). The formation of lyotropic aggregates will occur above a defined temperature the so-called Krafft-eutectic temperature. The Krafft-temperature (T_k) is a specific temperature above which a hydrated solid amphiphile dissolves into assemblies (Laughlin, 1992 and 1994). Below this temperature the amphiphile precipitates as a hydrated solid.

TABLE 1.1: Examples for different classes of amphiphilic systems.

Systems of single phases (homogeneous systems)	Systems of multiple phases (heterogeneous systems)
Solid phases	Emulsions
Liquid crystalline phases	Suspensions
Isotropic solutions	Vesicles
Micellar solutions	Foams
Microemulsions	Gels
Vesicle solutions	

1.2 Structure-property relationships

The aggregation of amphiphiles often does not depend on the exact chemical structure but more general on the overall shape of the lipid (see for example Tschierske, 2001, and references cited herein). Minden *et al.*, (2000) showed that it is possible to reduce the demanding stereochemistry of glycolipids to a more simple model. It was found that the exact configuration of the carbohydrate headgroup (e.g. gluco, galacto) has its main influence on

the transition temperatures of the compounds, but not on the phase sequence (see for example Vill *et al.*, 2000; Minden *et al.*, 2000; Minden *et al.*, 2002b). Thus the principle molecular structure can be reduced to the type and position of linkage between the carbohydrate headgroups. An overview of the general classes of amphiphiles is given in figure 1.2.

With reference to figure 1.2 it can be seen that the types of amphiphiles can be divided into three general classes. Type A has a rod-like structure, an example of these compounds would be alkyl glucosides or alkyl lactosides and cellobiosides. The alkyl chain is typically connected to the carbohydrate headgroup in β-position and, in the case of disaccharides, the two sugar moieties are also connected via a β-linkage at the anomeric centre. Compounds of type B can be divided into two subcategories: slightly wedge-shaped and tilted compounds. Typical molecules of this type would be for example alkyl-β-maltosides where the two Glucose units of the carbohydrate headgroup are connected via a α1→4 linkage or alkyl melibiosides where a Galactose moiety is linked α1→6 to a Glucose moiety. Type C represents a class of common biological lipids, the diacyl- or dialkyl glycosyl glycerols. These compounds are often termed "Y-shaped" lipids and can be found as normal (one polar head, two chains) or inverted (two polar heads, one chain) types.
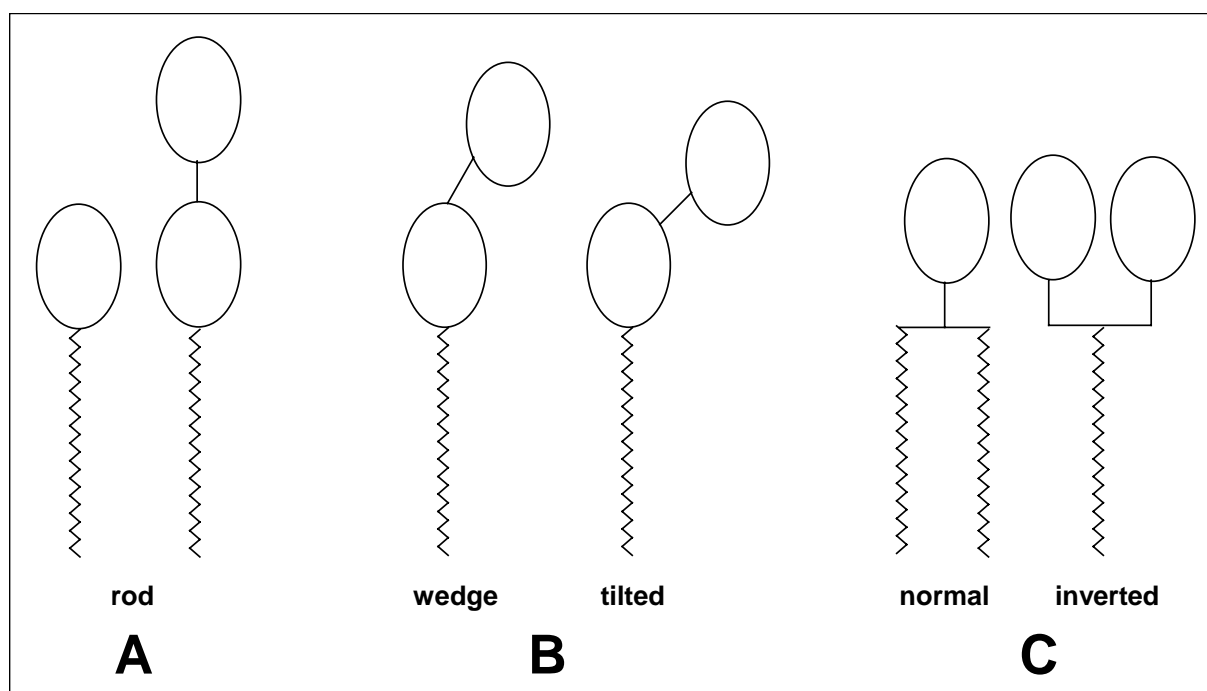

FIGURE 1.2: Types of amphiphiles (Minden *et al.*, 2000).

This simple structural description of amphiphiles has been successfully applied to the liquid crystalline properties of alkyl glycosides and glycosyl diacyl glycerols (Vill *et al.*, 2000; Minden *et al.*, 2000; Minden *et al.*, 2002a; Minden *et al.*, 2002b). It can also be used to

describe other carbohydrate headgroups or a different linkage of the alky chain to those headgroups.

1.3 Micelles

Liquid crystalline phases of alkyl glycosides and glycolipids have been extensively investigated. Micellar phases of synthetic alkyl glycosides and glycolipids on the other hand are less well known and most work is done on commercially available compounds. A concise description of the structure-property relationship between the micellar phases and the molecular structure is still missing.

In aqueous solution amphiphilic molecules form monolayer films at the air-water interface, further added amphiphiles are packed into this adsorption-film until the surface is completely covered by a monolayer. At this point, the so-called critical micelle concentration (*CMC*), further increase of the concentration of amphiphiles leads to the formation of micelles (Holmberg *et al.*, 2003a). The surface tension of the solution is lowered with increasing concentration, according to the adsorption-isotherm of Gibbs (Hiernez, 1977; Gibbs, 1976). After reaching the *CMC*, the surface tension stays constant.

The micellar forms can be very different, simple spherical micelles can be found, as well as long rod-like aggregates, which behave similar to solutions of polymers (Holmberg *et al.*, 2003a). The micellar form depends on the molecular structure. For example, in the case of tridecyl and tetradecyl maltoside elongation of the alkyl chain by one methylene group leads to the formation from spherical (Minden *et al.*, 2000) to polymer-like micelles (Ericsson *et al.*, 2005; Heerklotz *et al.*, 2004).

1.3.1 Geometric packing of amphiphilic molecules in micelles

The formation of aggregates above the *CMC* can be described in terms of a geometrical packing analysis. The two main forces that control the self-assembly into aggregate structures in water arise from the behaviour at the air-water interface. One force derives from the association of the molecules due to a hydrophobic attraction at the interfacial area, while the other, repulsive force arises from the nature of the headgroups, requiring the contact of the hydrophilic head with water. According to Tanford (1980) these 'opposing forces' are acting mainly at the interface between the hydrophilic and hydrophobic parts. The balance of these two forces is the optimal headgroup area (a_0) or an energetic minimum of the interfacial area (a) per molecule (See also Figure 1.3).
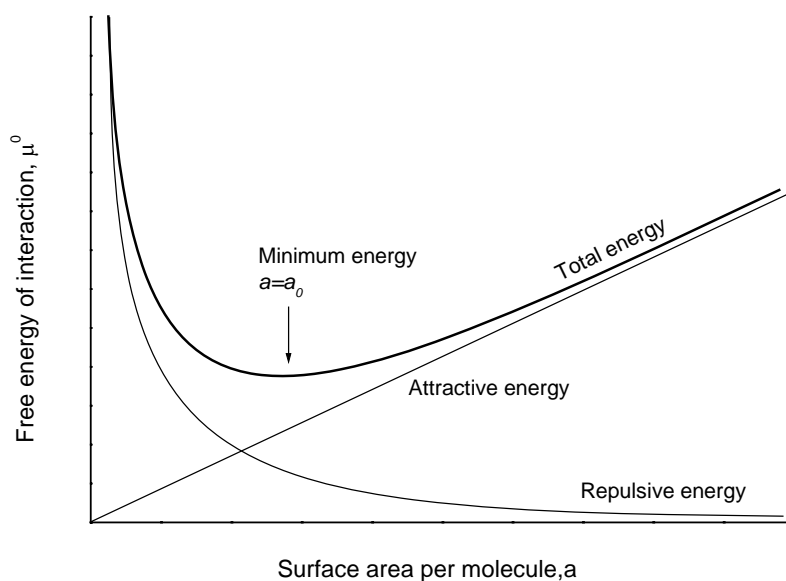
FIGURE 1.3: Position of the optimal headgroup area (a_0) at the minimum of the total energy of the repulsive (headgroup) and attractive (hydrophobic) forces (Israelachvili, 1992a).

From this the interfacial energy per molecule can be expressed as:

$$\mu_N^0 = 2\gamma a_0 + \frac{\gamma}{a}\left(a - a_0\right)^2 \tag{1.1}$$

with: γ: interfacial free energy per unit area

        a :   surface area per molecule

        a_0 :   optimal surface area per molecule

        μ_N^0 : interfacial energy per molecule

where the attractive interaction from the interfacial tension force (Parsegian, 1966; Jönnson and Wennerström, 1981) and the repulsive contributions arising from steric, hydration and electrostatic forces of the headgroup (Isrealachvili *et al.*, 1980; Puwada and Blanckstein, 1990) are taken into account.

With knowledge of the preferred interfacial area and the geometric properties of the molecules the most favoured structures that arise from these can now be predicted.
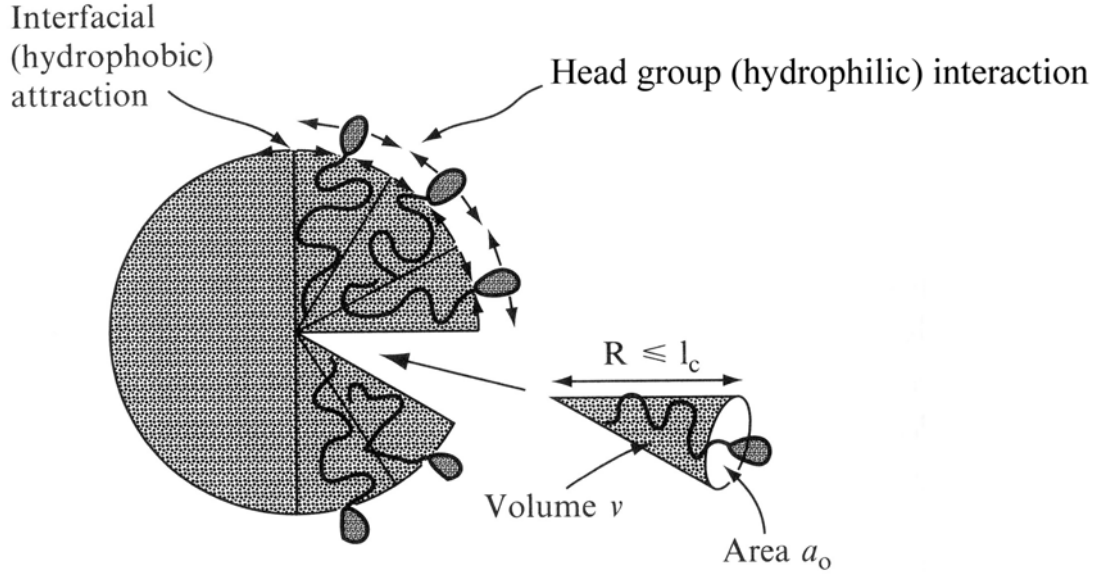
FIGURE 1.4: Geometric packing of amphiphilic molecules into spherical micelles (Reprinted from ISRAELACHVILI, J.N., *Intermolecular and Surface Forces*, 2nd ed., p.368, Copyright 1992, with permission from Elsevier).

The most simple micellar form is a sphere. As shown in Figure 1.4 a sphere can be divided into cones. According to Israelachvili (1992a) the molecular geometry of the amphiphile-cone in the micelle depends on the optimal headgroup area a_0, the volume of the hydrophobic alkyl chain v and its maximum length l_{max}. The chain cannot extend this length, so it is more commonly referred to as the critical chain length l_c. According to Tanford (1980) the critical chain length is given by

$$l_c \le l_{max} \approx \left(0.15 + 0.1265 n_c\right) \text{nm} \tag{1.2}$$

with: n_c :   number of carbon atoms

        l_c :   critical chain length

        l_{max} : maximum chain length

and the volume of the chain by

$$v \approx (27.4 + 26.9 n_c) \times 10^{-3} \, \text{nm}^3 \tag{1.3}$$

with: v : chain volume

The aggregation number N is assumed to be the ratio between the volume of the micellar core V_{mic} and the chain volume v:

$$N = \frac{V_{mic}}{v} = \frac{4\pi R_{mic}^3}{3v} \tag{1.4}$$

with: V_{mic} : volume of the micellar core

N :   aggregation number

R_{mic} : radius of the micellar core

Also N can be expressed as the ratio between the micellar area A_{mic} at the surface and the headgroup cross-section area a_0:

$$N = \frac{A_{mic}}{a_0} = \frac{4\pi R_{mic}^2}{a_0} \qquad (1.5)$$

with: A_{mic} : Surface area of the micelle

From Eq. 1.4 and 1.5 follows:

$$\frac{v}{R_{mic} a_0} = \frac{1}{3} \qquad (1.6)$$

Since R_{mic} cannot exceed the maximum chain length of the surfactant alkyl chain the term on the left side in Eq. 1.6 is limited by

$$\frac{v}{l_{max} a_0} \leq \frac{1}{3} \qquad (1.7)$$

for a spherical micelle. The ratio described in Eq. 1.7 is called Critical Packing Parameter (*CPP*). Amphiphiles do not form only spherical micelles, since for smaller values of a_0 Eq. 1.7 will be $v / a_0\ l_c > 1/3$. The aggregates that can be formed and the corresponding *CPP* values are shown in table 1.2.

TABLE **1.2:** Supramolecular structures depending on the packing shape and the critical packing parameter (*CPP*), according to Israelachvili (1992).

CPP	*Packing shape*	*Structures formed*
< 1/3	Cone	Spherical micelles
1/3 - 1/2	Truncated cone	Cylindrical micelles
1/2 - 1	Truncated cone	Flexible bilayers, vesicles
~ 1	Cylinder	Planar bilayers
> 1		Inverted structures

The interaction and the chirality of complex headgroups (e.g. carbohydrates) are not captured within the model of the *CPP*. The *CPP* can be easily calculated from the headgroup area at

the air-water interface which can be measured by surface tension experiments. The structures that are formed by carbohydrate-based lipids on the other hand often do not correspond with that predicted by the *CPP*.

1.4 Structural characterisation of supramolecular aggregates

Physical, technical, biophysical and biological properties have been reported for lipids (for recent reviews see for example Koynova and Caffrey, 1994; Mannock and McElhaney, 2004 and references cited herein). The connection of these properties with the molecular structure of these compounds gives a structure-property relationship, which provides a different understanding of certain functions of these lipids. Useful methods for the characterisation of the physical and biophysical properties can be concluded from the general phase behaviour of lipids (Figure 1.5).
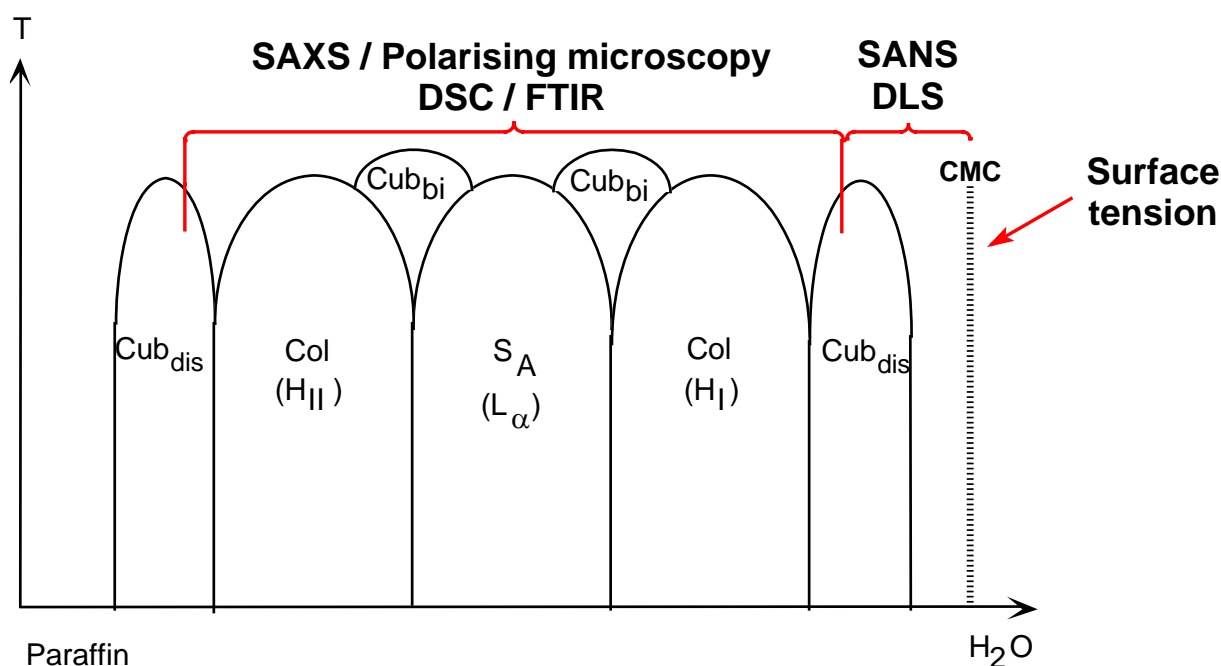

FIGURE 1.5: Physical characterisation methods for determining structural properties of amphiphilic compounds (SAXS - Small-angle x-ray scattering; DSC - Differential scanning calorimetry; FTIR - Fourier Transform Infrared spectroscopy of the chain order; SANS - Small-angle neutron scattering; DLS - Dynamic light scattering).

As shown in figure 1.5 the method of choice depends on the concentration of the amphiphile in the solvent. It is assumed that the aggregation of amphiphiles starts at a certain point, the critical micelle concentration (*CMC*).

The *CMC* can be determined using various methods, where the most common one is the surface tension method. The micellar phase region can be characterised by using small-angle neutron scattering (SANS) or dynamic light scattering (DLS). A combination of the methods provides a comprehensive picture of the structure of the aggregates. The structure of higher ordered phases in water, especially cubic, hexagonal and lamellar phases, can be determined best by using small-angle x-ray scattering (SAXS). Micellar phases can also be characterised using this method, but its use is limited to water contents of no more than 95% above which it becomes impossible to substract scattering signals of aggregates from the residual background. A qualitative phase diagram of the lyotropic phases can be obtained by polarising microscopy using the contact preparation technique. The thermotropic phases and phase transitions can be characterised as well. For phase transition temperatures and the characterisation of the phases differential scanning calorimetry (DSC) is very common. Nevertheless, it is often not possible to determine the phase region of metastable phases (e.g. cubic phases). In this case the combination of DSC and polarising microscopy will be useful. Additional structural information regarding the conformation of the hydrophobic molecular part in water can be obtained by using Fourier-Transform Infrared Spectroscopy (FTIR). A combination of these methods gives a complete picture of the supramolecular aggregate structure of the investigated amphiphile.

1.4.1 Surface tension

There are several possible ways for the determination of the CMC of an amphiphilic molecule. The most common one for surfactants and amphiphiles is the use of the de Noüy ring method. A platinum ring is submerged in an aqueous solution of the amphiphile and the maximum force that is required to pull the ring through the surface is determined. The surface tension is then calculated using

$$\sigma = \sigma^* \cdot F = \frac{P}{2\pi \cdot (R_1 + R_2)} \cdot F \qquad (1.8)$$

with: σ :   surface tension

σ^* :   measured surface tension

F :   correction factor

P :   maximum force on pulling the ring through the surface,

R_1 / R_2 : inner radius / outer radius of the ring

The correction factor F in Eq. 1.8 includes the hydrostatic lifted volume, temperature, ring geometry and the density of the solution.

Besides the *CMC* other useful data can be obtained. For non-ionic surfactants the surface tension is related to the adsorption of a molecule at air-liquid interface through the Gibbs-equation (Hiernez, 1977; Gibbs, 1976)

$$\partial\sigma = -\sum_{i=1}^{n}\Gamma_i\partial\mu_i \qquad (1.9)$$

with: Γ: surface concentration of component i

μ: chemical potential of component i

from Eq. 1.9 the surface concentration of the amphiphile can be derived:

$$\Gamma = -\frac{1}{RT}\left[\frac{d\sigma}{d\ln c}\right] \qquad (1.10)$$

with: R : molar gas constant

T : temperature

c : concentration

At the air-water interface only monolayer adsorption is assumed, therefore the adsorbed amount of amphiphile is inversely proportional to the area per molecule at the interface

$$a_0 = \frac{1000}{6.023\Gamma} \quad \text{(in Å}^2\text{/molecule)} \qquad (1.11)$$

with: a_0 : headgroup area at the air-water interface

and can be used for the calculation of the Critical Packing Parameter (*CPP*).

1.4.2 Small-angle scattering (SANS and SAXS)

Information regarding the structure, especially the structural parameters of supramolecular aggregates, is necessary for a thorough characterisation of amphiphilic compounds. The use of x-ray or neutron radiation is one of the most important tools. The scattering of the radiation occurs for x-rays on the electron system of the atoms and for neutrons directly on the nucleus. According to Braggs equation (Eq. 1.12),

$$\frac{1}{d} = \frac{2\cdot\sin\theta}{\lambda} \qquad (1.12)$$

with: d : distance between the different scattering layers

θ : scattering angle

λ : wavelength

it is obvious that the scattering angle depends on the size of the structure. Large structures, like micelles will scatter at small angles and vice versa. The great advantage of neutron scattering compared to x-ray scattering lies in the fact that neutron scattering length densities (b) for hydrogen and deuterium are very different (b_H = -0.374 x 10^{-12} cm $\leftrightarrow$ b_D = 0.667 x 10^{-12} cm). Thus the scattering curves of normal and heavy water are different and this offers the possibility to measure solutions at very low concentrations.
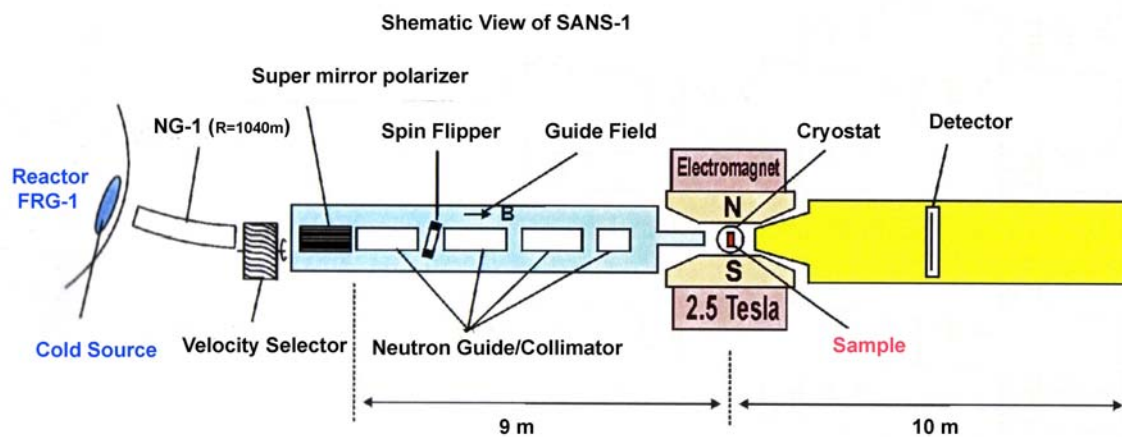
FIGURE 1.6: Schematic view of the small-angle scattering instrument SANS-1 at the GKSS research centre (Taken from: Schreyer *et al.*, 2004, reprinted with permission).

Neutron scattering experiments described in this thesis were carried out using the FRG-1 reactor at the GKSS research centre in Geesthacht, Germany. The experimental setup of the SANS-1 instrument designed for the investigation of colloidal systems (Stuhrmann *et al.*, 1995) is shown in figure 1.6. The research reactor FRG-1 has a thermal neutron source power of five megawatts. It provides a constant neutron flux of 1.4 x 10^{14} n/cm^2. The neutrons are sent through beam-holes to the different experiments. For the SANS-1 experiment the neutrons are guided first through a curved beam-line (NG-1), where the gamma-irradiation is cut off. Next the neutron-beam passes a velocity selector where only neutrons of the desired speed can pass. The beam passes the collimator line and is sent onto the sample. The wavelength of the cold polarised neutrons is λ = 8.1 Å with a wavelength resolution of ±10 %. The samples are kept in a thermostated sample holder for isothermal conditions. With the SANS-1 instrument it is possible to measure five samples in one cycle. A two-dimensional

[3]He-counter is used for the detection of the scattered neutrons. The active area of the detector is 55 x 55 cm^2 with an effective pixel size of 0.7 x 0.7 cm^2. The detector is placed in a vacuum-pipe and the sample-to-detector distance can be varied from 0.7 to 9 m. This allows coverage of scattering vectors from 0.005 to 0.25 Å^{-1}.

The raw scattering data have to be corrected for the incoherent background scattering of the solvent and are normalised to the concentration. The further analysis of the scattering data can be done in two different ways. First a model-independent approach is used, the indirect Fourier Transformation method (IFT) (Glatter, 1977; Pedersen, 1997). The IFT-routine gives information about the shape, radius and mass of the studied aggregates. With this information it is possible to select appropriate models that can then be applied to the scattering data. From a 'best fit' further information, e.g. overall length, flexibility or aggregation number, can be calculated. More detailed informations about the chosen models and data analysis are given in the subsequent chapters. Data analysis is done using computer programs. For the analysis of the raw data the programs "*SANSI*" and "*ri*" from the GKSS program library were used. Model fits were performed using the program "*LQRES*" from Prof. Jan Skov Pedersen (University of Aarhus). The IFT-analysis was made using the program "*Glatter*" by Prof. O. Glatter and J.S. Pedersen.

1.4.3 Fourier Transform Infrared Spectroscopy (FTIR)

Another method for the characterisation of the supramolecular structures of glycolipids is the FTIR spectroscopy (see for example Brandenburg and Seydel, 1998, and references cited herein). The state of order of the alkyl or acyl chains of glycolipids influences their molecular shape. It is assumed that the chains can have two main states, the gel (β-phase) and the liquid crystalline (α-phase) state. The transition between the α- and the β-phase takes place at a given phase transition temperature T_c. The value of this chain melting temperature T_c depends firstly on the number, length and degree of unsaturation of the acyl chains and secondly on the conformation, charge density, its distribution within the headgroup region and the nature and size of the saccharide moiety. IR spectroscopy allows the study of the motional freedom of the absorbing groups within the molecules and the changes due to temperature, pH, solutes, hydrogen and/or salt binding as well as interaction with agents. In many analyses of glycolipids, FTIR spectroscopy is applied complementary to other techniques, such as NMR and mass spectrometry, merely as a tool to monitor functional groups like sulfate, phosphate, etc. Phase transitions, which are often observed with changing water content, can be observed by FTIR-spectroscopy, but it is not possible to correlate this transition with its supramolecular structure. The phases have to be determined by other methods auch as small-angle x-ray scattering. Figure 1.7 shows an example of these orientation measurements. The lipid sample

in aqueous buffer is spread on the surface of the crystal and the totally reflected polarised light allows the analysis of thin multilayers. For the evaluation of the gel-to-liquid crystalline phase behaviour, the peak position of the symmetric stretching vibration of the methylene band ν_s (CH_2) approximately 2850 cm^{-1} is often chosen, which is a sensitive marker of lipid order (Brandenburg and Seydel, 1990).
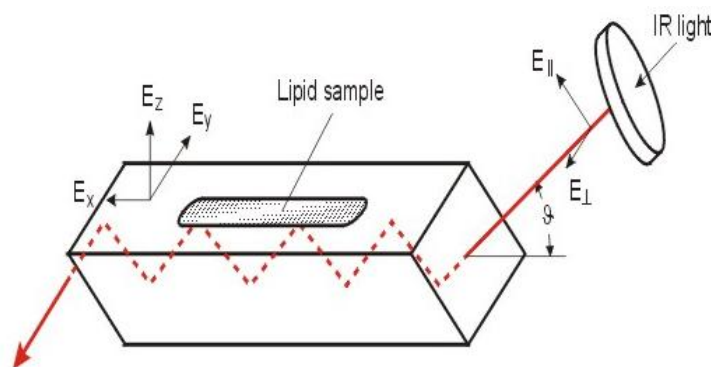

FIGURE 1.7: Orientation measurements (IR dichroism) via an attenuated total reflectance unit (Copyright by FZ Borstel, reprinted with permission).

1.5 Industrial Applications

An important technical feature of amphiphiles is the use as foaming agents or cleansers (Ananthapadmanabhan *et al.*, 2004; Holmberg *et al.*, 2003b) in products for domestic or household use.

Foams are defined as a dispersion of a gas in a liquid or solid. They are divided into two different classes: Non-stable or transient foams and stable foams (Holmberg *et al.*, 2003b). Whereas transient foams can only be characterised by the dynamic foam height, using the Bikerman method (Bikerman, 1953), stable foams are characterised by their foaming ability and foam stability. A pure liquid itself cannot form foams a surface active substance is required.

Cleansers are usually mixtures of amphiphilic surfactants and cosurfactants designed to uplift and solubilise dirt from skin. Beside this function, the formation of foam is desired and often regarded as an aspect of quality by the consumer. Therefore much attempt has been made by the industry to create formulations with a good cleansing and foaming ability (see for example Engels *et al.*, 1998). The foaming behaviour can be determined by using the industrial standard foam test according to Ross and Miles (DIN53902-2, 1977; Ross and Miles, 1941). A more simple method, working in a similar way, but requiring only small amounts of substance for each test, is shown in figure 1.8. By shaking a defined volume of a solution of

the amphiphile in water in a defined manner, the foaming ability can be determined. The foam stability is then defined as the volume of foam that remains 30 minutes after agitation of the cylinder. The experiment is repeated several times until the deviation stays constant.
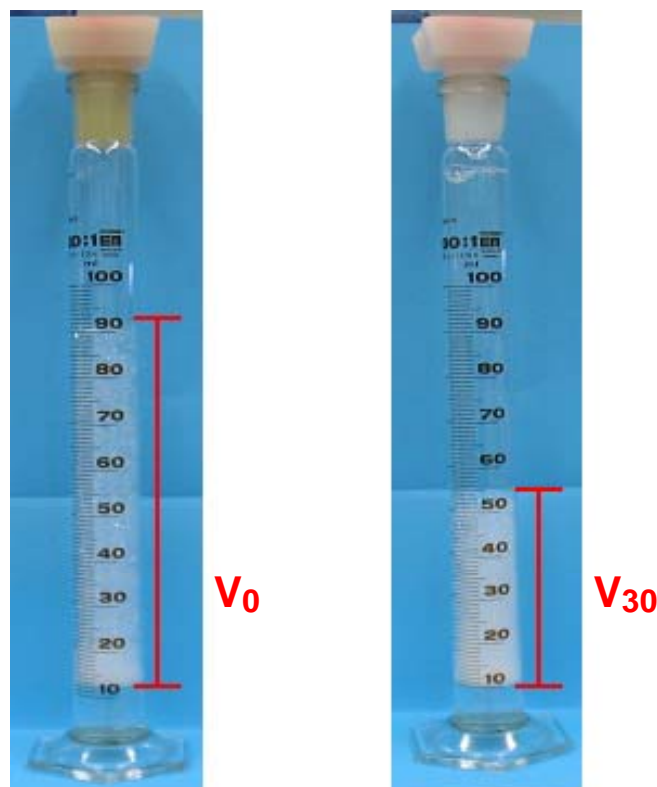
FIGURE 1.8: Foam test similar to the Ross-Miles test method. Left: Foaming ability (V_0 - Foam volume direct after agitation). Right: Foam stability (V_{30} - Foam volume after 30 min.).

Compounds showing a good foaming ability have to be tested for their use in consumer products. The foaming properties obtained from the Ross-Miles test often do not correlate with the formation of foam on skin or hair. This is tested by foaming a defined amount of hair with a defined amount of test solution. The formed foam is investigated by light microscopy immediately afterwards. Thus it is possible to get information about the structure of the foam and the size distribution of the air bubbles inside the foam.

The determination of the foam heights allows a first selection. Compounds showing a good foaming ability are then tested for their foaming ability on hair or skin. The foam structure is another criteria in the invetsigation of the amphiphiles. Spherical foams with a narrow size distribution of small air bubbles are preferred and are regarded as foams of a good quality for the use in a consumer product (J. Schreiber, personal communication).

Compounds showing a good foaming ability in the Ross-Miles test, but not on skin or hair, are also of interest; for example as ingredients in foaming bath or as laundry detergent.

1.6 Previous work

1.6.1 Synthesis

Several synthetic strategies have been employed to the synthesis of carbohydrate-based amphiphiles and glycolipids. Several structural types have gained interest as lipids for biological investigations, liquid crystals or surfactants and detergents.

Alkyl glycosides

Alkyl glycosides are commonly used as detergents and emulgators. Several approaches are available for the synthesis of these compounds. The synthesis of the pure α- and β-anomeres has been performed in different ways. Peracetylated glycosyl-halides have commonly been used for the synthesis of alkyl monosaccharides in four steps (for example Noller and Rockwell, 1938; Rosevar *et al.*, 1980; Ma *et al.*, 1994). Also the synthesis of short-chained alkyl maltosides has been performed in this way (Boyd *et al.*, 2000). The use of the α-halides only produce products with β-configuration (D-gluco and D-galacto series). The neighbouring group-effect of acetyl on C-2 of the sugar ring, forces the aglycon into the *trans* position (Paulsen, 1982). The synthesis of an α-anomer is slightly more complicated as it requires a thermodynamically less stable β-halide and a neighbouring group at C-2 that does not participate in the substitution reaction.

It is a more convenient method to use a peracetylated saccharide as glycosyl donor. Under catalysis of a Lewis acid the acetoxy group at C-1 is substituted by the aglycon (Banoub and Bundle, 1979). The β-anomer can be isolated under kinetic control, whereas the α-anomer is prepared under thermodynamic control (Böcker and Thiem, 1989). The use of boron trifluoride etherate for example was found to give the desired β-anomer after a reaction time of 5 hours (Vill *et al.*, 2000), also the degree of anomerisation was found to be very low. The synthesis of α-anomers using tin(IV)chloride or ferric(III)chloride as Lewis acid has been described for the synthesis of several alkyl α-mono- and disaccharides (Vill *et al.*, 2000; Minden *et al.*, 2000; Chatterjee and Nuhn, 1998).

Derivatives of alkyl glycosides

The synthesis of glycolipids with a spacer between the carbohydrate head and the lipophilic tail has only been described sparingly, for these compounds have no natural structural analogues. Most similar to natural compounds is the building-block sugar-ethanolamine-fatty acid, as the *N*-acyl ethanolamine spacer unit is similar to the ceramide subunit. Therefore Miura *et al.* (1996) synthesised a few lactose-based compounds of this structural type with

four different fatty acids. However, the synthetic route provided the compounds only in very poor yields and furthermore the starting materials are expensive.

A different aim is the use of ethyleneglycol spacer to increase the distance between the carbohydrate headgroup and surface in vesicles (Nuhn *et al.*, 1994, Bendas *et al.*, 1996). Falk *et al.* (1995) synthesised a series of n-alkyl-ethylenglycol α-monosaccharides using FeCl$_3$ as Lewis acid in excellent yields, they also report that the β-anomeres were obtained in moderate yields. The synthesis of (2-dodecyloxy-ethyl) β-D-lactopyranosides as an intermediate in the synthesis of a sulfated lipid using trimethylsilyl trifluoromethansulfonate has also been described (Yoshida *et al.*, 1995), but to date this is the only example for long-chain n-alkyl ethylenglycol lipids with disaccharide carbohydrate headgroups.

Another class of alkyl glycoside derivatives are the *N*-acyl glycosylamines where the hydroxy group at C-1 of the sugar ring is replaced by an amino group. Several synthetic pathways have been used for the synthesis of these surfactants. One way uses the direct reaction of the freshly prepared glycosylamine with the fatty acid chloride in methanol (Lubineau *et al.*, 1995). The great disadvantage is that most of the glycosylamines derived from disaccharides are not soluble in the solvents needed for the reaction. Therefore a different pathway uses peracetylated glycosylamines. The method described by Masuda and Shimizu (1998) starts from the peracetylated α-glycosyl bromide. The bromide is substituted by an azido-group that is converted into the glycosyl amine.

Glyco glycero lipids

Glyco glycero lipids and especially glycosyl 1,3-dialkyl, 1,2-diacyl glycerols and diglycosyl 2-acyl glycerols have created much interest due to their possible role in biological processes (see for example Ishizuka and Yamakawa, 1985; Curatolo, 1987). Therefore different synthetic strategies have been employed for the synthesis of these compounds. A simple and convenient method for the synthesis of glycosyl 1,3-dialkyl glycerols has been described by Minamikawa *et al.* (1994). This synthetic route starts with the peracetylated sugar, which is deprotected on C-1. Next the α-trichloracetimidate is prepared which is then reacted with the dialkyl glycerol under Lewis acid catalysis. After deprotection of the sugar the final compounds are obtained in good to excellent yields.

The synthesis of glycosyl diacyl glycerols is sligthly more complicated and requires different synthetic strategies depending on the type of fatty acid chain. Mannock *et al.* (1987, 1990) described a procedure for the synthesis of glycosyl diacyl glycerols with saturated fatty acid chains, which gives the final products in a few steps. Nevertheless the sugar headgroup is deprotected in the last step using hydrazine hydrate. Hence this method is not suitable for the preparation of lipids with unsaturated acyl chains as the double bond will be destroyed during the deprotection step. Nagatsu *et al.* (1994) and Minden *et al.* (2002b) used an alternative

method introducing intermediate changes to the protective group which can be easily removed afterwards under reductive conditions.

For the synthesis of inverted glyco glycero lipids with one hydrophobic chain and two sugar heads only a few examples can be found (Minden *et al.*, 2002b; Schmidt and Jankowski, 1996).

1.6.2 Structure-property relationship

The influence of the molecular structure of amphiphiles on the supramolecular self-assembly can provide solutions to possible functions (see for example Hato, 2001; Ellens *et al.*, 1989; Lindblom and Rilfors, 1989; Curatolo, 1987; Tanaka *et al.*, 2004; Brandenburg and Seydel, 1990; Tschierske, 2002). Despite the importance of this structure-property relationship, only a little is known about it to date. The main problem arises from the fact that the molecular structure of glycosides is often over-simplified. The molecular structure of disaccharide or higher alkyl glycosides is understood as only a combination of two or more sugar units regardless of the real molecular structure. Möller *et al.* for example state *"...alkyl glucosides (C_nG_m) with different hydrocarbon chain length and different numbers of glucose units."* (Möller *et al.*, 1998) and thus consider the type of sugar linkage as unimportant. It can also be found that different disaccharides (e.g. lactose and Maltose) are regarded to be similar, despite the fact that the molecular structure is totally different (Södermann and Johansson, 2000).

1.6.3 Micelles formed by glycolipids and surfactants

Numerous publications deal with the investigation of micelles formed by sugar-based surfactants (see for example Holmberg, 2001; Stubenrauch, 2001; Hoffmann and Platz, 2001, and references cited herein; Tschierske, 1996, and references cited herein). The subjects of these investigations are very different although the number of compounds investigated is small. Commercially available compounds have mainly been investigated, and there are only a few examples of investigations dealing with synthetic or natural amphiphiles. The results obtained for similar compounds are often different. This might be explained by the different techniques used for the characterisation of the micellar phase region. Whereas the use of small-angle scattering techniques dominates, other methods e.g. light scattering or NMR-self-diffusion measurements are also used.

Monosaccharide Headgroups

Octyl-β-D-glucopyranoside (**Glc-β-C8**). **Glc-β-C8** has long been known as a good foamer and is used as surfactant and detergent in many applications (see for example Shinoda *et al.*, 1959; Shinoda *et al.*, 1996, and references cited herein). It is thus not surprising that the micellar structure of this compound has also been investigated. However, the aggregation behaviour of **Glc-β-C8** in dilute solution is still not sufficiently explained. Focher *et al.* (1989) found a hydrodynamic radius of 28 Å for **Glc-β-C8** which cannot be correlated with a spherical micellar shape. Directly above the *CMC* the results from NMR self-diffusion experiments point on a non-spherical shape of the micelles as reported by Nilsson *et al.* (1998). The study of the micellar phase region by SAXS and SANS gives results which can be described by a cylindrical core-shell model (Zhang *et al.*, 1999). Also the micellar phase region extends from the *CMC* up to 60 wt% of lipid (Nilsson *et al.*, 1996) without a structural change (He *et al.*, 2000).

The micellar shape and length as well as the phase diagram indicate a dramatic change with increasing alkyl chain length from seven to ten carbon atoms. Zhang *et al.* (1999) compared the micelle length of heptyl-, octyl and nonyl-β-D-glucoside and found that at the same molar concentration the size of micelles increases from 16 Å for heptyl-β-D-glucopyranoside (**Glc-β-C7**) to 45.6 Å for **Glc-β-C8** and finally to 1600 Å for nonyl-β-D-glucopyranoside (**Glc-β-C9**). Additionally Nilsson *et al.* (1998) postulated a rod-like shape for the micelles formed by **Glc-β-C9** and decyl-β-D-glucopyranoside (**Glc-β-C10**).

Interestingly, **Glc-β-C10**, displays two micellar phases at concentrations between 0.1 and 17 wt% of surfactant (Nilsson *et al.*, 1998). The aggregation number of the dilute micellar phase lies in the range of 200 and 400 molecules per micelle, whereas in concentrated micellar phases aggregation numbers of >600 can be found, possibly belonging to large wormlike aggregates or branched micelles (Nilsson *et al.*, 1998).

The phase diagram of **Glc-β-C9** was found to be similar to that of **Glc-β-C8** (Nilsson *et al.*, 1998). A broad micellar phase region, which, upon increasing concentration, is sequentially followed by a hexagonal, bicontinuous cubic, and a lamellar phase change. Also for **Glc-β-C9** different results for the micellar structure are reported. Whereas one group postulates the formation of spherical micelles (Majhi and Blume, 2001) at concentrations near the *CMC*, Nilsson *et al.* suggest that nonspherical aggregates are formed at concentrations immediately above the *CMC* (Nilsson *et al.*, 1998). At higher concentration **Glc-β-C9** forms stiff, elongated structures, which grow in one dimension with increasing concentration (Ericsson *et al.*, 2004). The structure could be described more specificly by a model for thread-like micelles.

Disaccharide Headgroups

Octyl-, dodecyl-, tridecyl and tetradecyl β-D-maltoside have been extensively investigated due to their good solubility in water, e.g. the Krafft-temperature is below 20 °C.

For example the micellar structure of octyl-β-D-maltoside was determined to be spherical and does not change size or shape throughout the whole concentration range of the micellar phase (He *et al.*, 2002; Aoudia and Zana, 1998). The micellar size and shape at different temperatures was reported to be similar too. For the micellar shape of dodecyl-β-D-maltoside (**Mal-β-C12**) different results can be found in the literature. Focher *et al.* (1989) estimated a spherical shape by using a combination of dynamic light scattering and NMR-self diffusion experiments. Later on a micellar shape was determined for **Mal-β-C12** by small-angle scattering methods, but while one publication calculated an ellipticity of e = 0.75 (Cecutti *et al.*, 1991), another publication postulated an oblate ellipsoid with e = 0.59 (Dupuy *et al.*, 1997). In addition to these differences all three authors found that the micellar shape does not change with increasing concentration throughout the whole micellar phase range and that with an increase of the alkyl chain length, a change of the micellar shape occurs at lower concentration. As reported by Heerklotz *et al.* (2004), the formation of elliptical micelles was observed for tridecyl-β-D-maltoside (**Mal-β-C13**) at low and medium concentration. At higher concentrations a sphere-to-rod phase transition takes place. For tetradecyl-β-D-maltoside (**Mal-β-C14**) the transition already occurs at low concentrations (~ 10 mM). In the concentration range from 10 to 300 mM the formation of rod-like micelles can be observed before a liquid crystalline phase is formed. According to Ericsson *et al.* (2005) **Mal-β-C14** forms polymer-like micelles at medium concentrations that grow with increasing concentration. These micelles show length scales of 1700 Å (1 wt% lipid) at 35 °C, which increase up to 3800 Å for a concentration of 5 wt% of lipid. At higher temperatures the length of micelles even increases.

Beside normal alkyl glycosides synthetic surfactants containing amine or amide groups have also been investigated for their ability to form micelles in aqueous solution. Dupuy *et al.* (1996, 1998) and Auvray *et al.* (2001) investigated several short chained (*N*-alkylamino)-lactitols with alkyl chains of 8 to 12 carbon atoms, (*N*-dodecyl)-lactobionamide and (*N*-acetyl *N*-dodecyl)-lactosylamine. The open-ring lactitols form elliptical micelles with an axis ratio of ~ 0.7 from C8 to C12 alkyl chains length. The total radius and the aggregation increase linearly with increasing chain length. The open-ring lactobionamide shows a similar micellar structure as the corresponding lactitol. Only the (*N*-acetyl *N*-dodecyl)-lactosylamine forms spherical micelles with a smaller aggregation number than the other compounds. A dramatic change of the aggregate structure occurs when the alkyl chain length is increased. Bhattacharya and Acharya (2000) found that the (*N*-hexadecyl)-lactitol as well as the (*N*-hexadecyl)-maltitol no longer form micelles but vesicles with diameters between 500 and

800 Å. Conversely (*N*-hexadecyl) lactosylamine and maltosylamine still form micelles but with a radius of more than 80 Å, which is more than twice the radius of the (*N*-dodecyl)-lactosylamine, indicating that the molecular structure becomes unfavourable for the formation of micelles with increasing chain length.

Anomeric linkage $\alpha \leftrightarrow \beta$

The influence of the anomeric linkage of the alkyl chain to the sugar headgroup has been investigated for octyl glucoside (**Glc-α-C8** and **Glc-β-C8**) and for dodecyl maltoside (**Mal-α-C12** and **Mal-β-C12**). Focher *et al.* (1989) were the first to report that the type of anomeric linkage of the alkyl chain changes the phase behaviour in dilute solution completely. Whereas **Glc-β-C8** was found to form small micelles, the α-anomer does not form micelles but large non-spherical structures instead. A less dramatic difference in the aggregate formation was found by Dupuy *et al.* (1997) for the two anomers of dodecyl maltoside. As reported before, **Mal-β-C12** was found to form elliptical micelles with a total radius of 34.4 Å and an ellipticity of ε =0.59, while the α-anomer **Mal-α-C12** forms spherical micelles of smaller size with an average radius of 24 Å. The main difference can be seen in the aggregation number *N*. In the case of **Mal-α-C12**, where a micelle is formed by 75 molecules, micelles of the β-anomer require nearly twice as many molecules (*N* = 132).

Branched chains

Branched alkyl chains are commonly used to enhance solubility in water by lowering the Krafft-temperature. Detailed studies of the higher ordered phases of lipids bearing methylated, ethylated or higher branched chains are known (see for example Hato, 2001, and references cited herein) but studies of the micellar phases are scarce. Hato *et al.* (2002) observed a micellar phase for (3,7,11,15-tetramethylhexadecyl)-β-D-maltoside, but no closer characterisation was given. The monosaccharides with the same type of alkyl chain did not form a micellar phase. A similar result was found for (2,4,6,8-tetramethyldecyl)-β-D-glucoside and galactoside as well as for (3,7,11-trimethyldodecyl)-β-D-glucoside (Milkereit *et al.*, 2004). The molecular shape of the compounds only allows the formation of a lamellar phase, but no other phases are formed with increased water content. Single branched compounds on the other hand retain the ability of micelle formation. Nilsson *et al.* (1997) found micellar phases for four different glucosides with 2-ethylhexyl, isooctyl, 2-propylheptyl and isodecyl alkyl chains.

Mixed micelles

Mixed micelles of two or more different amphiphiles or surfactants are of interest, because new properties often arise from the addition of a second surfactant (Holmberg *et al.*, 2003c).

Examples of mixed micellar systems have been described (Hines, 2001 and references cited herein). Different effects can be observed by mixing different surfactants: change of the shape of micelles, aggregation number and length scale. These effects can be antagonistic (destabilisation) or protagonistic (stabilisation). For example the addition of sodium dodecyl sulfate (**SDS**) to micelles of the EO-surfactant $C_{12}E_6$ reduces the aggregation number owing to a growth of the electrostatic interaction of the headgroups (Garamus, 2003). The addition of **SDS** to micelles of the alkyl glycoside **Mal-β-C12** does not change the mean aggregation number of the elliptical micelles: the growth of the electrostatic interaction leads only to an increase of the ellipticity of the micelles with increasing molar fraction of **SDS** (Bucci *et al.*, 1991). A positive effect on the micellar growth has been reported by Lainez *et al.* (2004). The addition of the cationic surfactant tetradecyltrimethylammonium bromide to micelles of **Glc-β-C8** increases the aggregation number as the molar fraction of cationic surfactant increases. Alkyl poly glucoside (APG) itself can be regarded as a mixed micelle system. It is a complex mixture of different α- and β-glucosides with different alkyl chain lengths and a varying degree of polymerisation of the Glucose units. These systems are difficult to analyse due to the inhomogenous distribution of the alkyl glucosides. Nevertheless it is reported that APG derived from alcohol blends of short chain length ($C_{8/10}G_{1.5}$-APG) form spherical micelles whereas the medium chain derivatives ($C_{12/14}G_{1.5}$-APG) form rod-like micelles (Platz *et al.*, 1995). Furthermore effects can be induced by the addition of hexanol to micelles formed by the short-chain $C_{8/10}G_{1.5}$-APG (Stradner *et al.*, 2000). The globular micelles of the pure APG start to grow to rod-like micelles at very low hexanol content at slightly higher hexanol concentration the formation of giant polymer- (or worm)-like micelles is observed. On the other hand the addition of small amounts of n-butanol to micellar solutions of the pure amhiphil **Glc-β-C8** completely changes the shape of micelles from a rod-like geometry to anisotropic micelles (Möller *et al.*, 1998).

Other amphiphile or lipid structures

Formation of micelles can also be observed for more complex structures. Gulik *et al.* (1995) found that even the complex gangliosides GM1 and acetyl GM1 form spherical micelles in dilute aqueous solution. Interestingly these compounds form a discontinous cubic phase with increased concentration, which is normally very difficult to characterise. Non-typical amphiphiles are able to form micelles as well. For example the formation of spherical micelles was observed for a bolaamphiphile with two *N*-aza-18-crown-6 headgroups and a C16-alkyl chain (Caponetti *et al.*, 2004).

From all these results it becomes obvious, that sugar-based amphiphiles already show complex aggregation behaviour in the micellar solution. The properties are difficult to generalize, especially for disaccharide compounds, due to a limited amount of data. It is also

difficult to apply results obtained for typical surfactants, e.g. EO-based or ionic to sugar-surfactants, due to the differences in the polar headgroup region.

1.7 Aims

In the preceding introduction a general overview was given about the aggregation of amphiphilic compounds, aggregation models, the main characterisation methods and the current state of scientific research. In the subsequent chapters of this thesis the synthesis of different types of amphiphilic compounds is described, with structural variations of the carbohydrate headgroup and the lipophilic tail. Furthermore, the characterisation of the lyotropic aggregates and phases, as well as technical features of the synthesised compounds, are presented. Finally, the results are combined to derive structure-property relationship with three main aims:

I. A general overview for the micelle formation of carbohydrate-based amphiphiles with respect to their chemical structures.

II. The influence of the molecular structure on the formation of higher-ordered phases.

III. A characterisation of the physicochemical properties of these compounds in their pure state and in solution.

The main individual tasks can be subdivided as follows:

- Synthesis of new carbohydrate-based amphiphiles and lipids   *(Chapter 2, 4, 6, 9, 10 and Appendix A)*

- Investigation of the micellar structure of amphiphiles   *(Chapter 2, 3, 4, 5, 8, 9 and Appendix B)*

- Determination of the higher-ordered phases of glycolipids and amphiphiles   *(Chapter 7)*

- Influence of the structure of lipophilic tails from different natural sources   *(Chapter 4 and 7)*

- Investigation of the liquid crystalline properties *(**Chapter 2, 4, 7, 9 and 10**)*

- Influence of cosurfactants on the micellar structure *(**Chapter 3**)*

- Other physicochemical properties, e.g. *CMC*, surface tension, solubility and foaming *(**Chapter 3, 4, 5, 9, 11 and Appendix B**)*

- More general models for the relationship between the molecular structures of carbohydrate-based amphiphiles and the micellar form and the formation of foams *(**Chapter 11**)*

1.7 References

ANANTHAPADMANABHAN, K.P., MORRE, D.J., SUBRAMANYAN, K., MISRA, M., MEYER, F., Cleansing without compromise: the impact of cleansers on the skin barrier and the technology of mild cleansing, *Dermatol. Ther.*, 17, **2004**, 16-25.

AOUDIA, M., ZANA, R., Aggregation behaviour of sugar surfactants in aqueous solutions: Effect of temperature and the addition of nonionic polymers, *J. Colloid Interface Sci.*, 206, **1998**, 158-167.

AUVRAY, X., PEPITAS, C., DUPUY, C., LOUVET, S., ANTHORE, R., RICO-LATTES, I., LATTES, A., Small-angle x-ray diffraction study on the thermotropic and lyotropic phases of five cyclic and acyclic disaccharides: Influence of the linkage between the hydrophilic and hydrophobic moieties, *Eur. Phys. J. E*, 4, **2001**, 489-504.

BANOUB, J., BUNDLE, D.R., Stannic tetrachloride catalysed glycosylation of 8-ethoxycarbonyloctanol by cellobiose, lactose and maltose octaacetates: synthesis of α- and β-glycosidic linkages, *Can. J. Chem.*, 57, **1979**, 2085-2090.

BENDAS, G., WILHELM, F., RICHTER, W., NUHN, P., Synthetic glycolipids as membrane-bound cryoprotectants in the freeze-drying process of liposomes, *Eur. J. Pharm. Sci.*, 4, **1996**, 211-222.

BHATTACHARYA, S., ACHARYA, S.N.G., Vesicle and tubular microstructure formation from synthetic sugar-linked amphiphiles. Evidence of vesicle formation from single-chain amphiphiles bearing a disaccharide headgroup, *Langmuir*, 16, **2000**, 87-97.

BIKERMAN, J.J., *Foams: Theory and Industrial Applications*, Reinhold Publishing, New York, **1953**, 189-242.

BLUNK, D., PRAEFKE, K., VILL, V., Amphotropic liquid crystals. In: DEMUS, D., GOODBY, J., GRAY, G.W., SPIEß, H.-W., VILL, V. (Eds.), *Handbook of Liquid Crystals*, Vol. 3, Wiley-VCH, Weinheim, **1998**, pp. 305-340.

BÖCKER, T., THIEM, J., Synthese und Eigenschaften von Kohlenhydratetensiden, *Tenside, Surf. Det.*, 26, **1989**, 318-324.

BOYD, B.J., DRUMMOND, C.J., KRODKIEWSKA, I., GRIESER, F., How chain length, headgroup polymerization, and anomeric cinfiguration govern the thermotropic and lyotropic liquid crystalline phae behaviour and the air-interfacial adsorption of glucose-based surfactants, *Langmuir*, 16, **2000**, 7359-7367.

BRANDENBURG, K., SEYDEL, U., Infrared spectroscopy of glycolipids, *Chem. Phys. Lipids*, 96, **1998**, 23-40.

BRANDENBURG, K., SEYDEL, U., Investigation into the fluidity of lypopolysaccharide and free lipid A membrane systems by Fourier-transform infrared spectroscopy and differential scanning calorimetry, *Eur. J. Biochem.*, 191, **1990**, 229-236.

BUCCI, S., FAGOTTI, C., DEGIORGIO, V., PIAZZA, R., Small-angle neutron-scattering study of ionic-nonionic mixed micelles, *Langmuir*, 7, **1991**, 824-826.

CAPONETTI, E., CHILLURA-MARTINO, D., LA MESA, C., MUZZALUPO, R., PEDONE, L., Structural and transport properties of bola C-16 micelles in water and aqueous electrolyte solutions, *J. Phys. Chem. B*, 108, **2004**, 1214-1223.

CECUTTI, C., FOCHER, B., PERLY, B., ZEMB, T., Glycolipid self-assembly: micellar structure, *Langmuir*, 7, **1991**, 2580-2585.

CHATTERJEE, S.K., NUHN, P., Stereoselective α-glycosidation using FeCl₃ as a Lewis acid catalyst, *Chem. Commun.*, **1998**, 1729-1730.

CURATOLO, W., The physical properties of glycolipdis, *Biochim. Biophys. Acta*, 906, **1987**, 137-160.

CURATOLO, W., The physical properties of glycolipds, *Biochim. Biophys. Acta*, 906, **1987**, 111-136.

DIN53902-2: Prüfung von Tensiden; Bestimmung des Schäumungsvermögens, Modifiziertes Ross-Miles-Verfahren, **1977**.

DUPUY, C., AUVRAY, X., PEPITAS, C., ANTHORE, R., COSTES, F., RICO-LATTES, I., LATTES, A., Small-angle x-ray and neutron scattering study of the micellization of (*N*-alkylamino)-1-deoxylactitols in water, *Langmuir*, 12, **1996**, 3162-3172.

DUPUY, C., AUVRAY, X., PEPITAS, C., RICO-LATTES, I., LATTES, A., Anomeric effects on the structure of micelles of alkyl maltosides in water, *Langmuir*, 13, **1997**, 3965-3967.

DUPUY, C., AUVRAY, X., PEPITAS, C., RICO-LATTES, I., LATTES, A., Influence of structure of polar head on the micellization of lactose-based surfactants. Small-Angle x-ray and neutron scattering study, *Langmuir*, 14, **1998**, 91-98.

ELLENS, H., SIEGEL, D.P., ALFORD, D., YEAGLE, P.L., BONI, L., LIS, L.J., QUINN, P.J., BENTZ, J., Membrane fusion and inverted phases, *Biochemistry*, 28, **1989**, 3692-3703.

ENGELS, T., v.RYBINSKI, W., SCHMIEDEL, P., Structure and dynamics of surfactant-based foams, *Progr. Colloid Polym. Sci.*, 111, **1998**, 117-128.

ERICSSON, C.A., SÖDERMAN, O., GARAMUS, V.M., BERGSTRÖM, M., ULVENLUND, S., Effects of temperature, salt and deuterium oxide on the self-aggregation of alkylglycosides in dilute solution. 1. *n*-Nonyl-β-D-glucoside, *Langmuir*, 20, **2004**, 1401-1408.

ERICSSON, C.A., SÖDERMAN, O., GARAMUS, V.M., BERGSTRÖM, M., ULVENLUND, S., Effects of temperature, salt, and deuterium oxide on the self-aggregation of alkyl glycosides in dilute solution. 2. *n*-Tetradecyl-β-D-maltoside, *Langmuir*, 21, **2005**, 1507-1515.

FAIRHURST, C.E., FULLER, S., GRAY, J., HOLMES, M.C, TIDDY, G.J., Lyotropic surfactant liquid crystals. In: DEMUS, D., GOODBY, J., GRAY, G.W., SPIEß, H.-W., VILL, V. (Eds.), *Handbook of Liquid Crystals*, Vol. 3, Wiley-VCH, Weinheim, **1998**, 341-392.

FALK, W., CHATTERJEE, S., RATTAY, B., NUHN, P., BENECKE, P., ORTWEIN, J., Synthesis of glycolipids as membrane bound stabilizing carbohydrates, *Liebigs Ann.*, 9, **1995**, 1673-1679.

FOCHER, B., SAVELLI, G., TORRI, G., VECCHIO, G., MCKENZIE, D.C., NICOLI, D.F., BUNTON, C.A., Micelles of 1-alkyl glucoside and maltoside: Anomeric effects on structure and induced chirality, *Chem. Phys. Lett.*, 158, **1989**, 491-494.

GARAMUS, V.M., Formation of mixed micelles in salt-free aqueous solutions of sodium dodecyl sulfate and $C_{12}E_6$, *Langmuir*, 19, **2003**, 7214-7218.

GIBBS, J.W., On the equilibrium of heterogeneous substances, *Trans. Connect. Acad.*, 3, **1976**, 375-381.

GLATTER, O., A new method for the evaluation of small-angle scattering data, *J. Appl. Crystalogr.*, 10, **1977**, 415-421.

GULIK, A., DELACROIX, H., KIRSCHNER, G., LUZZATI, V., Polymorphism of ganglioside-water systems: a new class of micellar cubic phases. Freeze-fracture election microscopy and x-ray scattering studies, *J. Phys. II*, 5, **1995**, 445-464.

HATO, M., MINAMIKAWA, H., SALKAR, R.A., MATSUTANI, S., Alkylglycosides with an isoprenoid-type hydrophobic chain can afford greater control of aqueous phase structures at low temperatures, *Langmuir*, 18, **2002**, 3425-3429.

HATO, M., Synthetic glycolipid / water systems, *Curr. Opin. Colloid Interface Sci.*, 6, **2001**, 268-276.

HE, L.-Z., GARAMUS, V.M., FUNARI, S.S., MALFOIS, M., WILLUMEIT, R., NIEMEYER, B., Comparison of small-angle scattering methods for the structural analysis of octyl-β-D-maltopyranoside micelles, *J. Phys. Chem. B*, 106, **2002**, 7596-7604.

HE, L.-Z., GARAMUS, V.M., NIEMEYER, B., HELMHOLZ, H., WILLUMEIT, R., Determination of micelle structure of octyl-β-glucoside in aqueous solution by small angle neutron scattering and geometric analysis, *J. Mol. Liq.*, 89, **2000**, 239-249.

HEERKLOTZ, H., TSAMALOUKAS, A., KITA-TOKARCZYK, K., STRUNZ, P., GUTBERLET, T., Structural, volumetric and thermodynamic characterization of a micellar sphere-to-rod transition, *J. Am. Chem. Soc.*, 126, **2004**, 16544-16552.

HIERNEZ, P.C., *Principles of Colloid and Surface Chemistry*, Marcel Dekker, New York, **1977**.

HINES, J.D., Theoretical aspects of micellisation in surfactant mixtures, *Curr. Opin. Colloid Interface Sci.*, 6, **2001**, 350-356.

HOFFMANN, B., PLATZ, G., Phase and aggregation behaviour of alkyl glycosides, *Curr. Opin. Colloid Interface Sci.*, 6, **2001**, 171-177.

HOLMBERG, K., JÖNSSON, B., KRONBERG, B., LINDMAN, B., *Surfactants and polymers in aqueous solution*, 2nd ed., Wiley & Sons, Chichester, **2003a**, 32-36.

HOLMBERG, K., JÖNSSON, B., KRONBERG, B., LINDMAN, B., *Surfactants and Polymers in Aqueous Solution*, 2nd ed., John Wiley & Sons, Chichester, **2003b**, 39-66

HOLMBERG, K., JÖNSSON, B., KRONBERG, B., LINDMAN, B., *Surfactants and Polymers in Aqueous Solution*, 2nd ed., John Wiley & Sons, Chichester, **2003c**, 119-138.

HOLMBERG, K., Natural Surfactants, *Curr. Opin. Colloid Interface Sci.*, 6, **2001**, 148-159.

ISHIZUKA, I., YAMAKAWA, T., Glycolipids, In: WIEGANDT, H. (Ed.), *New Comprehensive Biochemistry*, Vol. 10, Elsevier, **1985**, 101-197.

ISRAELACHVILI, J.N., *Intermolecular and Surface Forces*, 2nd ed., Academic Press, London, **1992a**, 366-394.

ISRAELACHVILI, J.N., *Intermolecular and Surface Forces*, 2nd ed., Academic Press, London, **1992b**, p. 368.

ISREALACHVILI, J.N., MARCELJA, S., HORN, R.G., Physical principles of membrane organisation, *Quart. Rev. Biophys.*, 13, **1980**, 121-200.

JÖNNSON, B., WENNERSTRÖM, H., Thermodynamics of ionic amphiphile-water systems, *J. Coll. Interf. Sci.*, 80, **1981**, 482-496.

KOYNOVA, R., CAFFREY, M., Phases and phase transitions of the glycoglycerolipids, *Chem. Phys. Lipids*, 69, **1994**, 181-207.

LAINEZ, A., DEL BURGO, P., JUNQUERA, E., AICART, E., Mixed micelles formed by *n*-octyl-β-D-glucopyranoside and tetradecylammonium bromide in aqueous media, *Langmuir*, 20, **2004**, 5745-5752.

LAUGHLIN, R.G., *The aqueous phase behaviour of surfactants*, Academic press, London, **1994**.

LAUGHLIN, R.G., The role of swelling methods in surfactant phase science: past, present, and future, *Adv. Colloid Interface Sci.*, 41, **1992**, 57-79.

LINDBLOM, G., RILFORS, L., Cubic phases and isotropic structures formed by membrane lipids - possible biological relevance, *Biochim. Biophys. Acta*, 988, **1989**, 221-256.

LUBINEAU, A., AUGÉ, J., DROUILLAT, B., Improved synthesis fo glycosylamines and a straightforward preparation of *N*-acylglycosylamines as carbohydrate-based detergents, *Carbohydr. Res.*, 266, **1995**, 211-219.

MA, Y.-D., TAKADA, A., SUGIURA, M., FUKUDA, T., MIYAMOTO, T., WATANABE, J., Thermotropic liquid crystals based on oligosaccharides. n-alkyl 1-*O*-β-D-cellobiosides, *Bull. Chem. Soc. Jpn.*, 67, **1994**, 346-351.

MAJHI, P. R.; BLUME, A., Thermodynamic characterization of temperature-induced micellization and demicellization of detergents studied by differential scanning calorimetry, *Langmuir*, **2001**, *17*, 3844-3851.

MANNOCK, D.A., LEWIS, R.N.A.H., MCELHANEY, R.N., An improved procedure of the preparation of 1,2-di-*O*-acyl-3-*O*-(β-D-glucopyranosyl)-sn-glycerols, *Chem. Phys. Lipids*, 43, **1987**, 113-137.

MANNOCK, D.A., LEWIS, R.N.A.H., MCELHANEY, R.N., The chemical synthesis and physical characterisation of 1,2-di-*O*-acyl-3-*O*-(β-D-glucopyranosyl)-sn-glycerols, an important class of membrane glycolipids, *Chem. Phys. Lipids*, 55, **1990**, 157-179.

MANNOCK, D.A., MCELHANEY, R.N., Thermotropic and lyotropic phase properties of glycolipid diasteromers: role of headgroup and interfacial interactions in determinig phase behaviour, *Curr. Opin. Colloid Interface Sci.*, 8, **2004**, 426-447.

MASUDA, M., SHIMIZU, T., Synthesis of novel a,w-type 1-glucosamide and 1-galactosamide bolaamphiphiles, *J. Carbohydr. Chem.*, 17, **1998**, 405-416.

MILKEREIT, G., MORR, M., THIEM, J., VILL, V., Thermotropic and lyotropic properties of long chain alkyl glycopyranosides. Part III: pH-sensitive headgroups, *Chem. Phys. Lipids*, 127, **2004**, 47-63.

MINAMIKAWA, H., MURAKAMI, T., HATO, M., Synthesis of 1,3-di-*O*-alkyl-2-*O*-(β-D-glycosyl)glycerols bearing oligosaccharides as hydrophilic groups, *Chem. Phys. Lipids*, 72, **1994**, 111-118.

MINDEN, V.H.M., BRANDENBURG, K., SEYDEL, U., KOCH, M.H.J., GARAMUS, V.M., WILLUMEIT, R., VILL, V., Thermotropic and lyotropic properties of long chain alkyl glycopyranosides. Part II: Disaccharide headgroups, *Chem. Phys. Lipids*, 106, **2000**, 157-179.

MINDEN, V.H.M., MILKEREIT, G., VILL, V., Effects of carbohydrate headgroups on the stability of induced cubic phases in binary mixtures of glycolipids, *Chem. Phys. Lipids*, 120, **2002a**, 45-56.

MINDEN, V.H.M., MORR, M., MILKEREIT, G., HEINZ, E., VILL, V., Synthesis and mesogenic properties of glycosyl diacylglycerols, *Chem. Phys. Lipids*, , 114, **2002b**, 55-80.

MIURA, Y., ARAUI, T., YAMAGATA, T., Synthesis of amphiphilic lactosides that possess a lactosylceramide-mimicking *N*-acyl structure: Alternative universal substrates for *endo*-type glycosylceramidases, *Carbohydr. Res.*, 289, **1996**, 193-199.

MÖLLER, A., LANG, P., FINDENEGG, G.H., KEIDERLING, U., Location of butanol in mixed micelles with alkyl glucosides studied by SANS, *J. Phys.Chem. B*, 102, **1998**, 8958-8964.

NAGATSU, A., WATANABE, M., IKEMOTO, K., HASHIMOTO, M., MURAKAMI, N., SAKAKIBARA, J., TOKUDA, H., NISHINO, H., IWASHIMA, A., YAZAWA, K., Synthesis and structure-anti-tumor-promoting activity relationship of monogalactosyl diacylglycerols, *Bioorg. Med. Chem. Lett.*, 4, **1994**, 1619-1622.

NILSSON, F., SÖDERMAN O., JOHANSSON, I., Four different C_8G_1-alkylglucosides. Anomeric effects and the influence of straight vs branched hydrocarbon chains, *J. Colloid Interface Sci.*, 203, **1998**, 131-139.

NILSSON, F., SÖDERMAN, O., HANSSON, P., JOHANSSON, I., Physical-chemical properties of C_9G_1 and $C_{10}G_1$ β-Alkyl glycosides. Phase diagrams and aggregate size/structure, *Langmuir*, 14, **1998**, 4050-4058.

NILSSON, F., SÖDERMAN, O., JOHANSSON, I., Physical-chemical properties of some branched alkyl glucosides, *Langmuir*, 13, **1997**, 3349-3354.

NILSSON, F., SÖDERMAN, O., JOHANSSON, I., Physical-chemical properties of the *n*-octyl-β-D-glucoside/water system. A phase diagram, self-diffusion NMR, and SAXS study, *Langmuir*, 12, **1996**, 902-908.

NOLLER, C.R., ROCKWELL, W.C., The preparation of some higher alkylglucosides, *J. Am. Chem. Soc.*, 60, **1938**, 2076-2077.

NUHN, P., PFAFF, T., BENDAS, G., WILHELM, F., CHATTERJEE. S.K., Infrarotspektroskopische Untersuchungen an lyophilierten Liposomen zur Charakterisierung der Wechselwirkung von freien und membrangebundenen Zuckern mit Phospholipiden, *Arch. Pharm.*, 327, **1994**, 429-433.

PARSEGIAN, V.A., Theory of liquid-crystal phase transitions in lipid + water systems, *Trans. Faraday Soc.*, 62, **1966**, 848-860.

PAULSEN, H., Fortschritte bei der selektiven chemischen Synthese komplexer Oligosaccharide, *Angew. Chem.*, 94, **1982**, 184-201.

PEDERSEN, J. S., Analysis of small-angle scattering data from colloids and polymer solutions: modeling and least-squares fitting, *Adv. Colloid Interface Sci.*, 70, **1997**, 171-210.

PLATZ, G, PÖLIKE, J., THUNIG, C., HOFMANN, R., NICKEL, D., v. RYBINSKI, W., Phase behaviour, lyotropic phases, and flow properties of alkyl glycosides in aqueous solution, *Langmuir*, 11, **1995**, 4250-4255.

PRADE, H., MIETHCHEN, R., VILL, V., Thermotrop flüssigkristalline Kohlenhydrat-Amphiphile, *J. Prakt. Chem.*, 337, **1995**, 427-440.

PUWADA, S., BLANCKSTEIN, D., Molecular-thermodynamic approach to predict micellization, phase behavior and phase separation of micellar solutions. I. Application to nonionic surfactants, *J. Chem. Phys.*, 92, **1990**, 3710-3724.

RILFORS, L., LINDBLOM, G., WIESLANDER, A., CHRISTIANSON, A., Membrane Fluidity. In: KATES, M. AND MANSON, L.A. (Eds.), *Biomembranes*, Vol. 12, Plenum Press, New York, **1984**, 205-245.

ROSEVAR, P., VANAKEN, T., BAXTER, J., FERGUSON-MILLER, Alkyl glycoside detergents: A simple synthesis and their effects on kinetic and physical properties of cytochrome c oxidase, *Biochemistry*, 19, **1980**, 4108-4115.

ROSS, J., MILES, G.D., An apparatus for comparison of foaming properties of soaps and detergents, *Oil and Soap*, 18, **1941**, 99-131.

SCHMIDT, R.R., JANKOWSKI, K., New types of nonionic surfactants with sugar head groups, *Liebigs Ann.*, 4, **1996**, 867-879.

SCHREYER, A., VOLLBRANDT, J., WILLUMEIT, R., *GeNF - Experimental Reports 2003*, Geesthacht, **2004**.

SHINODA, K., CARLSSON, A., LINDMAN, B., On the importance of hydroxyl groups in the polar head-group of nonionic surfactants and membrane lipids, *Adv. Colloid Interface Sci.*, 64, **1996**, 253-271.

SHINODA, K., YAMANAKA, T., KINOSHITA, K., Surface chemical properties in aqueous solutions of non-ionic surfactants octyl glycol ether, α-octyl glyceryl ether and octyl glucoside, *J. Phys. Chem.*, 63, **1959**, 648-650.

SIEGEL, D. P., Inverted micellar intermediates and the transitions between lamellar, cubic, and inverted hexagonal phases. I. Mechanism of the $L_\alpha \leftrightarrow H_{II}$ phase transitions, *Biophys. J.*, 49, **1986**, 1155-1170.

SIEGEL, D. P., Inverted micellar intermediates and the transitions between lamellar, cubic, and inverted hexagonal phases. II. Implications for membrane-membrane interactions and membrane fusion, *Biophys. J.*, 49, **1986**, 1171-1183.

SIEGEL, D. P., Inverted micellar intermediates and the transitions between lamellar, cubic, and inverted hexagonal amphiphile phases. III. Isotropic and inverted cubic state formation via intermediates in transitions between L_α and H_{II} phases, *Chem. Phys. Lipids*, 42, **1986**, 279-301.

SIEGEL, D. P., BANSCHBACH, J., ALFORD, D., ELLENS, H., LIS, L., QUINN, P. J., YEAGLE, P. L., BENTZ, J., Physiological levels of diacylglycerols in phospholipid membranes induce membrane fusion and stabilize inverted phases, *Biochemistry*, 28, **1989**, 3703-3709.

SÖDERMANN, O., JOHANSSON, I., Polyhydroxyl-based surfactants and their physico-chemical properties and applications, *Curr. Opin. Colloid Interface Sci.*, 4, **2000**, 391-401.

STRADNER, A., GLATTER, O., SCHURTENBERGER, P., A hexanol-induced sphere-to-flexible cylinder transition in aqueous alkyl polyglucoside solutions, *Langmuir*, 16, **2000**, 5354-5364.

STUBENRAUCH, C., Sugar surfactants - aggregation, interacial, and adsorption phenomena, *Curr. Opin. Colloid Interface Sci.*, 6, **2001**, 160-170.

STUHRMANN, H.B., BURKHARDT, N., DIETRICH, G., JÜNEMANN, R., MEERWINCK, W., SCHMITT, M., WADZACK, J., WILLUMEIT, R., ZHAO, J., NIERHAUS, K.H., Proton- and deuteron spin targets in bioligical structure research, *Nucl. Instr. & Meth.*, A356, **1995**, 133-137.

TANAKA, M., SCHIEFER, S., GEGE, C., SCHMIDT, R.R., FULLER, G.G., Influence of subphase conditions on interfacial viscoelastic properties of synthetic lipids with gentiobiose head groups, *J. Phys. Chem. B*, 108, **2004**, 3211-3214.

TANFORD, C., *The Hydrophobic Effect: Formation of Micelle and Biological Membranes*, Wiley and Sons, New York, **1980**.

TSCHIERSKE, C., Molecular self-organization of amphotropic liquid crystals, *Progr. Polym. Sci.*, 21, **1996**, 775-852.

TSCHIERSKE, C., Non-conventional soft matter, *Ann. Rep. Progr. Chem., Ser. C*, 97, **2001**, 191-267.

TSCHIERSKE, C., Liquid Crystalline materials with complex mesophase morphologies, *Curr. Opin. Colloid Interf. Sci.*, 71, **2002**, 69-80.

VILL, V., v.MINDEN, H.M., KOCH, M.H.J., SEYDEL, U., BRANDENBURG, K., Thermotropic and lyotropic properties of long chain alkyl glycopyranosides. Part I: Monosaccharide headgroups, *Chem. Phys. Lipids*, 104, **2000**, 75-91.

YOSHIDA, H., IKEDA, K., ACHIWA, K., HOSHINO, H., Synthesis of sulfated cerebroside analogs having mimicks of ceramide and their anti-human immunodefiency virus type 1 activities, *Chem. Pharm. Bull.*, 43, **1995**, 594-602.

ZHANG, R., MARONE, P.A., THIYAGARAJAN. P., TIEDE, D.M., Structure and molecular fluctuations of *n*-Alkyl-β-D-gluopyranoside micelles determined by x-ray and neutron scattering, *Langmuir*, 15, **1999**, 7510-7519.

Chapter 2

Synthesis and Mesogenic Properties

of a Y-shaped Glyco Glycero Lipid

Synthesis and mesogenic properties of a Y-shaped glyco-glycero-lipid

G. Milkereit [a], V.M. Garamus [b], K. Veermans [a], R. Willumeit [b], V. Vill [a],*

[a] *Institute of Organic Chemistry, University of Hamburg, Martin-Luther-King-Platz 6, 20146 Hamburg, Germany*
[b] *GKSS Research Centre, Max Planck Str., Geesthacht 21502, Germany*

Abstract

We synthesised a new glycoglycerolipid [1,3-di-*O*-(β-D-glucopyranosyl)-2-deoxy-2-amino-*N*-palmitoyl-*sn*-glycerol] with a Y-shaped structure bearing two sugar head groups and only one fatty acid chain. Instead of an ester linkage between the glycerol and the fatty acid an amido function was introduced. The mesogenic properties were investigated using polarising microscopy and are discussed with respect to similar compounds. The lyotropism was measured using the contact preparation method and small-angle neutron-scattering.
© 2004 Elsevier Ireland Ltd. All rights reserved.

Keywords: Glyco-glycero-lipids; Amphiphiles; Lyotropic cubic phases; Small-angle neutron-scattering

1. Introduction

Glyco-glycero-lipids are known to be important constituent of many cell membranes. Naturally occurring glyco-glycero-lipids normally have a Y-shaped structure (Fig. 1a) with a polar carbohydrate head group linked to a 1,2- or 1,3-di-*O*-acyl or alkyl-*sn*-glycerol (Ishizuka and Yamakawa, 1985; Minden et al., 2002a,b; Mannock et al., 1987, 1990, 2001; Hinz et al., 1996; Six et al., 1983; Kuttenreich et al., 1988; Nagatsu et al., 1994; Minamikawa et al., 1994). But only a few compounds with an inverse structure (Fig. 1b) were reported (Minden et al., 2002a; Fischer et al., 1994).

All of these amphotropic molecules form both thermotropic liquid crystalline phases in their pure state upon heating and lyotropic polymorphism can be found on the addition of solvent. The driving force of the mesophase formation in case of amphiphiles is a micro phase separation leading to an aggregate structure with separated regions for the lipophilic and hydrophilic molecular parts.

The structures of the common lyotropic and thermotropic aggregates have been investigated extensively (Curatolo, 1987; Prade et al., 1995; Blunk et al., 1998; Jeffrey and Wingert, 1992).

The synthesis of glycolipids is often very tedious, requires multistep synthesis, and the introduction of other functional groups than alkoxy or esters (e.g.

* Corresponding author. Tel.: +49-40-42838-4269; fax: +49-40-42838-4325.
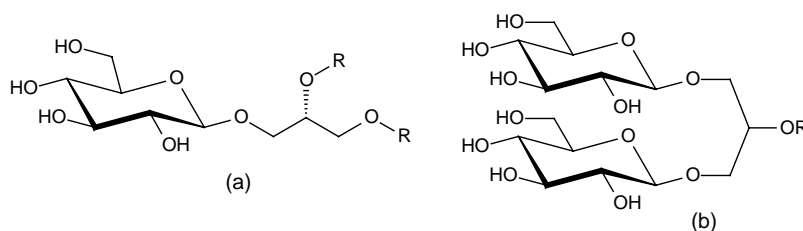*E-mail address:* vill@liqcryst.chemie.uni-hamburg.de (V. Vill).

Fig. 1. (a) Normal Y-shaped glyco-glycero-lipid and (b) inverted structure.

phosphate, nitrogen, sulphur) makes the synthesis often more complicated.

We report about the easy synthesis of a new glyco-glycero-lipid with an inverted Y-shaped structure. An amido group substituted the oxygen at the carbon-2 in order to make the molecule more polar. The thermotropic and the lyotropic properties are discussed; the results from small-angle-neutron-scattering are presented.

2. Results and discussion

2.1. Synthesis

Fig. 2 shows the synthetic route used for the preparation of N-palmitoyl-1,3-di-O-(β-D-glucopyranosyl)-2-deoxy-2-amino-sn-glycerol.

In an earlier paper we reported the synthesis of an 1,3-di-O-glucosyl-2-O-acyl-sn-glycerol (Minden et al., 2002a) that required a multistep synthesis with several protecting and deprotecting steps. The synthesis of the title compound should afford less synthetic steps. We started with commercial available 2-amino-1,3-propanediol (Serinol). For glycosylation the amino function had to be protected. We used in this case the benzyloxycarbonyl group (cbz) as protective group. On treatment of **1** with benzyl chloroformate according to the procedure described by Harada et al. (1996) we obtained 2-benzyloxycarbonylamino-1,3-propanediol in 40% yield. 1,2,3,4,6-penta-O-acetyl-β-D-glucopyranoside was prepared according to the literature (Fischer and Helferich, 1911).

The glycosylation reaction was carried using the method described by Vill et al. (1986), but instead of tin tetrachloride boron trifluoride etherate, a more efficient Lewis acid for the synthesis of β-glycosides (Ferrier and Furneaux, 1976) was used for glycosyla-

tion reaction. The desired product was obtained in a yield of 15%, besides this an amount of ∼3% monoglycosylated product could be separated from the reaction mixture, however, the reaction time exceeded 18 h, but no α-product was detected.

One could expect that it would make more sense using other glycosylation procedures, e.g. for the synthesis of the lipid 2-O-oleoyl-1,2-di-O-β-D-glucopyranosyl-sn-glycerol the key glycosylation step was carried out using a variation of the Königs–Knorr procedure (Helferich and Ost, 1962), or using the trichloracetimidate procedure (Schmidt and Stumpp, 1983) for the synthesis of 1,3-diglycosylated 2-acyl-glycerol esters (Milkereit and Vill, unpublished), due to higher yields. But this holds not true for this glycosylation reaction. The problem seems to be a lower reactivity of the amino alcohol, because even using the trichloracetimidate procedure, the yield was around 15–16% and two more synthetic steps for the synthesis of the imidate are necessary.

In the next step the cbz group was removed by hydrogenation. The reaction was somehow tedious and the product had to be purified by silica gel chromatography. The amino glycerol **3** was reacted with palmitoyl chloride using the method described by Masuda et al. (2000), however, dichlormethane was used as solvent instead of N,N-dimethylformamide. After chromatographic purification compound **4** was obtained in 45% yield. In the last step the compound was deacetylated using the Zemplen procedure, leading to the desired lipid N-palmitoyl-1,3-di-O-β-D-glucopyranosyl-2-deoxy-2-amino-sn-glycerol (**5**) in 94% yield.

2.2. Thermotropic properties

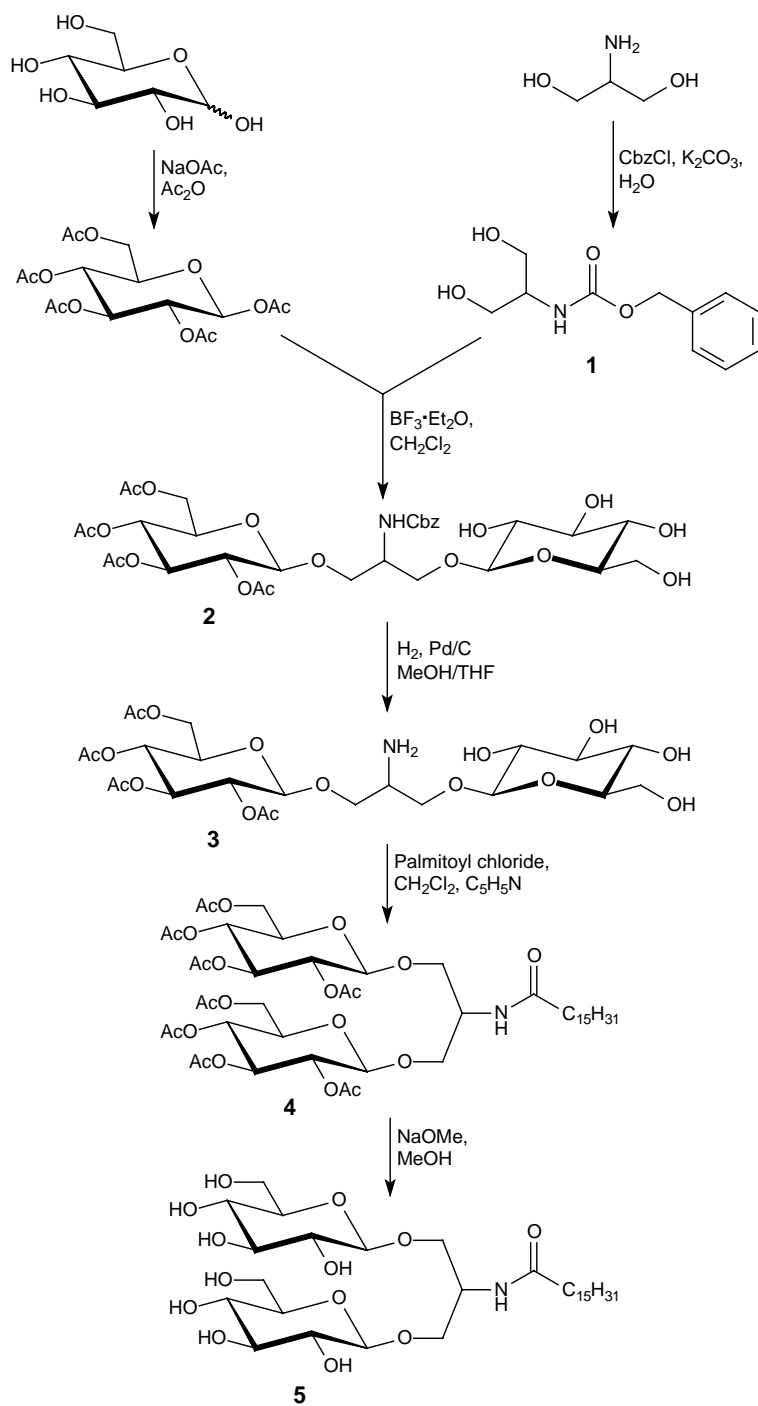Table 1 shows the thermotropic properties of the synthesised compound, together with the data of some

Fig. 2. Synthesis of *N*-palmitoyl-1,3-di-*O*-β-ᴅ-glucopyranosyl-2-deoxy-2-amino-*sn*-glycerol.

Table 1
Thermotropic properties of the synthesised lipid, together with some literature data for comparison (**A**, **B**: Schmidt and Jankowski, 1996; Schmidt and Vill, unpublished results; **C**: Fischer et al., 1994; **D**: Minden et al., 2002a)
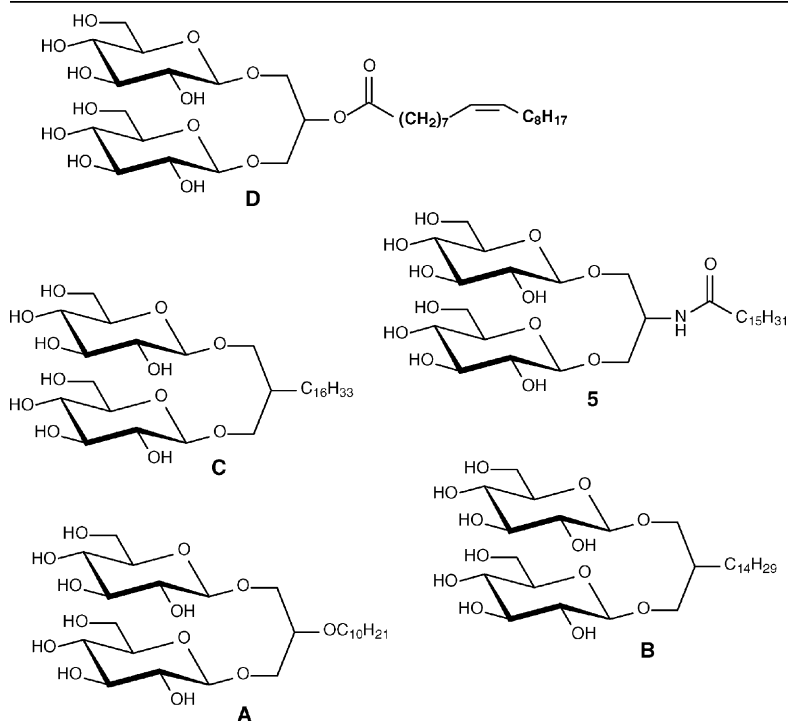
5	g	?	col	65	cub				134	I
A	Cr	115	disc						149.5	I
B	Cr	111			cub				205	I
C	Cr	110	disc	125	cub				175	I
D	Cr	< 20	col	72	cub	156	S$_A$		217	I

similar mesogenes for comparison (**A**, **B**: Schmidt and Jankowski, 1996; Schmidt and Vill, unpublished results; **C**: Fischer et al., 1994; **D**: Minden et al., 2002a).

It depicts clearly the influence of the type of linkage between the alkyl chain and the glycerol moiety, the chain length and type of chain.

The type of chain has the strongest effects on the melting point. An unsaturation in the hydrophobic part of the molecule (**D**) leads to liquid crystallinity even at ambient temperature, due to a disturbed packing of the chains. Compounds **A**, **B** and **C** with saturated alkyl chains show no liquid crystal phases at ambient temperature. Hence the kind of linkage has for these three compounds no remarkable influence on the melting point. For compound **5** the influence of the kind of linkage is more significant. Compared to **D** one would expect for a palmitoyl ester a much higher melting temperature, but the palmitoyl amid **5** has a very unusual melting behaviour, due to a much more complex hydrogen bond network, that differs from the ester. The compound is in glass state at ambient temperature, with a phase transitions temperature to the columnar

phase that could not be clearly determined. On cooling the phase transition from the columnar phase to the glass state could only be seen in the "breaking" of the glass at low temperatures. The length of the hydrophobic chain can be seen in the different kind of phases occurring with varying chain length. For compound **B** and **C**, increasing the chain length with two methylene groups leads to a second phase. For compounds **A**, **D** and **5** the polymorphism increases with increasing chain length (the type of linkage is not considered), starting with only a columnar-discotic phase for the short chain compound to a columnar, cubic and lamellar phase diagram for the C_{18}-chain. Compound **5** forms a columnar phase of type I, the hydrophilic/hydrophobic interface curved towards the hydrocarbon chain region. As a fact of frustration, a cubic phase is formed between 65 and 134 °C, since the columnar phase is already destabilised due to the increased volume of the fluid hydrocarbon chain region. A S_A phase cannot be formed, because the hydrocarbon chain length is to short to accommodate the hydrophilic headgroup, which is too broad compared to the hydrocarbon chain. Compound **D** becomes at higher temperatures rod-like, and is able to form a S_A phase, but the fluidity maximum of the hydrophobic chain of compound **5** is not enough to form a S_A phase.

2.3. Lyotropic properties

The lyotropism was measured using the contact preparation technique. Compound **5** displayed in the contact with water the phase sequence:

(100% water)   cub H_I (100% lipid)

The occurrence of the hexagonal phase with the hydrophilic sugar moieties curved towards the water region was expected, more interesting is the cubic phase. For compound **D** even two cubic phases were found (Minden et al., 2002a), but the structure was not further investigated.

The cubic phase can have two possible shapes, discontinuous and bicontinous phases. Whereas the discontinous cubic phases are based upon various packing of spherical or slightly anisotropic micelles, the bicontinous cubic phases with interwoven fluid structures are based upon underlying infinite periodic minimal surfaces (Fairhurst et al., 1998).

In the next step we investigated the structure of the lyotropic aggregates with small-angle neutron-scattering. For the investigation of micellar structures this method provides significant structural information (He et al., 2002), and for the investigation of discontinous cubic phases information of the size and shape of the micelles in isotropic micellar phases it is helpful to unravel the structure of the cubic phase.

2.4. Analysis of SANS data

2.4.1. Model-independent approach

The pair distribution function $p(r)$ of scattering length density gives in many cases information about the overall shape and dimension of micelles (Glatter and Kratky, 1982). Because the scattering data is only measured in a finite range, a traditional Fourier transformation cannot be performed, instead an indirect Fourier transformation can be used (Glatter, 1977; Pedersen, 1997). The $p(r)$ function is approximated by linear combination of a finite number of cubic B-spline functions, giving the expression:

$$p(r) = \sum_{i=1}^{N} a_i \varphi_i(r) \qquad (1)$$

After calculating the $p(r)$ function we are able to calculate integral parameters of the micelle, like $d\Sigma(0)/dW$ expressing the scattering at the so called "zero" angle and R_g the radius of gyration (Glatter, 1977; Glatter and Kratky, 1982), which is given by:

$$R_g^2 = \frac{\int_0^{D_{max}} p(r) r^2 \, dr}{2 \int_0^{D_{max}} p(r) \, dr} \qquad (2)$$

with an upper limit for the maximum particle size of D_{max}.

2.4.2. Modelling

To obtain specific structural information about the micelle it is necessary to fit the experimental data by the different models of micellar structures. Looking at the results from the contact preparation, it seemed to be enough to use a spherical and an ellipsoidal model to fit the data.

The differential cross-sections of neutron-scattering per unit volume by an ensemble of monodisperse spherical-like objects with negligible interaction can

be written as:

$$\frac{d\Sigma(q)}{d\Omega} = \frac{d\Sigma(0)}{d\Omega F^2(q) + B_{inc}} \qquad (3)$$

where $d\Sigma(0)/dW$ depends on the concentration of micelles (n), the volume of micelle (V) and the difference in the scattering length densities between micelles and solvent leading to the equation:

$$\frac{d\Sigma(0)}{d\Omega} = n(\langle\rho\rangle - \rho_s)^2 V^2 \qquad (4)$$

$\langle\rho\rangle$ and ρ_s describe the average of the neutron-scattering length densities of aggregates and solvent, respectively, and B_{inc} stands for the residual scattering background.

The form factor $F^2(q)$ expresses the scattering cross-section of one particle. Eq. (5) stands for the form factor for spherical and elliptical micelles

$$F^2(q) = \int_0^{\pi/2} \left[f(q,\beta) \right]^2 \sin\beta \, d\beta \qquad (5)$$

In the case of an ellipsoid with three semiaxes a, a, εa the function $f(q,\beta)$ can be written as:

$$f(q,\beta) = \frac{3[\sin x - x \cos x]}{x^3} \qquad (6)$$

where β is the angle between the vector q and the axis of the particle and $x = qb[\sin^2\beta + \varepsilon^2\cos^2\beta]^{1/2}$. For $\varepsilon = 1$, Eq. (6) describes the scattering of spherical aggregates with $a = b = r$.

The models described above were applied to fit the experimental data.

2.5. Structural analysis

Two different concentrations were measured (0.07 and 0.1 wt.%). At both besides the smaller aggregates some larger aggregates are formed, exceeding the measurement range of SANS. On further increasing the concentration the smaller aggregates stay nearly the same size, therefore, the large aggregates have to grow, but it is not observable on the present data due to limited q-range.

From this point of view, it seems to be useful to analysis only the data for the medium concentration, because the aggregates have for all concentrations nearly the same size, and at medium concentration the smaller aggregate can be investigated besides the larger aggregate.
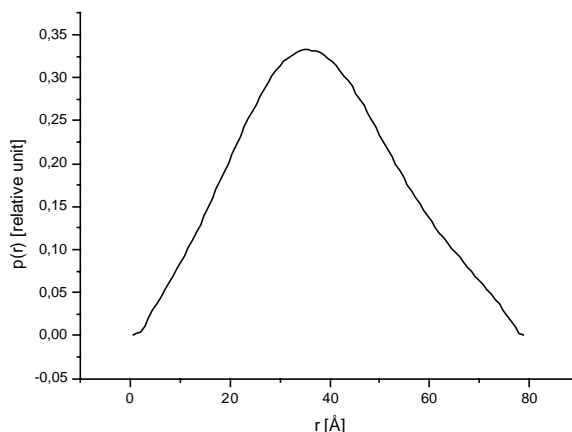
Fig. 3. Pair distribution function (for $c = 7.0 \times 10^{-4}$ g mL^{-1}).

The pair distance distribution function calculated by the IFT method is shown in Fig. 3. It gives an indication that a spherical shape is more probable, due to its nearly Gaussian form, therefore, the models for spherical and ellipsoidal micelles were fitted to the data. The fitting results are shown in Fig. 4, showing the model fit for spherical micelles and the data, the fit for ellipsoidal micelles is not shown. The application of ellipsoidal model gives the value of parameter ε is equal to 1, i.e. spherical shape. The structural results calculated from the model fitting results are summarised in Table 2.
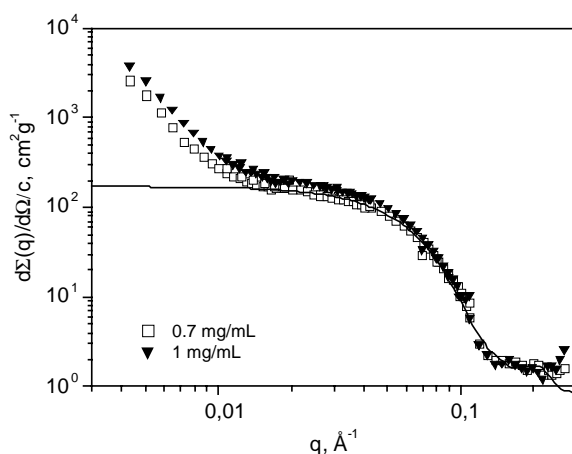
Fig. 4. Scattering data for $c = 7.0 \times 10^{-4}$ g mL^{-1} (empty squares) and $c = 10.0 \times 10^{-4}$ g mL^{-1} (solid triangles) together with the model fit for spherical micelles (solid line).

Table 2
Results of SANS data analysis by model independent approach (IFT), R_g and $d\Sigma(0)/d\Omega/c$, model fitting, r and calculated parameter of aggregates, i.e. radius of equivalent sphere

Radius of gyration, R_g (Å)	29.2 ± 0.2
Radius of equivalent sphere (Å)	37.7 ± 0.3
Radius of sphere from model fitting, r (Å)	36 ± 2
Scattering at "zero"-angle, $d\Sigma(0)/d\Omega/c$ (cm^2 g^{-1})	172 ± 1
Apparent molar mass of micelle, M_{app} (g M^{-1})	$(8.4 \pm 0.4) \times 10^4$
Radius of equivalent sphere (Å)	29.6 ± 1.5

The fitting of the data shows another interesting result of the experiments. It can be seen, that the fitted curve is close to the experimental data. But it is remarkable that at low q values, the curves of the model fit and the experimental data diverge, and this discrepancy is cannot be explained as an experimental error. We assume that in this experiment we observed the formation of a non-micellar aggregate besides the spherical micelles. The lowest part of experimental data ($q < 0.01$ Å^{-1}) was analysed by power law

$$\frac{d\Sigma(q)}{d\Omega} \sim q^{-\alpha}. \tag{7}$$

The obtained value of α is equal to 2.7 ± 0.1 which points on the formation of aggregates with a relation between the mass (M) and linear sizes (r) as $M \sim r^{2.7}$ for a length scale of $r > 300$ Å.

This change of micellar form is similar to a second or higher order phase transition, but it is not the same as the main liquid crystalline phase transition. However, from the neutron-scattering data it was not possible to obtain information about the space group of a possible cubic phase, this information may be provided by X-ray diffraction experiments.

The results in Table 2 describe the local structure of the micelle in a solution of heavy water. The model fits showed that the micelles are spherical with the radius in the range of 36–38 Å. The results of model independent analysis and model fitting give the consistent values. The radius of micelle corresponds to the length of the molecule, which is equal to ~31 Å. This molecule length is the value for the length of the "dry molecule", under real conditions the hydration of the carbohydrate headgroup increases the volume of

the polar group, and therefore, the length of molecule. From another point of view, the radius of the micelle obtained from SANS analysis is the average value, which is affected by the polydispersity of the aggregates and by the fluctuation of the micellar surface. That is why the obtained value of the micellar radius (36 Å), which is higher due to the above mentioned effects of hydration, polydispersity and fluctuation of surface, is in good agreement with the length of the "dry molecule" (31 Å).

On the other hand there is some disagreement between the radius of equivalent sphere calculated from radius of gyration (R_g) and the scattering at "zero"-angle ($d\Sigma(0)/d\Omega/c$). It is straight forward to get the mass and volume of the micelle from $d\Sigma(0)/d\Omega/c$. In the present calculations we have taken into account that eight H-atoms of hydroxyl functions of the sugar head groups are under H–D exchange. The value of equivalent sphere obtained from $d\Sigma(0)/d\Omega/c$ is equal to 29.6 Å which is significant lower than the values obtained from R_g (IFT) and model fitting. This difference can be explained by the beginning of the phase separation, i.e. the co-existence of two different kinds of aggregates (large particles of the hexagonal phase and small spherical micelles). The Scattering data were normalised by total concentration of surfactant but in the interval of the scattering vector q (0.01–0.25 Å^{-1}) analysed by IFT method only the scattering from the small spherical aggregates is significant. That is why, actual values of the micellelar mass (volume) should be larger and the corresponding radius of equivalent sphere also. Taking into account these difficulties one can conclude the observation of spherical micelles with a radius of 36–38 Å and an aggregation number of about 200.

3. Summary

A new synthetic strategy was employed successful to synthesise an unusual glyco-glycero-lipid. The mesogenic properties are strongly influenced by the amide linkage of the fatty acid chain to the hydrophilic part of the molecule. The investigation of the lyotropic structure by small-angle neutron-scattering revealed an interesting lyotropism. The micellar structure was determined and the size of the micelle was calculated

by standard procedures. Another interesting observation is the phase transition that seems to occur in the measured concentration range. The micelles stay the same size, whereas with increasing concentration all molecules are used for building up the new phase. Interesting is that many inverted Y-mesogenes exhibit thermotropic and lyotropic cubic phases. The structure enables the formation of cubic structures, perhaps this structure facilitates the formation of cubic phases in biological processes.

4. Experimental section

4.1. Polarising microscopy

An Olympus BH optical polarising microscope equipped with a Mettler FP 82 hot stage and a Mettler FP 80 central processor was used to identify thermal transitions and characterise anisotropic textures.

For the contact preparation a small amount of sample was placed on a microscope slide and covered with a cover glass before heating to the S_A phase. Afterwards a small amount of solvent was placed on the slide at the edge of the cover glass. As soon as the solvent had moved under the cover glass and the sample was completely surrounded with the solvent, it was placed again for some seconds on the hot stage at a temperature of 100–120 °C and the phase behaviour was investigated immediately afterwards by polarising microscopy.

4.2. Small-angle neutron-scattering

Small-angle neutron-scattering experiments were made with the SANS-1 experiment at the FRG1 research reactor at GKSS research Centre, Geesthacht, Germany (Stuhrmann et al., 1995). Four sample-to-detector distances (from 0.7 to 9.7 m) were employed to cover the range of scattering vectors q from 0.005 to 0.25 Å^{-1}. The neutron wavelength λ was 8.1 Å with a wavelength resolution of 10% (full-width at half-maximum value).

The samples were kept in quartz cells (Hellma) with a path length of 5 mm. The samples were placed in a thermostated sample holder, for isothermal conditions. The raw spectra were corrected for the background from the solvent, sample cell, and other sources, by

conventional procedures (Wignall and Bates, 1986). The two-dimensional isotropic scattering spectra were azimuthally average, converted to an absolute scale, and corrected for detector efficiency by dividing by the incoherent scattering spectra of pure water (Wignall and Bates, 1986) which was measured with a 1-mm path-length quartz cell (Hellma).

The average excess scattering length density per unit mass $\Delta\rho_m$ of the surfactant in deuterated water was determined from the known chemical composition, it was equal to $\Delta\rho_m = -4.297 \times 10^{10}$ cm g^{-1} for the full protonated and in the case of H–D exchange of eight H atoms $\Delta\rho_m = -3.528 \times 10^{10}$ cm g^{-1}.

4.3. Materials

Dry solvents were obtained from Fluka or Merck, all other solvents were freshly distilled before use. Deuterium oxide was purchased from Deutero. Thin-layer chromatography was performed on silica gel (Merck GF$_{254}$), and detection was effected by spraying with a solution of: (a) ethanol–sulphuric acid (9:1) or (b) ethanol–molybdic phosphoric acid (99:1) followed by heating. Column chromatography was performed using silica gel 60 (Merck, 0.063–0.200 nm, 230–400 mesh). NMR spectra were recorded on a Bruker AMX 400 or a Bruker DRX 5001 spectrometer (m$_c$: centred multiplett; d: doublet; t: triplet; dd: double doublet; dt: double triplet).

4.4. Synthesis

4.4.1. N-(Carbonylbenzyloxy)-2-amino-propane-1,3-diol (1)

Benzyl chloroformate (8.4 mL; 10.2 g; 60 mmol) was added dropwise to a stirred solution of 5 g (54.8 mmol) Serinol (2-amino-1,3-propanediol) and 8.3 g (60 mmol) potassium carbonate in 40 mL of water at 5 °C. The mixture was stirred for an additional hour at 5 °C and then extracted four-times with 50 mL ethyl acetate. The combined organic extracts were dried over magnesium sulphate and solvent was removed in vacuo. The residue was recrystallised from acetone/n-hexane. Yield: 4.93 g (40%).

^{1}H NMR (400 MHz, pyridine-d$_5$): $\delta = 5.07$–5.15 (m, 5H, H-arom.), 4.92 (s, 2H, CH$_2$-benzyl.),

4.15–4.22 (m, 2H, H-1a, H-3a), 4.06–4.14 (m, 2H, H-1b, H-3b), 3.92–4.02 (m, 1H, H-2).

4.4.2. N-(Carbonylbenzyloxy)-1,3-di-O-(2,3,4,6-tetra-O-acetyl-β-D-glucopyranosyl)-2-deoxy-2-amino-sn-glycerol (2)

1,2,3,4,6-Penta-O-acetyl-β-D-glucopyranosid (11.7 g; 30 mmol) and 2.3 g (10 mmol) N-carbonylbenzyloxy-2-amino-1,3-propanediol were dissolved in 150 mL anhydrous dichlormethane under an atmosphere of dry nitrogen. Boron trifluoride etherate (3.81 mL; 4.3 g; 30 mmol) was added dropwise at 0 °C and the solution was stirred 18 h at ambient temperature. After the reaction had been quenched with a saturated solution of sodium hydrogen carbonate, the organic layer was separated and the aqueous layer extracted two-times with dichlormethane. The combined organic phases were washed twice with water (100 mL), dried over magnesium sulphate and solvent was removed in vacuo. The residue was purified by silica gel chromatography (ethyl acetate–light petroleum, bp 50–70 °C, 2:1). Yield: 1.30 g (15%).

^{1}H NMR (500 MHz, CDCl$_3$+TMS): δ = 7.28–7.37 (m, 5H, H-arom.), 5.19, 5.20 (je dd,1H, H-3′, H-3″), 5.07, 5.08 (je dd, 1H, H-4′, H-4″), 4.99, 5.01 (je dd, 1H, H-2′, H-2″), 4.58, 4.62 (je d, 1H, CH$_2$-benzyl.), 4.52, 4.55 (je d, 1H, H-1′, H-1″), 4.24, 4.26 (je dd, 1H, H-6a′, H-6a″), 4.10, 4.14 (je dd, 1H, H-6b′, H-6b″), 3.96, 3.88 (je dd, H-1a, H-3a), 3.59–3.70 (m, 4H, H-1b, H-3b, H-5′, H-5″), 3.41 (m$_c$, 1H, H-2), 2.07, 2.06 (je s, 3H, OAc), 2.02 (s, 6H, OAc), 2.00 (s, 9H, OAc), 1.94 (s, 3H, OAc); $^3J_{1',2'}$ = 8.1 Hz, $^3J_{2',3'}$ = 9.7 Hz, $^3J_{3',4'}$ = 9.7 Hz, $^3J_{4',5'}$ = 9.7 Hz, $^3J_{5',6a'}$ = 4.6 Hz, $^3J_{5',6b'}$ = 2.6 Hz, $^2J_{6a',b'}$ = 12.2 Hz, $^3J_{1'',2''}$ = 8.1 Hz, $^3J_{2'',3''}$ = 9.7 Hz, $^3J_{3'',4''}$ = 9.7 Hz, $^3J_{4'',5''}$ = 9.7 Hz, $^3J_{5'',6a''}$ = 4.6 Hz, $^3J_{5'',6b''}$ = 2.6 Hz, $^2J_{6a'',b''}$ = 12.2 Hz, $^3J_{1a,2}$ = 3.1 Hz, $^2J_{1a,b}$ = 10.7 Hz, $^3J_{3a,2}$ = 3.1 Hz, $^3J_{3a,b}$ = 10.7 Hz.

^{13}C NMR (125 MHz, CDCl$_3$ + TMS): δ = 172.63 (C=O, amid), 170.64, 170.28, 170.24, 169.98, 169.35, 169.26 (C=O, OAc), 138.32 (C$_{quart}$-arom.), 128.42, 127.74, 127.59 (C-arom.), 101.21, 101.14 (C-1′, C-1″), 72.8, 72.70 (C-3′, C-3″), 72.41 (C-benzyl.), 71.88 (C-5′, C-5″), 71.38, 71.29 (C-2′, C-2″), 70.35, 69.22 (C-1, C-3), 68.39 (C-4′, C-4″), 61.88 (C-6′, C-6″), 52.03 (C-2), 20.74, 20.60, 20.18 (–CH$_3$, OAc).

4.4.3. 1,3-Di-O-(2,3,4,6-tetra-O-acetyl-β-D-glucopyranosyl)-2-deoxy-2-amino-sn-glycerol (3)

A mixture of 682 mg (0.77 mmol) 2 and 40 mg Pd/C (10%) in 100 mL methanol/tetrahydrofurane (1:1 v/v) was stirred under 1 atm of hydrogen. After 2 days TLC showed the reaction to be complete. The catalyst was removed by filtration. The mother liquor evaporated in vacuo and the resulting residue purified by silica gel chromatography (chloroform–methanol 9:1). Yield: 567 mg (97%).

^{1}H NMR (400 MHz, CDCl$_3$ + TMS): δ = 5.19 (dd, 2H, H-3′, H-3″), 5.07, 5.08 (je dd, 1H, H-4′, H-4″), 4.99 (m$_c$, 2H, H-2′, H-2″), 4.52, 4.54 (je d, 1H, H-1′, H-1″), 4.23–4.26 (m, 2H, H-6a′, H-6a″), 4.11, 4.13 (je dd, 1H, H-6b′, H-6b″), 3.58–3.91 (m, 6H, H-1a, H-3b, H-1b, H-3b, H-5′, H-5″), 3.09 (m$_c$, 1H, H-2), 2.08, 2.05 (je s, 3H, OAc), 2.01 (s, 6H, OAc), 2.00, 1.98, 1.95, 1.93 (je s, 3H, OAc); $^3J_{1',2'}$ = 8.1 Hz, $^3J_{3',2'}$ = 9.7 Hz, $^3J_{3',4'}$ = 9.7 Hz, $^3J_{4',5'}$ = 9.7 Hz, $^3J_{5',6b'}$ = 2.6 Hz, $^2J_{6a',b'}$ = 12.2 Hz, $^3J_{1'',2''}$ = 8.1 Hz, $^3J_{3'',2''}$ = 8.1 Hz, $^3J_{3'',4''}$ = 9.7 Hz, $^3J_{5'',6''}$ = 2.6 Hz, $^3J_{6a'',b''}$ = 12.2 Hz.

4.4.4. N-(Palmitoyl)-1,3-di-O-(2,3,4,6-tetra-O-acetyl-β-D-glucopyranosyl)-2-deoxy-2-amino-sn-glycerol (4)

Compound 3 (560 mg; 0.74 mmol) and 75 μL (73.2 mg; 0.9 mmol) pyridine were dissolved in 25 mL anhydrous dichlormethane. At 0 °C a solution of 224 μL (203 mg; 0.74 mmol) palmitoyl chloride in 1 mL anhydrous dichlormethane was added slowly. Afterwards the solution was stirred 30 min at 0 °C and overnight at ambient temperature. The organic phase was washed twice with a saturated solution of sodium hydrogen carbonate (10 mL) and once with water (5 mL), dried over magnesium sulphate, and evaporated in vacuo. The residue was purified by silica gel chromatography (ethyl acetate–light petroleum, bp 50–70 °C 2:1). Yield: 330 mg (45%).

^{1}H NMR (500 MHz, CDCl$_3$ + TMS): δ = 5.19, 5.21 (je dd, 1H, H-3′, H-3″), 5.07, 5.08 (je dd, 1H, H-4′, H-4″), 4.99, 5.02 (je dd, 1H, H-2′, H-2″), 4.53, 4.56 (je d, 1H, H-1′, H-1″), 4.24, 4.26 (je dd, 1H, H-6a′, H-6a″), 4.10, 4.13 (je dd, 1H, H-6b′, H-6b″), 3.89, 3.96 (je dd, 1H, H-1a, H-3a), 3.59–3.69 (m, 4H, H-1b, H-3b, H-5′, H-5″), 3.41 (m$_c$, 1H, H-2), 2.21 (m, 2H, Alkyl-α-CH$_2$), 2.07, 2.05 (je s, 3H, OAc),

2.03 (s, 6H, OAc), 2.00 (s, 9H, OAc), 1.94 (s, 3H, OAc), 1.49–1.59 (m, 2H, Alkyl-β-CH$_2$), 1.19–1.31 (m, 24H, Alkyl-CH$_2$), 0.85 (t, 3H, Alkyl-CH$_3$); $^3J_{1',2'} = 8.1$ Hz, $^3J_{2',3'} = 9.7$ Hz, $^3J_{3',4'} = 9.7$ Hz, $^3J_{4',5'} = 9.7$ Hz, $^3J_{5',6a'} = 4.6$ Hz, $^3J_{5',6b'} = 2.6$ Hz, $^2J_{6a',b'} = 12.2$ Hz, $^3J_{1'',2''} = 8.1$ Hz, $^3J_{2'',3''} = 9.7$ Hz, $^3J_{3'',4''} = 9.7$ Hz, $^3J_{4'',5''} = 9.7$ Hz, $^3J_{5'',6a''} = 4.6$ Hz, $^3J_{5'',6b''} = 2.6$ Hz, $^2J_{6a'',b''} = 12.2$ Hz, $^3J_{1a,2} = 3.1$ Hz, $^2J_{1a,b} = 10.7$ Hz, $^3J_{3a,2} = 3.1$ Hz, $^3J_{3a,b} = 10.7$ Hz.

^{13}C NMR (125 MHz, CDCl$_3$ + TMS): $\delta = 172.51$ (C=O, amid), 170.63, 170.29, 170.18, 169.70, 169.35, 169.27 (C=O, OAc), 101.25, 101.19 (C-1′, C-1″), 72.86, 72.72 (C-3′, C-3″), 71.87 (C-5′, C-5″), 71.38, 71.30 (C-2′, C-2″), 70.35, 69.22 (C-1, C-3), 68.45 (C-4′, C-4″), 61.84 (C-6′, C-6″), 52.08 (C-2), 25.96, 24.83, 24.69, 24.17, 23.18, 22.70, 21.18 (Alkyl-CH$_2$), 20.74, 20.61, 20.19 (–CH$_3$, OAc), 14.08 (Alkyl-CH$_3$).

4.4.5. N-(Palmitoyl)-1,3-di-O-(β-D-glucopyranosyl)-2-deoxy-2-amino-sn-glycerol (5)

Compound **4** (325 mg; 0.33 mmol) was dissolved in 25 mL dry methanol and sodium methoxide was added (pH 8–9). The solution was stirred at ambient temperature until TLC revealed the reaction to be complete. The reaction mixture was neutralised using Amberlyst IR 120 ion exchange resign (protonated form), filtrated and evaporated in vacuo. The product was recrystallised from methanol. Yield: 201 mg (94%).

^{1}H NMR (400 MHz, d$_4$-methanol): $\delta = 4.33, 4.34$ (je d, 1H, H-1′, H-1″), 4.04, 4.09 (je d, 1H, H-1a, H-3a), 3.81–3.94 (m, 4H, H-1b, H-3b, H-6a′, H-6a″), 3.65–3.73 (m, 2H, H-6b′, H-6b″), 3.26–3.42 (m, 7H, H-2, H-3′, H-4′, H-5′, H-3″, H-4″, H-5″), 3.22, 3.23 (je dd, 1H, H-2′, H-2″), 2.39 (t, 2H, Alkyl-α-CH$_2$), 1.59–1.67 (m, 2H, Alkyl-β-CH$_2$), 1.30–1.41 (m, 24H, Alkyl-CH$_2$), 0.93 (t, 3H, Alkyl-CH$_3$); $^3J_{1',2'} = 8.1$ Hz, $^3J_{2',3'} = 9.2$ Hz, $^3J_{1'',2''} = 8.1$ Hz, $^3J_{1a,2} = 4.1$ Hz, $^2J_{1a,b} = 11.2$ Hz, $^3J_{3a,2} = 5.7$ Hz, $^3J_{3a,b} = 11.1$ Hz.

Acknowledgements

References

Blunk, D., Praefke, K., Vill, V., 1998. Amphotropic liquid crystals. In: Demus, D., Goodby, J., Gray, G.W., Spiess, H.-W., Vill, V. (Eds.), Handbook of Liquid Crystals, vol. 3. Wiley-VCH, Weinheim, pp. 305–340.

Curatolo, W., 1987. The physical properties of glycolipids. Biochim. Biophys. Acta 779, 381–401.

Fairhurst, C.E., Fuller, S., Gray, J., Holmes, M.C., Tiddy, G.J., 1998. Lyotropic surfactant liquid crystals. In: Demus, D., Goodby, J., Gray, G.W., Spiess, H.-W., Vill, V. (Eds.), Handbook of Liquid Crystals, vol. 3. Viley-VCH, Weinheim, pp. 341–392.

Ferrier, R.J., Furneaux, R.H., 1976. Synthesis of 1,2-*trans*-related 1-thioglycoside esters. Carbohydr. Res. 52, 63–68.

Fischer, E., Helferich, B., 1911. Über neue synthetische glycoside. Liebigs Ann. Chem. 383, 68–91.

Fischer, S., Fischer, H., Diele, S., Pelzl, G., Jankowski, K., Schmidt, R.R., Vill, V., 1994. On the structure of the thermotropic cubic mesophase. Liq. Cryst. 17, 855–861.

Glatter, O., 1977. Data evaluation of small-angle scattering: calculation of the radial electron density distribution by means of indirect Fourier transformation. Acta Phys. Aust. 47, 83–102.

Glatter, O., Kratky, O. (Eds.), 1982. Small-Angle-X-ray Scattering. Academic Press, London.

Harada, H., Morie, T., Hirokawa, Y., Kato, S., 1996. An efficient synthesis of 6-substituted aminohexahydro-1*H*-1,4-diazepines from 2-substituted aminopropenals. Chem. Pharm. Bull. 44 (12), 2205–2212.

He, L., Garamus, V.M., Funari, S.S., Malfois, M., Willumeit, R., Niemeyer, B., 2002. Comparison of small-angle scattering methods for the structural analysis of octyl-β-maltopyranoside micelles. J. Phys. Chem. B 106, 7596–7604.

Helferich, B., Ost, W., 1962. Synthese einiger β-D-xylopyranoside. Chem. Ber. 95, 2612–2615.

Hinz, H.-J., Tenchova, R., Tenchov, B., Quinn, P.J., 1996. Lamellar-non-lamellar phase transitions in synthetic glycoglycerolipids studied by time-resolved X-ray diffraction. Liq. Cryst. 20, 469–482.

Ishizuka, I., Yamakawa, T., 1985. Glycolipids. In: Wiegandt, H. (Ed.), New Comprehensive Biochemistry, vol. 10. Elsevier, pp. 101–197.

Jeffrey, G.A., Wingert, L.M., 1992. Carbohydrate liquid crystals. Liq. Cryst. 12, 179–202.

Kuttenreich, H., Hinz, H.-J., Inczedy-Marcsek, M., Koynova, R., Technov, B., Laggner, P., 1988. Polymorphism of synthetic 1,2-di-*O*-alkyl-3-*O*-β-D-galactopyranosyl-*sn*-glycerols of different alkyl chain length. Chem. Phys. Lipids 47, 245–260.

Mannock, D.A., Lewis, R.N.A.H., McElhaney, R.N., 1987. An improved procedure for the preparation of 1,2-di-*O*-acyl-3-O-(β-D-glucopyranosyl)-*sn*-glycerols. Chem. Phys. Lipids 43, 113–127.

Mannock, D.A., Lewis, R.N.A.H., McElhaney, R.N., 1990. The chemical synthesis and physical characterisation of 1,2-di-*O*-acyl-3-*O*-(β-D-glucopyranosyl)-*sn*-glycerols, an important class of membrane glycolipids. Chem. Phys. Lipids 55, 309–321.

Mannock, D.A., Harper, P.E., Gruner, S.M., McElhaney, R.N., 2001. The physical properties of glycosyl diacylglycerols. Calorimetric, X-ray diffraction and Fourier transform spectroscopic studies of a homologous series of 12-di-*O*-acyl-3-*O*-(β-D-galactopyranosyl)-*sn*-glycerols. Chem. Phys. Lipids 111, 139–161.

Masuda, M., Vill, V., Shimizu, T., 2000. Conformational and thermal phase behaviour of oligomethylene chains constrained by carbohydrate hydrogen-bond networks. J. Am. Chem. Soc. 122, 12327–12333.

Minamikawa, H., Murakami, T., Hato, M., 1994. Synthesis of 1,3-di-*O*-alky-2-*O*-(β-D-glycosyl)glycerols bearing oligosaccharides as hydrophilic groups. Chem. Phys. Lipids 72, 111–118.

Minden, V.H.M., Morr, M., Milkereit, G., Heinz, E., Vill, V., 2002a. Synthesis and mesogenic properties of glycosyl diacylglycerols. Chem. Phys. Lipids 114, 55–80.

Minden, V.H.M., Milkereit, G., Vill, V., 2002b. Effects of carbohydrate headgroups on the stability of induced cubic phases in binary mixtures of glycolipids. Chem. Phys. Lipids 120, 45–56.

Nagatsu, A., Watanabe, M., Ikemoto, K., Hashimoto, M., Murakami, N., Sakakibara, J., Tokuda, H., Nishino, H., Iwashima, A., Yazawa, K., 1994. Synthesis and structure–anti-tumor-promoting activity relationship of monogalactosyl diacylglycerols. Bioorg. Med. Chem. Lett. 4, 1619–1622.

Pedersen, J.S., 1997. Analysis of small-angle scattering data from colloids and polymer solutions: modelling and leastsquares fitting. Adv. Colloid Interf. Sci. 70, 171–210.

Prade, H., Miethchen, R., Vill, V., 1995. Thermotrop flüssig-kristalline Kohlenhydrat-amphiphile. J. Prakt. Chem. 337, 427–440.

Schmidt, R.R., Stumpp, M., 1983. Synthese von 1-thioglycosiden. Liebigs Ann. Chem. 1249–1256.

Schmidt, R.R., Jankowski, K., 1996. New types of nonionic surfactants with sugar head groups. Liebigs Ann. 4, 867–879.

Six, L., Rueß, K.-P., Liefländer, M., 1983. An efficient synthesis of 12-*O*-dialkyl-3-*O*-β-D-glycosyl-*sn*-glycerols. Tetrahedron Lett. 24, 1229–1232.

Stuhrmann, H.B., Burkhardt, N., Dietrich, G., Jünemann, R., Meerwinck, W., Schmitt, M., Wadzack, J., Willumeit, R., Zhao, J., Nierhaus, K.H., 1995. Nucl. Instrum. Methods 356, 133–137.

Vill, V., Böcker, T., Thiem, J., Fischer, F., 1986. Studies on liquid crystalline glycosides. Liq. Cryst. 6, 349–356.

Wignall, G.D., Bates, F.S., 1986. Absolute calibration of small-angle neutron-scattering data. J. Appl. Crystallogr. 20, 28–40.

Chapter 3

Micellar Structure of a

Sugar-based Bolaamphiphile in pure Solution

and Destabilizing Effects in Mixtures of Glycolipids

Micellar structure of a sugar based bolaamphiphile in pure solution and destabilizing effects in mixtures of glycolipids

Vasil M. Garamus [a,*], Götz Milkereit [b], Sven Gerber [b], Volkmar Vill [b]

[a] *GKSS Research Centre, Max-Planck-Straße 1, Abt. WFS – Geb. 03 D-21502 Geesthacht, Germany*
[b] *Institute of Organic Chemistry, University of Hamburg, Martin-Luther-King-Platz 6, D-20146 Hamburg, Germany*

Abstract

We have synthesized a new type of bolaamphiphile with disaccharide headgroups at the polar terminus and an alkyl chain of 12 carbon atoms. The self organization properties of the pure compound in dilute aqueous solutions have been investigated using surface tension measurements critical micelle concentration (CMC) and small angle neutron scattering (aggregate structure). Additionally, we have used the bolaamphiphile as a dopant to solutions of octyl-β-D-glucoside. Addition of bolaamphiphile shifts the CMC to higher values compared to ideal mixing and decreases the size of micelles.
© 2004 Elsevier B.V. All rights reserved.

1. Introduction

Glyco glycero lipids are known to be important constituents of many cell membranes. Naturally occurring glyco glycerol lipids normally have an Y-shaped structure with a polar carbohydrate head group linked to an 1,2- or 1,3-di-*O*-acyl or alkyl-*sn*-glycerol [1–5]. Additionally, cell membranes consist of a wide variety of lipids (e.g. phospholipids, alkyl glycosides). Whereas the above mentioned lipid compositions are mainly occurring in plant and bacteria cell membranes, a special kind of glycolipids can be found in a few bacteria that can exist in very hostile environments. These lipids, the so-called bolaamphiphiles, are characteristic for their unusual chemical structure. The principal structure is shown in Fig. 1. The non polar part of the lipids is connected on both ends of the chain to polar head groups. The difference to normal lipids can be seen in the formation of the lipid bilayer. Normal lipids build up bilayers with one molecule on each side of the membrane, whereas bolaamphiphiles form bilayers where the

inner and outer sides of the membrane consist of only one molecule. Bolaamphiphiles show unusual high melting points as reported by Mitsutoshi [6] and this property can be a possible explanation for the temperature resistance of the cell membrane of *archaebacteria* [7]. Until now only very few data are available regarding bolaamphiphiles [8] and especially data of the sugar based ones can hardly be found.

We have synthesized a new bolaamphiphile with two disaccharide head groups, linked to an alkyl chain consisting of 12 carbon atoms. The lyotropic properties of the pure compound were investigated using small angle neutron scattering and surface tension measurements. In a second experiment, the mixture of the bolaamphiphile with the well known surfactant octyl-β-D-glucoside is studied.

2. Materials and methods

2.1. Synthesis

Synthesis of 1,12-Bis-[4''-*O*-(α-D-glucopyranosyl)-β-D-glucopyranosyl)]-dodecane (**MDM**) will be published elsewhere. The purity of this compound was 99%

* Corresponding author. Fax: +49-4152-871356.
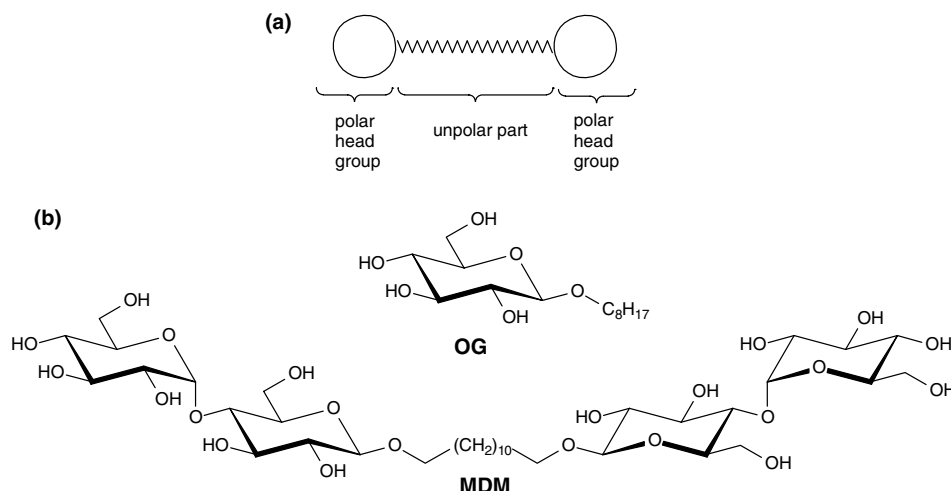*E-mail address:* vasyl.haramus@gkss.de (V.M. Garamus).

Fig. 1. (a) Principal structure of bolaamphiphiles; (b) investigated compounds: Octyl-β-D-glucopyranoside (**OG**); 1,12-Bis-[4″-*O*-(α-D-glucopyranosyl)-β-D-glucopyranosyl]-dodecane (**MDM**).

(Fig. 1). Octyl β-D-glucopyranoside (**OG**) was prepared from 1-octanol and 1,2,3,4,6-penta-*O*-acetyl-β-D-glucopyranoside according to standard procedures [9]. The compound was obtained in a purity of 99.8% (Fig. 1).

2.2. Surface tension

Surface tension was measured on a Krüss K6 tensiometer (Krüss, Germany), using the de Noüy ring method. Measurements were carried out using bidestilled water with a surface tension of $\sigma = 72$–73 mN/m. Correction for the ring geometry and the hydrostatic lifted volume of liquid was made using the method described by Harkins and Jordan or by Zuidema and Waters [10,11]. The reproducibility between measurements on different samples was ± 1 mN/m.

2.3. Small angle neutron scattering

Small angle neutron scattering experiments were performed on the SANS-1 instrument at the FRG-1 research reactor in GKSS Research Centre, Geesthacht, Germany [12]. Four sample-to-detector distances (from 0.7 to 9.7 m) were employed to cover the range of scattering vectors q from 0.005 to 0.25 Å^{-1}. The neutron wavelength λ was 8.1 Å with a wavelength resolution of 10% (full-width-at-full-maximum).

The solutions were prepared in D$_2$O (Deutero GmbH, purity 99.98%). The samples were kept in quartz cells (Hellma) with a path length of 5 mm. The samples were placed in a thermostated holder, for isothermal conditions $T = 25.0 \pm 0.5$ °C. The raw spectra were corrected for the background from the solvent, sample cell, and other sources, by conventional procedures [13,14] and converted to an absolute scale.

The average excess scattering length density per unit mass $\Delta\rho_m$ of the surfactant in deuterated water was determined from the known chemical composition, it was equal to $\Delta\rho_m = -4.883 \times 10^{10}$ cm/g for **OG** and $\Delta\rho_m = -3.34 \times 10^{10}$ cm/g for **MDM**.

3. Results and discussion

3.1. Determination of critical micelle concentration

Surface tension measurements were performed to obtain the critical micelle concentration (CMC) of the mixture solutions with different fractions of **OG** in the mixture of **OG** and **MDM**. The CMC values were obtained as intersection of linear extrapolated values of the surface tension below and above the CMC [15].

Fig. 2 shows the CMC values of the mixtures together with the theoretical curve for the CMCs of ideal mixing surfactants which was calculated within the regular solution theory using [16,17]

$$\frac{1}{\text{CMC}_{\text{mix}}} = \frac{\alpha}{f_1 \text{CMC}_1} + \frac{1-\alpha}{f_2 \text{CMC}_2}, \tag{1}$$

where f_1, f_2 the activity coefficients of **OG** and **MDM** in mixed micelles (for ideal mixing $f_1 = f_2 = 1$). CMC$_1$ corresponds to **OG**/water mixture (19.7 ± 1.9 mM) and CMC$_2$ corresponds to **MDM**/water ones (0.44 ± 0.03 mM).

It is easy to see that the experimental values of the CMC are always higher than the values expected for an ideal mixing. It shows that there is some repulsive interaction between the surfactant molecules. It can be expected that the parameters f_1 and f_2 are larger than 1 and the corresponding parameter β, which is related to an interaction between surfactants in mixed micelles, is positive [16,17].
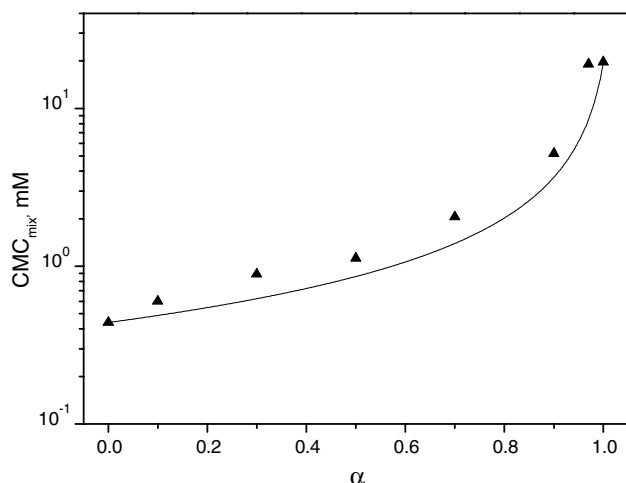
Fig. 2. CMC as a function of surfactant composition of **OG** and **MDM** mixtures (symbols) and ideal mixing curve (solid line). α is the molar fraction of **OG**.

3.2. Determination of micellar structure

SANS data were collected for the following solutions: **OG** in D$_2$O (0.01 g/mL, 34.2 mM); **MDM** in D$_2$O (0.01 g/mL, 11.8 mM); the mixture of **OG**(0.01 g/mL, 34.2 mM) and of **MDM** (0.001 g/mL; 1.18 mM) in D$_2$O at 25 °C. The scattering curves for **OG** and **MDM** obtained by small angle neutron scattering are shown in Fig. 3. The scattering intensities of compounds **OG** and **MDM** are very different. **OG** represents the typical scattering for anisotropic aggregates (short rod-like aggregates) which were reported earlier [18]. In the case of **MDM** solutions, we have observed strong scattering in the
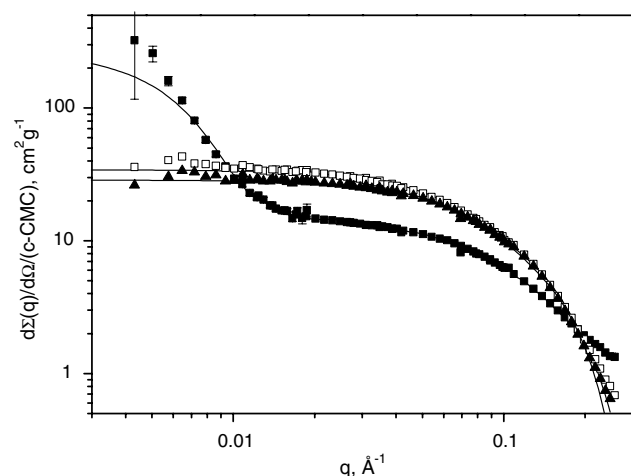

Fig. 3. SANS data of solutions of pure 1,12-bis-[4″-*O*-(α-D-glucopyranosyl)-β-D-glucopyranosyl]-dodecane 0.01 g/mL (filled squares), pure Octyl-β-D-glucopyranoside 0.01 g/mL (empty squares) and mixture of OG (0.01 g/mL) with 0.001 g/mL of MDM in D$_2$O, $T = 25$ °C. Solid lines are fits by IFT (**MDM**) and cylindrical model (**OG** and mixture).

lower q region which points to the presence of very large aggregates. But there is also a significant scattering at the higher q range, i.e., it is a sign of smaller aggregates, too. It seems that there are populations of aggregates with different sizes. The scattering curve of the mixed solution is similar to the curve of pure **OG**, as it should be expected due to the very small molar fraction of added **MDM**, although the curve is lower than the scattering curve of the pure **OG** solution. This could mean a decreasing of the micelles upon the addition of **MDM**.

In the case of **MDM**/D$_2$O solution, we have used a model independent analysis, i.e., indirect Fourier transformation method (IFT) which does not demand any a priori information about the structure of the studied aggregates [19].

The overall shape and dimensions of studied aggregates can be estimated from the pair distribution function $p(r)$. The scattering intensities are written in the form of pair distribution function by Fourier transform which, for an isotropic sample, can be expressed as

$$\mathrm{d}\Sigma(q)/\mathrm{d}\Omega = 4\pi \int_0^\infty p(r) \frac{\sin qr}{qr} \mathrm{d}r. \tag{2}$$

The pair distribution function is connected with the contrast $\Delta\rho(r)$ (difference between scattering length density of aggregate at point r, $\rho(r)$, and averaged scattering length density of solvent ρ_s, $\Delta\rho(r) = \rho(r) - \rho_s$) via an autocorrelation function of the contrast

$$p(r) = r^2 \int \Delta\rho(u)\Delta\rho(r+u)u^2 \mathrm{d}u. \tag{3}$$

In IFT method the pair distribution function of an aggregate with finite maximal dimensions D_{max} is approximated by a linear combination of a finite number, N, of cubic B-splines, evenly distributed in the interval $[0, D_{max}]$:

$$p(r) = \sum_{i=1}^N a_i\varphi_i(r), \tag{4}$$

where a_i is the coefficient of the ith cubic B-spline $\varphi_i(r)$. a_i are fitting parameters which are optimized using a least-squares method of minimization together with smoothness constraint.

The IFT analysis has been performed twice: i) for the whole q range (fit is shown in Fig. 3) and ii) for large q range ($q > 0.02$ Å^{-1}). The aim of this additional procedure is to get information about scattering of small aggregates only (large q). The obtained $p(r)$ functions are shown in Fig. 4. As we have expected there are two maxima (whole q range analysis) at $r \sim 15$ Å and $r \sim 350$ Å. Analysis of large q range (empty symbols) and whole q interval (filed symbols) gives the consistent results for interval of r for small particles. It points that the difference in size of aggregates is so large that there is no overlapping in scattering curve. The size of large
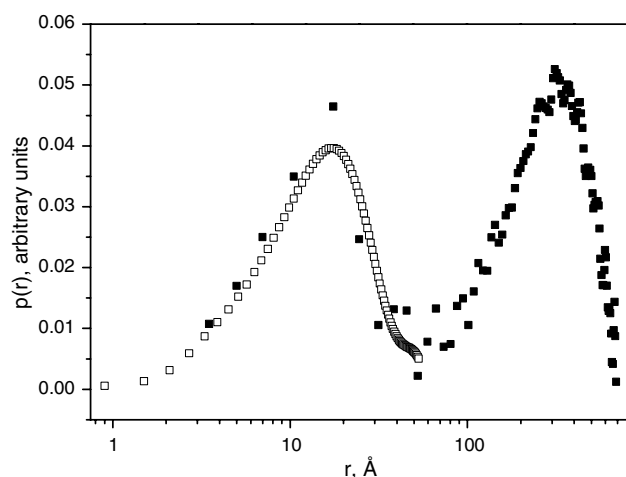
Fig. 4. Pair distance distribution function obtained by IFT analysis for solution of **MDM** (empty symbols are results of analysis of only the large q part of spectra, $q > 0.02$ Å^{-1}).

aggregates should be considered with caution due to limited q range. It can be expected that the larger aggregate radius is not smaller than 350 Å. From the radius of smaller aggregates ($\sim$15 Å) and known molecular structure one can determine the aggregation number of **MDM** aggregate as $\sim$14.

The scattering data of **OG**/D$_2$O solution and of **OG**/**MDM**/D$_2$O mixture were modeled by population of rod-like particles. For a mono-disperse system of anisotropical interactive particles, which is a reasonable approximation for micelles at low concentrations, the scattering cross-section d$\Sigma(q)$/dΩ can be described in a decoupling approximation by [20]

$$d\Sigma(q)/d\Omega = nP(q)S'(q), \tag{5}$$

where

$$P(q) = \left\langle |F(q)|^2 \right\rangle, \tag{6}$$

$$S'(q) = 1 + \beta(q)[S(q) - 1], \tag{7}$$

$$\beta(q) = |\langle F(q)\rangle|^2 / \left\langle |F(q)|^2 \right\rangle. \tag{8}$$

The inner brackets $\langle \ \rangle$ in Eqs. (6) and (8) represent an average weighted by the distribution of particle sizes and/or orientations, n is the number density (corresponding to the concentration) of the particles in the solution, $P(q)$ is the form factor, $F(q)$ is the amplitude of the form factor, $S(q)$ is the structure factor, and $S'(q)$ is the effective structure factor modified by the anisotropy and polydispersity of particles. In the case of cylindrical particles, $F(q)$ is expressed as

$$F(q) = \Delta\rho V \frac{\sin(qL/2\cos\beta)2J_1(qR\sin\beta)}{(qL/2\cos\beta)(qR\sin\beta)}, \tag{9}$$

where $\Delta\rho$ is the average difference in scattering density between the particles and the solvent, V is the volume of

a particle, L is the length of the cylinder, R is the radius of the cylinder, J_1 is the first-order Bessel function, and β is the angle between the q vector and the axis of the cylinder [21].

Fig. 3 shows a reasonable agreement between experimental data and model fits. The values of the fit parameters show that micelles become smaller upon addition of **MDM** to the solution, i.e., length of micelles decreases from $L = 74 \pm 4$ Å (aggregation number $\sim$80) for the pure **OG** solution to $L = 63 \pm 3$ Å (aggregation number $\sim$68) for the **OG**–**MDM** mixture. The radius of cross-section does not change $R = 12 \pm 1$ Å.

As reported by Caponetti et al. [22], the size of micelles formed by bolaform (non-carbohydrate surfactant) can be reduced upon the addition of salt, in our case, we reduced the size of micelles formed by normal alkyl glucoside by the addition of a bolaamphiphile.

Previously [18], we have got length of **OG** micelle $L = 96 \pm 2$ Å for 100 mM solution. One can conclude that micelles grow with concentration of **OG**.

From present SANS data, we cannot say how much **MDM** is present in micelles. This question can be answered by using deuterated **OG**. One can expect that the fraction of **MDM** is small.

4. Conclusions

A new carbohydrate based bolaamphiphile (**MDM**) has been synthesized and described by surface tension and small angle neutron scattering. **MDM** shows quite low CMC values and population of supramolecular aggregates with different length scales (small $r \sim 15$ Å and large $r \sim 350$ Å). The interaction of **MDM** with octyl glucoside (**OG**) is antagonistic, which is confirmed by a higher mixture CMC compared to the ideal mixing expectation (the value of parameter β is positive) and a decreasing of length of **OG** micelles upon addition of small amount of **MDM** to the solution (from 74 to 63 Å). The results are unexpected, because due to the very similar chemical structure of the investigated compounds (**OG**, one gluco-headgroup; **MDM**, two gluco-based-headgroups) normally an increase in the size of micelles would be expected. The biological relevance of this effect is under investigation.

References

[1] I. Isjizuka, T. Yamakawa, in: H. Wiegandt (Ed.), New Comprehensive Biochemistry, vol. 10, Elsevier, 1985.
[2] H.M. von Minden, M. Morr, G. Milkereit, E. Heinz, V. Vill, Chem. Phys. Lipids 114 (2002) 55.
[3] D.A. Mannock, R.N.A.H. Lewis, R.N. McElhaney, Chem. Phys. Lipids 43 (1987) 113.
[4] D.A. Mannock, R.N.A.H. Lewis, R.N. McElhaney, Chem. Phys. Lipids 55 (1990) 309.

[5] D.A. Mannock, P.E. Harper, S.M. Gruner, R.N. McElhaney, Chem. Phys. Lipids 111 (2001) 139.

[6] M. Mitsutoshi, V. Vill, T. Shimizu, J. Am. Chem. Soc. 122 (2000) 12327.

[7] Y. Rivaux, N. Noiret, H. Patin, New. J. Chem. (1998) 857.

[8] O. Kandler, in: M.J. Danson, D.W. Hough, G.G. Lunt (Eds.), The Archebacteria: Biochemistry and Biotechnolgy, Portland Press, London, 1992, p. 195.

[9] G. Milkereit, M. Morr, J. Thiem, V. Vill, Chem. Phys. Lipids 127 (2004) 47.

[10] F. Harkins, O. Jordan, J. Phys. Chem. 58 (1954) 825.

[11] H.H. Zuidema, G.W. Waters, Indus. Eng. Chem. 13 (1941) 312.

[12] H.B. Stuhrmann, N. Burkhardt, G. Dietrich, R. Jünemann, W. Meerwinck, M. Schmitt, J. Wadzack, R. Willumeit, J. Zhao, K.H. Nierhaus, Nucl. Instr. and Meth. A 356 (1995) 133.

[13] G.D. Wignall, F.S. Bates, J. Appl. Cryst. 20 (1986) 28.

[14] J.S. Pedersen, D. Posselt, K. Mortensen, J. Appl. Cryst. 23 (1990) 321.

[15] B. Jönsson, B. Lindmann, K. Holmberg, B. Kronberg, Surfactants and Polymers in Aqueous Solution, second ed., Wiley, New York, 2003.

[16] J.H. Clint, J. Chem. Soc., Faraday Trans. 71 (6) (1975) 1327.

[17] P.M. Holland, Adv. Colloid Interface Sci. 26 (1986) 111.

[18] L.-Z. He, V.M. Garamus, B. Niemeyer, H. Helmholz, R. Wilumeit, J. Mol. Liq. 89 (2000) 239.

[19] O. Glatter, J. Appl. Cryst. 10 (1977) 415.

[20] M. Kotlarchyk, S.H.J. Chen, J. Chem. Phys. 79 (1983) 2461.

[21] J.S. Pedersen, Adv. Colloid Interface Sci. 70 (1997) 171.

[22] E. Caponetti, D. Chillura-Martino, C. La Messa, R. Muzzalupo, L. Pedone, J. Phys. Chem. B 108 (2004) 1214.

Chapter 4

Comparison of the Supramolecular Structures of
two Glycolipids with Chiral and Non-chiral
Methyl Branched Alkyl Chains from Natural Sources

Comparison of the Supramolecular Structures of Two Glyco Lipids with Chiral and Nonchiral Methyl-Branched Alkyl Chains from Natural Sources

Götz Milkereit,[†] Vasil M. Garamus,[‡] Jun Yamashita,[§] Masakatsu Hato,[§] Michael Morr,[||] and Volkmar Vill*,[†]

Institute of Organic Chemistry, University of Hamburg, Martin Luther King Platz 6, D-20146 Hamburg, Germany, GKSS Research Centre, Max Planck Straße 1, D-21502 Geesthacht, Germany, Nanotechnology Research Institute, AIST, 1-1-1 Higashi, Tsukuba Central 5, Tsukuba, Ibaraki 305-8565, Japan, and Gesellschaft für Biotechnologische Forschung mbH, Mascheroder Weg 1, D-38124 Braunschweig, Germany

Two alkyl glycosides with the same type of disaccharide headgroups (melibiose) and different methyl-branched alkyl chains, short chiral [(2R,4R,6R,8R)-2,4,6,8-tetramethyldecyl, extracted from an animal source] and long nonchiral (3,7,11,15-tetramethylhexadecyl, from a plant source), were synthesized. The supramolecular aggregate structure formed in dilute solutions was investigated by small-angle neutron scattering and surface tension measurements. The lyotropic phase diagram was studied by differential scanning calorimetry and water penetration scans. The thermotropic phase behavior was investigated by polarizing microscopy. The compounds showed unusual phase behavior: (i) The liquid-crystalline polymorphism is reduced to only form smectic A phases in the pure state; the formation of lyotropic phases such as hexagonal or lamellar phases was not observed. (ii) The compound with the longer nonchiral alkyl chain is more soluble in water than the one with the shorter chiral chain, most likely because of the different flexibilities of the chains. (iii) For the long-chain compound, the formation of micelles is observed, whereas the short-chain compound forms large disklike/bilayer aggregates. The method of methylation of the chain controls the self-assembly and can explain different biological functions for either plants (variable temperature) or animals (constant temperature).

1. Introduction

The first observation of lyotropic liquid-crystalline phase behavior was in 1884 when Koch observed unusual optical textures upon the investigation of aqueous dispersions of extracts from tuberculosis bacteria.[1] The observation of thermotropic liquid crystallinity is also related to alkylated carbohydrates. Fischer and Helferich observed a double melting of hexadecyl-β-D-glucopyranoside.[2] These amphotropic molecules that form both thermotropic and lyotropic mesophases gained much interest during recent years.[3−7] They are mainly nontoxic and biodegradable and can be obtained from renewable sources.

The principal phase behavior of these compounds is shown in Figure 1.[8,9] A typical amphiphile is represented by a vertical line and usually exhibits only one mesophase, but in the case of an unusual geometry of the hydrophilic headgroup, polymorphism can occur. In this case, cubic phases may also be observed,[10] while simple amphiphiles normally exhibit only a smectic A (S_A) phase thermotropically.[11]

Deviation from the previously mentioned vertical line may also be seen upon the addition of solvents, the most common of which is water, because of its biological relevance. Whereas small amounts of water will not change the phase type and transition temperatures, larger amounts will introduce new phases, such as cubic and columnar phases ($H_{I/II}$). Upon the
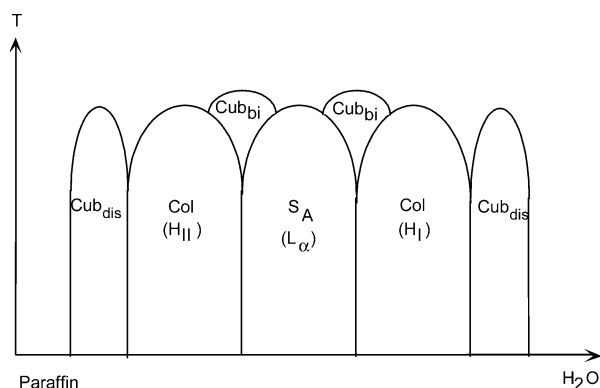
Figure 1. Principal phase behavior of amphiphilic compounds.[8,9]

addition of paraffin, it is possible to induce inverse phases (e.g., inverse micelles), with the polar headgroup curved away from the solvent.

The discontinuous cubic phases are based upon various packings of spherical or slightly anisotropic micelles, whereas the bicontinuous cubic phases with interwoven fluid porous structures are based upon underlying infinite periodic minimal surfaces.[12] This phase, in particular, is of great biological interest.[13−18] The lamellar (L_α) phase with its multibilayer structure has long been well-known to biologists, but there is much evidence today that the bicontinuous cubic phase may play an important role in processes such as membrane fusion.

A problem in lipid and surfactant investigations is solubility. Surfactants that are soluble in water show no polymorphism that would be interesting for biophysical investigations, whereas compounds that show this polymorphism are often not soluble

* Corresponding author. Phone: +49 40-42 838 4269. Fax: +49 40-42 838 4325. E-mail: vill@liqcryst.chemie.uni-hamburg.de.
† University of Hamburg.
‡ GKSS Research Centre.
§ Nanotechnology Research Institute, AIST.
|| Gesellschaft für Biotechnologische Forschung mbH.
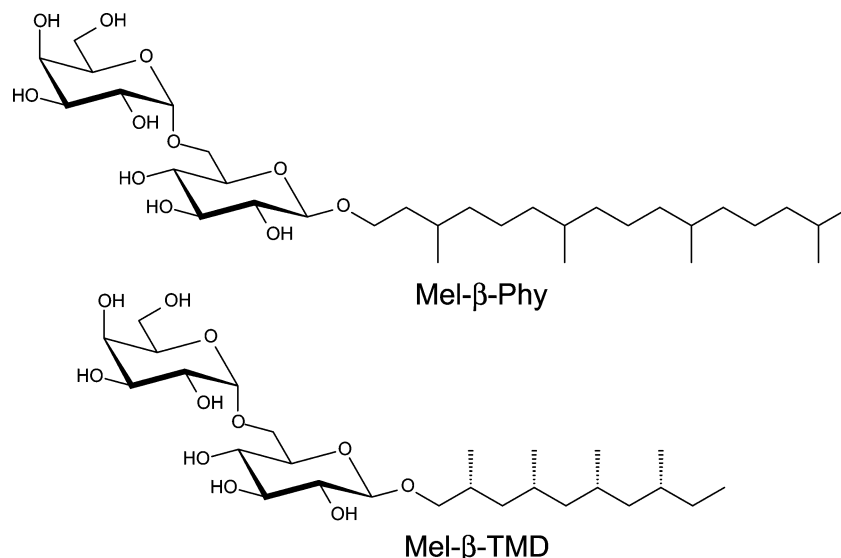
Figure 2. Chemical structures of the investigated glycolipids 1-*O*-[(2″*R*,4″*R*,6″*R*,8″*R*)-2″,4″,6″,8″-tetramethyldecyl]-6-*O*-(α-D-galactopyranosyl)-β-D-glucopyranoside (Mel-β-TMD) and 1-*O*-(3″,7″,11″,15″-tetramethylhexadecyl)-6-*O*-(α-D-galactopyranosyl)-β-D-glucopyranoside (Mel-β-Phy).

in water because of the length of the alkyl chain. With increasing chain length, the melting temperature and the Krafft temperature (or gel to liquid-crystalline phase transition; T_K) rise. For example, T_c of dodecyl-maltoside is below 25 °C and rises for stearyl-maltoside to 40 °C.[19]

To circumvent this problem, alkyl glycosides with unsaturated chains were synthesized;[19,20] the melting point and T_c could be lowered by this to below 0 °C. The disadvantage of these molecules is the lability of the double bond, which is unstable in oxidative environments and often not stable during chemical modifications. A different approach is the use of methyl-branched alkyl chains, with a homogeneous alternating sequence of branching. There are two main sources for this type of chain. The isoprenoid-type alcohols can be obtained from plant sources, as short-chain (gernaniol) and long-chain alcohols (phytanol). Several lipids of these plant-based carbohydrates were synthesized, and their lyotropic properties were thoroughly investigated.[21−26] A shorter-chained methyl-branched fatty alcohol can be obtained from animal sources. The preen gland of the domestic goose is a source for the chiral alcohol (2*R*,4*R*,6*R*,8*R*)-tetramethyldecanol. Several glyco glycero lipids and alkyl glycosides with this type of alcohol have been synthesized.[27−29] These compounds also showed liquid-crystalline phase behavior at ambient temperature.

For biological model systems, it is often necessary to also test lipids with an uncommon carbohydrate headgroup. Whereas, for technical applications, glucosides and maltosides are used, uncommon or expensive carbohydrate headgroups are less frequently used and investigated. Nevertheless, it is useful if the results obtained for branched maltosides (T_K is lowered) can be applied to other disaccharide compounds. Additionally, it would be interesting to see if these compounds would then still show a phase behavior similar to that of the *n*-alkyl analogues, which is often much more complex than that of glucosides or maltosides.

In this paper, we report about the synthesis of two different alkyl glycosides with the same disaccharide headgroups and different alkyl chains (Figure 2). As a carbohydrate headgroup, we chose the α1→6-linked sugar melibiose, consisting of a galactose moiety and a glucose moiety. These α1→6-linked headgroups are of particular interest because they show a much more complex polymorphism than the commonly used α1→4- or β1→4-linked disaccharides (for example, maltose or lactose).

As alkyl chains, we chose the phytanyl chain with a chain length of 16 methylene groups (4 additional methylene groups in the branched part) and the (all-*R*) tetramethyldecyl chain with a chain length of 10 methylene groups (4 additional methylene groups in the branched part). The thermotropic properties were studied using polarizing microscopy, the lyotropic phase sequence was studied by the contact preparation method, and differential scanning calorimetry was performed at defined water concentrations. The critical micelle concentration (cmc) was measured by the surface tension method, and additionally, geometric properties were calculated from this. The micellar aggregate structures in dilute solution were investigated using small-angle neutron scattering (SANS).

2. Materials and Methods

2.1. Materials. α-D-Melibiose monohydrate was purchased from Acros Organics. Solvents were distilled prior to use. 6-*O*-(2′,3′,4′,6′-Tetra-*O*-acetyl-α-D-galactopyranosyl)-1,2,3,4-tetra-*O*-acetyl-β-D-glucopyranoside (melibiose peracetate) was prepared according to standard procedures. 3,7,11,15-Tetramethylhexadecan-1-ol was prepared by hydrogenation of 3,7,11,15-tetramethylhexadec-2-en-1-ol (Merck, Darmstadt) in the presence of palladium on charcoal (10%; Fluka) as described by Minamikawa et al.[21,30] The chiral fatty alcohol (2*R*,4*R*,6*R*,8*R*)-tetramethyldecan-1-ol was prepared using extracts from rump glands of *Anser a.f. domesticus*.[31,32]

Thin-layer chromatography (TLC) was performed on silica gel (Merck GF254), and detection was effected by spraying with a solution of ethanol/sulfuric acid (9:1, v/v), followed by heating. Column chromatography was performed using silica gel (Merck, 0.063−0.200 mm, 230−400 mesh). NMR spectra were recorded on a Bruker AMX 400 or DRX5001 spectrometer (m_c = centered multiplet, d = doublet, t, = triplet, dd = double doublet, and dt = doublet triplet). *J* values are given in hertz.

2.2. Synthesis. *1-O-[(2″R,4″R,6″R,8″R)-2″,4″,6″,8″-Tetramethyldecyl]-6-O-(2′,3′,4′,6′-tetra-O-acetyl-α-D-galactopyranosyl)-2,3,4-tri-O-acetyl-β-D-glucopyranoside (**1**).* Totals of 3.39 g (5 mmol) of melibiose peracetate and 1.07 g (5 mmol) of (2*R*,4*R*,6*R*,8*R*)-2,4,6,8-tetramethyldecan-1-ol were dissolved in 50 mL of dry dichloromethane under an atmosphere of dry nitrogen. A total of 994 mg (880 µL; 7 mmol) of boron trifluoride etherate was added, and the solution was stirred for

Comparison of the Structures of Two Glyco Lipids

J. Phys. Chem. B, Vol. 109, No. 4, 2005 **1601**

6 h at ambient temperature until TLC revealed the reaction to be complete. The reaction was quenched with 50 mL of a saturated solution of sodium hydrogen carbonate, the organic layer was separated, and the aqueous layer was extracted twice with dichloromethane. The combined organic phases were washed twice with water, dried over magnesium sulfate, and evaporated in vacuo. The residue was purified by column chromatography [light petroleum (bp 50−70 °C)/ethyl acetate (2:1)]. Yield: 0.99 g (24%). $C_{40}H_{64}O_{18}$ (860.2967). ^{1}H NMR (400 MHz, CDCl$_3$ + TMS): δ 5.38 (dd, 1H, H-4′), 5.28 (dd, 1H, H-3′), 5.14 (t, 1H, H-3), 5.09 (d, 1H, H-1′), 5.04 (dd, 1H, H-2′), 5.02 (t, 1H, H-4), 4.87 (dd, 1H, H-2), 4.40 (d, 1H, H-1), 4.17 (m$_c$, 1H, H-5′), 3.99−4.08 (m, 3H, H-6a, H-6a′, H-6b′), 3.69 (dd, 1H, H-6b), 3.58 (ddd, 1H, H-5), 3.53 (m$_c$, 1H, H-αa), 3.23 (m$_c$, 1H, H-αb), 2.06, 1.99 (je 1, 3H, OAc), 1.98 (s, 6H, OAc), 1.97, 1.94, 1.91 (each s, 3H, OAc), 1.78 (m$_c$, 1H, H-β), 1.57 (m$_c$, 1H, H-δ), 1.55 (m$_c$, 1H, H-ζ), 1.40 (m$_c$, 1H, H-θ), 1.37 (m$_c$, H-ιa), 1.32 (m$_c$, 1H, H-γa), 1.22 (m$_c$, H-ηa), 1.19 (m$_c$, 1H, H-ϵa), 1.03 (m$_c$, 1H, H-ιb), 0.95 (d, 3H, CH$_3$-β), 0.86−0.92 (m, 2H, H-γb, H-ϵb), 0.88 (d, 3H, CH$_3$-δ), 0.86 (t, 3H, alkyl-CH$_3$), 0.81−0.85 (m, 1H, H-ηb), 0.84 (d, 3H, CH$_3$-θ), 0.82 (d, 3H, CH$_3$-ζ); $^3J_{1,2}$ = 8.1, $^3J_{2,3}$ = 9.7, $^3J_{3,4}$ = 9.7, $^3J_{4,5}$ = 9.7, $^3J_{5,6a}$ = 4.8, $^3J_{5,6b}$ = 2.6, $^3J_{6a,b}$ = 11.2, $^3J_{1',2'}$ = 3.6, $^3J_{2',3'}$ = 10.7, $^3J_{3',4'}$ = 3.5, $^3J_{4',5'}$ = 1.3, $^3J_{CH_3-\beta,\beta}$ = 6.6, $^3J_{CH_3-\delta,\delta}$ = 6.6, $^3J_{CH_3-\zeta,\zeta}$ = 6.6, $^3J_{CH_3-\theta,\theta}$ = 6.6, $^3J_{alkyl-CH_3,\iota}$ = 6.6. ^{13}C NMR (400 MHz, CDCl$_3$ + TMS): δ 170.52, 170.30, 170.18, 169.84, 169.32, 169.28 (C=O, OAc), 101.42 (C-1), 96.75 (C-1′), 75.08 (C-α), 72.94 (C-3), 72.61 (C-5), 71.32 (C-2), 69.10 (C-4), 68.05, 68.03 (C-4′, C-2′), 67.42 (C-3′), 66.47 (C-5′), 66.39 (C-6), 61.60 (C-6′), 45.36 (C-ϵ), 44.58 (C-η), 41.03 (C-γ), 31.52 (C-θ), 30.35 (C-β), 28.81 (C-ι), 27.43 (C-ζ), 27.31 (C-δ), 21.11 (CH$_3$-δ), 20.98 (CH$_3$-ζ), 20.77, 20.70, 20.67, 20.64 (−CH$_3$, OAc), 20.08 (CH$_3$-θ), 17.78 (CH$_3$-β), 11.24 (alkyl-CH$_3$).

1-O-[(2″R,4″R,6″R,8″R)-2″,4″,6″,8″-Tetramethyldecyl]-6-O-(α-D-galactopyranosyl)-β-D-glucopyranoside (Mel-β-TMD). A total of 0.97 g (1.16 mmol) of **1** was dissolved in 50 mL of anhydrous methanol, and sodium methoxide was added (pH 8−9). The solution was stirred at ambient temperature until TLC revealed the reaction to be complete. It was neutralized using Dowex 50WX ion-exchange resin (protonated form), filtered, and evaporated in vacuo. The product was recrystallized from propan-2-ol. Yield: 588 mg (94%). $C_{26}H_{50}O_{11}$ (538.3353). $[\alpha]^{20}_D$ +52 (c 0.8, MeOH). HIRESFAB-MS (m/z): 561.6758 [M + Na]$^+$. ^{1}H NMR (500 MHz, methanol-d$_4$): δ 4.89 (d, 1H, H-1′), 4.31 (d, 1H, H-1), 4.01 (dd, 1H, H-6a), 3.90−3.95 (m, 2H, H-4′, H-5′), 3.88 (dt, 1H, H-αa), 3.69−3.80 (m, 4H, H-2′, H-3′, H-6a′, H-6b, H-6b′), 3.68 (dd, 1H, H-αa), 3.58 (dt, 1H, H-αb), 3.50 (ddd, 1H, H-5), 3.48 (dd, 1H, H-αb), 3.43 (dd, 1H, H-4), 3.38 (dd, 1H, H-3), 3.21 (dd, 1H, H-2), 1.93 (m$_c$, 1H, H-β), 1.61−1.65 (m, 2H, H-δ, H-ζ), 1.49 (m$_c$, 1H, H-θ), 1.44 (m$_c$, H-ιa), 1.42 (m$_c$, 1H, H-γa), 1.32 (m$_c$, H-ηa), 1.27 (m$_c$, 1H, H-ϵa), 1.10 (m$_c$, 1H, H-ιb), 0.99 (d, 3H, CH$_3$-β), 0.96 (m$_c$, 1H, H-γb), 0.95 (m$_c$, 1H, H-ϵb), 0.94 (d, 3H, CH$_3$-δ), 0.93 (t, 3H, alkyl-CH$_3$), 0.92 (d, 3H, CH$_3$-θ), 0.90 (d, 3H, CH$_3$-ζ), 0.88 (m$_c$, 1H, H-ηb); $^3J_{1,2}$ = 8.1, $^3J_{2,3}$ = 9.2, $^3J_{3,4}$ = 9.2, $^3J_{4,5}$ = 9.2, $^3J_{5,6a}$ = 4.1, $^3J_{5,6b}$ = 2.0, $^2J_{6a,b}$ = 11.2, $^3J_{1',2'}$ = 4.1, $^3J_{H-\alpha a,\beta}$ = 7.6, $^3J_{H-\alpha b,\beta}$ = 5.1, $^3J_{H-\alpha a,b}$ = 9.2, $^3J_{CH_3-\beta,\beta}$ = 6.6, $^3J_{CH_3-\delta,\delta}$ = 6.6, $^3J_{CH_3-\zeta,\zeta}$ = 6.6, $^3J_{CH_3-\theta,\theta}$ = 6.1, $^3J_{alkyl-CH_3,\iota}$ = 6.6.

1-O-(3″,7″,11″,15″-Tetramethylhexadecyl)-6-O-(2′,3′,4′,6′-tetra-O-acetyl-α-D-galactopyranosyl)-2,3,4-tri-O-acetyl-β-D-glucopyranoside (2). Totals of 3.39 g (5 mmol) of melibiose peracetate, 1.49 g (5 mmol) of 3,7,11,15-tetramethylhexadecan-1-ol, and 994 mg (880 μL; 7 mmol) of boron trifluoride etherate in 50 mL of anhydrous dichloromethane were reacted as described

for compound **1**. Yield: 1.28 g (28%). $C_{46}H_{76}O_{18}$ (944.3906). ^{1}H NMR (400 MHz, CDCl$_3$ + TMS): δ 5.42 (dd, 1H, H-4′), 5.32 (dd, 1H, H-3′), 5.18 (dd, 1H, H-3), 5.18 (dd, 1H, H-3), 5.13 (d, 1H, H-1′), 5.08 (dd, 1H, H-2′), 5.04 (dd, 1H, H-4), 4.90 (dd, 1H, H-2), 4.45 (d, 1H, H-1), 4.28 (ddd, 1H, H-5′), 4.08 (dd, 1H, H-6a′), 4.03 (dd, 1H, H-6b′), 3.80 (dt, 1H, H-αa), 3.73 (dd, 1H, H-6a), 3.62 (ddd, 1H, H-5), 3.55 (dd, 1H, H-6b), 3.42 (dt, 1H, H-αb), 2.10, 2.09, 2.01, 2.00, 1.97, 1.95 (each s, 3H, OAc), 1.45−1.64 (m, 4H, H-γ, H-η, H-λ, H-o), 0.98−1.64 (m, 20H, CH$_2$-β, CH$_2$-δ, CH$_2$-ϵ, CH$_2$-ζ, CH$_2$-υ, CH$_2$-ι, CH$_2$-χ, CH$_2$-μ, CH$_2$-ν, CH$_2$-ξ), 0.87 (d, 3H, CH$_3$-δ), 0.84 (d, 6H, CH$_3$-η, CH$_3$-λ), 0.81 (d, 6H, CH$_3$-o, CH′$_3$-o); $^3J_{1,2}$ = 8.1, $^3J_{2,3}$ = 9.7, $^3J_{3,4}$ = 9.7, $^3J_{4,5}$ = 9.7, $^3J_{5,6a}$ = 5.1, $^3J_{5,6b}$ = 2.5, $^3J_{6a,b}$ = 11.2, $^3J_{1',2'}$ = 3.6, $^3J_{2',3'}$ = 10.7, $^3J_{3',4'}$ = 3.1, $^3J_{4',5'}$ = 1.0, $^3J_{5',6a'}$ = 5.6, $^3J_{5',6b'}$ = 6.6, $^3J_{6a',b'}$ = 11.2, $^3J_{\alpha a,\beta-CH_2}$ = 6.1, $^3J_{\alpha b,\beta-CH_2}$ = 6.6, $^3J_{\alpha a,b}$ = 9.7, $^3J_{CH_3,CH_2}$ = 6.6.

1-O-(3″,7″,11″,15″-Tetramethylhexadecyl)-6-O-(α-D-galactopyranosyl)-β-D-glucopyranoside (Mel-β-Phy). A total of 1.20 g (1.31 mmol) of **2** was deprotected as described for compound Mel-β-TMD. Yield: 741 mg (91%). $C_{32}H_{62}O_{11}$ (622.4292). $[\alpha]^{20}_D$ +48 (c 1.0, MeOH). HIRESFAB-MS (m/z): 645.0382 [M + Na]$^+$. ^{1}H NMR (400 MHz, methanol-d$_4$): δ 4.89 (d, 1H, H-1′), 4.31 (d, 1H, H-1), 4.01 (dd, 1H, H-6a), 3.90−3.95 (m, 2H, H-4′, H-5′), 3.52−3.86 (m, 6H, H-2′, H-3′, H-6a′, H-6b, H-6b′, H-αa, H-αb), 3.50 (ddd, 1H, H-5), 3.43 (dd, 1H, H-4), 3.38 (dd, 1H, H-3), 3.21 (dd, 1H, H-2), 1.65−1.75 (m, 4H, H-γ, H-η, H-λ, H-o), 1.01−1.64 (m, 20H, CH$_2$-β, CH$_2$-δ, CH$_2$-ϵ, CH$_2$-ζ, CH$_2$-υ, CH$_2$-ι, CH$_2$-χ, CH$_2$-μ, CH$_2$-ν, CH$_2$-ξ), 0.94 (d, 3H, CH$_3$-δ), 0.84 (d, 6H, CH$_3$-η, CH$_3$-λ), 0.90 (d, 6H, CH$_3$-o, CH′$_3$-o); $^3J_{1,2}$ = 8.1, $^3J_{2,3}$ = 9.2, $^3J_{3,4}$ = 9.2, $^3J_{4,5}$ = 9.2, $^3J_{5,6a}$ = 4.1, $^3J_{5,6b}$ = 2.0, $^2J_{6a,b}$ = 11.2, $^3J_{1',2'}$ = 4.1.

2.3. Surface Tension. Surface tension was measured on a Krüss K6 tensiometer (Krüss), using the de Noüy ring method. Measurements were carried out using bidistilled water with a surface tension of σ = 72−73 mN/m. All values were corrected for the temperature. Corrections for the ring geometry and the hydrostatic lifted volume of the liquid were made using the method described by Harkins and Jordan[33] or by Zuidema and Waters.[34]

2.4. SANS. SANS experiments were performed with the SANS-1 instrument at the FRG1 research reactor at the GKSS Research Centre.[35] Four sample-to-detector distances (from 0.7 to 9.7 m) were employed to cover the range of scattering vectors q from 0.005 to 0.25 Å^{-1}. The neutron wavelength λ was 8.1 Å with a wavelength resolution of 10% (full-width at full-maximum).

The solutions were prepared in D$_2$O (Deutero GmbH; purity 99.98%). The samples were kept in quartz cells (Hellma) that had a path length of 5 mm. The samples were placed in a thermostated holder for isothermal conditions T = 25.0 ± 0.5 and 50.0 ± 0.5 °C. The raw spectra were corrected for the background from the solvent, sample cell, and other sources by conventional procedures.[36] The two-dimensional isotropic scattering spectra were azimuthally averaged, converted to an absolute scale, and corrected for detector efficiency by dividing them by the incoherent scattering spectra of pure water,[36] which was measured with a 1 mm pathlength quartz cell (Hellma).

The average excess scattering-length density per unit mass ($\Delta\rho_m$) of the surfactant in deuterated water was determined from the known chemical composition, and it was equal to −4.92 × 10^{10} cm/g for compound Mel-β-Phy and −4.51 × 10^{10} cm/g for compound Mel-β-TMD.

2.5. Polarizing Microscopy and Contact Preparation. An Olympus BH optical polarizing microscope equipped with a
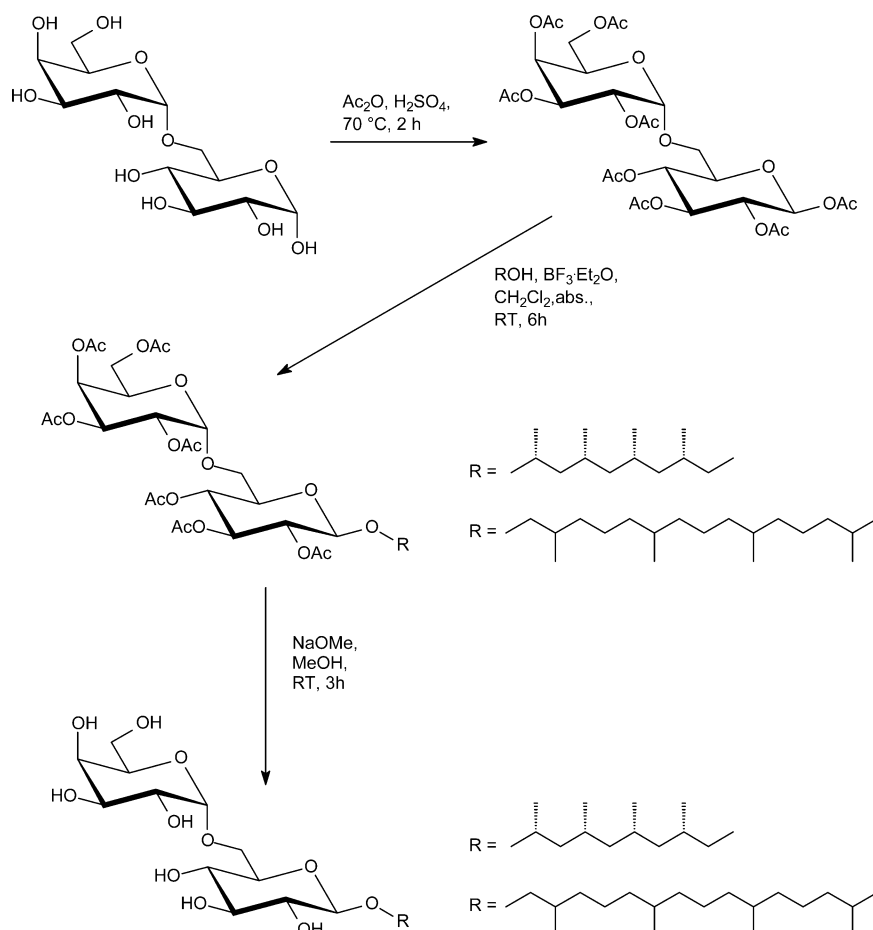
Figure 3. Synthetic procedure for the preparation of Mel-β-TMD and Mel-β-Phy.

Mettler FP 82 hot stage and a Mettler FP 80 central processor was used to identify thermal transitions and characterize anisotropic textures.

For the contact preparation, a small amount of sample was placed on a microscope slide and covered with a cover glass before heating it to the liquid-crystalline phase (S_A or Col). Afterward, a small amount of solvent was placed on the slide at the edge of the cover glass. As soon as the solvent had moved under the cover glass and the sample was completely surrounded by the solvent, it was again placed, for a few seconds, on the hot stage at a temperature of 100−120 °C, and the phase behavior was investigated immediately afterward by polarizing microscopy.

2.6. Differential Scanning Calorimetry (DSC). The thermal phase behavior of the investigated compounds was investigated using a Seiko SSC/560U differential scanning calorimeter. The lipid/water mixtures were sealed in silver DSC capsules. To fully develop crystals of Mel-β-Phy, the samples (49 wt % lipid) were incubated at −20 °C for 3 h before a heating run was initiated at a rate of 0.2 °C/min. For Mel-β-TMD, the samples (54 wt % lipid) were incubated at −40 °C for 3 h before initiating a heating run at a rate of 0.4 °C/min. A cooling run was not performed because of a great degree of supercooling of the samples.

3. Results and Discussion

3.1. Compounds and Synthesis. Figure 3 shows the synthetic route for the preparation of the investigated compounds. Although the preparations of both glycosides follow the same route, the alcohols needed for the preparations were prepared

in different ways. Phythanol (3,7,11,15-tetramethylhexadecan-1-ol), for the preparation of Mel-β-Phy, was prepared by a simple catalytic hydrogenation of phythol (3,7,11,15-tetra-methylhexadec-2-en-1-ol), as described by Minamikawa et al.[21,30]

The chiral methyl-branched fatty alcohol (2R,4R,6R,8R)-2,4,6,8-tetramethyldecanol was prepared from natural sources as described by Morr et al.[31,32] Using extracts from the preen glands of the domestic goose (*Anser a.f. domesticus*), the alcohol is prepared in a multistep synthesis by transesterification, Spaltrohr distillation, and reduction of the fatty acid methyl ester. The alcohol was obtained with a diastereomeric excess of more than 99%.

The synthesis of compounds Mel-β-TMD and Mel-β-Phy was carried out using standard procedures.[6] Protection of the sugar in acetic acid anhydride/sulfuric acid afforded the β-peracetate in a good yield. The glycosylation reaction using boron trifluoride etherate as a Lewis acid gave the desired β-glycosides. Deprotection using the standard Zemplén procedure finally led to the desired products.

3.2. Thermotropic Liquid-Crystalline Properties. The thermotropic properties were investigated using polarizing microscopy. The following liquid-crystalline phases and transition temperatures were found (Cr = crystalline; g = glass; I = isotropic):

Mel-β-TMD	Cr	<20.0	S_A	156.9	I
Mel-β-Phy	g	?	S_A	178.6	I

Compound Mel-β-TMD, with the short alkyl chain, is already a liquid crystal at ambient temperature. The compound forms a

Comparison of the Structures of Two Glyco Lipids

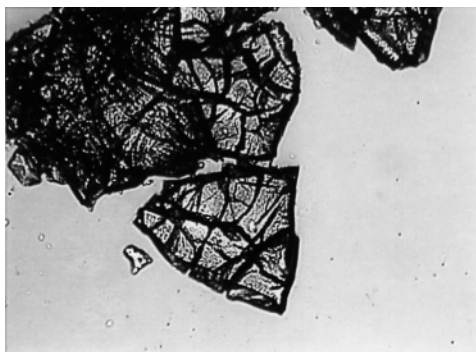*J. Phys. Chem. B, Vol. 109, No. 4, 2005* **1603**

Figure 4. Water-penetration scan for Mel-β-Phy at 23 °C ($\times$40). There was no sign of water penetration, and crystals remained, even after 24 h of contact with water. When the temperature exceeded 40 °C, the crystals melted and quickly turned into a transparent isotropic solution (see text).

Figure 5. Heating curve of a 49 wt % Mel-β-Phy/water system (heating rate: 0.2 °C/min).

S$_A$ phase over the whole temperature range. Compound Mel-β-Phy also exclusively forms a L$_\alpha$ phase. The clearing temperature is 21.7 K higher compared to that of Mel-β-TMD. Both compounds cannot be obtained in a crystalline form, like most of the known branched-chain glycolipids. The glass temperature (T_g) of Mel-β-TMD is below room temperature, whereas Mel-β-Phy has a T_g above room temperature. It forms a rigid glass structure with cracks resulting from shrinking during cooling of the glassy state.

Unfortunately, no reliable data on the thermotropic and lyotropic phase sequence and transition temperatures for the corresponding *n*-decyl-, *n*-hexadecyl-, or *n*-eicosanyl-melibiosides can be found. Despite this, the data for the *n*-dodecyl- and *n*-octadecyl-melibiosides[19] provide sufficient information for a comparison. *n*-Dodecyl-melibioside forms a cubic phase above the melting point (155 °C) upon heating, whereas upon cooling from the isotropic phase, a S$_A$ phase is formed. However, *n*-octadecyl-melibioside has a melting point of 152 °C, and above that, a S$_A$ phase is formed throughout the whole temperature range up to the clearing temperature (262 °C).

The melting point is lowered in both cases. In the case of the tetramethyldecyl chain, the effect is even much stronger than that for the tetramethylhexadecyl chain. This means that the distance between the methyl groups in the branching has to be taken into account. With decreasing distances between the methyl groups, the disturbance of the packing density in the chains rises. Another effect is the change in the molecular shape. The molecular geometry of *n*-dodecyl-melibioside lies between a rodlike and a wedge-shaped structure, which can be seen from the phases formed. The tetramethyldecyl chain then leads to a stable rodlike structure; thus, a stable thermotropic S$_A$ phase is formed. Mel-β-Phy also forms a S$_A$ phase, but compared to *n*-octadecyl-melibioside, the temperature range of this phase is small, indicating that the shape is still rodlike. However, upon heating, a change of shape is favored.

3.3. Thermal and Lyotropic Phase Behavior of the Lipid/Water Systems. *Mel-β-Phy/Water System.* Water-penetration (contact-penetration) experiments of Mel-β-Phy displayed rather unusual phase behavior. Dry Mel-β-Phy was in the glass state at ambient temperature (23 °C) and did not show any sign of water penetration, even after 2 days of contact with water (see Figure 4). With increasing temperature (above 35 °C), the glass disappeared rapidly, forming a clear transparent solution. This may be attributable to the dissolving of Mel-β-Phy in water. Solutions of Mel-β-Phy then showed a moderate foaming ability. Because of the rapid change upon heating, it was not possible to observe any stable water-penetration textures that are gener-
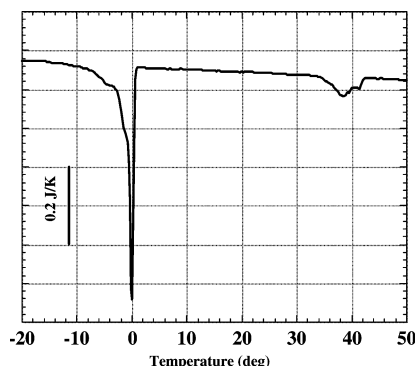
ally observed in water-penetration experiments. Upon cooling of the transparent aqueous solution, the solid again started to appear below 20 °C. This observation is consistent with the DSC measurements. Figure 5 shows a typical example of the DSC thermogram of the Mel-β-Phy/water system (49 wt %), in which an endothermic peak ($\Delta H = 38$ kJ/mol) associated with the glass $\leftrightarrow$ L$_\alpha$ phase transition of Mel-β-Phy was observed between 33 and 43 °C. The endothermic peak that starts at about -15 °C and ends at about 1 °C belongs to the melting of frozen water in the Mel-β-Phy/water system. Compared to normal ice melting, the water started to melt at significantly lower temperatures. This suggests that the melting of ice in the Mel-β-Phy/water system, occurring throughout a wide temperature range, is a result of different water organization.

Mel-β-TMD/Water System. Dry Mel-β-TMD exhibited birefringent textures at 23 °C. Upon addition of water, an isotropic region started to grow from the Mel-β-TMD/water interface, with a concomitant decrease in the birefringent Mel-β-TMD region (see Figure 6). The birefringent Mel-β-TMD region eventually disappeared, resulting in a two-phase-coexistence system of the isotropic phase (I) and the aqueous system (W). As seen in Figure 6c, the isotropic (most probably Mel-β-TMD-rich) phase dispersed as spherical liquid droplets in an aqueous solution phase. Thus, the isotropic phase observed in the water-penetration scan (Figure 6a,b) was not a cubic phase. The turbid two-phase state remained unaltered at least up to 70 °C. When the two-phase solution was incubated at 4 °C, the liquid droplets transformed into birefringent solid particles.

The observation is consistent with the DSC thermogram of the Mel-β-TMD/water system (54 wt %). The thermogram consists of two endothermic peaks. The lower endothermic peak is most presumably the one associated with the melting of frozen water in the Mel-β-TMD/water system. The second peak, overlapping with the first endothermic peak, is associated with the phase transition of Mel-β-TMD. The endotherm completed at about 18 °C (indicated by an arrow in Figure 7).

To summarize the results, the Mel-β-Phy/water system displayed a T_K of about 33 °C, above which the system formed an isotropic transparent solution with moderate foaming ability. This indicates that Mel-β-Phy is soluble in water by forming normal micelles at temperatures above its T_K. Compound Mel-β-TMD, on the other hand, was not soluble in water, even at temperatures above its T_K. The Mel-β-TMD/water system forms a two-phase solution that consists of a lipid-rich phase and an aqueous solution (most probably built up by isotropic disklike aggregates/bilayer aggregates; see section 3.5). As shown in section 3.5, the concentration of Mel-β-TMD in the aqueous solution is about 10^{-3} g/mL ($\sim$18 times the cmc). Thus, Mel-β-Phy, with its phytanyl chain (a total of 20 carbon atoms), is
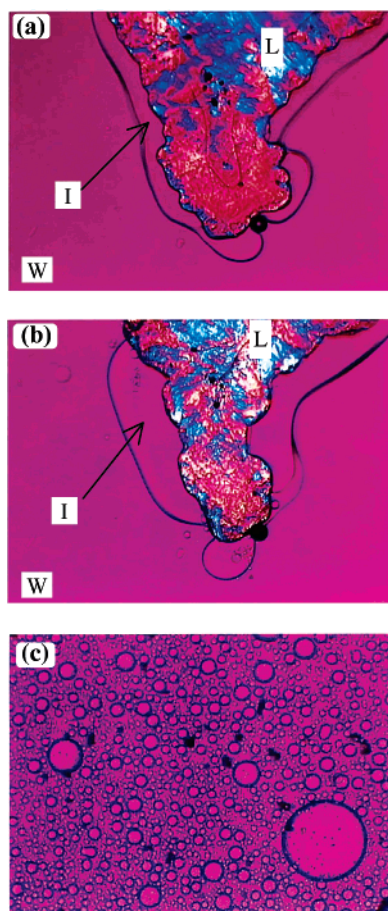
Figure 6. Water-penetration scan of Mel-β-TMD at 23 °C (×40). W: water region. I: isotropic region. L: lipid region. Microscopic pictures at (a) 2 min of water penetration and (b) 5 min of water penetration. (c) Microscopic picture of a 3 wt % Mel-β-TMD/water system at 23 °C (×40). Spherical droplets of the water-swollen lipid phase (disklike/bilayer aggregates) are dispersed in the aqueous solution phase.

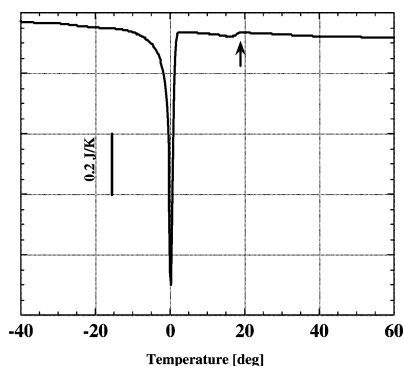**Figure 7.** Heating curve of a 54 wt % Mel-β-TMD/water system (heating rate: 0.4 °C/min).

more soluble in water than Mel-β-TMD, with its smaller hydrophobic chain (a total of 14 carbon atoms in the hydrophobic chain). A definite explanation will need a more detailed phase diagram, but a reason for this unexpected behavior might be found in the difference between the branched alkyl chains. In comparison to that of *n*-alkyl chains, the flexibility of the alkyl chain should be reduced, in the cases of both the phytanyl and tetramethyldecyl chains.[37] Nevertheless, the phytanyl chain should show some flexibility with its alternating $-(CH_2)_3-$ CHCH_3$-$ sequence. However, the tetramethyldecyl chain, with the alternating $-CH_2-CHCH_3-$ sequence, should show less flexibility. This is also indicated by the absence of the symmetric

stretching vibration band in Fourier transform infrared spectroscopy, which is found upon the investigation of glycosyl diacyl glycerols with tetramethyldecyl chains,[29] that is a sensitive marker of the alkyl and acyl chain order.[38] This can result in a rigid structure of compound Mel-β-TMD, even above T_K. The hydration and self-assembly that occurs upon the addition of water will be energetically more unfavorable than it will for the more flexible Mel-β-Phy.

Second, the good aqueous solubility of Mel-β-Phy appears to be in marked contrast to the phase behavior of another phytanyl-chained glycolipid, 1-*O*-phythanyl-β-D-maltoside, β-Mal_2(Phyt). Having a common phytanyl chain, their molecular structures differ only in their headgroup part, for example, melibiose for Mel-β-Phy and maltose for β-Mal_2(Phyt). It is interesting to note that the β-Mal_2(Phyt)/water system forms a water (dilute aqueous lipid solution) and a L_α two-phase region followed by a one-phase region of the L_α phase as the lipid concentration increases.[39] This again adds an intriguing example in which the saccharide headgroup has a significant effect on the physical behavior of glycolipid/water systems.[40]

Lowering T_K by using branched alkyl chains instead of *n*-alkyl chains is a common method employed in surfactant chemistry.[41] Unfortunately, no literature data are available on the T_K values of *n*-tetradecyl- or *n*-eicosanyl-melibiosides. Only data for *n*-dodecyl-melibioside ($T_K < 0$ °C) and *n*-octadecyl-melibioside ($T_K = 67.5$ °C) can be found.[19] From these data, the values for *n*-tetradecyl-glycoside (20−30 °C) and *n*-eicosanyl-glycoside (80−100 °C) can be estimated. When these values are compared with the DSC results, the difference between the branched chains is again visible. Whereas T_K of Mel-β-Phy (33 °C) is significantly lower than even that for octadecyl-melibioside, T_K of Mel-β-TMD (18 °C) seems to be in the same range as those for the corresponding *n*-alkyl analogues.

3.4. Surface Tension and Geometric Properties. Table 1 shows the geometrical properties of the investigated compounds. The carbon-chain volume and the extended chain length were calculated according to the method described by Tanford.[42] For the calculations, we assumed that the volume of the carbon chains totaled 14 and 20 carbon atoms for Mel-β-TMD and Mel-β-Phy, respectively. For the chain length, we assumed that the branching of the chain does not affect the chain length; therefore, the chain length will be, in the case of Mel-β-TMD, 10 carbon atoms and, in the case of Mel-β-Phy, 16 carbon atoms.

In Figure 8, the adsorption isotherms of the investigated compounds at the air solution interface are shown. The interfacial absorption behavior was investigated at 40 °C. Both compounds formed homogeneous solutions in the measured concentration range; no phase separation occurred, and no multiphase systems formed. No phase separation occurred above the cmc for compound Mel-β-Phy. For Mel-β-TMD at a concentration of 1×10^{-3} g/mL, the solution became cloudy, indicating the formation of bigger aggregates/phases or a solubility limit.

The data obtained from the surface tension measurements are presented in Table 1.

The cmc value of Mel-β-TMD is higher than that of compound Mel-β-Phy, which has a longer alkyl chain. The decrease of the cmc from Mel-β-TMD to Mel-β-Phy is in accordance with the theory predicting a decrease in cmc values with an increase in the alkyl chain length.[43]

From the pre-cmc slope, the headgroup area per molecule at the air−water interface was calculated. From this, the critical packing parameters (CPPs) were calculated.[41] As shown in Table 1, CPP predicts the formation of a bilayer structure for the

Comparison of the Structures of Two Glyco Lipids

J. Phys. Chem. B, Vol. 109, No. 4, 2005 **1605**

TABLE 1: Adsorption of Mel-β-TMD and Mel-β-Phy at the Air$-$Aqueous-Solution Interface and Data Calculated from the Pre-cmc Slope, $T = 40$ °C

	cmc [mM L^{-1}]	cmc [g/mL]	γ_{cmc} [mN/m]	γ_{min} [mN/m]	carbon chain volume[a] v_c [Å^3]	extended chain length[b] l_c [Å]	headgroup area[c] a_0 [Å^2]	critical packing parameter[d] $v_c/l_c a_0$
Mel-β-TMD	$0.1 \pm 2 \times 10^{-2}$	5.4×10^{-5}	35.6	35.2	404	14.15	23.1 ± 4	~1
Mel-β-Phy	$0.03 \pm 1 \times 10^{-2}$	1.87×10^{-5}	~36	~36	565.4	21.74	37 ± 15	0.7

[a] The values were calculated using $v_c = 27.4 + 26.9 n_c$. [b] Calculated with $l_c = 1.5 + 1.265 n_c$.[42] [c] Calculated from the pre-cmc slope. [d] Calculated from the carbon chain volume, the extended chain length, and the headgroup area per molecule at the air$-$water interface obtained from the pre-cmc slope.
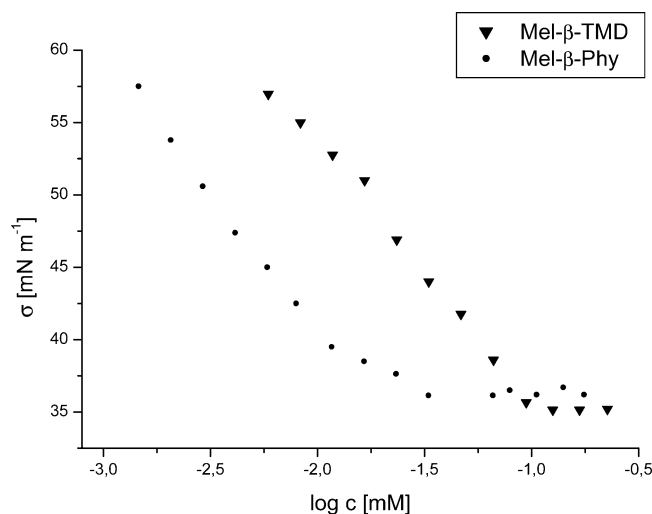
Figure 8. Surface tension plots for Mel-β-TMD and Mel-β-Phy at 40 °C.

Figure 9. Scattering curves and model fits for solutions of Mel-β-TMD ($c = 1.0 \times 10^{-3}$ g/mL; empty symbols) and Mel-β-Phy ($c = 5.0 \times 10^{-4}$ g/mL; filled symbols) in D$_2$O, $T = 50$ °C. The curves are normalized to the concentration of surfactant in aggregates ($c -$ cmc). The solid lines represent fits or approximations. The arrow points to the position of the maximum in the scattering data of Mel-β-TMD.

shorter-chained lipid Mel-β-TMD. For compound Mel-β-Phy, the prediction of the micellar shape is more difficult. The error in the determination of a_0 from the pre-cmc slope is very high because it is difficult to estimate the correct part in the slope of the curve (the value of CPP predicts a cylindrical structure of the micelles).
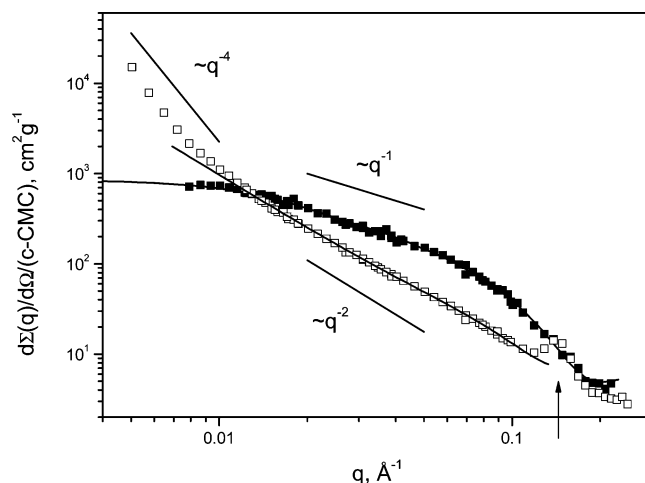
3.5. Analysis of SANS Data. SANS data were collected for solutions of Mel-β-TMD ($c = 1.0 \times 10^{-3}$ g/mL) and Mel-β-Phy ($c = 5.0 \times 10^{-4}$ g/mL) in D$_2$O at a temperature of 50 °C for Mel-β-Phy and 20, 50, and 70 °C for Mel-β-TMD. These concentrations are approximately 20$-$25 times the cmc value for both compounds. A detailed description of the analysis of the SANS data is given in the appendix.

The obtained scattering curves are very different for the two glycosides (shown in Figure 9). Compound Mel-β-TMD shows a high scattering at the lowest interval of the scattering vector ($q < 0.01$ Å^{-1}). At an intermediate q range (0.01$-$0.1 Å^{-1}), the scattering curve changes and shows a disklike behavior according to d$\Sigma(q)$/d$\Omega \sim q^{-2}$. For large values of q, a diffraction maximum ($q \approx 0.15$ Å^{-1}) is observed.

In contrast, the scattering curve of the lipid Mel-β-Phy shows a rodlike behavior at an intermediate range of the scattering vector (d$\Sigma(q)$/d$\Omega \sim q^{-1}$).

It can be assumed that the two lipids form different aggregate structures in an aqueous solution: (1) Mel-β-TMD forms large aggregates with partial-plane or disk-shaped substructures. (2) Mel-β-Phy forms small rodlike aggregates.

Mel-β-Phy Solutions. We started the analysis of the scattering data for compound Mel-β-Phy by applying the indirect Fourier transformation (IFT) method developed by Glatter,[44] using the version reported by Pedersen.[45] This model-independent approach needs only minor additional (model) information on the possible aggregate structure: dimensions (spherelike, rodlike, or disklike) and a maximal value of the diameter, cross-sectional

diameter, or thickness, respectively. The IFT routine for rodlike aggregates was applied to the large q part ($q > 0.02$ Å^{-1}). The large q part is chosen to ensure the validity of the approximation for rodlike aggregates (infinite long cylinder) $q > 1/L$, where L is the length of the cylinder.

We obtained the following values for the parameters: $R_{CS,g} = 13.4 \pm 0.2$ Å (the corresponding radius of the homogeneous circular cross section of Mel-β-Phy aggregates is 19.0 ± 0.4 Å) and $M_L = (1.4 \pm 0.1) \times 10^{-13}$ g/cm (this gives ~13 Mel-β-Phy molecules per 10 Å of aggregate length and ~90 Å^2 per one Mel-β-Phy molecule at the surface of the cylinder). The radius of the cylindrical cross section, calculated from the radius of gyration, points to an extended conformation of the alkyl chain in the rodlike aggregates (Table 1).

The analysis was continued with the model fitting. A cylindrical model was chosen and applied to the experimental data. In Figure 9, the experimental data and the applied model are shown. The applied model and the experimental scattering curve fit together throughout the whole interval of the scattering vector q. Using the data, we calculated the radius ($R = 19.2 \pm 0.4$ Å) and the length of the cylinder ($L = 290 \pm 10$ Å). The radii of the cylinder obtained by the two different methods (IFT analysis and model fitting) are in accordance. Both of the methods gave consistent results, which can be interpreted as the formation of short cylindrical aggregates in dilute solution. The results are summarized in Table 2.

The observations of the water-penetration scans of Mel-β-Phy are consistent with the results from SANS. Above T_K, Mel-β-Phy forms cylindrical micelles at a concentration that is 27 times above the cmc. The formation of micelles is similar to that of the *n*-alkyl counterparts. For example, for *cis*-9-

TABLE 2: Results of SANS Data Analysis by a Model-Independent Approach (IFT), Model Fitting, and Calculated Parameter of Aggregates for Mel-*β*-Phy (*c* = 5.0 × 10⁻⁴ g/mL, *T* = 50 °C)

micellar shape	cylindrical
radius of cylindrical cross section [Å]	19.0 ± 0.4
length [Å]	290 ± 10
mass per unit length [g/cm]	$(1.4 \pm 0.1) \times 10^{-13}$
number of molecules per 1 nm of length	~13
surface area per molecule [Å²]	90

TABLE 3: Results of SANS Data Analysis by Model-Independent Approach (IFT), Model Fitting, and Calculated Parameter of Aggregates for Mel-*β*-TMD (*c* = 1.0 × 10⁻³ g/mL, *T* = 25, 50, and 70 °C)

micellar shape	bilayer/large aggregates
radius [Å]	~4000 Å (large aggregates)
thickness of layer for [Å]	39 ± 2 (bilayer)
repeat distance between layers [Å]	$40-50$ (bilayer)
mass per surface unit [g/cm²]	$(8.3 \pm 0.5) \times 10^{-10}$ (bilayer)
surface area per molecule [Å²]	100 (bilayer)

octadecenyl-melibioside, the formation of long cylindrical micelles was observed.[38]

For compound Mel-*β*-Phy, the area per headgroup in the micelles obtained from the SANS data is about $2-3$ times higher than that at the liquid−air interface (Table 2). This shows that, in the micelle, a wedge-shaped packing of the molecules with a dense hydration of the carbohydrate headgroup can be assumed, whereas at the liquid−air interface, a nearly rodlike packing of the monolayers occurs.

*Mel-*β*-TMD Solution.* The scattering data of Mel-*β*-TMD show the so-called Porod behavior at the lowest interval of q ($q < 0.01$ Å⁻¹). It points to a smooth and sharp interface between large aggregates and the surrounding solvent. The following parameters of smaller disklike/bilayer aggregates were obtained from the analysis of the intermediate part of the scattering curve: a radius gyration of thickness of $R_{T,g} = 11.4 \pm 0.4$ Å (the corresponding thickness of bilayers of Mel-*β*-TMD is 39 ± 2 Å) and a mass per surface unit of $M_S = (8.3 \pm 0.5) \times 10^{-10}$ g/cm² (100 Å² per one Mel-*β*-TMD molecule in the surface of the bilayer).

We can summarize the results of the structural analysis as follows: Large aggregates ($R \sim 4000$ Å) are formed. The surface is smooth/sharp. Substructural units are disklike particles with a thickness of approximately 40 Å, and the formation of ordered bilayers with a repeat distance between the layers of $d \sim 40-50$ Å is observed. It is probable that we observed a phase transition at this concentration. The results are summarized in Table 3.

For compound Mel-*β*-TMD, the headgroup area in the bilayer obtained from SANS is about 4 times higher than that at the liquid−air interface (Table 3). This is due to the formation of different aggregates in solution that makes the calculation of the exact concentration in the single aggregates impossible. From the theoretical point of view, it is expected that the headgroup area in the bilayer should be in a range similar to that at the air−water interface.[41]

Contrary to the results obtained for solutions of Mel-*β*-Phy, compound Mel-*β*-TMD formed no micelles at a concentration of 1×10^{-3} g/mL (18 times above the cmc). In this case, the formation of large aggregates/lipid bilayers was observed. This can again be an indication that the alkyl chain of Mel-*β*-TMD is very rigid, which makes the formation of micelles, even at low concentrations, unfavorable. Nevertheless, concentrations below this were not investigated; thus, the formation of micelles in a very narrow concentration range near the cmc cannot be

excluded. For example, *n*-tetradecyl-melibioside forms spherical micelles.[38]

The CPP values calculated from the surface tension data (section 3.4) are in accordance with the results from the SANS analysis. Mel-*β*-Phy forms cylindrical micelles (CPP ~ 0.7), whereas Mel-*β*-TMD forms bilayer aggregates (CPP ~ 1).

4. Conclusions

Two new glycolipids with methyl-branched alkyl chains of different lengths and chiralities were synthesized. The combination of different analytical standard methods (polarizing microscopy, contact preparation, DSC, surface tension measurements, and SANS) gave a comprehensive characterization of the biophysical properties in the pure state and in an aqueous solution. The effect of the branching is obvious. The compounds show liquid-crystalline phase behavior near or at ambient temperature, although the phase behavior is changed. *n*-Alkyl-melibiosides exhibit a more complex polymorphism leading to the formation of lamellar, cubic, and columnar mesophases, because of the wedge-shaped geometry of the molecules, than was found for the investigated compounds. The use of methyl-branched alkyl chains instead of *n*-alkyl chains led to a general change of the physical properties. It is interesting to note that the solubility of Mel-*β*-TMD is low even above T_K. This is similar to the observations made for the tetramethyldecyl wax esters of the preen glands, which are responsible for the good water protection of the feathers of the domestic goose.[46] The method of methylation of the chain controls the self-assembly and can explain different biological functions for plants (variable temperature) and animals (constant temperature). The different influences of the branched chains can be used for the applications. Mel-*β*-Phy shows normal surfactant behavior starting with micelle formation and can be used as a sugar surfactant, exhibiting a galactose residue at the end of the disaccharide head. Conversely, Mel-*β*-TMD will form stable bilayers and can be used for building model membranes with an unusual carbohydrate head or more simple stabilized membranes.

The main observations that were made can be summarized as follows.

(1) Similar properties of Mel-*β*-Phy and Mel-*β*-TMD:

(a) The liquid-crystalline polymorphism is reduced to only form S_A phases in the pure state; the formation of lyotropic phases, such as hexagonal or lamellar phases, was not observed.

(b) No cubic or columnar phases were formed, because of the branched alkyl chains, therefore changing the molecular shape from wedge-shaped to a rodlike shape.

(c) The stability of the liquid-crystalline phase is increased.

(d) The melting points and T_K's are lowered.

(2) Differences between Mel-*β*-Phy and Mel-*β*-TMD:

(a) Mel-*β*-Phy forms cylindrical micelles.

(b) The less flexible TMD chain disables the formation of a large micellar solution region; compound Mel-*β*-TMD forms disklike aggregates/bilayers of small or medium size instead because no birefringent textures were observed for this phase region (Figure 6).

(c) Mel-*β*-TMD is not very soluble in water, even above T_K.

(d) Mel-*β*-Phy has a greater hydrophobic moiety than Mel-*β*-TMD, but it is more soluble in water, as a result of the more flexible phytanyl chain.

Comparison of the Structures of Two Glyco Lipids

J. Phys. Chem. B, Vol. 109, No. 4, 2005 **1607**

Appendix: Analysis of SANS Data

Mel-β-Phy Solutions. The scattering intensities for rodlike aggregates are written via the cross-sectional pair distance distribution function $p_{CS}(r)$:

$$d\Sigma(q)/d\Omega = \left(\frac{\pi}{q}\right) 2\pi \int_0^\infty p_{CS}(r) \, J_0(qr) \, dr \qquad (1)$$

where J_0 is the zeroth-order Bessel function.

The $p_{CS}(r)$ function is given by[44]

$$p_{CS}(r) = \frac{c - \text{cmc}}{2\pi M_L} \int r \Delta\rho(\mathbf{r}') \, \Delta\rho(\mathbf{r} + \mathbf{r}') \, d\mathbf{r}' \qquad (2)$$

where $\Delta\rho(r)$ is the contrast [difference between the scattering-length density of aggregates at the point r, $\rho(r)$, and the averaged scattering-length density of the solvent, ρ_s; $\Delta\rho(r) = \rho(r) - \rho_s$]; the vectors $\mathbf{r}$ and $\mathbf{r}'$ are lying in the cross-sectional plane.

The pair distance distribution function is expressed as a sum of N b splines evenly distributed in the interval $[0, D_{max}]$. The values of the coefficients are calculated numerically by a least-squares fitting of the IFT model curve to the experimental data. In the present study, the values of D_{max} were carefully chosen to give both good fits to the experimental data and smooth p_{CS}-(r) functions.

At the large q range ($q > 0.02$ Å^{-1}), the experimental data and the fitted curves coincide very well (data not shown).

The Gaussian shape of the pair distribution function is characteristic of almost-homogeneous cylindrical aggregates formed by compound Mel-β-Phy. Here, we got a first estimation of the cross-sectional diameter of approximately 40 Å, which is obtained from the maximum distance of $p_{CS}(r)$.

After determination of the pair distance distribution function, the mass per unit length of the aggregate M_L and the radius of gyration of the cross section of the micelle $R_{CS,g}$ will be calculated. The radius of gyration can be written as

$$R_{CS,g} = \left[\frac{\int_0^\infty r^2 p_{CS}(r) \, dr}{2 \int_0^\infty p_{CS}(r) \, dr} \right]^{1/2} \qquad (3)$$

The analysis was continued with the model fitting. A cylindrical model was chosen and applied to the experimental data. The model scattering cross section used for the fitting is based on the integral equation theory for polymers and the polymer reference interaction site model. For the isotropic solution of rigid cylinders, the scattering cross section was taken as[47]

$$d\Sigma(q)/d\Omega/(c - \text{cmc}) = M\Delta\rho_m^2 \frac{P_{cyl}(q)}{1 + \beta c(q) \, P_{rod}(q, L - 2\langle R \rangle)} \qquad (4)$$

where $\beta = [1 - S(0)]/S(0)$, with $S(0)$ being the structure factor calculated by the rigid cylinder model; that is, for a solution of isotropic rigid cylinders, $S(0)$ is calculated from the expression for the osmotic compressibility as determined in the scaled particle approximation:

$$S(0) = \frac{(1 - B - C)^4}{[1 + 2(B + C)]^2 + 2D[1 + B + (5/4)C]} \qquad (5)$$

In this equation, $B = \pi R^2 L n$, $C = 4/3 \pi R^3 n$, $D = 1/2 \pi R L^2 n$, L is the length of the cylinders, R is the radius of the cylinders, and n is the number concentration of the cylinders.

$P_{cyl}(q)$ is the form factor of a cylinder of length L and radius R:[48]

$$P_{cyl}(q) = 4 \int_0^{\pi/2} \left\{ \frac{\sin[qL/(2 \cos \beta)] 2J_1[qR \sin \beta]}{[qL/(2 \cos \beta)][qR \sin \beta]} \right\}^2 \sin \beta \, d\beta \qquad (6)$$

where J_1 is the first-order Bessel function.

$P_{rod}(q,L)$ is the form factor of an infinitely thin rod of length L:

$$P_{rod}(q) = 2Si(qL)/(qL) - 4 \sin^2(qL/2)/(q^2 L^2) \qquad (7)$$

where

$$Si(x) = \int_0^x t^{-1} \sin t \, dt$$

The function $c(q)$ is related to the Fourier transform of the "direct" correlation function, which we approximated by the Fourier transform of the correlation hole around each site:[45,47]

$$c(q) = \frac{3[\sin(qD') - qD' \cos(qD')]}{(qD')^3} \qquad (8)$$

where the diameter of the correlation hole is chosen as $D' = 2R$.

In the final fit, four parameters were fitted: the length of the micelle, the cross-sectional radius, a correction factor for the absolute scale, and a residual background. The correction factor for the absolute scale takes small errors of the concentration into account, and it is expected to be close to unity. The correction factor for the absolute scale variation is within 5% of unity, which reflects the accuracy of the absolute calibration of SANS data and of the surfactant concentration. The experimental data and the applied model are shown in Figure 9.

Mel-β-TMD Solution. The scattering data of Mel-β-TMD show the so-called Porod behavior at the lowest interval of q ($q < 0.01$ Å^{-1}):[48]

$$d\Sigma(q)/d\Omega \sim Aq^{-4} \qquad (9)$$

This points to a smooth and sharp interface between aggregates formed by Mel-β-TMD and the surrounding solvent. The parameter A is connected with the interfacial area S by

$$A = 2\pi \Delta\rho^2 S \qquad (10)$$

First, the parameter A was obtained from a fitting procedure at the lowest q region. With knowledge of the volume fraction of the surfactant and with the assumption that the formed aggregates are spherical, the size of the aggregates was estimated to be $R \sim 4000$ Å. This means that, even at this very low concentration, compound Mel-β-TMD forms not only simple micelles but large aggregates as well. Most probably, these are some sheets of lipid bilayers, which, with a further increase of concentration, will form a lamellar phase.

The position of the diffraction maximum in the scattering curve is connected to the distance between bilayers:

$$d = 2\pi/q_{max} \qquad (11)$$

From the quite-broad maximum in the SANS curve, d can be estimated to be 40−50 Å.

Next, the interval of q from 0.01 to 0.1 Å^{-1} was analyzed by the IFT method. This interval shows the scattering behavior ($d\Sigma$-$(q)/d\Omega \sim q^{-2}$) of disklike (bilayer) aggregates.

The scattering intensities for disklike aggregates are written in the form of the thickness pair distance distribution function $p_T(r)$:

$$d\Sigma(q)/d\Omega = \left(\frac{2\pi}{q^2}\right)\pi\int_0^\infty p_T(r)\cos(qr)\,dr \qquad (12)$$

The $p_T(r)$ function is given by[44]

$$p_T(r) = \frac{c - cmc}{2\pi M_S}\int \Delta\rho(\mathbf{r}')\,\Delta\rho(\mathbf{r} + \mathbf{r}')\,d\mathbf{r}' \qquad (13)$$

with r corresponding to the coordinate in the x direction and M_S corresponding to the mass per surface units of disklike aggregates.

Now we are able to describe the intermediate q interval for disklike aggregates by IFT (Figure 9). Similar to the method used for rodlike aggregates, the radius of gyration (thickness of $R_{T,g}$) and the mass per surface unit M_S can be calculated from $p_T(r)$.

References and Notes

(1) Koch, R. *Mitt. K. Gesundsheitsamt* **1884**, *2*, 1−88.

(2) Fischer, E.; Helferich, B. *Liebigs Ann. Chem.* **1911**, *383*, 68−91.

(3) Södermann, O.; Johansson, I. *Curr. Opin. Colloid Interface Sci.* **2000**, *4*, 391.

(4) Jeffrey, G. A. *Mol. Cryst. Liq. Cryst.* **1984**, *110*, 221−237.

(5) Böcker, T.; Thiem, J. *Tenside, Suractants, Deterg.* **1989**, *26*, 318−324.

(6) Vill, V.; Böcker, T.; Thiem, J.; Fischer, F. *Liq. Cryst.* **1989**, *6*, 349−356.

(7) Boullanger, P. Amphiphilic Carbohydrates as a Tool for Molecular Recognition in Organized Systems. In *Topics in Current Chemistry*; Drigenz, H., Thiem, J., Eds.; Springer: Berlin, 1998; Vol. 187, pp 275−312.

(8) Prade, H.; Miethchen, R.; Vill, V. *J. Prakt. Chem./Chem.−Ztg.* **1995**, *337*, 427−440.

(9) Blunk, D.; Praefke, K.; Vill, V. Amphotropic Liquid Crystals. In *Handbook of Liquid Crystals*; Demus, D., Goodby, J., Gray, G. W., Spiess, H.-W., Vill, V., Eds.; Wiley-VCH: Weinheim, Germany, 1998; Vol. 3, pp 305−340.

(10) Fischer, S.; Fischer, H.; Diele, S.; Pelzl, G.; Jankowski, K.; Schmidt, R. R.; Vill, V. *Liq. Cryst.* **1994**, *17*, 855−861.

(11) Jeffrey, G. A.; Wingert, L. M. *Liq. Cryst.* **1992**, *12*, 179−202.

(12) Fairhurst, C. E.; Fuller, S.; Gray, J.; Holmes, M. C.; Tiddy, G. J. Lyotropic Surfactant Liquid Crystals. In *Handbook of Liquid Crystals*; Demus, D., Goodby, J., Gray, G. W., Spiess, H.-W., Vill, V., Eds.; Wiley-VCH: Weinheim, Germany, 1998; Vol. 3, pp 341−392.

(13) Lindblom, R.; Rilfors, R. *Biochim. Biophys. Acta* **1989**, *988*, 221−256.

(14) Ellens, H.; Siegel, D. P.; Alford, D.; Yeagle, P. L.; Boni, L.; Lis, J.; Quinn, P. J.; Bentz, J. *Biochemistry* **1989**, *28*, 3692−3703.

(15) Siegel, D. P. *Biophys. J.* **1986**, *49*, 1155−1170.

(16) Siegel, D. P. *Biophys. J.* **1986**, *49*, 1171−11783.

(17) Siegel, D. P. *Chem. Phys. Lipids* **1986**, *42*, 279−301.

(18) Siegel, D. P.; Banschbach, J.; Alford, J.; Ellens, H.; Lis, L. J.; Quinn, P. J.; Yeagle, P. L.; Bentz, J. *Biochemistry* **1989**, *28*, 3703−3709.

(19) Minden, v. H. M.; Brandenburg, K.; Seydel, U.; Koch, M. H. J.; Garamus, V.; Willumeit, R.; Vill, V. *Chem. Phys. Lipids* **2000**, *106*, 157−179.

(20) Vill, V.; Minden, v. H. M.; Koch, M. H. J.; Seydel, U.; Brandenburg, K. *Chem. Phys. Lipids* **2000**, *104*, 75−91.

(21) Minamikawa, H.; Hato, M. *Langmuir* **1997**, *13*, 2564−2571.

(22) Minamikawa, H.; Hato, M. *Langmuir* **1998**, *14*, 4503−4509.

(23) Korchowiec, B. M.; Baba, T.; Minamikawa, H.; Hato, M. *Langmuir* **1998**, *17*, 1853−1859.

(24) Hato, M. *Curr. Opin. Colloid Interface Sci.* **2001**, *6*, 268−276.

(25) Hato, M.; Minamikawa, H.; Salkar, R. A.; Matsutani, S. *Langmuir* **2002**, *18*, 3425−3429.

(26) Salkar, R. A.; Minamikawa, H.; Hato, M. *Chem. Phys. Lipids* **2004**, *127*, 65−75.

(27) Minden, v. H. M.; Morr, M.; Milkereit, G.; Heinz, E.; Vill, V. *Chem. Phys. Lipids* **2002**, *114*, 55−80.

(28) Milkereit, G.; Morr, M.; Thiem, J.; Vill, V. *Chem. Phys. Lipids* **2004**, *127*, 47−63.

(29) Milkereit, G.; Gerber, S.; Brandenburg, K.; Koch, M. H. J.; Morr, M.; Seydel, U.; Vill, V. To be published.

(30) Minamikawa, H.; Murakami, T.; Hato, M. *Chem. Phys. Lipids* **1994**, *72*, 111−118.

(31) Morr, M.; Wray, V.; Fortkamp, J.; Schmid, R. D. *Liebigs Ann. Chem.* **1992**, *5*, 433−440.

(32) Morr, M.; Fortkamp, J.; Ruehe, S. *Angew. Chem.*, *Int. Ed. Engl.* **1992**, *36*, 2460−2462.

(33) Harkins, F.; Jordan, O. *J. Phys. Chem.* **1954**, *58*, 825.

(34) Zuidema, H. H.; Waters, G. W. *Ind. Eng. Chem.* **1941**, *13*, 312−313.

(35) Stuhrmann, H. B.; Burkhardt, N.; Dietrich, G.; Jünemann, R.; Meerwinck, W.; Schmitt, M.; Wadzack, J.; Willumeit, R.; Zhao, J.; Nierhaus, K. H. *Nucl. Instrum. Methods* **1995**, *A356*, 133−137.

(36) Wignall, G. D.; Bates, F. S. *J. Appl. Crystallogr.* **1986**, *20*, 28−40.

(37) Shinoda, W.; Mikami, M.; Baba, T.; Hato, M. *J. Phys. Chem. B* **2003**, *107*, 14030−14035.

(38) Garamus, V. M.; Milkereit, G.; Vill, V. To be published.

(39) Hato, M.; Minamikawa, H.; Salkar, R. A.; Matsutani, S. *Prog. Colloid Polym. Sci.* **2004**, *123*, 56−60.

(40) Hato, M.; Minamikawa, H. *Langmuir* **1996**, *12*, 1658−1665.

(41) Israelachvili, J. N. *Intermolecular and Surface Forces*, 2nd ed.; Academic Press: London, 1992.

(42) Tanford, C. *The Hydrophobic Effect: Formation of Micelle and Biological Membranes*; Wiley and Sons: New York, 1980.

(43) Jönsson, B.; Lindmann, B.; Holmberg, K.; Kronberg, B. *Surfactants and Polymers in Aqueous Solution*, 2nd ed.; John Wiley & Sons: Chichester, U.K., 2003.

(44) Glatter, O. *J. Appl. Crystallogr.* **1977**, *10*, 415−421.

(45) Pedersen, J. S. *Adv. Colloid Interface Sci.* **1997**, *70*, 171−210.

(46) Jacob, J. *Fortschr. Chem. Org. Naturst.* **1976**, *34*, 373.

(47) Schweizer, K. S.; Curro, J. G. *Chem. Phys.* **1990**, *149*, 105−127.

(48) Feigin, L. A.; Svergun, D. I. *Structure Analysis by Small-Angle X-ray and Neutron Scattering*; Plenum Press: New York, 1987.

Chapter 5

Structures of Micelles Formed by Alkyl Glycosides
with Unsaturated Alkyl Chains

Structures of micelles formed by synthetic alkyl glycosides with unsaturated alkyl chains

Götz Milkereit [a], Vasil M. Garamus [b,*], Koen Veermans [a], Regine Willumeit [b], Volkmar Vill [a]

[a] *Institute of Organic Chemistry, University of Hamburg, Martin-Luther-King-Platz 6, 20146 Hamburg, Germany*
[b] *GKSS Research Centre, Max Planck Str., 21502 Geesthacht, Germany*

Abstract

Three new alkyl glycosides with similar molecular structures (oleyl and oleoyl alkyl chains and various head groups: disaccharide, trisaccharide and disaccharide with an additional amidoethoxy spacer) were synthesized and their supramolecular structure in aqueous solution was investigated. Small angle neutron scattering, surface tension measurement and the contact preparation method were applied to get molecular structure–property relationships. Although the chemical structures differ only in small details, their CMC values, lyotropic phase behaviour, surface area per surfactant molecule in the micelle and at the liquid–air interface, and the size and shape of the micelles are very different. We have found three different types of aggregates: spherical, cylindrical and polymer-like micelles in dilute solutions.
© 2004 Elsevier Inc. All rights reserved.

Keywords: Alkyl glycosides; Small angle neutron scattering; Polymer-like micelles; Surface tension

1. Introduction

The unique properties of solutions of amphiphilic molecules in polar (e.g., water) and nonpolar (e.g., paraffin) solvents are well known [1]. The molecular structure of amphiphilic compounds has a great influence on the formation of specific structures like spherical, rod-like and worm-like micelles, vesicles and lamellar aggregates. Other properties such as the CMC, solubility of nondissolved substances or phase boundaries also depend on the molecular shape of the amphiphile [2]. The delicate balance between opposite forces associated with the hydrophobic and the hydrophilic parts of the molecule plays a key role especially in the case of long chain surfactants.

During the last decade biodegradable nontoxic surfactants synthesized from renewable sources have become more and more attractive as ingredients for consumer, health and industrial products. Alkyl glycosides bearing carbohydrate head groups as the polar parts are good candidates for this so-called "green" or "natural" surfactants [3].

The synthesis of these new environmentally compatible surfactants sharing similar properties with those of conventional surfactants demands also the intensive study of their self-assembly behaviour. Regarding this aspect, alkyl glycosides are significantly less studied compared to ionic or nonionic PEO-based surfactants. There are many differences in self-organization between glycosides, and ionic and PEO-based surfactants. More specifically, alkyl glycosides carry no charge but still have rigid carbohydrate headgroups. Therefore they share features with PEO-based and ionic surfactants. At the very least the chirality of carbohydrate head groups has a great influence on the self-assembly in solution, a characteristic missing for normal surfactants [4].

Actual reviews addressing the relationship between the structure of alkyl glycosides and their aggregation behaviour can be found in the literature [5,6]. To date mainly short and medium chained alkyl glycosides have been in-

vestigated. The results show that an increase of the alkyl chain length usually leads to the destabilization of the hexagonal phase in favour of the lamellar phase due to a decreasing curvature of the surfactant monolayer and an increase of the critical packing parameter (CPP) of the surfactant molecules. An increase of the polar head group from mono- to disaccharides was found to cause thermotropic and lyotropic polymorphism [7,8]. The shape of the micelles also changes; for example, the disaccharide *n*-octyl *β*-D-maltopyranoside forms spherical micelles in a wide range of concentrations but the corresponding monosaccharide *n*-octyl *β*-D-glucopyranoside forms rod-like micelles [9,10].

Whereas mainly the higher ordered lyotropic phases of glycolipids are investigated, yet [11–13] little data is available on the micellar structures of glycolipids.

In this paper we report our results on the investigation of a set of synthetic alkyl glycosides with unsaturated alkyl chains in dilute aqueous solutions. These compounds are very important in modern researches because nearly 50% of the natural occurring lipids contain unsaturated alkyl chains. The great difference compared to technical surfactants, for example APGs, is the purity of present compounds, and a defined chemical composition of the carbohydrate headgroup and the anomeric linkages of the monosaccharides in the head and of the alkyl chain. To derive structure–property relationship the alkyl chain type was kept constant and the polar head group was changed systematically. This gives us the possibility to investigate the influence of the head group size and chemical nature on the aggregation properties of solutions.

The size and shape of the aggregates in dilute solutions (micellar L_1 phase) were studied by small angle neutron scattering (SANS). The CMC was investigated using surface tension and the lyotropic phase behaviour by contact preparation methods. We have observed that the micellar structure changes from large polymer-like aggregates to smaller mostly stiff rod-like objects and further to relatively small, nearly spherical micelles with increasing size of the surfactant head group.

2. Materials and methods

2.1. Synthesis

*(cis-9-octadecenyl)-4-O-(α-*D*-glucopyranosyl)-β-*D*-glucopyranoside (**OM**)*

The synthesis of this compound is described in Ref. [8]. The purity of this compound has been found to be 99.9%. The molecular structure is presented in Fig. 1.

*(cis-9-octadecenyl)-4-O-[4′-O-(α-*D*-glucopyranosyl)-α-*D*-glucopyranosyl]-β-*D*-glucopyranoside (**OMT**)*

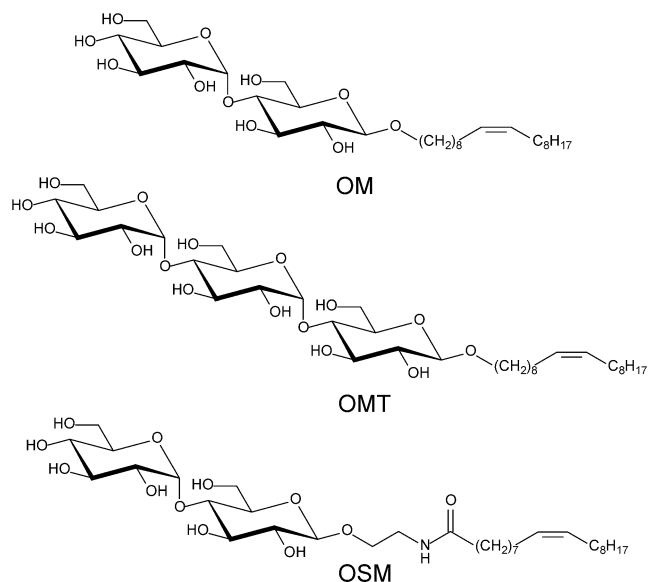Synthesis of this compound will be described elsewhere [G. Milkereit, V. Vill, unpublished results]. Purity of this

Fig. 1. Chemical structures of (*cis*-9-octadecenyl)-4-*O*-(α-D-glucopyranosyl)-β-D-glucopyranoside (**OM**), (*cis*-9-octadecenyl)-4-*O*-[4′-*O*-(α-D-glucopyranosyl)-α-D-glucopyranosyl]-β-D-glucopyranoside (**OMT**), [*N*-(*cis*-9-octadecenoyl)-2″-ethylamino]-4-*O*-(α-D-glucopyranosyl)-β-D-glucopyranoside (**OSM**).

compound has been found to be 99%. The molecular structure is presented in Fig. 1.

*1-O-[N-(cis-9-octadecenoyl)-2″-amino-ethyl]-4-O-(2′,3′,4′,6′-tetra-O-acetyl-α-*D*-glucopyranosyl)-2,3,6-tri-O-acetyl-β-*D*-glucopyranoside (**OSM**)*

Synthesis of this compound will be described elsewhere [G. Milkereit, V. Vill, unpublished results]. The purity has been found to be 99.9% and the molecular structure is also presented in Fig. 1.

2.2. Polarising microscopy

An Olympus BH optical polarising microscope equipped with a Mettler FP 82 hot stage and a Mettler FP 80 central processor was used to identify thermal transitions and characterize anisotropic textures.

For the contact preparation a small amount of sample was placed on a microscope slide and covered with a cover glass before heating to the liquid crystalline phase (S_A or Col). Afterwards a small amount of solvent was placed on the slide at the edge of the cover glass. As soon as the solvent had moved under the cover glass and the sample was completely surrounded by the solvent, it was placed again for several seconds on the hot stage at a temperature of 100 to 120 °C and the phase behaviour was investigated immediately afterwards by polarising microscopy. The following abbreviations were used to describe the lyotropic phases: L_α, lamellar; H_1, hexagonal (normal type); V_1, bicontinuous cubic phase; cub, discontinuous cubic phase; and ch, lyotropic cholesteric phase.

2.3. Surface tension

Surface tension was measured on a Krüss K6 Tensiometer (Krüss, Germany), using the de Noüy ring method. All measurements were carried out using bidistilled water with a surface tension of $\sigma = 72–73$ mN/m. For each sample the experiment was repeated three times in order to obtain constant values. All values were first corrected for the temperature. Correction for the ring geometry and the hydrostatic lifted volume of liquid were made using the method described by Harkins and Jordan or by Zuidema and Waters for values <25 mN/m [14,15]. The excess surface concentration Γ [mol m^{-2}] was calculated from the modified Gibbs adsorption equation [16,17],

$$\Gamma = -\frac{1}{RT}\left[\frac{\partial \sigma}{\partial \ln c}\right],\tag{1}$$

where σ is the surface tension (N m^{-1}), R the gas constant, T the temperature [K] and c the surfactant concentration [mM L^{-1}]. From Eq. (1) the area occupied by each molecule at the air–water interface can be calculated via

$$a_0 = \frac{10^{20}}{\Gamma N_A},\tag{2}$$

where N_A is Avogadro's number.

2.4. Small angle neutron scattering

Small angle neutron scattering experiments were made using the SANS-1 experiment at the FRG1 research reactor at the GKSS Research Centre, Geesthacht, Germany [18]. Four sample-to-detector distances (from 0.7 to 9.7 m) were employed to cover the range of scattering vectors q from 0.005 to 0.25 Å^{-1}. The neutron wavelength λ was 8.1 Å with a wavelength resolution of 10% (full-width-at-half-maximum value).

The solutions were prepared in D$_2$O (Deutero GmbH, purity 99.98%). The samples were kept in quartz cells (Hellma) with a path length of 5 mm. The samples were placed in a thermostated sample holder for isothermal conditions $T = 25.0 \pm 0.5\,°C$. The raw spectra were corrected for the background from the solvent, sample cell and other sources using conventional procedures [19]. The two-dimensional isotropic scattering spectra were azimuthally averaged, converted to an absolute scale and corrected for the detector efficiency by dividing by the incoherent scattering spectra of pure water [19], which was measured with a 1-mm-path-length quartz cell (Hellma).

The average excess scattering length density per unit mass $\Delta\rho_m$ of the surfactant in deuterated water was determined from the known chemical composition. This was found to be equal to -4.64×10^{10} cm/g for compound **OM**, -4.11×10^{10} cm/g for compound **OMT** and -4.44×10^{10} cm/g for compound **OSM**.

3. Results

3.1. Compounds

The chemical structures of the investigated compounds are shown in Fig. 1. All compounds have the same type of unsaturated alkyl chain although compounds **OMT** and **OSM** are modifications of **OM**.

The two glucose units of the maltose head group of **OM** and **OSM** are linked $\alpha 1 \to 4$, whereas the trisaccharide head group of **OMT** has three glucose units with a $\alpha 1 \to 4$ linkage. The oleyl chain of compound **OM** and **OMT** is linked directly to the sugar unit; **OSM** has a C$_2$-spacer between the carbohydrate head group and the carboxylic chain, increasing the polar part of the molecule.

3.2. Lyotropic properties

The lyotropic liquid crystalline properties were investigated using the contact preparation technique. This method allows to study the whole phase sequence from the pure liquid crystal to pure water. The results are summarised in Table 1. All investigated compounds displayed complex lyotropic phase behaviour upon the addition of water. This is in contrast to their thermotropic properties, where all compounds exhibited only a single liquid crystalline phase (Smectic A/lamellar for compounds **OM** and **OSM** and a columnar phase of the normal type for compound **OMT**). These phases can also be found in the lyotropic phase sequence for the lowest water concentration. The normal alkyl glycoside **OM** shows that with increasing water content a hexagonal phase is formed next. The phase transition does not occur directly but via a bicontinuous cubic phase [8]. Beyond the hexagonal phase a less anisotropic phase is formed which, to date, has been observed only for a few alkyl glycosides yet [8]. This is assumed to be a lyotropic cholesteric phase.

The introduction of a spacer between the sugar head group and the alkyl chain does not change the phase sequence, but the increase in polarity induced by the amidic function of compound **OSM** leads to changes in the range of the phases. The lyotropic lamellar phase decreases slightly, whereas a broad hexagonal phase is formed. Again, we have observed a possible lyotropic cholesteric phase. The ability to form strong hydrogen bonding networks is typical for amidic functions in glycolipids [21].

Table 1

Lyotropic phase sequence of the synthesized compounds in the contact preparation with water

OM	L$_\alpha$	V$_1$	H$_1$		ch	
OMT			H$_1$	cub		
OSM	L$_\alpha$	V$_1$	H$_1$		ch	
Pure surfactant						Water

The water content increases from the left side (pure surfactant) to the right side (pure water) of the diagram. (Data for compound OM were taken from ref. [8].)
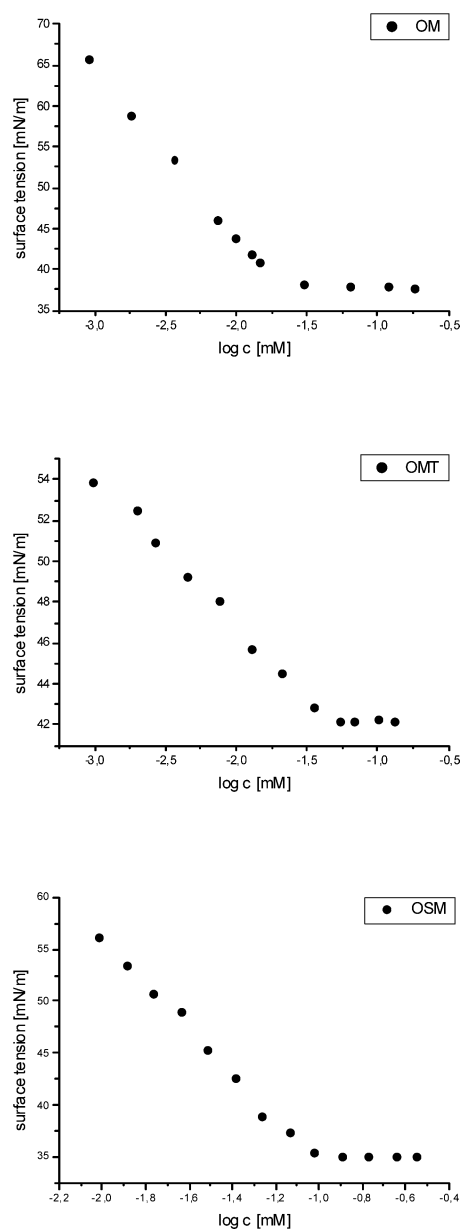
Fig. 2. Surface tension plots for **OM**, **OMT** and **OSM** at 25 °C.

If the disaccharide head group is exchanged by a trisaccharide head group (compound **OMT**), the lyotropism changes completely. The balance between the hydrophilic and the hydrophobic part of the amphiphile is changed in favour of the hydrophilic part and this favours the formation of a hexagonal structure. Interestingly, a discontinuous cubic phase is formed at the highest water concentration.

3.3. Surface tension and geometric properties

The adsorption isotherms for all three compounds at the liquid–air interface are presented in Fig. 2. The interfacial adsorption behaviour of the compounds was investigated at 25 °C and it was observed that all compounds formed homogeneous solutions and that no phase separation occurred or multi-phase systems were formed. Above the CMC no phase separation could be observed. Table 2 presents the data obtained from the surface tension measurements. The surface area per surfactant molecule at the liquid–air interface determined from the pre-CMC slope was used for calculating the CPP (Eq. (2)). The carbon chain volume and the extended chain length of the investigated compounds were calculated using the Tanford method [20]. For the "normal" alkyl glycosides **OM** and **OMT** a chain length of 18 carbon atoms was used for calculation and for the carboxylic acid chain of compound **OSM** the hydrophobic part of the chain was regarded to be only 17 carbon atoms. For compounds **OM** and **OSM** a cylindrical shape should be expected ($1/3 <$ CPP $< 1/2$) and for compound **OMT** a spherical shape is possible (CPP $< 1/3$).

The CMC decreases in the order **OSM** $>$ **OMT** $>$ **OM**. Compound **OM** shows the lowest CMC value, as expected, due to the favourable balance between the hydrophilic and hydrophobic molecule parts. The CMC for compound **OMT** is only two times higher than that of **OM**, which is unexpected whereas for **OSM** it is more than four times higher. This cannot be explained only by changes in the polarity of the head group; in this case it is more likely that the stereochemistry of the carbohydrate head group has a very strong influence on the interaction between the molecules even in dilute solutions. This holds especially true for the trisaccharide **OMT** where the long-range chirality transfer should be much higher than for disaccharides [22]. Taking this into account, it can be assumed that with increasing concentration of the surfactant the diastereomeric interaction between the sugar head groups of **OMT** is getting much stronger than for the disaccharide head groups. This is the reason why the formation of micelles is more favoured for compound **OMT**. The CMC is therefore lower than the extrapolated value from compound **OM**.

3.4. Analysis of SANS data

Three different concentrations were measured for each compound (1×10^{-4}, 5×10^{-4} and 1×10^{-3} g/mL). The concentration of 5×10^{-4} g/mL is of particular interest because it is 10–50 times higher than the CMC (Table 2). The concentration of 5×10^{-4} g/mL will be in the region of the dilute micellar L_1 phase, where an overlapping of micelles will not occur. In the concentration range from 1×10^{-4} to 1×10^{-3} g/mL a significant change in size and shape of the micelles was not observed. SANS data for a concentration of 5×10^{-4} g/mL are shown in Fig. 3 (all measured scattering data are provided as Supplementary Material). The scattering intensities were normalized to the concentration of the alkyl glycosides in the micelles by dividing by $c - $ CMC. The values of the scattering intensities and the shapes of the scattering curves are different for alkyl glycosides with different head groups, which points to the difference in the size and shape of the micelles. The values of the scattering intensities are in the order **OM** $>$ **OSM** $>$ **OMT**. In

Table 2
Adsorption of **OM**, **OMT** and **OSM** at the air–aqueous solution interface and data calculated from the CMC and the pre-CMC slope, $T = 25\,°C$

	CMC [mM L^{-1}]	CMC [g/mL]	γ_{CMC} [mN m^{-1}]	γ_{min} [mN m^{-1}]	Carbon chain volume[a] υ_c [Å^3]	Extended chain length[b] l_c [Å]	Head group area[c] a_0 [Å^2]	Packing parameter[d] $\upsilon_c/(l_c a_0)$
OM	$0.02 \pm 2 \times 10^{-4}$	1.2×10^{-5}	37.8 ± 1	37.8 ± 1	511.6	24.27	47 ± 5	0.45
OMT	$0.042 \pm 2 \times 10^{-3}$	3.2×10^{-5}	42.5 ± 1	42.2 ± 1	511.6	24.27	128 ± 11	0.16
OSM	$0.09 \pm 1 \times 10^{-3}$	5.8×10^{-5}	35.5 ± 1	35.1 ± 1	484.7	23.01	47 ± 5	0.45

[a] The values were calculated using $\upsilon_c = 27.4 + 26.9 n_c$.
[b] Calculated with $l_c = 1.5 + 1.265 n_c$ [20].
[c] Calculated from the pre-CMC slope.
[d] Calculated from the carbon chain volume and the extended chain length and the head group area obtained from the surface tension measurements.

the case of dilute solutions this reflects directly the variation of the micellar size. Compound **OM** forms the largest micelles whereas compound **OMT** forms the smallest ones. Next, the slope of the scattering intensities at low q regions $(\mathrm{d}\Sigma(q)/\mathrm{d}\Omega \sim q^{-\alpha})$ suggests the shape of the formed aggregates: rod-like for compounds **OM** and **OSM** ($\alpha \approx 1$) and nearly spherical for compound **OMT** ($\alpha \approx 0$).

We have started the analysis of SANS data by applying the indirect Fourier transformation method (IFT) developed by Glatter [23] in the version of Pedersen [24]. This model-independent approach needs only minor additional (model) information on the possible aggregate structure: dimensions (sphere-like, rod-like or disk-like) and maximal value of the diameter and cross-section diameter and thickness, respectively.

The IFT routine for spherical aggregates was applied to the data obtained for compound **OMT**, and the IFT routine for rod-like aggregates was applied to the large q part ($q > 0.02$ Å^{-1}) of the data for compounds **OM** and **OSM**. The large q part is chosen to ensure the validity of the approximation for infinitely long cylinder $q > 1/L$, where L is the length of the cylinder.

The scattering intensities for spherical micelles are evaluated using the pair distance distribution function $p(r)$ or via the cross-section pair distance distribution function $p_{CS}(r)$ for rod-like micelles. The normalized $p(r)$ and $p_{CS}(r)$ functions are given by [25]

$$p(r) = \frac{c - \mathrm{CMC}}{4\pi M} \int r^2 \Delta\rho(\mathbf{r}') \Delta\rho(\mathbf{r}' + \mathbf{r})\, \mathrm{d}\mathbf{r}', \qquad (3)$$

where $\Delta\rho(r)$ is the contrast (difference between scattering length density of aggregates at point r, $\rho(r)$, and the averaged scattering length density of the solvent ρ_s, $\Delta\rho(r) = \rho(r) - \rho_s$) and

$$p_{CS}(r) = \frac{c - \mathrm{CMC}}{2\pi M_L} \int r \Delta\rho(\mathbf{r}') \Delta\rho(\mathbf{r} + \mathbf{r}')\, \mathrm{d}\mathbf{r}'. \qquad (4)$$

In the case of rod-like aggregates, the vectors $\mathbf{r}$ and $\mathbf{r}'$ are in the cross-section plane.

The pair distance distribution function is expressed as a sum of N b-splines evenly distributed in the interval $[0, D_{max}]$ and the values of the coefficients are calculated numerically by a least-squares fitting of the IFT model curve

to the experimental data. In the present study, the values of D_{max} were carefully chosen to give both good fits to the experimental data and smooth $p(r)$ or $p_{CS}(r)$ functions.

The experimental data and fitted curves (Fig. 3) coincide perfectly, taking the limited q range of the analysis for compounds **OM** and **OSM** ($q > 0.02$ Å^{-1}) into account. The pair distance distribution function exhibits a shape that is characteristic for a homogeneous sphere for compound **OMT** (Fig. 4a) and an almost homogeneous locally cylindrical structure for compounds **OM** and **OSM** (Fig. 4b). We obtained a first estimate of the diameter of the sphere from the maximum distance of $p(r)$, and the cross-sectional diameter from the maximum distance of $p_{CS}(r)$, which are approximately 70 and 50 Å, respectively (pair distance distribution functions obtained for other concentrations are available as Supplementary Material).

After determination of the pair distance distribution functions it is straightforward to get the mass of the aggregates M (spherical micelles, compound **OMT**) or the mass per unit length of the aggregate M_L (rod-like micelles, compounds **OM** and **OSM**) and the radius of gyration of the excess scattering length density of the whole micelle R_g (compound **OMT**) or of cross section of the micelle $R_{CS,g}$ (compounds **OM** and **OSM**).

The values of the parameters obtained by the IFT method are shown in Table 3. It is easy to see that the characteristics of the cross section for compounds **OM** and **OSM** are very similar, which suggests that locally the structure of the micelles is not affected by increasing the polar group by the amidoethoxy part. The radius of cylindrical cross section calculated from the radius of gyration (approximation to a homogeneous structure) is equal to ~25 Å which points to a flexible conformation of the alkyl chain. In the case of the spherical micelle formed by compound **OMT**, the radius of the sphere was calculated in a similar way and its value is significantly larger (35 Å) which points to a more extended conformation of the alkyl chain than for compound **OMT**.

The next step in the analysis is the modelling of studied systems by some kind of structures and comparison of the experimental data and model curves, which represent the scattering from the applied model. The model-independent analysis, together with the contact preparation method and

Fig. 4. Pair distance distribution function: (a) for compound **OMT**— spherical geometry and (b) for compounds **OM** (filled symbols) and **OSM** (empty symbols) rod-like geometry—pair distance distribution function of the cross section.

Table 3
Results of SANS data analysis by model-independent approach (IFT), model fitting and calculated parameters of aggregates for all three compounds at $c = 5 \times 10^{-4}$ g/mL

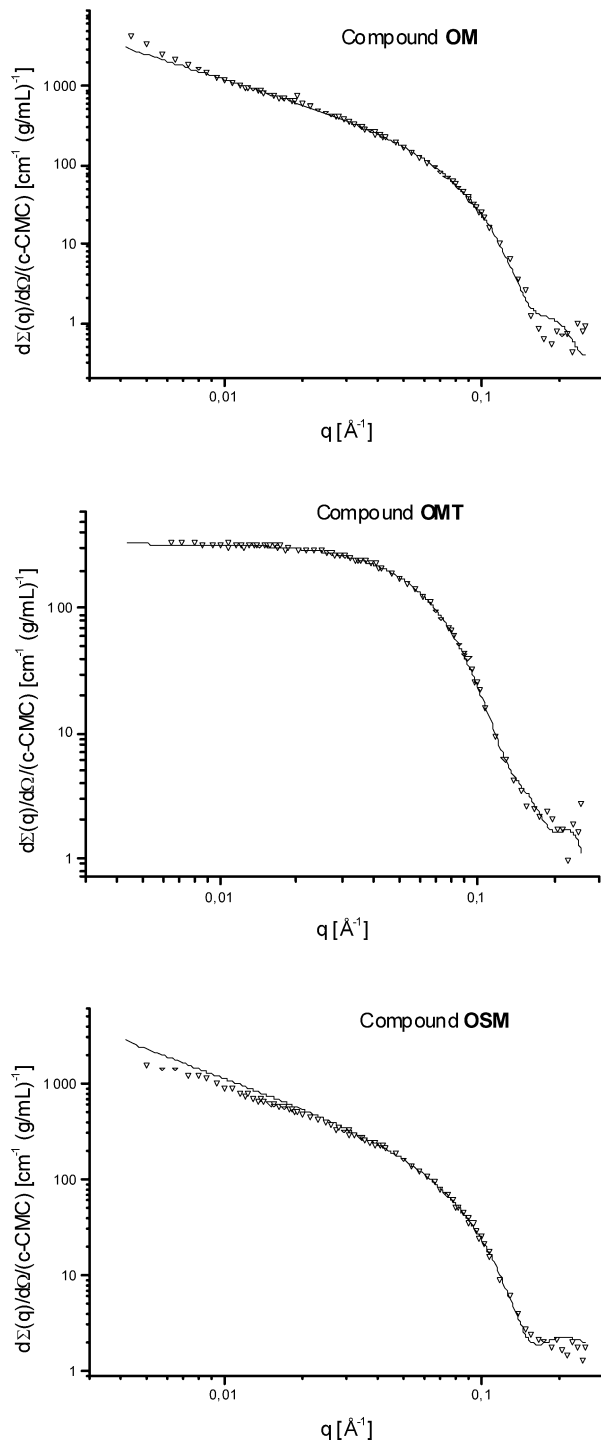|	OM	OMT	OSM
Micellar shape	Polymer-like	Sphere	Cylinder
Radius of cylindrical cross section [Å]	25 ± 1	–	25 ± 1
Length or radius for **OMT** [Å]	1200 ± 200	35 ± 1	600 ± 100
Mass of micelle, $\times 10^{6}$ [g/M]	1.3 ± 0.3	0.12 ± 0.01	0.68 ± 0.10
Mass per unit length, $\times 10^{-13}$ [g/cm]	1.8 ± 0.1	–	2.0 ± 0.1
Number of molecules per 1 nm of length	19 ± 2	–	20 ± 2
Surface area per molecule [Å^2]	80 ± 8	90 ± 10	80 ± 8

Fig. 3. Scattering data for $c = 5.0 \times 10^{-4}$ g/mL (empty triangles) with the IFT fits (solid lines) for rod-like (**OM**), spherical (**OMT**) and rod-like (**OSM**) micelles.

surface tension measurements, gives us enough information to select a specific model.

In general, it was assumed that all studied systems are dilute solutions, which means the scattering intensities depend only on the size and shape of the micelles and the interaction between micelles is small. This should be reasonable for noncharged micelles in dilute solutions (for volume frac-
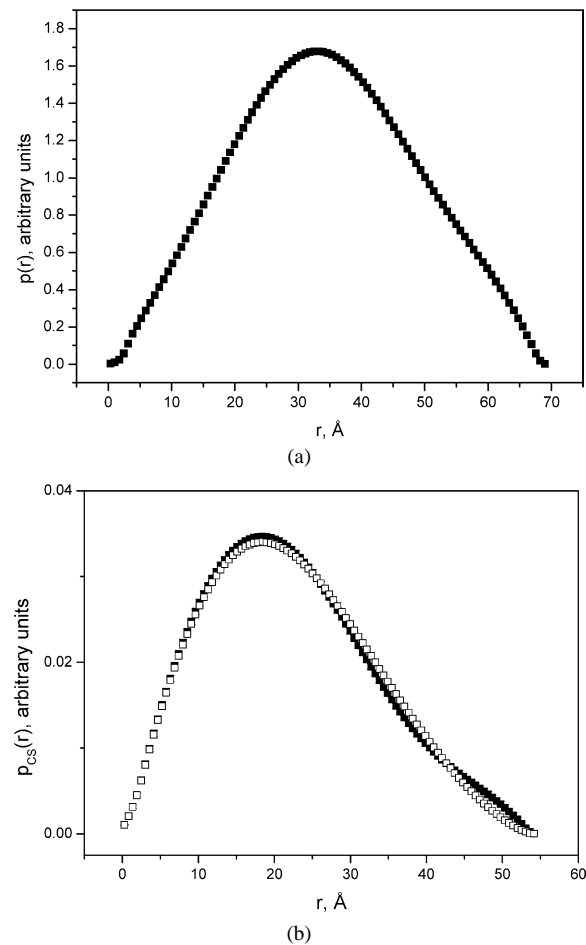
tions which are less than 0.05%). In this case the scattering intensities are

$$d\Sigma(q)/d\Omega = n\langle |F(q)|^2 \rangle. \tag{5}$$

The values inside the brackets $\langle\ \rangle$ represent an average weighted by the distribution of particle sizes and/or orientations, n is the number density (corresponding to the concentration) of the particles in the solution, $F(q)$ is the amplitude of the form factor,

$$F(q) = V\Delta\rho f(q, V, \text{sh}), \qquad (6)$$

where V is the volume of the micelle, $\Delta\rho$ is the contrast of scattering length densities between the particles and the solvent, and the scattering function $f(q, V, \text{sh})$ depends on the volume (size) and the shape sh of the micelles.

The simplest situation is for compound **OMT**, where the IFT method describes the experimental data perfectly and the shape of $p(r)$ is symmetrical (homogeneous sphere). The scattering function for an ellipsoid of revolution with semi-axes b, b and a ($a = \varepsilon b$) was taken in the fitting procedure [25].

The fitting of the scattering data from a solution of compound **OMT** by the model of an ellipsoid of revolution shows the same quality of agreement as in the case of the IFT method. The obtained value of the parameter of anisotropy ε is equal to 1 within statistical errors (different initial values were checked). This means that micelles formed by compound **OMT** (three monosaccharide units in the head group) are spherical with a small polydispersity. The obtained radius is equal to 35 ± 1 Å. We did not apply more complicated models, for example two shell aggregates, because it would significantly increase the number of fitting parameters and demand additional experimental data (SAXS and/or SANS on partially deuterated compounds).

For compounds **OM** and **OSM** the model-independent approach IFT shows some disagreement for the lower q values. This could mean that the studied aggregates are not ideal infinitely long cylinders in a scale range l larger than $\sim$100 Å ($l \sim q^{-1}$). The behaviour of the scattering intensity at low q regions reflects the overall structure of the studied aggregates or, in other words, the crossover of scattering from a local cylindrical structure to overall or intermediate structural units of studied micelles. It should be pointed out that the deviations are different: compound **OM** shows higher scattering than infinitely long cylinders and compound **OSM** shows lower scattering than infinitely long cylinders.

Compound **OSM** shows, at the lower q region ($q < 0.01$ Å^{-1}), the typical crossover of finite size, rod-like particles (stiff cylinders), i.e., from $\mathrm{d}\Sigma(q)/\mathrm{d}\Omega \sim q^{-1}$ ($L^{-1} < q < R_{CS}^{-1}$) to $\mathrm{d}\Sigma(q)/\mathrm{d}\Omega \sim \exp(-q^2 R_g^2)$ ($L^{-1} > q$), where L is the cylinder length, R_{CS} is the cross-sectional radius, R_g is the radius of the gyration of cylinder. We have applied the model of stiff cylinders [25] to the data of compound **OSM** and the model curve is in good agreement with the experimental data. The obtained radius of cross section is equal to 25 ± 1 Å which is in agreement with the IFT analysis and suggests a circular and homogeneous cross section. The length of the micelles L is about 600 ± 100 Å. Due to limited experimental data at lower q regions, the determination of the cylindrical length is of lower accuracy which

points on the order of magnitude of the micellar size. This value should be considered with caution and points to some lower limits of the micellar length.

The deviation in the experimental data (higher values than the IFT analysis, which is presented in Fig. 3) in the case of **OM** can be explained as scattering from flexible rods. It looks like that there is a crossover from the scattering of a cylindrical cross section $\mathrm{d}\Sigma(q)/\mathrm{d}\Omega \sim q^{-1}$ ($l_p^{-1} < q < R_{CS}^{-1}$) to the scattering of a coil $\mathrm{d}\Sigma(q)/\mathrm{d}\Omega \sim q^{-2}$ (θ solvent) or $\mathrm{d}\Sigma(q)/\mathrm{d}\Omega \sim q^{-5/3}$ (good solvent) for the interval of the scattering vectors ($L^{-1} < q < l_p^{-1}$), where l_p is the persistence length of flexible aggregates (polymer-like micelles) and L is the contour length of the micelles. The persistence length describes the flexibility of polymer-like micelles as an average cosine between the directions of two different parts of the micelle versus the contour length between these parts using the expression $\langle\cos\psi\rangle = \exp(-L/l_p)$.

In the modelling of the scattering curves and the determination of the persistence length, the powerful approach based on intensive studies (renormalization group theory, Monte Carlo simulation and scattering techniques) of Pedersen and Schurtenberger should be applied [26,27]. The flexibility of the aggregates can be obtained by fitting the full range of scattering curves. The scattering intensities are in the form of

$$\mathrm{d}\Sigma(q)/\mathrm{d}\Omega/(c - \text{CMC}) \sim S_{\text{wc}}(q, L, l_p)S_{CS}(q, R), \qquad (7)$$

where $S_{\text{wc}}(q, L, l_p)$ is the single chain scattering function for a semi-flexible chain with excluded-volume effects of the contour length L and the persistence length l_p. A detailed expression for $S(q, L, l_p)$ can be found in Refs. [26, 27]. $S_{CS}(q, R)$ is the scattering of the cross section of semi-flexible aggregates [24].

The results and fits are shown in the Holtzer (bending rod) presentation $q \times \mathrm{d}\Sigma(q)/\mathrm{d}\Omega/(c - \text{CMC})$ in Fig. 5. The model gives a satisfactory reproduction of the upturn of the scattering data, which points to the flexibility of the formed
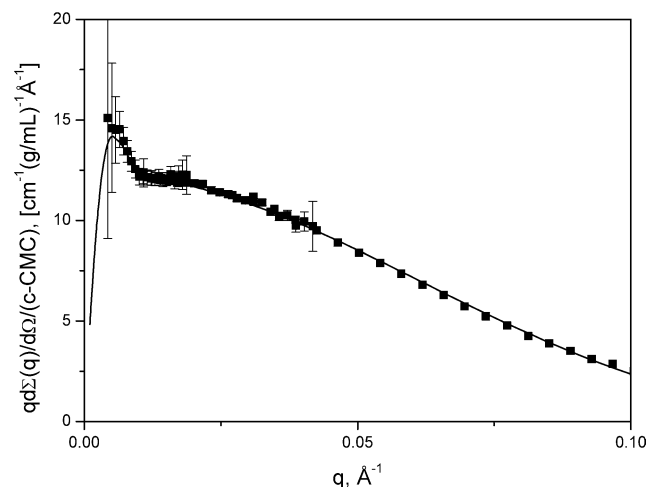

Fig. 5. Model fits using the flexible chain model (Eq. (12)) and experimental data OM (5×10^{-4} g/mL) in Holtzer (bending rod) representation.

aggregates. We have obtained the values of contour length 1200 ± 200 Å, persistence length 300 ± 50 Å and the radius of cross section 25 ± 1 Å.

The obtained values of contour length are affected by the polydispersity of the micelles and the fact that real small q values that are needed for the study of such long aggregates were not achieved. In Ref. [26] the polydispersity was first fixed to $M_w/M_n = 2$ and then the value of the average contour length was determined by fitting. In our case **OM** micelles may be quite polydisperse, but we do not know the range of distributions, and that is why it was not possible to include the polydispersity in the fitting of the scattering data. The persistence length is affected by interactions between the micelles and should be extrapolated to the value at 'zero concentration.' The intramicellar interaction is taken into account.

The obtained values of contour length ($\sim$1200 Å) and persistence length ($\sim$300 Å), together with the value of the radius of the cross section (25 Å), seem to be reasonable. These values support our assumption that the formed aggregates are long and flexible.

4. Discussion

4.1. Surface area occupied by surfactant molecules

The surface area occupied by the surfactant molecules (**OM**, **OMT** and **OSM**) in the micelles (SANS data, Table 3) and at the liquid–air interface (surface tension data, Table 2) can be compared. In the case of cylindrical aggregates (**OM** and **OSM**) it can be estimated that $A_s = 2\pi R_{CS} M_s / M_L N_A$, where R_{CS} is the radius of the cylindrical cross section, M_s is the molar mass of a surfactant molecule and N_A is Avogadro's number. The calculation is performed for the surface of an infinite cylinder, which should give larger values than obtained by the measurements at the liquid–air interface (planar surface). Note that the choice of a separation surface between the surfactant molecules and water molecules in the micelle cannot be considered as a neutral plane surface. However, it is well known that in heavy water the excess neutron scattering length density from the polar groups of surfactant molecules is much lower than that for the alkyl chains. Therefore errors made by using the above-described expression should not be too large. The values obtained for the surface area of **OM** and **OSM** molecules are identical within experimental errors ($A_s = 80 \pm 8$ Å^2). The same procedure was applied for **OMT** micelles, taking the spherical shape of the formed micelles into account (i.e., $A_s = 4\pi R^2 M_s / M N_A$ where R is the radius of a spherical micelle). In this case the value is slightly higher (90 ± 9 Å^2).

The values of the surface area per surfactant molecules for **OM**, **OMT** and **OSM** obtained from SANS and surface tension measurements show the same trends. Compound **OMT** shows the maximum of occupied surface area, although **OMT** has the largest (volume) polar head group. We

found the same values for the surface area of compounds **OM** and **OSM** in micelles and at the liquid–air interface. From this it can be concluded that the amidoethoxy spacer of **OSM** does not change the volume of the polar head group, the local structure of micelles or the structure at the liquid–air interface significantly. The higher values for the surface area obtained for micelles compared to the values for the liquid–air interface (compounds **OM** and **OSM**) are not surprising. Due to the local circular geometry of cylindrical aggregates the polar groups of **OM** and **OSM** molecules cannot cover the micellar surface and occupy more surface area; this part of the micelle area is not covered by the polar head group [28].

In case of compound **OMT** the situation is more complicated. The surface area per **OMT** molecule is higher (128 Å^2) at the liquid–air interface (planar geometry) than in the micelle (90 Å^2) with its spherical geometry. This discrepancy can be explained in different ways. The first explanation could be a difference in the direction of the polar groups at the interface, meaning that in the micellar aggregates the polar head group is directed perpendicularly to the micelle–solvent interface, and at the liquid–air interface the angle between the polar head group and the interface is less than 90°. Another explanation is the decrease of the effective size of the polar group due to specific diastereomeric interactions. This effect also has an influence on the CMC values as mentioned in Section 3. **OMT** shows a columnar phase in the thermotropic phase diagram, which is an indication for the nonlinear shape of the molecule. For **OMT** a banana-shaped structure is to be expected. **OM** is more linear and shows therefore a thermotropic lamellar phase. The effect is already known from starch, where the sugar groups are twisted in a helix [29].

4.2. Flexibility of micelles formed by OM and OSM

Micelles formed by **OM** show a flexibility and the value of the persistence length is equal to $\sim$300 Å. If we compare the values of l_p for different systems (ionic surfactant/salt/water mixtures, nonionic surfactants or microemulsions) obtained via different experimental methods and analysis approaches, the bandwidth of the presented results ranges from 100 to 1700 Å [30] for rod-like micelles. Smaller persistence length values ($\sim$200 Å) obtained by analysis taking an intra- and interchain interaction into account were reported for shorter surfactants with saturated alkyl chains (C16E6 in D_2O [31], lecithin microemulsions in cyclohexane [32], or in deuterated isooctane [30] or TDAO/NaCl/D_2O mixtures [33]). For mixtures of APGs with hexanol in aqueous solution an increase of the micellar size and flexibility was reported [34]. Nevertheless, the results presented in the literature are of less use, especially the APGs often used are statistical mixtures of different APGs. The anomeric linkage between the sugars in the head and between the alkyl chain and the sugars are an average of α- and β-linkages. Effects

of the anomeric linkage on the formation of micelles are reported in the literature (see, for example, [35]).

Assuming that the analysis procedure was similar it can be suggested that we observed an increase of rigidity for polymer-like micelles formed by long chain alkyl glycosides. There are a few possible reasons for the observed effect: (i) longer and stiffer alkyl chains due to the double bond with *cis*-conformation in the middle of the chain; (ii) bigger repulsive interactions among the polar head groups resulting in a similar behaviour to that of electrostatic interactions in charged micelles and giving a significant increase of the persistence length.

We could not observe the flexibility for rod-like micelles formed by compound **OSM**. The absence of flexibility in the data could have two possible reasons: (1) the persistence length of **OSM** is larger than the micellar length, and/or (2) the contour length of the micelles is so small, that the flexibility is not detectable. Looking at the similar volumes of the polar head groups of **OSM** and **OM** molecules it would be reasonable that the persistence length should be not smaller than 300 Å (the value obtained for **OM** micelles). As the micelles have a contour length of about 600 Å (Table 3), they are almost two times as long as the persistence length. It is known that flexibility cannot be observed in a scattering experiment for such short semi-flexible chains [27].

Therefore it can be concluded that the contour length of **OSM** micelles is too small for flexibility to be observed in our studies.

4.3. Relationship between the molecular structure and properties of long chain alkyl glycoside solutions

In this paper we have investigated different properties of surfactant solutions: the CMC, the lyotropic phase behaviour and the structures of micelles regarding the variation of the polar head group of long unsaturated alkyl chain surfactant. It is observed that the local structure of the formed aggregates follows simple geometrical considerations the so-called critical packing parameter. The significant increase of the polar group size from disaccharides (**OM** and **OSM**, with a CPP between 1/3 and 1/2, Table 2) to trisaccharides (**OMT**, CPP < 1/3) shows the change of micellar type from rod-like to spherical-like micelles. The lyotropic phase behaviour also changes according to the CPP values, whereas the biggest difference is observed between the disaccharides (**OM** and **OSM**) and the trisaccharide (**OMT**). We have observed a discontinuous cubic phase at higher water content (**OMT** mixtures), which was not observed for the **OM** and **OSM** solutions. A discontinuous cubic phase is based on various packing of spherical micelles [4]. In this work the size and shape of spherical micelles in the dilute micellar phase were characterized. It is likely that the size and shape of the micelles are similar to those of the micelles that build up the discontinuous cubic phase with increasing concentration.

The lyotropic cholesteric phase found for compounds **OM** and **OSM** in the lyotropic phase diagram also fits well to the micellar shapes. The interaction of cylindrical aggregates will be chiral in nature in the case of glycolipids, leading to a twisted ordering of the micelles.

The effect of the amidoethoxy spacer (**OSM**) is more complicated. Micelles formed by **OSM** are shorter than **OM** ones. This should be related to an additional energy of transfer, which is necessary for the molecule with the amidoethoxyspacer to move from the solvent to the micelle. Nevertheless, the effect of amidic functions, forming directed hydrogen bonding networks and resulting in more rigid structures, also plays an important role. Therefore the formation of micelles is less favoured for **OSM** compared to **OM**.

5. Conclusions

The combination of different experimental methods (surface tension, contact preparation method and small angle neutron scattering) and the systematic variation of the polar carbohydrate head group morphology of long unsaturated alkyl chain surfactants gives new information about the structure–property relationship of aqueous solutions of long chain alkyl glycosides. The local structure of the formed aggregates varies from cylindrical for the disaccharide surfactants (polymer-like micelles for compound **OM** or short cylinders for compound OSM) to spherical for the trisaccharide surfactant (compound **OMT**), which is in accordance with the critical packing parameter approach. The lyotropic phase behaviour is also in accordance with the CPP consideration. The variation of CMCs and surface area per surfactant molecule in micelles and at the liquid–air interface reflects the fine effects of hydrogen bonding networks for the amidoethoxy spacer (compound **OSM**) and the specific interactions between the long polar head groups (compound **OMT**).

Supplementary material

The online version of this article contains additional supplementary material.

Please visit DOI: 10.1016/j.jcis.2004.10.039.

References

[1] W. Curatolo, Biochim. Biophys. Acta 906 (1987) 111–136.

[2] B. Jönsson, B. Lindmann, K. Holmberg, B. Kronberg, Surfactants and Polymers in Aqueous Solution, Wiley, New York, 1998, p. 423.

[3] M. Hato, H. Minamikawa, K. Tamada, T. Baba, Y. Tanabe, Adv. Colloid Interface Sci. 80 (1999) 233.

[4] C.E. Fairhurst, S. Fuller, J. Gray, M.C. Holmes, G.J. Tiddy, in: D. Demus, J.W. Goodby, G.W. Gray, H.-W. Spiess, V. Vill (Eds.), Handbook of Liquid Crystals, vol. 3, Wiley–VCH, Weinheim, 1998, p. 341.

[5] C. Stubenrauch, Curr. Opin. Colloid Interface Sci. 6 (2001) 160.

[6] O. Soderman, I. Johansson, Curr. Opin. Colloid Interface Sci. 4 (2000) 391.

[7] V. Vill, H.M. von Minden, M.H.J. Koch, U. Seydel, K. Brandenburg, Chem. Phys. Lipids 104 (2000) 75.

[8] H.M. von Minden, K. Brandenburg, U. Seydel, M.H.J. Koch, V.M. Garamus, R. Willumeit, V. Vill, Chem. Phys. Lipids 106 (2000) 157.

[9] L.-Z. He, V.M. Garamus, S.S. Funari, M. Malfois, R. Willumeit, B. Niemeyer, J. Phys. Chem. B 106 (2002) 7596.

[10] L.-Z. He, V.M. Garamus, B. Niemeyer, H. Helmholz, R. Willumeit, J. Mol. Liq. 89 (2000) 239.

[11] J.M. Seddon, Biochim. Biophys. Acta 1031 (1990) 1.

[12] U. Seydel, K. Brandenburg, M.H.J. Koch, E.T. Rietschel, Eur. J. Biochem. 186 (1989) 325.

[13] G. Milkereit, M. Morr, J. Thiem, V. Vill, Chem. Phys. Lipids 127 (2004) 47.

[14] F. Harkins, O. Jordan, J. Phys. Chem. 58 (1954) 825.

[15] H.H. Zuidema, G.W. Waters, Ind. Eng. Chem. 13 (1941) 312.

[16] P.C. Hiernez, Principles of Colloid and Surface Chemistry, Dekker, New York, 1977.

[17] J.W. Gibbs, Trans. Conect. Acad. 3 (1976) 375.

[18] H.B. Stuhrmann, N. Burkhardt, G. Dietrich, R. Jünemann, W. Meerwinck, M. Schmitt, J. Wadzack, R. Willumeit, J. Zhao, K.H. Nierhaus, Nucl. Instrum. Methods A 356 (1995) 133.

[19] G.D. Wignall, F.S. Bates, J. Appl. Cryst. 20 (1986) 28.

[20] C. Tanford, The Hydrophobic Effect: Formation of Micelle and Biological Membranes, Wiley, New York, 1980.

[21] G. Milkereit, V.M. Garamus, K. Veermans, R. Willumeit, V. Vill, Chem. Phys. Lipids 131 (2004) 51.

[22] H.M. von Minden, V. Vill, M. Pape, K. Hiltrop, J. Colloid Interface Sci. 236 (2001) 108.

[23] O. Glatter, J. Appl. Crystalogr. 10 (1977) 415.

[24] J.S. Pedersen, Adv. Colloid Interface Sci. 70 (1997) 171.

[25] L.A. Feigin, D.I. Svergun, Structure Analysis by Small-Angle X-Ray and Neutron Scattering, Plenum, New York, 1987.

[26] G. Jerke, J.S. Pedersen, S.U. Egelhaaf, P. Schurtenberger, Phys. Rev. E 56 (1997) 5772.

[27] J.S. Pedersen, P. Schurtenberger, Macromolecules 29 (1996) 7602.

[28] J.N. Israelachvili, Intermolecular and Surface Forces, Academic Press, London, 1991, p. 312.

[29] A. Imberty, H. Chanzy, S. Perez, A. Buleon, V. Tran, J. Mol. Biol. 201 (1988) 365.

[30] L. Magid, J. Phys. Chem. B 102 (1998) 4064.

[31] P. Schurtenberger, C. Cavaco, F. Tiberg, O. Regev, Langmuir 12 (1996) 2894.

[32] P. Schurtenberger, C. Cavaco, J. Phys. II 3 (1993) 1279.

[33] V.M. Garamus, J.S. Pedersen, H. Kawasaki, H. Maeda, Langmuir 16 (2000) 6431.

[34] A. Stradner, O. Glatter, P. Schurtenberger, Langmuir 16 (2000) 5354.

[35] B. Focher, G. Savelli, G. Torri, G. Vecchio, D.C. McKenzie, D.F. Nicoli, C.A. Bunton, Chem. Phys. Lett. 158 (1989) 491.

Chapter 6

Synthesis and Mesogenic Properties
of Glycosyl Dialkyl- and Diacylglycerols
bearing Saturated, Unsaturated and
Methyl Branched Fatty Acid and
Fatty Alcohol Chains.
Part I: Synthesis

Synthesis and mesomorphic properties of glycosyl dialkyl- and diacyl-glycerols bearing saturated, unsaturated and methyl branched fatty acid and fatty alcohol chains
Part I. Synthesis

Götz Milkereit [a], Sven Gerber [a], Klaus Brandenburg [b], Michael Morr [c], Volkmar Vill [a, *]

[a] *Institute of Organic Chemistry, University of Hamburg, Martin-Luther-King-Platz 6, 20146 Hamburg, Germany*
[b] *Research Center Borstel, Leibniz-Zentrum für Medizin und Biowissenschaften, Parkallee 10, 23845 Borstel, Germany*
[c] *Gesellschaft für Biotechnologische Forschung mbH, Mascheroder Weg 1, 38124 Braunschweig, Germany*

Abstract

Glycosyl dialkyl- and diacyl-glycerols bearing saturated, unsaturated or chiral methyl branched chains in the tail and disaccharide and trisaccharide carbohydrate headgroups were synthesised. Standard procedures were used for the preparation of the educts and the glyco lipids: trichloracetimidate procedure for the preparation of long-chained compounds, glycosylation using the β-peracetate and boron trifluoride etherate was successful for the preparation of lipids with a medium-alkyl chain length. Preparation of the ester was afforded in a multi-step synthesis according to published procedures. Thus, several lipids were synthesised in a few synthetic steps in good yields. The introduction of unsaturated or methyl branched chains lead to liquid crystallinity at ambient temperature, because these compounds will be used as model compounds for biological systems. The biophysical properties of these compounds will be reported in a following paper.
© 2005 Elsevier Ireland Ltd. All rights reserved.

Keywords: Glyco glycero lipids; Synthesis; Branched fatty acids; Trichloracetimidate procedure

1. Introduction

Glyco glycero lipids are known to be an important class of glycolipids. These lipids can be found as important constituents in cell membranes. In principle, these lipids consist of a carbohydrate headgroup as polar head while the unpolar tail is build up by glycerol esters or ethers of alkyl or acyl chains (Ishizuka and Yamakawa, 1985). Lipids with small headgroups (1–3 carbohydrate units in the head) can be found as major components of the cell membrane, whereas the more complex lipids are in-

volved in cell surface recognition processes (Curatolo, 1987).

In a preceding paper, we reported about the synthesis of glycosyl diacyl-glycerols with monosaccharide and disaccharide headgroups (Minden et al., 2002a), with unsaturated and chiral methyl branched fatty acid chains. These molecules showed liquid crystalline phases already at ambient temperature so biophysical properties could be investigated in the temperature range of biological systems (Minden et al., 2002b).

The great disadvantage of these compounds is the synthesis. The synthesis of a single diacyl-glycerol with unsaturated fatty acid chains requires at least nine synthetic steps, and the overall yield will be in the range of 3–26%.

Especially for physical characterisation and biological testing, enough substance has to be provided. Therefore, a relative short-synthetic procedure is needed to enable a rapid synthesis in good yields.

In recent years, Hato and co-workers prepared a new class of glycolipids with a 1,3-di-*O*-alkyl-sn-glycerol moiety. Mainly 1,3-dialkyl-glyco glycero lipids with *n*-dodecyl and *n*-tetradecyl alkyl chains and oligomaltose and cellobiose headgroups were synthesised in good to excellent yields (Minamikawa et al., 1994) and a relative short-synthetic sequence. The lyotropic properties of the oligosaccharide headgroups were thoroughly characterised (Hato, 2001; Hato and Minamikawa, 1996; Hato et al., 1998; Korchowiec et al., 2001). A few examples with methyl branched phytanyl chains can be found (Minamikawa and Hato, 1997). The amphiphilic properties of some of these compounds were in part similar to those observed for the unsaturated disaccharide compounds (Minden et al., 2002a).

From this observation, we synthesised a series of 1,3-dialkyl-glyco-glycerolipids with disaccharide (Maltose and Melibiose) and trisaccharide (maltotriose) headgroups. Different synthetic standard routes were employed to ensure a fast and efficient synthesis. To derive structure property relationships, different types of alkyl chains were used: unsaturated (*cis*-9-octadecenyl), saturated (*n*-tetradecyl) and chiral methyl branched ((2*R*,4*R*,6*R*,8*R*)-2,4,6,8-tetramethyldecyl). Additionally, a 1,2-diacyl-methyl branched maltoside and unsaturated 1-*O*-alkyl maltotrioside were synthesised. Even in case of 1,3-ethers, the unsaturated and methyl branched alkyl chains should prevent crystallisation.

The mesomorphic properties of the synthesised compounds are presented in a following paper (Milkereit et al., 2004, in press).

2. Results and discussion

First three different types of 1,3-substituted glycerols were synthesised using standard procedures (see for example, Bebernitz et al., 2001).

Synthesis of 1,3-di-*O*-tetradecyl-sn-glycerol and 1,3-di-*O*-(oleyl)-sn-glycerol is already described in the literature (see for example, Altenburger et al., 1992; Bear and Stanacev, 1965; Paltauf and Johnston, 1971).

The chiral methyl branched fatty acid (2*R*,4*R*, 6*R*,8*R*)-2,4,6,8-tetramethyldecanoic acid and the corresponding alcohol (2*R*,4*R*,6*R*,8*R*)-2,4,6,8-tetramethyldecanol were prepared from natural source as described by Morr et al. (1992, 1997). Using extracts from the preen glands of the domestic goose (*Anser a.f. domesticus*), the acid was prepared in a multi-step synthesis by transesterification, Spaltrohr distillation and saponification of the fatty acid methyl ester. The alcohol was prepared by reduction of the fatty acid methyl ester instead of the saponification step. The fatty acid and the alcohol were obtained with a diastereomeric excess of more than 99%. The alcohol was used for the synthesis of the new glycerol **3**. The fatty acid was used for the synthesis of the diacyl-glycerol instead, as described below. The synthesis of the aglycon **1** was carried out by reacting the sodium salt of *cis*-9-octadecenol with anhydrous 1,3-di-chlor-propan-2-ol. After purification, the product was obtained in low yields (21%). In a second attempt, epichlorhydrine was used instead, but this did not increase the yield considerably. The synthesis of compounds **2** and **3** was performed in a similar way. The salt of the alcohol was reacted with epichlorhydrine. The products were obtained in good yields, after chromatographic purification. In case of the synthesis of compounds **3**, non-reacted alcohol was nearly completely recovered.

For the preparation of the dialkyl-glyco glycero lipids, we used two different routes. As shown in Fig. 1, the glycerol with octadecenyl chains was reacted using the trichloracetimidate procedure (Schmidt, 1986; Schmidt and Kläger, 1985; Schmidt and Stumpp, 1983; Schmidt et al., 1984), which has been proven to
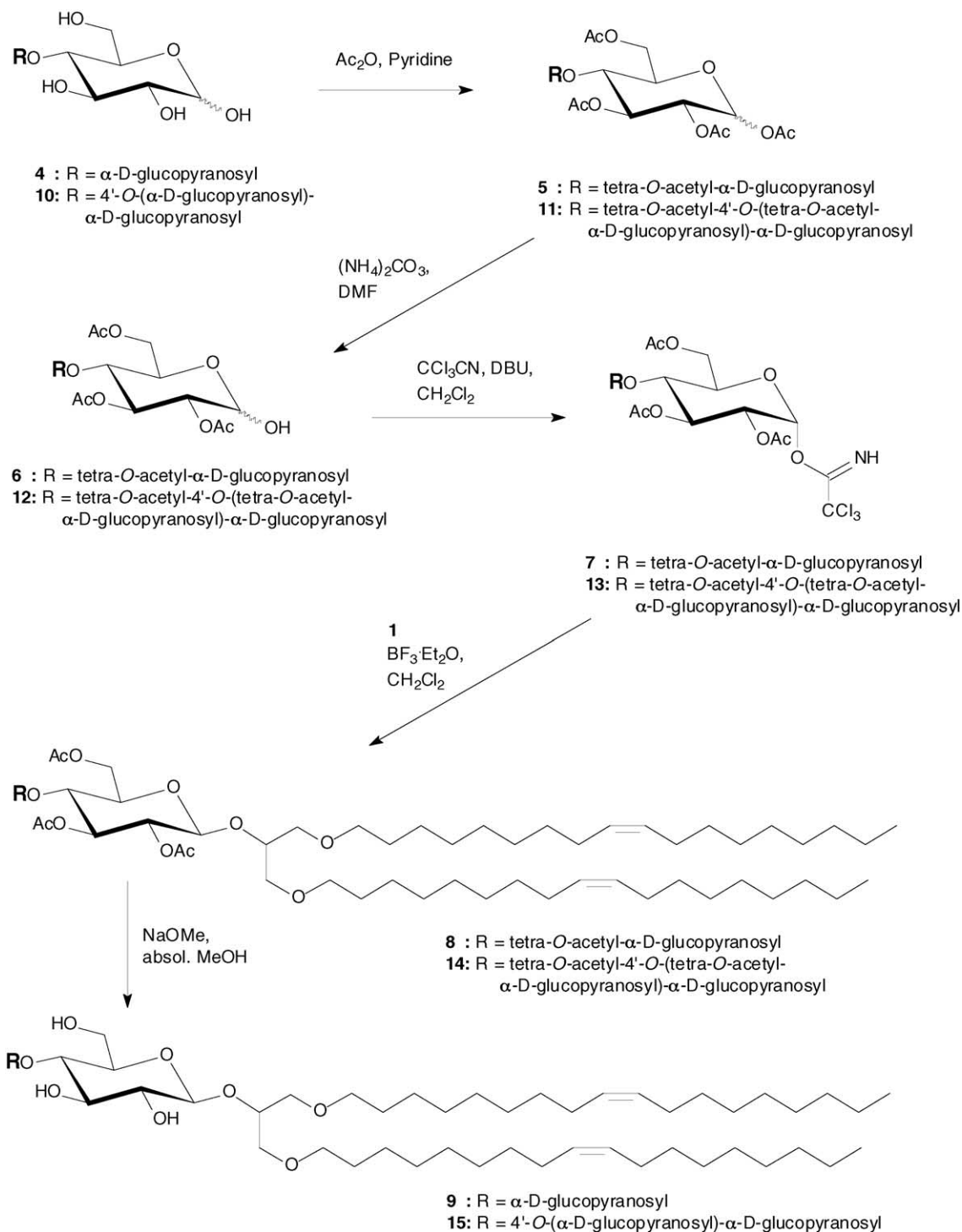
Fig. 1. Synthesis of 1,3-di-*O*-alkyl glyco glycero lipids via the trichloracetimidate route.

be useful in the preparation of glyco glycero lipids (Minamikawa et al., 1994). We started with the un-protected sugar, which was acetylated using acetic acid anhydride in pyridine to give the products **5** and **11** in excellent yields. Next, the peracetylated sac-charide was deprotected at the reducing terminus by treatment with an excess of ammonium carbonate in dimethylformamide at ambient temperature. Finally, the glycosyl donors **7** and **13** were prepared by react-ing trichloracetonitril in dichlormethane under basic conditions. However, 1,8-diazabicyclo[5.4.0]undec-7-

en (DBU) was used as base (Schmidt and Kinzy, 1994), instead of the often used sodium hydride (Schmidt and Stumpp, 1983) or caesium carbonate. The great advan-tage of this base is the change of colour during the reaction, indicating at this point that sufficient amount of base has been added. In the glycosylation coupling, the glycosyl donor was reacted with 1,3-di-*O*-(*cis*-9-octadecenyl)-glycerol **1** in the presence of trimethylsi-lyl trifluormethanesulfonate (one-to-one molar ratio). As reported by Minamikawa et al. (1994), the chem-ical structure of the donors and the acceptors had no
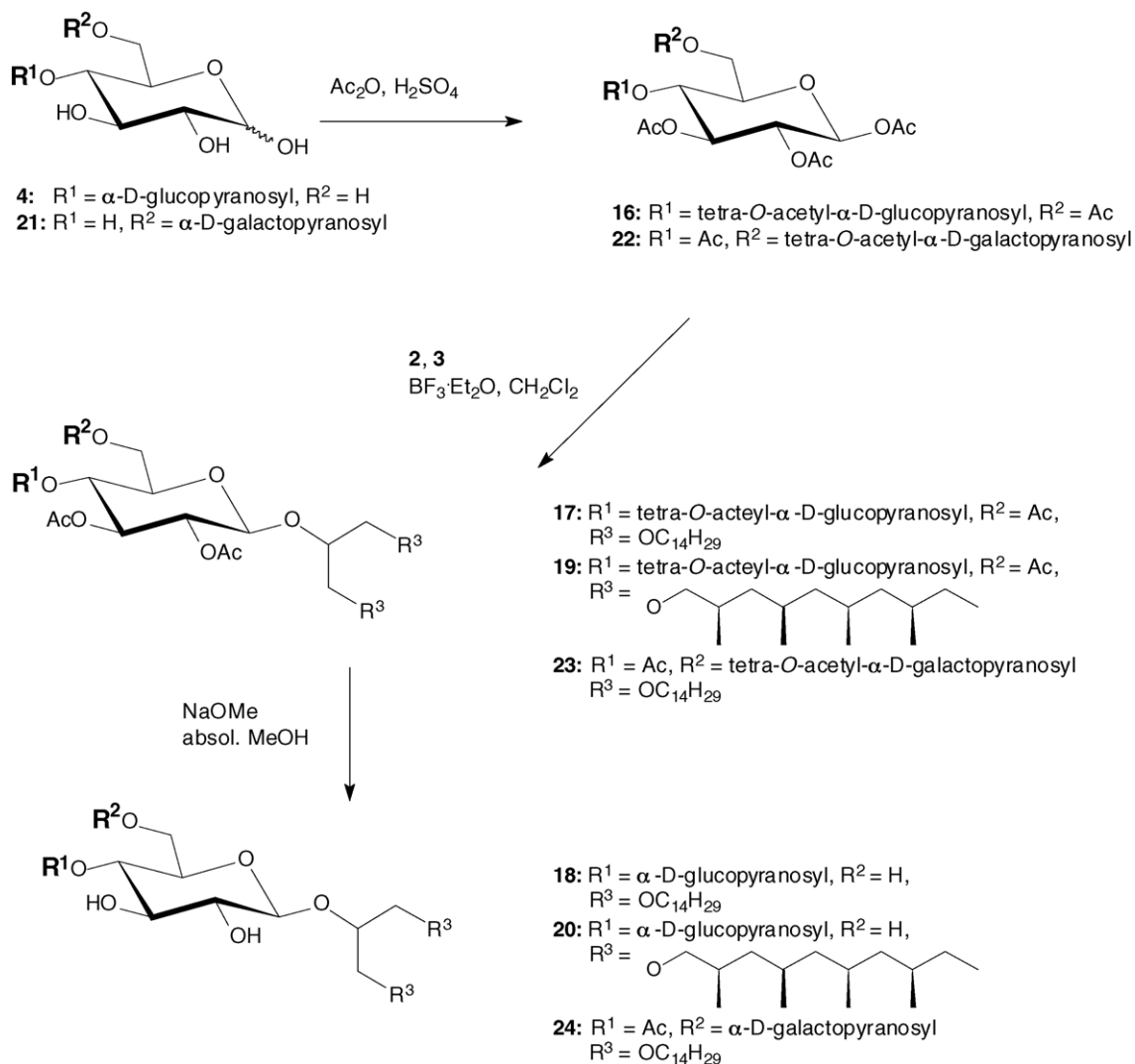
Fig. 2. Synthesis of 1,3-di-*O*-alkyl glyco glycerol lipids via the β-peracetate.

significant influence on the reaction, as can be seen in the similar yields of the disaccharide and trisaccharide product, respectively. Also the double bonds of the glycerol were stable during the reaction. The peracetylated lipids **8** and **14** were deprotected using sodium methoxide in anhydrous methanol to give the desired products **9** and **15**.

For the glycosylation reaction of the shorter-chained aglycons (Fig. 2), which should be more reactive, we used the standard procedure described by Vill et al. (1989). Protection of the sugar was afforded by reaction of the unprotected sugar in acetic acid anhydride with a catalytic amount of sulfuric acid, yielding the β-anomer in good yields. The β-peracetate

and the glycerols **2** and **3** were than reacted in anhydrous dichlormethane in the presence of boron trifluoride etherate. Deprotection of the product was afforded using sodium methoxide in anhydrous methanol. Although this glycosylation reaction is more likely useful for the preparation of alkyl glycosides, its use was in this case successful and the overall yields are comparable to the trichloracetimidate procedure. However, if the long-chained aglycon **1** was reacted with the β-peracetate, product **8** was obtained only in poor yields. This second synthetic route is therefore being useful if glycerols with alkyl chains of medium-chain length are used. In addition, the synthetic procedure is shorter by two steps.

Fig. 3. Synthesis of 1,2-di-*O*-[(2″*R*,4″*R*,6″*R*,8″*R*)-2″,4″,6″,8″-tetramethyl-decanoyl]-4-*O*-(α-D-glucopyranosyl)-β-D-glucopyranoside.

For comparison, the corresponding 1,2-diacyl-glycol glycerolipids and alkyl glycosides had to be synthesised. The corresponding 1,2-di-*O*-oleoyl glycerol maltoside was alr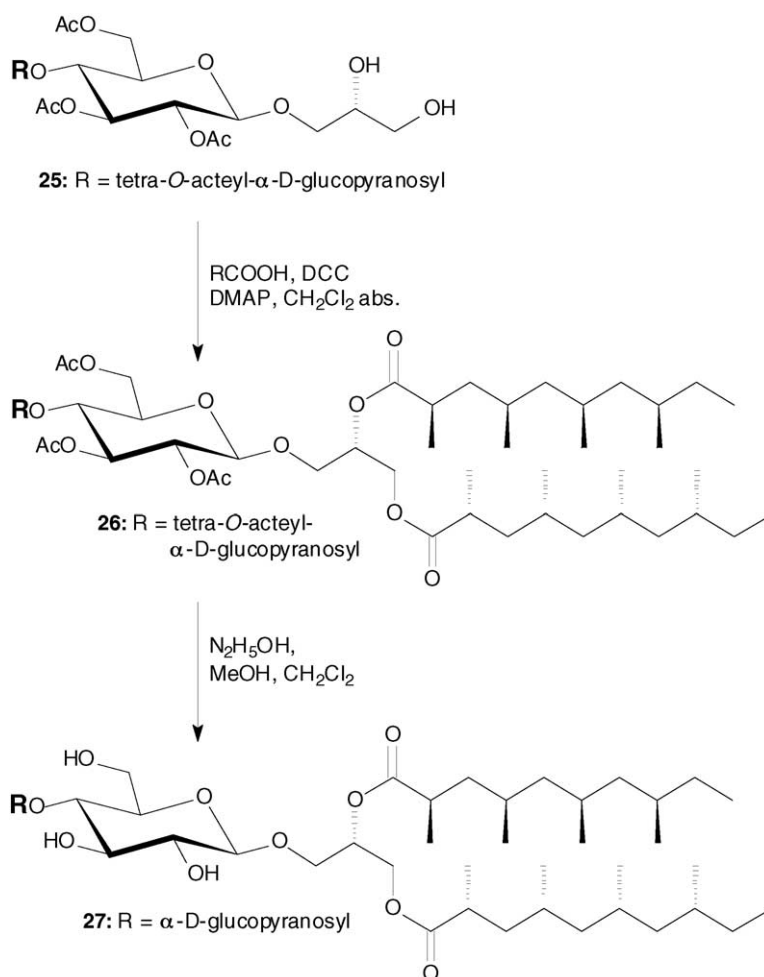eady synthesised by our group (Minden et al., 2002a), but no data are available on the corresponding 1,2-di-*O*-(2*R*,4*R*,6*R*,8*R*)-2,4,6,8-tetramethyldecanoyl glycerol glycoside. The synthesis of the 1,2-diacyl-glyco-glycero lipid **27** is partial shown in Fig. 3. The diol **25** was synthesised similar to the well-elaborated procedure from Mannock et al. (1987). The first step is a condensation of 1,2-di-*O*-benzyl-sn-glycerol with maltoseperacetate in abs. dichlormethane in the presence of boron trifluoride etherate (Minden et al., 2002a; Vill et al., 1989) to obtain the β-maltoside. It is again noteworthy that the easily accessible and optically pure 1,2-*O*-isopropylidene-sn-glycerol racemises during the Koenigs–Knorr condensation procedure (Wehrli and Pomeranz, 1969; Wickberg, 1958) or under Lewis acid catalysis, due to intramolecular migration of the isopropylidene group and cannot be used thus. After hydrogenolytic removal of the benzyl protective groups of compound, the glycerol **25** is afforded. This was esterified with (2*R*,4*R*,6*R*,8*R*)-2,4,6,8-tetramethyldecanoic acid using the DCC method (Hassner and Alexanian, 1978) and DMAP, yielding the ester **26**. After deacetylation under reductive conditions and a subsequent chromatographic purification, the glycosyl diacyl-glycerol **27** was obtained as a waxy solid.

The alkyl glycoside **29** was synthesised according to the method described by Vill et al. (1989). The β-maltotriose peracetete was reacted under catalysis of a lewis acid to give the desired alkly glycoside. Instead of tin tetrachloride, we used boron trifluoride etherate as Lewis acid (Ferrier and Furneaux, 1976; Minden et al., 2000) for the synthesis of the β-anomers. The compound could be separated by simply silica gel chromatography; no tedious ion-exchange chromatography was necessary. After deprotection in anhydrous methanol using catalytic amounts of sodium methoxide the compound was obtained in high purity. Compared to the synthesis of alkyl glycosides bearing monosaccharide or disaccharide carbohydrate headgroups (see for example, Böcker and Thiem, 1989; Minden et al., 2000; Vill et al., 2000), compound **29** was obtained only in poor yields. In this case, other methods should be used for the preparation.

Due to their liquid crystallinity at ambient temperature, the glycolipids **9**, **15**, **20**, **27** and **29** could not be recrystallised after the deprotection step. To ensure the high purity, which is necessary for the exact determination of the liquid crystalline transition temperatures **9**, **15** and **29** were purified by means of an additional gel filtration, whereas for compounds **20** and **27,** a subsequent silica gel chromatography was already successful. The products **18** and **24** were purified by recrystallisaton from methanol or propane-2-ol.

3. Conclusions

Different standard synthetic procedures were employed to the synthesis of several glyco lipids. The synthesised lipids are shown in Fig. 4. It was possible to obtain the lipids in short-synthetic steps in good overall yields, partially in Gram-scale. On our knowledge, we were the first to synthesise the 1,3-di-*O*-oleyl-lipids **9** and **15**, the oleyl-maltotrioside (**29**) and the chiral methyl branched lipids **20** and **27**. The 1,3-dialkyl-glycerols were synthesised in a fast and efficient way. For the glycosylation, two different routes were chosen depending on the aglycon. The long-chained glycerol bearing unsaturated alkyl chains was reacted with the carbohydrate using the trichloracetimidate method. The products were obtained in excellent yields for maltose and maltotriose headgroups. The synthesis of the medium and methyl branched glyco glycero lipids was done using a shorter-reaction sequence was chosen. The glycosylation of the β-peracetate using boron trifluoride etherate as Lewis acid also afforded the desired products. The yields were good for the preparation of the *n*-tetradecyl lipids (35 and 45%) but the use of the chiral methyl branched aglycon **3** led to lower yields. For the synthesis of the glycosyl dialkyl-glycerols, it is more likely to use the glycosylation via the peracetylated sugar. The reaction sequence is shortened by two steps including tedious chromatographic purification and the overall yields are comparable to that obtained with the trichloracetimidate procedure. For the synthesis of long-chain glycosyl dialkyl-glycerols and highly methyl branched glycerols, the trichloracetimidate procedure is superior to other methods. Another problem in the synthesis of biological interesting compounds is to obtain compounds that show low-melting points. Due to the need of liquid crystallinity at biological relevant

Fig. 4. Structures of the synthesised lipids.

4. Experimental section

4.1. Materials and methods

Peracetylated disaccharides were prepared according to the literature (Vill et al., 1989). Synthesis of 3-*O*-[4′-*O*-(2″,3″,4″,6″-tetra-*O*-acetyl-α-D-glucopyranosyl-2′,3′,6′-tri-*O*-acetyl-β-D-glucopyranosyl)-sn-glycerol (**25**) has been described in an earlier paper (Minden et al., 2002a). Synthesis of the chiral fatty acid (2*R*,4*R*,6*R*,8*R*)-2,4,6,8-tetramethyldecanoic acid and the corresponding alcohol was performed according to the procedure of Morr et al. (1992, 1997). *n*-Tetradecanol (purest grade) and maltose monohydrate were purchased from Fluka Chemie.

α-Melibiose monohydrate and maltotriose were purchased from Acros Organics.

Thin-layer chromatography (TLC) was performed on silica gel (Merck GF$_{254}$), and detection was effected by spraying with a solution of ethanol:sulfuric acid (9:1) followed by heating. Column chromatography was performed using silica gel (Merck, 0.063–0.200 mm, 230–400 mesh). NMR spectra were recorded on a Bruker AMX 400 or a Bruker DRX 5001 spectrometer (m$_c$, centred multiplet; d, doublet; t, triplet; dd, double doublet; dt, double triplet).

4.2. Synthesis

Deacetylation (general procedure 1):

The compound was dissolved in anhydrous methanol and sodium methoxide was added (pH 8–9). The solution was stirred at ambient temperature until TLC revealed the reaction to be complete. It was neutralised then using Amberlyst IR 120 ion-exchanger resign (protonated form), filtrated and evaporated in vacuo.

4.2.1. 1,3-Di-O-[(2′R,4′R,6′R,8′R)-2′,4′,6′,8′-tetra-methyl-decyl]-propan-2-ol (3)

The reaction was carried out as described for compound **2**, using 6 g (28 mmol) (2R,4R,6R,8R)-2,4,6,8-tetramethyldecane-1-ol, 644 mg (28 mmol) sodium and 1.3 g (1.1 mL; 14 mmol) epichlorhydrine in 100 mL of toluene. The product was purified by column chromatography (light petroleum b.p. 50–70 °C–ethyl acetate 20:1, then 9:1) to give slight yellow syrup.

Yield: 3.19 g (47%). $C_{31}H_{64}O_3$ (484.4855).

^{1}H NMR (500 MHz, CDCl$_3$ + TMS): δ = 3.84–3.90 (m, 1H, H-2), 3.34–3.44 (m, 8H, H-1a, H-1b, H-3a, H-3b, H-1a′, H-1b′), 2.57 (m, 2H, H-2′), 1.78 (m, 2H, H-3a′), 1.51–1.69 (m, 4H, H-4′, H-6′), 1.28–1.49 (m, 4H, H-8′, H-9a′), 1.16–1.25 (m, 10H, H-5a′, H-7a′, CH$_3$-2′), 0.97–1.12 (m, 4H, H-3b′, H-9b′), 0.80–0.95 (m, 4H, H-5b′, H-7b′), 0.90 (d, 6H, CH$_3$-4′), 0.85 (t, 6H, CH$_3$-10), 0.84 (m, 6H, CH$_3$-8′), 0.81 (d, 6H, CH$_3$-6′).

^{13}C NMR (125 MHz, CDCl$_3$ + TMS): δ = 72.20 (C-1, C-3), 76.50, 76.09 (C-1a′, C-1b′), 70.25 (C-2), 45.48, 44.88, 44.85 (C-5a′, C-5b′, C-7a′, C-7b′), 41.52, 41.30 (C-3a′, C-3b′), 31.58 (C-8a′, C-8b′), 31.08, 30.85 (C-2a′, C-2b′), 28.94, 28.90 (C-9a′, C-9b′), 28.09, 28.05 (C-4a′, C-4b′), 27.25, 27.23 (C-6a′, C-6b′), 21.69, 21.65, 21.64, 21.59, 21.48, 21.45 (CH$_3$-4a′, CH$_3$-4b′, CH$_3$-6a′, CH$_3$-6b′, CH$_3$-8a′, CH$_3$-8b′), 18.98 (CH$_3$-2a′, CH$_3$-2b′), 11.25 (CH$_3$-10a′, CH$_3$-10b′).

4.2.2. 1,3-Di-O-[cis-9-octadecenyl]-2-O-[4′-O-(2″,3″,4″,6″-tetra-O-acetyl-α-D-glucopyranosyl)-2′,3′,6′-tri-O-acetyl-β-D-glucopyranosyl]-sn-glycerol (8)

Seven hundred and eighty-one milligrams (1 mmol) **7**, 593 mg (1 mmol) **1** and 100 mg of freshly dried powdered molecular sieve (4 Å) were dissolved in 10 mL of anhydrous dichlormethane under an atmosphere of nitrogen. Under cooling (0 °C), 222 mg (1 mmol) trimethylsilyl trifluormethanesulfonate were added dropwise. Afterwards, the reaction mixture was stirred for 6 h at 0 °C. After TLC revealed the reaction to be complete, pyridine was added, 50 mL dichlormethane were added and the reaction mixture was filtered through Celite®. The organic phase was washed twice with 10 mL of a saturated solution of sodium hydrogen carbonate, and subsequently with 10 mL of water. The organic phase was dried over magnesium sulphate and solvent was removed under reduced pressure. The residue was purified by short-column chromatography (light petroleum b.p. 50–70 °C–ethyl acetate 4:1).

Yield: 1.0 g (83%). $C_{65}H_{110}O_{20}$ (1210.759).

^{1}H NMR (500 MHz, CDCl$_3$ + TMS): δ = 5.28–5.43 (m, 4H, H-olefin), 5.33 (d, 1H, H-1″), 5.29 (dd, 1H, H-3″), 5.17 (dd, 1H, H-3′), 4.98 (dd, 1H, H-4″), 4.79 (dd, 1H, H-2″), 4.72 (dd, 1H, H-2′), 4.71 (d, 1H, H-1′), 4.40 (dd, 1H, H-6a′), 4.19 (dd, 1H, H-6a″), 4.15 (dd, 1H, H.6b′), 3.97 (dd, 1H, H-6b″), 3.90 (dd, 1H, H-4′), 3.89 (ddd, 1H, H-5″), 3.80–3.87 (m, 1H, H-2), 3.59 (ddd, 1H, H-5′), 3.49 (d, 2H, H-1a, H-3a), 3.29–3.37 (m, 6H, H-1b, H-3b, α-CH$_2$), 2.06, 2.03, 1.97, 1.95 (each s, 3H, OAc), 1.93 (s, 6H, OAc), 1.92 (s, 3H, OAc), 1.86–1.99 (m, 8H, H-allyl.), 1.40–1.53 (m, 4H, β-CH$_2$), 1.12–1.33 (m, 44H, alkyl-CH$_2$), 0.81 (t, 6H, alkyl-CH$_3$); $^3J_{1',2'}$ = 8.6, $^3J_{2',3'}$ = 9.6, $^3J_{3',4'}$ = 9.6, $^3J_{4',5'}$ = 9.6, $^3J_{5',6a'}$ = 2.8, $^3J_{5',6b'}$ = 4.5, $^3J_{6a',b'}$ = 11.9, $^3J_{1'',2''}$ = 4.0, $^3J_{2'',3''}$ = 9.8, $^3J_{3'',4''}$ = 9.8, $^3J_{4'',5''}$ = 9.8, $^3J_{5'',6a''}$ = 4.1, $^3J_{5'',6b''}$ = 2.0, $^3J_{6a'',b''}$ = 12.5 Hz.

^{13}C NMR (125 MHz, CDCl$_3$ + TMS): δ = 170.55, 170.49, 170.27, 169.98, 169.60, 169.44 (C=O, OAc), 130.08 (C-olefin), 100.86, (C-1′), 96.06 (C-1″), 78.70 (C-2), 75.88 (C-3′), 73.48 (C-4′), 72.92 (C-2′), 72.63 (C-5′), 71.86 (α-CH$_2$), 71.31 (C-1, C-3), 70.38 (C-2″), 70.09 (C-3″), 69.25 (C-5″), 68.68 (C-4″), 63.46 (C-6′), 61.77 (C-6″), 33.36 (C-allyl), 32.57, 30.51, 30.26, 30.04, 29.89, 29.79, 29.71, 26.62 (alkyl-CH$_2$), 20.89, 20.78, 20.68, 20.64, 20.62, 20.60, 20.59 (CH$_3$, OAc), 14.13 (alkyl-CH$_3$).

4.2.3. 1,3-Di-O-[cis-9-octadecenyl]-2-O-[4′-O-(α-D-glucopyranosyl)-β-D-glucopyranosyl]-sn-glycerol (9)

Nine hundred and eighty-eight milligrams (0.815 mmol) **8** were deprotected using general procedure 1. The product was purified by gel filtration on a column of Serva LH-20 suspended in methanol.

Yield: 665 mg (89%). $C_{51}H_{96}O_{13}$ (916.6851).

FAB-HIRESMS: m/z = 939.6712 $[M + Na]^+$ (calc. 939.6749).

$[\alpha]_D^{20} = +22°$ (c = 0.17, MeOH)

^{1}H NMR (400 MHz, d$_4$-methanol): δ = 5.27–5.38 (m, 4H, H-olefin), 5.14 (d, 1H, H-1″), 4.31 (d, 1H, H-1′), 3.94–3.97 (m, 1H, H-2), 3.88 (dd, 1H, H-6a′), 3.79–3.87 (m, 3H, H-4″, H-6b′, H-6a″), 3.65–3.73

(m, 2H, H-5″, H-6b″), 3.61 (m, 2H, H-3′, H-3″), 3.56 (dd, 1H, H-4′), 3.43–3.50 (m, 3H, H-1a, H-3a, H-2″), 3.38 (ddd, 1H, H-5′), 3.24–3.29 (m, 3H, H-1b, H-3b, H-2′), 3.16–3.21 (m, 4H, alkyl-α-CH₂), 1.92–2.05 (m, 8H, −CH₂-allyl.), 1.48–1.57 (m, 4H, alkyl-β-CH₂), 1.16–1.41 (m, 44H, alkyl-CH₂), 0.88 (t, 3H, alkyl-CH₃); $^3J_{1',2'} = 8.1$, $^3J_{3',4'} = 9.2$, $^3J_{4',5'} = 9.3$, $^3J_{5',6a'} = 2.1$, $^3J_{5',6b'} = 5.6$, $^2J_{6a',b'} = 12.2$, $^3J_{1'',2''} = 3.6$ Hz.

4.2.4. 1,3-Di-O-[cis-9-octadecenyl]-2-O-{4′-O-[4″-O-(2‴,3‴,4‴,6‴-tetra-O-acetyl-α-D-glucopyranosyl)-2″,3″,6″-tri-O-acetyl-α-D-glucopyranosyl]-2′,3′,6′-tri-O-acetyl-β-D-glucopyranosyl}-sn-glycerol (14)

The reaction was carried out as described for **8** using 1.1 g (1 mmol) **13** and 593 mg (1 mmol) **1**. The product was purified using light petroleum b.p. 50–70 °C–ethyl acetate 1:1 as eluent.

Yield: 983 mg (70%). C₇₇H₁₂₆O₂₈ (1498.8436).

^{1}H NMR (400 MHz, CDCl₃ + TMS): $\delta = 5.25$–5.26 (m, 6H, H-3″, H-3‴, H-olefin), 5.20 (d, 2H, H-1″, H-1‴), 5.19 (dd, 1H, H-3′), 5.00 (dd, 1H, H-4‴), 3.79 (dd, 1H, H-2‴), 4.72 (d, 1H, H-1′), 4.71 (dd, 1H, H-2′), 4.67 (dd, 1H, H-2″), 4.35–4.42 (m, 2H, H-2, H-6a′), 3.80–4.27 (m, 11H, H-1a, H-3a, H-4′, H-4″, H-5′, H-5‴, H-6a″, H-6a‴, H-6b′, H-6b″, H-6b‴), 3.45–3.51 (m, 2H, H-1b, H-3b), 3.30–3.38 (m, 5H, H-5′, alkyl-α-CH₂), 2.09, 2.08, 2.03, 1.98, 1.97, 1.96, 1.95, 1.93, 1.92, 1.91 (each s, 3H, OAc), 1.44–1.51 (m, 8H, H-allyl.), 1.15–1.32 (m, 48H, alkyl-CH₂), 0.81 (t, 6H, alkyl-CH₃); $^3J_{1',2'} = 8.1$, $^3J_{2',3'} = 9.2$, $^3J_{3',4'} = 9.2$, $^3J_{1'',2''} = 3.8$, $^3J_{2'',3''} = 10.2$, $^3J_{1''',2'''} = 3.8$, $^2J_{2''',3'''} = 10.4$, $^3J_{3''',4'''} = 9.8$, $^3J_{4''',5'''} = 9.8$, $^3J_{CH_2,CH_3} = 6.9$ Hz.

^{13}C NMR (100 MHz, CDCl₃ + TMS): $\delta = 170.54$, 170.52, 170.29, 170.27, 169.97, 169.83, 169.59, 169.43 (C=O, OAc), 130.34, 130.25 (C-olefin), 100.65 (C-1′), 96.14, 96.11 (C-1″, C-1‴), 78.76 (C-2), 75.88 (C-3′), 74.38 (C-3″), 73.00, 72.87, 72.39, 72.11, 71.67 (C-4′, C-4″, C-5′, C-5″, C-5‴), 72.23, 72.19 (C-2′, C-2″), 70.92 (C-2‴), 70.49, 70.46 (C-α), 69.82 (C-3‴), 69.34, 69.29 (C-1, C-3), 68.36 (C-4‴), 63.50, 62.81, 61.83 (C-6′, C-6″, C-6‴), 33.02, 32.32, 30.19, 30.13, 30.08, 30.05, 29.93, 29.91, 29.72, 27.64, 26.55, 26.53, 23.09 (alkyl-CH₂), 21.31, 21.28, 21.21, 21.08, 21.05, 20.99, 20.96 (CH₃, OAc), 14.61, 14.58 (alkyl-CH₃).

4.2.5. 1,3-Di-O-[cis-9-octadecenyl]-2-O-{4′-O-[4″-O-(α-D-glucopyranosyl)-α-D-glucopyranosyl]-β-D-glucopyranosyl}-sn-glycerol (15)

Nine hundred and seventy-five milligrams (0.65 mmol) **14** were deprotected using general procedure 1. The product was purified by gel filtration on a column of Serva LH-20 suspended in methanol.

Yield: 647 mg (93%). C₅₇H₁₀₆O₁₈ (1078.7379).

FAB-HIRESMS: $m/z = 1101.7255$ $[M + Na]^+$ (calc. 1101.7277)

$[\alpha]_D^{20} = +45°$ ($c = 0.8$, MeOH)

^{1}H NMR (500 MHz, d₄-Methanol): $\delta = 5.26$–5.36 (m, 4H, H-olefin), 5.12 (d, 1H, H-1‴), 5.10 (d, 1H, H-1″), 4.43 (d, 1H, H-1′), 3.92–3.98 (m, 1H, H-2), 3.69–3.85 (m, 8H, H-4″, H-4‴, H-6a′, H-6a″, H-6a‴, H-6b′, H-6b″, H-6b‴), 3.50–3.66 (m, 7H, H-1a, H-3a, H-3′, H-3″, H-3‴, H-5″, H-5‴), 3.42–3.49 (m, 7H, H-1b, H-3b, H-4′, alkyl-α-CH₂), 3.40 (dd, 2H, H-2″, H-2‴), 3.33 (m_c, 1H, H-5), 3.20 (dd, 1H, H-2′), 1.91–2.04 (m, 8H, H-allyl.), 1.49–1.57 (m, 4H, β-CH₂), 1.16–1.39 (m, 44H, alkyl-CH₂), 0.87 (t, 6H, alkyl-CH₃); $^3J_{1',2'} = 8.1$, $^3J_{2',3'} = 9.1$, $^3J_{1'',2''} = 4.1$, $^3J_{2'',3''} = 9.8$, $^3J_{1''',2'''} = 4.1$, $^3J_{2''',3'''} = 9.8$, $^3J_{CH_2,CH_3} = 6.6$ Hz.

4.2.6. 1,3-Di-O-tetradecyl-2-O-[4′-O-(2″,3″,4″,6″-tetra-O-acetyl-α-D-glucopyranosyl)-2′,3′,4′-tri-O-acetyl-β-D-glucopyranosyl]-sn-glycerol (17)

3.39 g (5 mmol) Maltoseperacetate and 2.42 g (5 mmol) **2** were dissolved in 50 mL of dry dichlormethane under an atmosphere of dry nitrogen. 994 mg (880 μL; 7 mmol) boron trifluoride etherate were added and the solution was stirred for 6 h at ambient temperature until TLC revealed the reaction to be complete. The reaction was quenched with 50 mL of a saturated solution of sodium hydrogen carbonate, the organic layer was separated and the aqueous layer extracted twice with dichlormethane. The combined organic phases were washed twice with water, dried over magnesium sulphate and evaporated in vacuo. The residue was purified by column chromatography (light petroleum b.p. 50–70 °C–ethyl acetate 2:1).

Yield: 3.00 g (54%). C₅₇H₉₈O₂₀ (1102.6651).

^{1}H NMR (400 MHz, CDCl₃ + TMS): $\delta = 5.34$ (d, 1H, H-1″), 5.29 (dd, 1H, H-3″), 5.18 (t, 1H, H-3′), 4.98 (t, 1H, H-4″), 4.79 (dd, 1H, H-2″),

4.74 (dd, 1H, H-2′), 4.70 (d, 1H, H-1′), 4.40 (dd, 1H, H-6a′), 4.19 (dd, 1H, H-6a″), 4.15 (dd, 1H, H-6b′), 3.97 (dd, 1H, H-6b″), 3.91 (t, 1H, H-4′), 3.80–3.91 (m, 2H, H-2, H-5″), 3.59 (ddd, 1H, H-5′), 3.44–3.51 (m, 2H, H-1a, H-3a), 3.29–3.38 (m, 6H, H-1b, H-3b, alkyl-α-CH$_2$), 2.07, 2.03, 1.98, 1.96 (each s, 3H, OAc), 1.93 (s, 6H, OAc), 1.92 (s, 3H, OAc), 1.42–1.52 (m, 4H, β-CH$_2$), 1.16–1.25 (m, 44H, alkyl-CH$_2$), 0.81 (t, 6H, alkyl-CH$_3$); $^3J_{1',2'} = 8.1$, $^3J_{2',3'} = 9.7$, $^3J_{3',4'} = 9.7$, $^3J_{4',5'} = 9.7$, $^3J_{5',6a'} = 2.8$, $^3J_{5',6b'} = 4.8$, $^2J_{6a',6b'} = 12.2$, $^3J_{1'',2''} = 3.8$, $^3J_{2'',3''} = 9.7$, $^3J_{3'',4''} = 9.7$, $^3J_{4'',5''} = 9.7$, $^3J_{5'',6a''} = 4.1$, $^3J_{5'',6b''} = 2.3$, $^2J_{6a'',6b''} = 12.9$, $^3J_{CH_2,CH_3} = 6.6$ Hz.

^{13}C NMR (100 MHz, CDCl$_3$ + TMS): $\delta = 170.94$, 170.87, 170.62, 170.34, 170.05, 169.82 (C=O, OAC), 100.66 (C-1″), 95.94 (C-1′), 78.75 (C-2), 75.94 (C-3′), 73.25 (C-4′), 72.81 (C-2′), 72.43 (C-5′), 72.19, 72.10 (C-α), 71.66, 70.92 (C-1, C-3), 70.40 (C-2″), 70.09 (C-3″), 69.80 (C-5″), 68.47 (C-4″), 63.33 (C-6′), 61.94 (C-6″), 32.34, 30.12, 30.08, 29.95, 29.78, 26.56, 26.53, 23.11 (alkyl-CH$_2$), 21.35, 21.25, 21.11, 21.06, 21.00 (–CH$_3$, OAc), 14.54 (alkyl-CH$_3$).

4.2.7. 1,3-Di-O-tetradecyl-2-O-[4′-O-(α-D-glucopyranosyl)-β-D-glucopyranosyl]-sn-glycerol (18)

2.98 g (2.70 mmol) **17** were deprotected using general procedure 1. The product was recrystallised from methanol.

Yield: 2.10 g (90%). C$_{43}$H$_{84}$O$_{13}$ (808.5912).

MALDITOF-MS: $m/z = 831.6$ [$M + Na$]$^+$

Calc.		Found	
C 63.83			C 63.92
	H 10.46		H 10.58

$[\alpha]_D^{20} = +20°$ ($c = 1.0$, MeOH)

^{1}H NMR (500 MHz, d$_4$-Methanol): $\delta = 5.19$ (d, 1H, H-1″), 4.30 (d, 1H, H-1′), 3.94–3.96 (m, 1H, H-2), 3.89 (dd, 1H, H-6a′), 3.76–3.87 (m, 3H, H-4″, H-6b′, H-6a″), 3.66–3.73 (m, 2H, H-5″, H-6b″), 3.58–3.63 (m, 2H, H-3′, H-3″), 3.52 (dd, 1H, H-4′), 3.43–3.50 (m, 3H, H-1a, H-3a, H-2″), 3.39 (ddd, 1H, H-5′), 3.22–3.29 (m, 3H, H-1b, H-3b, H-2′), 3.17–3.21 (m, 4H, alkyl-α-CH$_2$), 1.41–1.50 (m, 4H, alkyl-β-CH$_2$), 1.16–1.35 (m, 44H, alkyl-CH$_2$), 0.88 (t, 6H, alkyl-CH$_3$); $^3J_{1',2'} = 8.1$, $^3J_{3',4'} = 9.1$,

$^3J_{4',5'} = 9.1$, $^3J_{5',6a'} = 2.1$, $^3J_{5',6b'} = 5.7$, $^2J_{6a',b'} = 12.1$, $^3J_{1'',2''} = 3.6$ Hz.

4.2.8. 1,3-Di-O-[(2′R,4′R,6′R,8′R)-2′,4′,6′,8′-tetramethyldecyl]-2-O-[4″-O-(2‴,3‴,4‴,6‴-tetra-O-acetyl-α-D-glucopyranosyl)-2″,3″,4″-tri-O-acetyl-β-D-glucopyranosyl]-sn-glycerol (19)

The reaction was carried out as described for **17** using 1.83 g (2.7 mmol) Maltoseperacetate, 1.3 g (2.7 mmol) **3** and 537 mg (475 μL; 3.78 mmol) boron trifluoride etherate. The product was purified using light petroleum b.p. 50–70 °C–ethyl acetate 2:1 as eluent.

Yield: 1.04 g (35%). C$_{57}$H$_{98}$O$_{20}$ (1102.6651)

^{1}H NMR (500 MHz, CDCl$_3$ + TMS): $\delta = 5.36$ (d, 1H, H-1‴), 5.28 (dd, 1H, H-3‴), 5.21 (dd, 1H, H-3″), 5.00 (t, 1H, H-4‴), 4.85 (dd, 1H, H-2‴), 4.76 (dd, 1H, H-2″), 4.74 (d, 1H, H-1″), 4.41 (dd, 1H, H-6a″), 4.19 (dd, 1H, H-6a‴), 4.14 (dd, 1H, H-6b‴), 3.96 (dd, 1H, H-6b‴), 3.92 (t, 1H, H-4″), 3.81–3.95 (m, 2H, H-2, H-5‴), 3.61 (ddd, 1H, H-5″), 3.44–3.50 (m, 2H, H-1a, H-3a), 3.28–3.40 (m, 6H, H-1b, H-3b, H-1a′, H-1b′), 2.56 (m, 2H, H-2′), 2.07, 2.03, 1.98, 1.96 (each s, 3H, OAc), 1.94 (s, 6H, OAc), 1.91 (s, 3H, OAc), 1.78 (m, 2H, H-3a′), 1.52–1.70 (m, 4H, H-4′, H-6′), 1.28–1.50 (m, 4H, H-8′, H-9a′), 1.16–1.26 (m, 10H, H-5a′, H-7a′, CH$_3$-2′), 0.98–1.13 (m, 4H, H-3b′, H-9b′), 0.79–0.95 (m, 4H, H-5b′, H-7b′), 0.90 (d, 6H, CH$_3$-4′), 0.85 (t, 6H, CH$_3$-10′), 0.83 (m, 6H, CH$_3$-8′), 0.79 (d, 6H, CH$_3$-6′). $^3J_{1',2'} = 8.1$, $^3J_{2',3'} = 9.7$, $^3J_{3',4'} = 9.7$, $^3J_{4',5'} = 9.7$, $^3J_{5',6a'} = 2.8$, $^3J_{5',6b'} = 4.8$, $^2J_{6a',6b'} = 12.2$, $^3J_{1'',2''} = 3.8$, $^3J_{2'',3''} = 9.7$, $^3J_{3'',4''} = 9.7$, $^3J_{4'',5''} = 9.7$, $^3J_{5'',6a''} = 4.1$, $^3J_{5'',6b''} = 2.3$, $^2J_{6a'',6b''} = 12.9$ Hz.

^{13}C NMR (100 MHz, CDCl$_3$ + TMS): $\delta = 170.98$, 170.90, 170.68, 170.34, 170.12, 169.92 (C=O, OAC), 100.54 (C-1‴), 95.98 (C-1″), 78.76 (C-2), 75.92 (C-3″), 73.26 (C-4″), 72.81 (C-2″), 72.43 (C-5″), 72.25, 72.14 (C-1a′, C-1b′), 71.98, 71.05 (C-1, C-3), 70.48 (C-2‴), 70.25 (C-3‴), 69.78 (C-5‴), 68.55 (C-4‴), 63.42 (C-6″), 61.98 (C-6‴), 45.48, 44.87, 44.84 (C-5a′, C-5b′, C-7a′, C-7b′), 41.51, 41.34 (C-3a′, C-3b′), 31.57 (C-8a′, C-8b′), 31.07, 30.86 (C-2a′, C-2b′), 28.93, 28.89 (C-9a′, C-9b′), 28.07, 28.03 (C-4a′, C-4b′), 27.26, 27.24 (C-6a′, C-6b′), 21.69, 21.65, 21.64, 21.59, 21.48, 21.45 (CH$_3$-4a′, CH$_3$-4b′, CH$_3$-6a′, CH$_3$-6b′, CH$_3$-8a′, CH$_3$-8b′), 21.36, 21.26, 21.12, 21.07, 21.01 (–CH$_3$, OAc), 18.98 (CH$_3$-2a′, CH$_3$-2b′), 11.25 (CH$_3$-10a′, CH$_3$-10b′).

4.2.9. 1,3-Di-O-[(2′R,4′R,6′R,8′R)-2′,4′,6′,8′-tetramethyldecyl]-2-O-[4′′-O-(α-D-glucopyranosyl)-β-D-glucopyranosyl]-sn-glycerol (20)

Nine hundred and fifty milligrams (0.86 mmol) **17** were deprotected using general procedure 1. The product was purified by silica gel chromatography (chloroform–methanol 10:1).

Yield: 522 mg (75%). $C_{43}H_{84}O_{13}$ (808.5912). MALDITOF-MS: $m/z = 831.5$ $[M + Na]^+$FAB-HIRESMS: $m/z = 831.5802$ $[M + Na]^+$ (calc. 831.581)

$[\alpha]_D^{20} = +25°$ ($c = 0.2$, MeOH)

^{1}H NMR (500 MHz, d$_4$-MeOH): $d = 5.21$ (d, 1H, H-1′′′), 4.40 (d, 1H, H-1′′), 3.94–3.96 (m, 1H, H-2), 3.43–3.50 (m, 2H, H-1a, H-3a), 3.75–3.95 (m, 4H, H-3′′, H-3′′′, H-4′′, H-4′′′) 3.52–3.70 (m, 6H, H-5′′, H-5′′′, H-6a′′, H-6a′′′, H-6b′′, H-6b′′′), 3.48 (dd, 1H, H-2′′′), 3.40 (dd, 1H, H-2′′), 3.22–3.29 (m, 6H, H-1b, H-3b, H-1a′, H.1a′, H-1b′, H-1b′), 2.54–2.65 (m, 2H, H-2′, H-2′), 1.69–1.79 (m, 2H, H-3a′, H-3a′), 1.47–1.65 (m, 4H, H-4′, H-4′, H-6′, H-6′), 1.31–1.47 (m, 4H, H-8′, H-8′, H-9a′, H-9a′), 1.11–1.23 (m, 10H, H-5a′, H-5a′, H-7a′, H-7a′, CH$_3$-2′, CH$_3$-2′), 1.01–1.11 (m, 4H, H-3b′, H-3b′′, H-9b′, H-9b′), 0.80–0.97 (m, 28H, H-5b′, H-5b′, H-7b′, H-7b′, CH$_3$-4′, CH$_3$-4′, CH$_3$-6′, CH$_3$-6′, CH$_3$-8′, CH$_3$-8′, CH$_3$-10′, CH$_3$-10′); $^3J_{1,2} = 9.7$, $^3J_{2,3} = 9.2$, $^3J_{1′,2′} = 4.1$, $^3J_{2′,3′} = 9.7$, $^2J_{\alpha a,\alpha\beta} = 12.2$, $^3J_{\alpha a,b-CH_2} = 7.1$, $^3J_{\alpha\beta,\beta-CH_2} = 7.6$ Hz.

4.2.10. 1,3-Di-O-tetradecyl-2-O-[6′-O-(2′′,3′′,4′′,6′′-tetra-O-acetyl-α-D-galactopyranosyl)-2′,3′,4′-tri-O-acetyl-β-D-glucopyranosyl]-sn-glycerol (23)

The reaction was carried out as described for **17** using 2.95 g (4.3 mmol) Melibioseperacetate, 2.3 g (4.3 mmol) **2** and 854 mg (760 μL; 6 mmol) boron trifluoride etherate. The product was purified using light petroleum b.p. 50–70 °C–ethyl acetate 2:1 as eluent.

Yield: 2.05 g (43%). $C_{57}H_{98}O_{20}$ (1102.6651).

^{1}H NMR (500 MHz, CDCl$_3$ + TMS): $\delta = 5.39$ (dd, 1H, H-4′′), 5.27 (dd, 1H, H-3′′), 5.13 (t, 1H, H-3′), 5,09 (d, 1H, H-1′′), 5.05 (dd, 1H, H-2′′), 5.04 (dd, 1H, H-4′), 4.83 (dd, 1H, H-2′), 4.71 (d, 1H, H-1′), 4.15 (m$_c$, 1H, H-5′), 4.00–4.08 (m, 2H, H-6a′′, H-6b′′), 3.82–3.87 (m, 1H, H-2), 3.68 (dd, 1H, H-6a′), 3.45–3.57 (m, 4H, H-1a, H-3a, H-5′, H-6b′), 3.29–3.37 (m, 6H, H-1b, H-3b, alkyl-α-CH$_2$), 2.06, 1.98, 1.97,

1.96, 1.93, 1.91 (each s, 3H, OAc), 1.43–1.51 (m, 4H, alkyl-β-CH$_2$), 1.14–1.28 (m, 44H, alkyl-CH$_2$), 0.81 (t, 6H, alkyl-CH$_3$); $^3J_{1′,2′} = 7.9$, $^3J_{2′,3′} = 9.5$, $^3J_{3′,4′} = 9.5$, $^3J_{4′,5′} = 9.7$, $^3J_{5′6a′} = 4.1$, $^2J_{6a′,b′} = 11.0$, $^3J_{1′′,2′′} = 3.8$, $^3J_{2′′,3′′} = 10.7$, $^3J_{3′′,4′′} = 3.5$, $^3J_{4′′,5′′} = 1.0$, $^3J_{CH_2,CH_3} = 6.9$ Hz.

^{13}C NMR (125 MHz, CDCl$_3$ + TMS): $\delta = 170.95$, 170.77, 170.74, 170.58, 170.16, 169.76, 169.70 (C=O, OAc), 100.94 (C-1′), 97.13 (C-1′′), 78.39 (C-2), 73.00 (C-3′), 72.17 (C-5′), 72.10, 71.92 (C-α), 71.38 (C-2′), 71.70, 70.97 (C-1, C-3), 69.37 (C-4′), 68.36, 68.31 (C-4′′, C-2′′), 67.85 (C-3′′), 66.85 (C-5′′), 66.83 (C-6′), 62.10 (C-6′′), 32.33, 30.12, 30.08, 29.96, 29.78, 26.58, 26.54, 23.10 (alkyl-CH$_2$), 21.23, 21.12, 21.04, 20.80 (−CH$_3$, OAc), 14.53 (alkyl-CH$_3$).

4.2.11. 1,3-Di-O-tetradecyl-2-O-[6′-O-(α-D-galactopyranosyl)-β-D-glucopyranosyl]-sn-glycerol (24)

1.95 g (1.77 mmol) **23** were deprotected using general procedure 1. The product was recrystallised from 2-propanol.

Yield: 1.27 g (89%). $C_{43}H_{84}O_{13}$ (808.5912). MALDITOF-MS: $m/z = 831.5$ $[M + Na]^+$

Calc.	C 63.86	Found	C 63.91
	H 10.46		H 10.10

$[\alpha]_D^{20} = +23°$ ($c = 0.8$, CH$_3$COCH$_3$)

^{1}H NMR (400 MHz, d$_4$-methanol): $\delta = 4.89$ (d, 1H, H-1′′), 4.31 (d, 1H, H-1′), 4.01 (dd, 1H, H-6a′), 3.90–3.95 (m, 2H, H-4′′, H-5′′, H-2), 3.69–3.80 (m, 5H, H-2′′, H-3′′, H-6a′′, H-6b′, H-6b′′), 3.50 (ddd, 1H, H-5′), 3.43–3.49 (m, 3H, H-1a, H-3a, H-4′), 3.38 (dd, 1H, H-3′), 3.20–3.28 (m, 3H, H-1b, H-3b, H-2′), 3.17–3.22 (m, 4H, alkyl-α-CH$_2$), 1.40–1.49 (m, 4H, β-CH$_2$), 1.16–1.36 (m, 44H, alkyl-CH$_2$), 0.88 (t, 6H, alkyl-CH$_3$); $^3J_{1′,2′} = 8.1$, $^3J_{2′,3′} = 9.2$, $^3J_{3′,4′} = 9.2$, $^3J_{4′,5′} = 9.2$, $^3J_{5′,6a′} = 4.1$, $^3J_{5′,6b′} = 2.0$, $^3J_{1′′,2′′} = 4.1$ Hz.

4.2.12. 1,2-Di-O-[(2′R,4′R,6′R,8′R)-2′,4′,6′,8′-tetramethyldecanoyl]-3-O-[4′′-O-(2′′′,3′′′,4′′′,6′′′-tetra-O-acetyl-α-D-glucopyranosyl)-2′′,3′′,6′′-tri-O-acetyl-β-D-glucopyranosyl]-sn-glycerol (26)

677.5 mg (0.95 mmol) 3-O-[4′-O-(2′′,3′′,4′′,6′′-tetra-O-acetyl-α-D-glucopyranosyl)-2,3,6-tri-O-acetyl-β-D-glucopyranosyl]-sn-glycerol (**25**), 435 mg (1.90 mmol) (2R,4R,6R,8R)-2,4,6,8-tetramethyldecanoic

acid, 393 mg (1.90 mmol) N,N′-dicyclohexyl-carbodiimide and a catalytic amount of 4-(1-pyrrolidinyl)pyridine were dissolved in 25 mL of dry dichlormethane and stirred at room temperature overnight, until TLC revealed the reaction to be complete. N, N′-dicyclohexylurea formed during the course of the reaction was filtered off, the solvent removed under reduced pressure and the resulting syrup purified by silica gel chromatography (light petroleum b.p. 50–70 °C–ethyl acetate 2:1).

Yield: 537 mg (49%). $C_{57}H_{94}O_{22}$ (1130.6237).

^{1}H NMR (500 MHz, CDCl$_3$ + TMS): δ = 5.36 (d, 1H, H-1‴), 5.30 (dd, 1H, H-3‴), 5.20 (dd, 1H, H-3″), 5.00 (dd, 1H, H-4‴), 5.16–5.23 (m, 1H, H-2), 4.81 (dd, 1H, H-2‴), 4.78 (dd, 1H, H-2″), 4.71 (d, 1H, H-1″), 4.41 (dd, 1H, H-6a″), 4.32 (dd, 1H, H-1a), 4.13–4.21 (m, 3H, H-1b, H-6b″, H-6a‴), 3.99 (dd, 1H, H-6b‴), 3.97 (dd, 1H, H-3a), 3.90 (t, 1H, H-4″), 3.85 (ddd, 1H, H-5‴), 3.66 (dd, 1H, H-3b), 3.60 (ddd, 1H, H-5″), 2.56 (m$_c$, 2H, H-2′, H-2′), 2.08, 2.07, 2.00, 1.98 (each s, 3H, OAc), 1.94 (s, 6H, OAc), 1.92 (s, 3H, OAc), 1.72–1.76 (m, 2H, H-3a′, H-3a′), 1.54–1.65 (m, 2H, H-6′, H-6′), 1.48–1.54 (m, 2H, H-4′, H-4′), 1.30–1.46 (m, 4H, H-8′, H-8′, H-9a′, H-9a′), 1.15–1.28 (m, 10H, H-5a′, H-5a′, H-7a′, H-7a′, CH$_3$-2′, CH$_3$-2′), 0.95–1.09 (m 4H, H-3b′, H-3b′, H-9b′, H-9b′), 0.80–0.94 (m, 28H, H-5b′, H-5b′, H-7b′, H-7b′, CH$_3$-4′, CH$_3$-4′, CH$_3$-6′, CH$_3$-6′, CH$_3$-8′, CH$_3$-8′, CH$_3$-10′, CH$_3$-10′); $^3J_{1',2'}$ = 8.1, $^3J_{2',3'}$ = 9.7, $^3J_{3',4'}$ = 9.7, $^3J_{4',5'}$ = 9.7, $^3J_{5',6a'}$ = 2.8, $^3J_{5',6b'}$ = 4.8, $^2J_{6a',6b'}$ = 12.2, $^3J_{1'',2''}$ = 3.8, $^3J_{2'',3''}$ = 9.7, $^3J_{3'',4''}$ = 9.7, $^3J_{4'',5''}$ = 9.7, $^3J_{5'',6a''}$ = 4.1, $^3J_{5'',6b''}$ = 2.3, $^2J_{6a'',6b''}$ = 12.9 Hz.

^{13}C NMR (125 MHz, CDCl$_3$ + TMS): δ = 176.95, 176.01 (C-1′, C-1′), 170.95, 170.86, 170.65, 170.25, 169.37, 169.18 (C=O, OAc), 101.16 (C-1‴), 96.01 (C-1″), 75.75 (C-3″), 73.24 (C-4″), 71.96 (C-2″), 71.13 (C-5″), 70.45 (C-2‴), 70.11 (C-3‴), 69.95 (C-5‴), 69.65 (C-2), 68.33 (C-4‴), 67.80 (C-3), 63.25 (C-6″), 62.14 (C-1), 61.85 (C-6‴), 45.34, 44.86, 44.82 (C-5a′, C-5b′, C-7a′, C-7b′), 40.91, 40.81 (C-3a′, C-3b′), 37.26, 37.17 (C-2a′, C-2b′), 31.53 (C-8a′, C-8b′), 28.98, 28.96 (C-9a′, C-9b′), 28.09, 28.06 (C-4a′, C-4b′), 27.25 (C-6a′, C-6b′), 21.35, 21.26, 21.12, 20.99, 20.70, 20.68, 20.64, 20.59, 20.48, 20.45, 19.92, 19.90 (OAc, CH$_3$-4a′, CH$_3$-4b′, CH$_3$-6a′, CH$_3$-6b′, CH$_3$-8a′, CH$_3$-8b′), 18.15 (CH$_3$-2a′, CH$_3$-2b′), 11.20 (CH$_3$-10a′, CH$_3$-10b′).

4.2.13. 1,2-Di-O-[(2′R,4′R,6′R,8′R)-2′,4′,6′,8′-tetramethyldecanoyl]-3-O-[4″-O-(α-D-glucopyranosyl)-β-D-glucopyranosyl]-sn-glycerol (27)

Five hundred and eighteen milligrams (0.46 mmol) **26** were dissolved in a mixture of 7 mL dry methanol and 3 mL dry dichlormethane. 0.18 mL (3.65 mmol) hydrazine hydrate (100%) were added to this solution and the mixture was heated at the temperature of reflux for 8 h. The solution was cooled in an ice-bath, neutralised with formic acid and the solvent removed in vacuo. The residue was submitted to chromatographic purification on silica gel (chloroform–methanol 15:1).

Yield: 166 mg (43%). $C_{43}H_{80}O_{15}$ (836.5497).

MALDITOF-MS: m/z = 859.4 $[M + Na]^+$

FAB-HIRESMS: m/z = 859.5388 $[M + Na]^+$ (calc. 859.5395)

$[\alpha]_D^{20}$ = +28° (c = 0.3, MeOH)

^{1}H NMR (500 MHz, d$_4$-MeOH + TMS): δ = 5.27 (m$_c$, 1H, H-2), 5.15 (d, 1H, H-1‴), 4.40 (dd, 1H, H-1a), 4.30 (d, 1H, H-1″), 4.21 (dd, 1H, H-1b), 3.97 (dd, 1H, H-3a), 3.89 (dd, 1H, H-6a″), 3.79–3.86 (m, 2H, H-6b″, H-6a‴), 3.64–3.72 (m, 2H, H-5‴, H-6b‴), 3.62 (t, 2H, H-3″, H-3‴), 3.55 (dd, 1H, H-4″), 3.45 (dd, 1H, H-2‴), 3.37 (ddd, 1H, H-5″), 3.27 (dd, 1H, H-4‴), 3.25 (dd, 1H, H-2″), 2.53–2.64 (m, 2H, H-2′, H-2′), 1.68–1.78 (m, 2H, H-3a′, H-3a′), 1.46–1.64 (m, 4H, H-4′, H-4′, H-6′, H-6′), 1.30–1.46 (m, 4H, H-8′, H-8′, H-9a′, H-9a′), 1.10–1.22 (m, 10H, H-5a′, H-5a′, H-8a′, H-8a′, CH$_3$-2′, −CH$_3$-2′), 0.99–1.10 (m, 4H, H-3b′, H-3b′, H-9b′, H-9b′), 0.79–0.94 (m, 28H, H-5b′, H-5b′, H-7b′, H-7b′, CH$_3$-4′, CH$_3$-4′, CH$_3$-6′, CH$_3$-6′, CH$_3$-8′, CH$_3$-8′, CH$_3$-10′, −CH$_3$-10′); $^3J_{1',2'}$ = 7.9, $^3J_{2',3'}$ = 9.1, $^3J_{3',4'}$ = 9.1, $^3J_{4',5'}$ = 9.3, $^3J_{5',6a'}$ = 1.9, $^3J_{5',6b'}$ = 4.4, $^2J_{6a',6b'}$ = 12.3, $^3J_{1'',2''}$ = 3.8, $^3J_{2'',3''}$ = 9.8, $^3J_{3'',4''}$ = 9.2, $^3J_{1a,2}$ = 2.8, $^3J_{1b,2}$ = 6.6, $^3J_{1a,1b}$ = 12.0, $^3J_{3a,2}$ = 5.4, $^3J_{3b,2}$ = 6.0, $^2J_{3a,3b}$ = 11.0 Hz.

^{13}C NMR (125 MHz, d$_4$-MeOH + TMS): δ = 177.03, 176.78 (C-1′, C-1′), 104.53 (C-1″), 102.83 (C-1‴), 81.10 (C-4″), 77.44, 74.88 (C-3″, C-3‴), 76.52 (C-5″), 74.57 (C-5‴), 74.30 (C-2″), 73.95 (C-2‴), 71.49 (C-2), 71.31 (C-4‴), 68.71 (C-3), 63.85 (C-1), 62.64 (C-6‴), 61.94 (C-6″), 45.31, 44.85 (C-5a′, C-5b′, C-7a′, C-7b′), 40.89, 40.82 (C-3a′,

C-3b′), 37.32, 37.27 (C-2a′, C-2b′), 31.52 (C-8a′, C-8b′), 28.98 (C-9a′, C-9b′), 28.09 (C-4a′, C-4b′), 27.24 (C-6a′, C-6b′), 20.60, 20.64, 20.48, 20.46, 19.91 (CH$_3$-4a′, CH$_3$-4b′, CH$_3$-6a′, CH$_3$-6b′, CH$_3$-8a′, CH$_3$-8b′),18.19, 18.14 (CH$_3$-2a′, CH$_3$-2b′), 11.20 (CH$_3$-10a′, CH$_3$-10b′).

4.2.14. (cis-9-Octadecenyl) 4-O-[4′-O-(2″,3″,4″, 6″-tetra-O-acetyl-α-D-glucopyranosyl)-2′,3′,6′-tri-O-acetyl-α-D-glucopyranosyl]-2,3,6-tri-O-acetyl-β-D-glucopyranoside (28)

4.23 g (4.4 mmol) β-D-Maltotrioseundecaacetate, 1.14 mL (1.34 g; 6.6 mmol) cis-9-octadecen-1-ol and 20 mg freshly dried powdered molecular sieve (0.4 nm) were dissolved in 50 mL of dry dichlormethane under a dry nitrogen atmosphere. 0.86 mL (679 mg; 6.8 mmol) boron trifluoride etherate were added dropwise. After 5 h, TLC revealed the reaction to be complete. The reaction was quenched with 50 mL of a saturated solution of sodium hydrogen carbonate, the organic layer was separated and the aqueous layer extracted twice with dichlormethane. The combined organic phases were washed twice with water, dried over magnesium sulphate and evaporated in vacuo. The resulting syrup was purified by column chromatography (light petroleum (b.p. 50–70 °C)–ethyl acetate 1:1).

Yield: 971 mg (19%). C$_{56}$H$_{86}$O$_{26}$ (1174.5407).

^{1}H NMR (500 MHz, CDCl$_3$ + TMS): δ = 5.30–5.40 (m, 4H, H-3′, H-3″, H-olefin), 5.25 (d, 2H, H-1′, H-1″), 5.22 (dd, 1H, H-3), 5.04 (dd, 1H, H-4″, 4.83 (dd, 1H, H-2″), 4.77 (dd, 1H, H-2), 4.71 (dd, 1H, H-2′), 4.48 (d, 1H, H-1), 4.41 (dd, 2H, H-6a, H-6a′), 4.29 (dd, 1H, H-6b), 4.21 (dd, 1H, H-6a″), 4.16 (dd, 1H, H-6b′), 4.03 (dd, 1H, H-6b″), 3.97 (m$_c$, 1H, H-5″), 3.93 (dd, 1H, H-4′), 3.91 (m$_c$, 1H, H-5′), 3.90 (dd, 1H, H-4), 3.81 (dt, 1H, H-αa), 3.67 (ddd, 1H, H-5), 3.40–3.45 (m, 1H, H-αb), 2.10, 2.09, 2.03, 1.98, 1.96, 1.95, 1.93, 1.92 (each s, 3H, OAc), 1.91 (s, 6H, OAc) 1.47–1.58 (m, 6H, H-allyl., β-CH$_2$), 1.17–1.38 (m, 22H, alkyl-CH$_2$), 0.85 (t, 3H, alkyl-CH$_3$); $^3J_{1,2}$ = 8.1, $^3J_{2,3}$ = 9.3, $^3J_{3,4}$ = 9.2, $^3J_{4,5}$ = 9.2, $^3J_{5,6a}$ = 2.4, $^3J_{5,6b}$ = 4.3, $^2J_{6a,b}$ = 12.1, $^3J_{1′,2′}$ = 4.1, $^3J_{2′,3′}$ = 10.4, $^3J_{3′,4′}$ = 9.2, $^3J_{4′,5′}$ = 9.2, $^3J_{5′,6a′}$ = 2.4, $^3J_{5′,6b′}$ = 3.8, $^2J_{6a′,b′}$ = 12.1, $^3J_{1″,2″}$ = 4.1, $^3J_{2″,3″}$ = 10.4, $^3J_{3″,4″}$ = 9.8, $^3J_{4″,5″}$ = 9.8, $^3J_{5″,6a″}$ = 3.5, $^3J_{5″,6b″}$ = 2.2, $^2J_{6a″,b″}$ = 12.6, $^3J_{αβ,β-CH_2}$ = 6.6, $^2J_{αa,b}$ = 9.5, $^3J_{CH_2,CH_3}$ = 6.6 Hz.

^{13}C NMR (125 MHz, CDCl$_3$ + TMS): δ = 170.58, 170.56, 170.53, 170.31, 169.88, 169.63, 169.47 (C=O, OAc), 130.38, 130.29 (C-olefin), 100.68 (C-1), 96.18, 96.15 (C-1′, C-1″), 75.91 (C-3), 73.04 (C-4′), 72.91 (C-4), 72.43 (C-2), 72.27 (C-3″), 71.23 (C-5), 70.97 (C-2′), 70.90 (C-α), 70.53 (C-2″), 70.50 (C-3′), 69.86 (C-5″), 69.37 (C-5′), 69.33 (C-4′), 63.54 (C-6), 62.85 (C-6′), 61.87 (C-6″), 31.95, 29.82, 29.56, 29.44, 29.36, 29.31, 27.26, 25.88, 22.73 (alkyl-CH$_2$), 21.35, 21.32, 21.25, 21.12, 21.09, 21.03, 21.00 (CH$_3$, OAc), 14.62 (alkyl-CH$_3$).

4.2.15. (cis-9-Octadecenyl) 4-O-[4′-O-(α-D-glucopyranosyl)-α-D-glucopyranosyl]-β-D-glucopyranoside (29)

Nine hundred and forty-two milligrams (0.8 mmol) **28** were deprotected using general procedure 1. The product was purified by gel filtration on a column of Serva LH-20 suspended in methanol.

Yield: 648 mg (98%). C$_{36}$H$_{66}$O$_{16}$ (754.4351).

FAB-HIRESMS: m/z = 777.4248 $[M + Na]^+$ (calc. 777.4279)

$[\alpha]_D^{20}$ = +40° (c = 0.1, MeOH)

^{1}H NMR (500 MHz, d$_4$-methanol): d = 5.20–5.41 (m, 2H, H-olefin), 5.16 (d, 1H, H-1″), 5.14 (d, 1H, H-1′), 4.17 (d, 1H, H-1), 3.78–3.91 (m, 6H, H-3″, H-6a, H-6a′, H-6a″,H-6b′, H.-6b″), 3.88 (dd, 1H, H-4″), 3.76 (m$_c$, 1H, H-5″), 3.58–3.69 (m, 3H, H-4′, H-5′, H-αa), 3.61 (dd, 1H, H-4), 3.47–3.56 (m, 3H, H-3′, H-6b, H-αb), 3.49 (dd, 1H, H-2″), 3.44 (dd, 1H, H-2′), 3.35 (m$_c$, 1H, H-5), 3.27 (dd, 1H, H-3), 3.21 (dd, 1H, H-2), 1.95–2.06 (m, 4H, H-allyl.), 1.59–1.65 (m, 2H, β-CH$_2$), 1.24–1.41 (m, 22H, alkyl-CH$_2$), 0.90 (t, 3H, alkyl-CH$_3$); $^3J_{1,2}$ = 8.1, $^3J_{2,3}$ = 9.1, $^3J_{3,4}$ = 9.3, $^3J_{4,5}$ = 9.2, $^3J_{1′,2′}$ = 3.8, $^3J_{2′,3′}$ = 9.8, $^3J_{1″,2″}$ = 3.8, $^3J_{2″,3″}$ = 9.8, $^3J_{4″,5″}$ = 9.8, $^3J_{CH_2,CH_3}$ = 6.8 Hz.

Acknowledgements

References

Altenburger, J.-M., Lebeau, L., Mioskowski, C., Schirlin, D., 1992. Synthesis of new glycerolipids linked to hydroxamate derivatives designed for two-dimensional crystallization of aminopeptidase M. Helv. Chim. Acta 75, 2538–2544.

Bear, E., Stanacev, N.Z., 1965. Phosphonolipids II. Synthesis of dialkyl-ʟ-glyceryl-(2-aminoethyl)phosphonates. J. Biol. Chem. 240, 44–48.

Bebernitz, G.R., Dain, J.G., Deems, R.O., Otero, D.A., Simpson, W.R., Strohschein, R.J., 2001. Reduction in glucose elvels in STZ diabetic rats by 4-(2,2-dimethyl-1-oxopropyl)benzoic acid: a prodrug approach for targeting the liver. J. Med. Chem. 44, 512–523.

Böcker, T., Thiem, J., 1989. Synthese und eigenschaften von kohlenhydrattensiden. Tenside Surf. Det. 26, 318–324.

Curatolo, W., 1987. The physical properties of glycolipids. Biochim. Biophys. Acta 906, 111–136.

Ferrier, R.J., Furneaux, R.H., 1976. Synthesis of 1,2-trans-related 1-thioglycosides esters. Carbohydr. Res. 52, 63–68.

Hassner, A., Alexanian, V., 1978. Direct room temperature esterification of carboxylic acids. Tetrahedron Lett. 46, 4475–4478.

Hato, M., Minamikawa, H., Seguer, J.B., 1998. Stereochemistry-dependent self-assembly in synthetic glycolipid/water systems: the aqueous phase structure of 1,3-di-*O*-dodecyl-2-(β-maltoheptaosyl)glycerol. J. Phys. Chem. B 102, 11035–11042.

Hato, M., Minamikawa, H., 1996. The effects of oligosaccharide stereochemistry on the physical properties of aqueous synthetic glycolipids. Langmuir 12, 1658–1665.

Hato, M., 2001. Synthetic glycolipid/water systems. Curr. Opin. Colloid Interface Sci. 6, 268–276.

Ishizuka, I., Yamakawa, T., 1985. Glycolipids. In: Wiegandt, H. (Ed.), New Comprehensive Biochemistry, vol. 10. Elsevier, pp. 101–197.

Korchowiec, B.M., Baba, T., Minamikawa, H., Hato, M., 2001. Forces that control pH-dependent aggregation of nonionic glycolipid vesicles. Langmuir 17, 1853–1859.

Mannock, D.A., Lewis, R.N.A.H., McElhaney, R.N., 1987. An improved procedure for the preparation of 1,2-di-*O*-acyl-3-*O*-(β-ᴅ-glucopyranosyl)-sn-glycerols. Chem. Phys. Lipids 43, 113–127.

Milkereit, G., Garamus, V.M., Veermans, K., Willumeit, R., Vill, V., 2004. Synthesis and mesogenic properties of a Y-shaped glyco glycerol lipid. Chem. Phys. Lipids 131, 51–61.

Milkereit, G., Gerber, S., Brandenburg, K., Koch, M.H.J., Morr, M.H.J., Seydel, U., Vill, V. Synthesis and mesomorphic properties of glycosyl dialkyl- and diacyl-glycerols bearing saturated, unsaturated and methyl branched fatty acid and fatty alcohol chains. Part II. Mesomorphic properties, Chem. Phys. Lipids, in press.

Minamikawa, H., Hato, M., 1997. Phase behaviour of synthetic phytanyl-chained glycolipid/water systems. Langmuir 13, 2564–2571.

Minamikawa, H., Murakami, T., Hato, M., 1994. Synthesis of 1,3-di-*O*-alkyl-2-*O*-(b-glycosyl)glycerols bearing oligosaccharides as hydrophilic groups. Chem. Phys. Lipids 72, 111–118.

Minden, v.H.M., Brandenburg, K., Seydel, U., Koch, M.H.J., Garamus, V., Willumeit, R., Vill, V., 2000. Thermotropic and lyotropic properties of long chain alkyl glycopyranosides. Part II. Disaccharide headgroups. Chem. Phys. Lipids 106, 157–179.

Minden, v.H.M., Morr, M., Milkereit, G., Heinz, E., Vill, V., 2002a. Synthesis and mesogenic properties of glycosyl diacylglycerols. Chem. Phys. Lipids 114, 55–80.

Minden, v.H.M., Milkereit, G., Vill, V., 2002b. Effects of carbohydrate headgroups on the stability of induced cubic phases in binary mixtures of glycolipids. Chem. Phys. Lipids 120, 45–56.

Morr, M., Wray, V., Fortkamp, J., Schmid, R.D., 1992. (2*R*,4*R*,6*R*,8*R*)-tetramethyldecan-und-undecansäure aus dem bürzeldrüsenwachs der hausgans, *Anser a.f. domesticus*: isolierung, synthese einiger derivate sowie der *rac*-2,4,6,8-tetramethyldecansäure. Liebigs Ann. Chem., 433–439.

Morr, M., Fortkamp, J., Rühe, S., 1997. Chirale methylverzweigte tenside und phospholipide: synthese und eigenschaften. Angew. Chem. 109, 2567–2569;
Morr, M., Fortkamp, J., Rühe, S., 1997. Chirale methylverzweigte tenside und phospholipide: synthese und eigenschaften. Angew. Chem. Int. Ed. Engl. 36, 2460–2462.

Paltauf, F., Johnston, J.M., 1971. Metabolism in vitro of enantiomeric 1-*O*-alkyl glycerols and 1,2- and 1,3-alkyl acyl glycerols in the intestinal mucosa. Biochim. Biophys. Acta 239, 47–56.

Schmidt, R.R., 1986. New methods of glycoside and oligosaccharide syntheses—are there alternatives to the Koenigs–Knorr method? Angew. Chem. Int. Ed. Engl. 25, 212–235.

Schmidt, R.R., Kinzy, W., 1994. Anomeric-oxygen activation for glycoside synthesis: the trichloroacetimidate method. Adv. Carbohydr. Chem. Biochem. 50, 21–123.

Schmidt, R.R., Kläger, R., 1985. Glycosylimidates. Part 15. Short synthesis of cerebrosides. Angew. Chem. Int. Ed. Engl. 24, 65–66.

Schmidt, R.R., Michel, J., Roos, M., 1984. Direkte synthese von *O*-α und *O*-β-glycosyl-imidaten. Liebigs Ann. Chem., 1343–1357.

Schmidt, R.R., Stumpp, M., 1983. Synthese von 1-thioglycosiden. Liebigs Ann. Chem., 1249–1256.

Vill, V., Böcker, T., Thiem, J., Fischer, F., 1989. Studies on liquid crystalline glycosides. Liq. Cryst. 6, 349–356.

Vill, V., Minden, v.H.M., Koch, M.H.J., Seydel, U., Brandenburg, K., 2000. Thermotropic and lyotropic properties of long chain alkyl glycopyranosides. Part I. Monosaccharide headgroups. Chem. Phys. Lipids 104, 75–91.

Wehrli, H.P., Pomeranz, Y., 1969. Synthesis of galactosyl glycerides and related lipids. Chem. Phys. Lipids 3, 357–370.

Wickberg, B., 1958. Synthesis of 1-glyceritol ᴅ-galactopyranosides. Acta Chem. Scan. 12, 1187–1201.

Chapter 7

Synthesis and Mesogenic Properties
of Glycosyl Dialkyl- and Diacylglycerols
bearing Saturated, Unsaturated and
Methyl Branched Fatty Acid and
Fatty Alcohol Chains.
Part II: Mesomorphic Properties

Synthesis and mesomorphic properties of glycosyl dialkyl- and diacyl-glycerols bearing saturated, unsaturated and methyl branched fatty acid and fatty alcohol chains
Part II. Mesomorphic properties

Götz Milkereit [a], Klaus Brandenburg [b], Sven Gerber [a], Michel H.J. Koch [c],
Michael Morr [d], Jörg Andrä [b], Ulrich Seydel [b], Volkmar Vill [a],*

[a] *Institute of Organic Chemistry, University of Hamburg, Martin-Luther-King-Platz 6, 20146 Hamburg, Germany*
[b] *Research Center Borstel, Leibniz-Zentrum für Medizin und Biowissenschaften, Parkallee 10, 23845 Borstel, Germany*
[c] *European Molecular Biology Laboratory, EMBL c/o DESY, Notkestr. 85, 22603 Hamburg, Germany*
[d] *Gesellschaft für Biotechnologische Forschung mbH, Mascheroder Weg 1, 38124 Braunschweig, Germany*

Abstract

The biophysical properties of a series of glycosyl dialkyl- and diacyl-glycerols bearing unsaturated or chiral methyl branched chains in the tail, and di- and trisaccharide carbohydrate headgroups are described. Thermotropism was investigated by polarising microscopy, the lyotropism was investigated by small angle X-ray diffraction and by the contact preparation method, and the gel to liquid crystalline phase transition by FT-IR-spectroscopy. The compounds displayed thermotropic Smectic A (SmA), cubic and columnar phases, whereas in the lyotropic phase diagram lamellar, hexagonal and cubic phases are found. The introduction of unsaturated or methyl branched chains leads to liquid crystallinity at ambient temperature. The difference between the 1,3-oleyl-glycerol maltoside and the corresponding 1,2-oleoyl-glycerol maltoside is small.
© 2005 Elsevier Ireland Ltd. All rights reserved.

Keywords: Glyco-glycero lipids; Cubic phases; Lamellar phases; Small-angle X-ray scattering; Infrared spectroscopy

1. Introduction

The observation of double melting of certain long chain alkyl glucopyranosides, e.g. hexadecyl-α-D-glucopyranoside by Fischer and Helferich (1911) was the first indication of thermotropic liquid crystalline properties in amphiphilic carbohydrates.

These amphiphilic molecules form both thermotropic liquid crystalline phases in their pure state upon heating and lyotropic liquid crystalline phases upon addition of solvent.

The driving force for the mesophase formation is a micro phase separation leading in the case of the amphiphilic molecules to an aggregate structure with separated regions for the lipophilic and hydrophilic moieties, enabling the maintenance of the van der Waals' interaction in the hydrophilic region.

The principal phase behaviour of these compounds is shown in Fig. 1 (Prade et al., 1995; Blunk et al., 1998). At a fixed amphiphile/water ratio, corresponding to a vertical line in the diagram, amphiphiles often display different phases as the temperature varies, especially if these compounds have an unusual geometry of the carbohydrate headgroup. In this case cubic phases may also be observed, while simple amphiphiles exhibit only a thermotropic Smectic A phase.

Deviation from the phase behaviour of the pure amphiphiles, that is only changed by the temperature will occur upon the addition of solvents. Whereas small amounts of e.g. water will not change the phase type and transition temperatures, larger amounts will induce new phases such as cubic and columnar phases ($H_{I/II}$). The discontinuous cubic phases are based upon various packing of spherical or slightly anisotropic micelles, whereas the bicontinuous cubic phases with interwoven fluid porous structures are based on underlying infinite periodic minimal surfaces (Fairhurst et al., 1998).

Due to the use as model compounds for biological systems, synthetic glycolipids have to be liquid crystalline already at or near ambient temperature.

In an earlier paper the synthesis of glycosyl diacylglycerol with mono- and disaccharide headgroups (Minden et al., 2002a), with unsaturated and chiral methyl branched fatty acid chains was described. These molecules displayed liquid crystalline phases already at ambient temperature, so that their biophysical properties could be investigated in the temperature range of biological systems (Minden et al., 2002b).

In recent years Hato and co-workers prepared a new class of glycolipids with a 1,3-di-*O*-alkyl-sn-glycerol moiety. Mainly 1,3-dialkyl-glyco-glycero lipids with *n*-dodecyl and *n*-tetradecyl alkyl chains and oligomaltose and cellobiose headgroups were synthesized in high yields (Minamikawa et al., 1994). The lyotropic properties of the oligosaccharide headgroups were thoroughly characterised (Hato et al., 1998; Korchowiec et al., 2001; Hato and Minamikawa, 1996; Hato, 2001). A few examples with methyl branched phytanyl chains can be found (Minamikawa and Hato, 1997). The amphiphilic properties of some of these compounds were in part similar to those observed for the unsaturated disaccharide compounds (Minden et al., 2002a).

We synthesized several dialkyl- and diacyl glycosyl glycerols, bearing saturated, unsaturated and methyl branched chains. Their biophysical properties are described below and discussed in terms of their chemical structures.

The thermotropic properties of the compounds were investigated by means of polarising microscopy. The lyotropic phase behaviour was characterised using different methods: The phase sequence by the contact preparation technique, the Krafft-temperature/$L_\beta \leftrightarrow L_\alpha$-phase transition by FT-IR-spectroscopy and the aggregate structure by small-angle X-ray scattering.
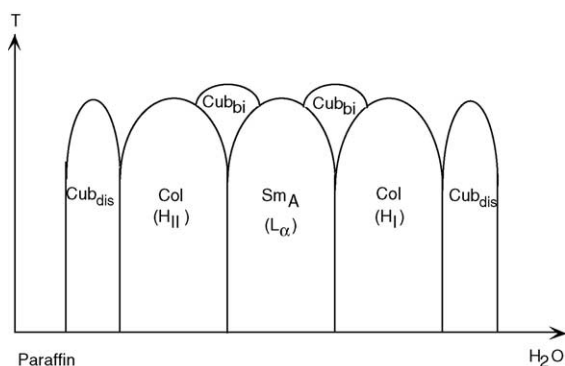
Fig. 1. Principal phase behaviour of amphiphilic compounds (Prade et al., 1995; Blunk et al., 1998).

2. Results and discussion

2.1. Thermotropic phase behaviour

The transition temperatures of the pure compounds are shown in Fig. 2. Due to its wedge shape the 1,3-dioleyl maltoside **1** forms an inverted columnar mesophase with the hydrophilic/hydrophobic interface curved towards the (minor) sugar component. Introduction of unsaturation into the alkyl chain led to liquid crystallinity already at ambient temperature, according to previous results (Vill et al., 2000; Minden et al., 2000, 2002a). The clearing temperature of **1** is 23.3 °C is lower than that of the corresponding 1,2-di-O-oleoyl-
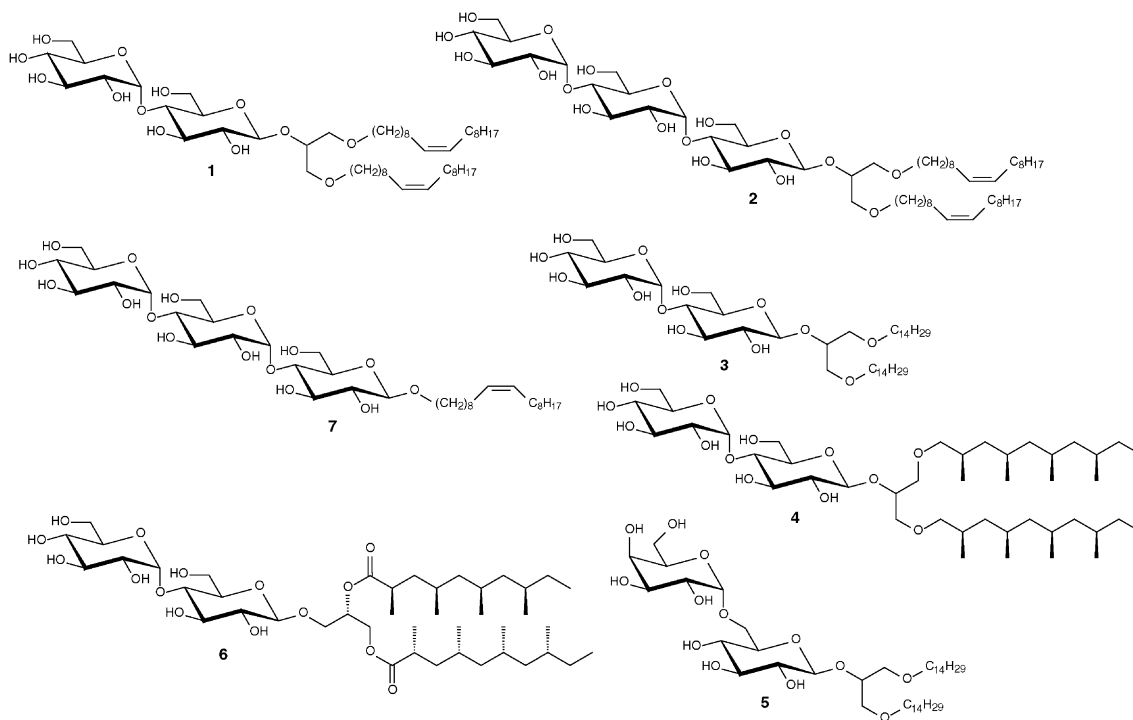
1	Cr	< 20.0	col				215.9	I
2	Cr	< 20.0		S$_A$			> 280	I[a]
3	Cr	92.5	col				228.7	d[b]
4	Cr	< 20.0		S$_A$			150.6	I
5	Cr	79.0		S$_A$	125.9	cub	158.6	I
6	Cr	< 20.0		S$_A$			153.3	I
7	Cr	?		(S$_A$)	?	col	233.0	d[b]

[a] The clearing temperature exceeded the temperature range of the hot stage

[b] The compounds decomposed above this temperature

Fig. 2. Transition temperatures of the synthetic compounds.

3-*O*-β-D-maltopyranosyl-sn-glycerol (Minden et al., 2002a). This might be attributed to the weaker interaction of the ether linkage compared to the ester linkage.

The carbohydrate headgroup of compound **2** has one more glucose unit than compound **1** and this leads to the formation of a lamellar Smectic A phase and a stabilization of the liquid crystalline phase of more than 65 °C. This might result from the balance between the long alkyl chains of the glycerol moiety and the trisaccharide headgroup, leading to a more rod-like packing of the molecules.

Saturated shorter alkyl chains lead to compound **3**. The hydrophobic part of the molecule is still dominant resulting in a wedge shaped structure, and to the formation of the inverted columnar phase. Nevertheless the stability of the liquid crystalline phase is reduced by ~60 °C due to a less wedge shaped molecular structure. The *n*-alkyl chain of this compound leads to a better chain packing compared to compound **1**, resulting in the higher melting temperature.

In compound **5** the $\alpha 1 \rightarrow 4$ diglucoside headgroup is replaced by a $\alpha 1 \rightarrow 6$ linked carbohydrate headgroup. This structural variation leads to the formation of Smectic A and broad cubic phases. The melting point is still high, due to the good packing of the alkyl chains. The reason for the different phase behaviour may be seen in the broad structure of the $\alpha 1 \rightarrow 6$ linked disaccharide headgroup, resulting in a rod-like shape at low temperatures (formation of the Smectic A phase). With increasing temperature the molecule becomes more and more wedge-shaped due to increased motion of the aliphatic chains, resulting in the formation of the cubic phase. The cubic phase is formed as a compromise, since the Smectic A phase is destabilised by the molecular moiety, but this destabilisation is not sufficient to enable the formation of a columnar phase beyond the cubic phase, as previously reported for compounds with longer alkyl chains (Minden et al., 2002a).

The alkyl chains of compound **4** again are shortened compared to compound **3**, resulting in a chain length of 10 carbon atoms per chain. In this case the alkyl chains are methyl branched leading to a melting temperature below 20 °C. Introduction of lateral branches in addition to unsaturation is a well known method in liquid crystal chemistry to prevent crystallisation.

The balance between the hydrophilic and the hydrophobic part again favours the formation of lamellar Smectic A phases. The same phase behaviour is observed for compound **6** the corresponding 1,2-ester, where the only difference to compound **4** can be observed in the stability of the liquid crystalline phase, which is slightly higher (~3 °C).

The methyl branching disturbs the interaction in the hydrophobic tail region as previously reported (Minden et al., 2002a) and therefore destabilises the mesophase, but enlarges its range, since the crystal to liquid crystal interconversion is much more strongly depressed.

This illustrates the wide range of usage of properties which can be produced using chiral methyl branched fatty acid/alcohol chains. This feature has been used for the preparation of phospholipids (Morr et al., 1997 and references cited herein), gluco-glycero lipids (Minden et al., 2002a), ferro- and antiferro-electric liquid crystals (Heppke et al., 1997), triphenylene-based liquid crystals (Schultz et al., 2002) as well as potent antimycotics (Morr et al., 1995; Kuwahara et al., 1994).

Compound **7** can be seen as the single chain counterpart of compound **2**. On reducing the size of the hydrophobic moiety of the molecule the balance between the hydrophilic and hydrophobic moiety is shifted towards the hydrophilic carbohydrate headgroup. The thermotropic textures become less distinguishable indicating that the shift of the balance is not very strong. It was not possible to determine an exact melting temperature but it can be assumed that it is below 50 °C. At lower temperatures there are indications of the formation of a lamellar Smectic A phase whereas at higher temperatures (above 100 °C) a columnar phase forms. A proof for the Smectic A phase is the observation of lyotropic lamellar structures (see Sections 2.2.1 and 2.2.2). In total the balance between the hydrophobic and hydrophilic moieties favours the formation of lamellar and columnar structures, due to a more labile balance between a rod-like structure and a wedge-shaped structure, which is favoured with increasing temperature.

2.2. Lyotropic phase behaviour

2.2.1. Contact preparation

Fig. 3 shows the lyotropic phase sequence in the contact preparation with water. Only the alkyl maltosides **1** and **3** display a lyotropic polymorphism. In both cases, three phases are formed with increasing water concentration: a H_{II} phase, a bicontinuous
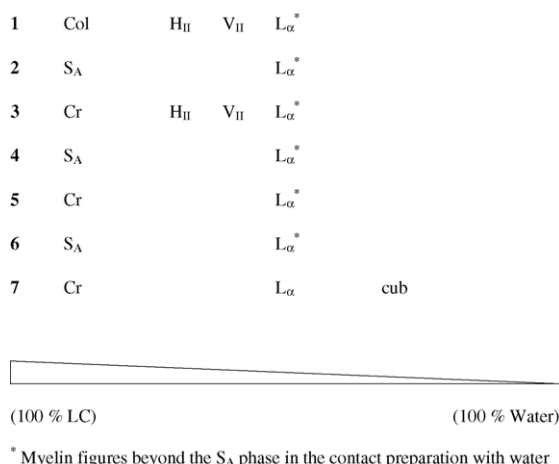
1	Col	H$_{II}$	V$_{II}$	L$_\alpha$*
2	S$_A$			L$_\alpha$*
3	Cr	H$_{II}$	V$_{II}$	L$_\alpha$*
4	S$_A$			L$_\alpha$*
5	Cr			L$_\alpha$*
6	S$_A$			L$_\alpha$*
7	Cr			L$_\alpha$	cub

(100 % LC)   (100 % Water)

* Myelin figures beyond the S$_A$ phase in the contact preparation with water

Fig. 3. Lyotropic phase sequence in the contact preparation with water.

cubic V$_{II}$ phase and a L$_\alpha$ phase. Furthermore, beyond the lamellar region towards higher water concentration myelin figures (Jeffrey and Wingert, 1992; Bouligand, 1998) can be found. Again, this phase sequence is the same as that of 1,2-di-*O*-oleoyl-3-*O*-β-D-maltopyranosyl-sn-glycerol (Minden et al., 2002a).

This phase behaviour might result from the increase in size of the headgroup with increasing hydration. As a result the molecule should become less wedge-shaped and finally even rod-shaped. This is in accordance with the observation of a cubic and finally a lamellar phase (rod-like shape of the molecules) at the highest water concentration.

The other lipids only form lamellar phases. Introduction of a third glucose moiety into the headgroup balances the hydrophobic and hydrophilic parts of the trisaccharide **2**, so that only a lamellar L$_\alpha$ phase can form. For the *n*-alkyl maltoside **3** and the methyl branched analogues **4** and **6** the balance between the molecular counterparts is achieved by shortening the alkyl chain. The position of the chain in the glycerol moiety (1,2 ↔ 1,3) and the type of linkage (ester ↔ ether) seem to have no influence on the lyotropic phase behaviour. Compound **5** with a Gal-α1 → 6-Glc disaccharide headgroup displayed, interestingly, only myelin figures besides the lamellar L$_\alpha$ phase. It might be expected that upon hydration a V$_I$ phase with the polar/unpolar interface curved towards the fluid hydrocar-

Fig. 4. (a) Peak position of the symmetric stretching vibration of the methylene groups ν_s(CH$_2$) vs. temperature for compounds **1**, **2** and **7** at different water contents (**1**: (■) 97.5% water; (□) 90% water; **2**: (▼) 97.5% water; (○) 90% water; **7**: (●) 97.5% water; (△) 90% water). (b) Peak position of the symmetric stretching vibration of the methylene groups ν_s(CH$_2$) vs. temperature for compound **1** at different water contents (●: 40% water, heating scan; ★: 40% water, cooling scan; ▼: 20% water, heating scan; ◇: 20% water, cooling scan).

bon chain region would form next. Since this phase was not found, the increase in size of the melibiose headgroup due to hydration seems not to suffice to become the dominating factor and to force the polar/nonpolar interface to curve towards the chain region.

The substitution of the dialkylglycerol moiety of the trisaccharide **2** by a single alkyl chain did not change the lyotropism much. In addition to the lamellar phase a cubic phase was found. The isotropic texture might be a hint to a discontinuous cubic phase, resulting from the packing of spherical micelles. The formation of a cubic phase again suggests that with increasing water content the rod-like shape is transformed into a slightly wedge-shaped structure.

2.2.2. Structural lyotropism

Analysis of the gel to liquid crystalline (β ↔ α) phase transition of the alkyl and acyl chains:

Above 20 °C all samples bearing unsaturated alkyl chains are in the liquid crystalline phase of the acyl, with the maltotriose-1-oleyl glycolipid having a significantly higher fluidity than the other two dialkylated glycolipids (Fig. 4). Interestingly, only maltose-1,3-oleyl (**1**) exhibits a sharp phase transition into a gel phase around 15 °C, with a wavenumber around 2850.5 cm^{-1}. This value is typical for other glycolipids such as lipopolysaccharides (Brandenburg and Seydel, 1990) but it is higher than it can be found for phospholipids (Brandenburg and Seydel, 1990). In contrast to the maltose compound **1**, the maltotriose compounds (**2** and **7**) exhibit very broad phase transitions over a temperature range of more than 20 °C, with wavenumber values corresponding to a relatively high fluidity even below −20 °C. Thus, the comparison of maltose-1,3-oleyl (**1**) with the maltotriose-1,3-oleyl (**2**) shows that addition of one monosaccharide to the headgroup drastically suppresses the gel phase at low temperatures. Regarding the dependence on water content (lyotropism), the phase behaviour is unchanged for all samples in the water concentration range from 90% to 97.5%.

However, reduction of the water content results in a drastic increase (fluidization) of the wavenumber values in the gel phase at water contents lower than 40%, as exemplified for maltose-1,3-oleyl (**1**) (Fig. 4b). Con-comitantly, a strong hysteretic behaviour – difference of the phase transition temperature between heating- and cooling-scan – is observed at 20% water content, which does not take place at water contents of 40% or higher.

The exchange of the unsaturated oleyl chains by the saturated *n*-alkyl chains of compounds **3** and **5** increases the phase transition temperatures (Fig. 5). A sharp transition can be observed for both compounds at a water content of 90%. Below 45 °C the maltoside **3** is in the gel phase, whereas the phase transition for the melibioside **5** already occurs at 27 °C. This significantly lower transition temperature is due to the wedge-shaped structure of the melibiose headgroup, leading to a less dense packing than for the only slightly wedge-shaped maltoside **3**.

Fig. 6 shows the phase behaviour of the maltoside **3** at different water contents. It is obvious that three phase transition sections are formed with changing water content. At high water content of 90% and 80% the main gel to liquid crystalline phase transition occurs at a temperature of 45 °C. With increasing amount of lipid (58% and 40% water) the transition temperature increases by around 5 °C, indicating a better packing of the chains in this structure. When the water content is below 40%, the transition temperature is lowered by 10 °C compared to a water content of 90%, indicating again the formation of a structure with a looser packing of the alkyl chains.
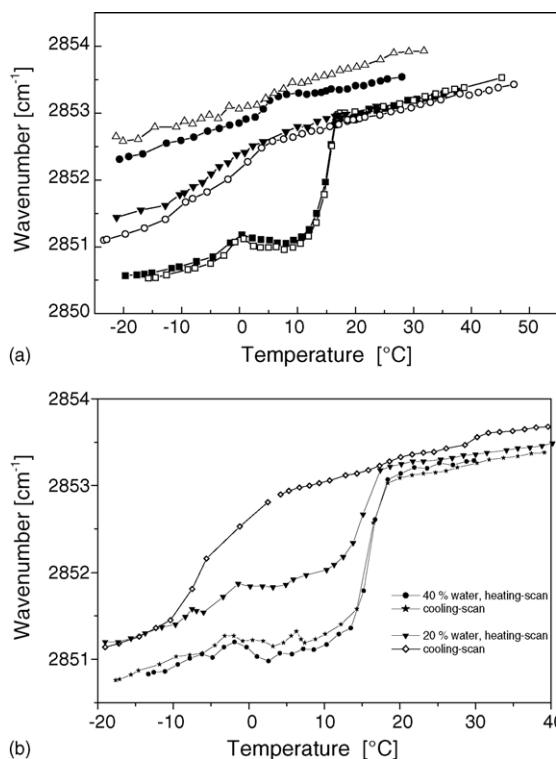

Fig. 5. Peak position of the symmetric stretching vibration of the methylene groups ν_s(CH$_2$) vs. temperature for compounds **3** and **5** at 90% water content (**3**: ■; **5**: □).

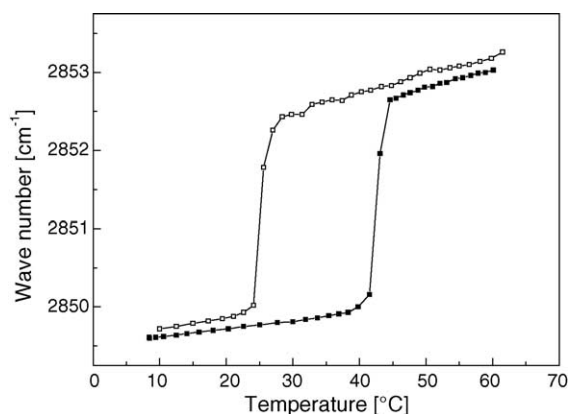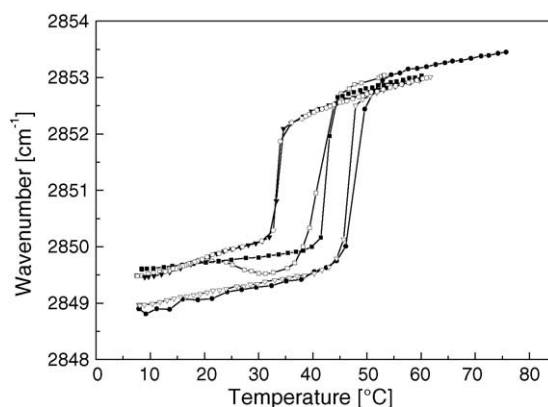Fig. 6. Peak position of the symmetric stretching vibration of the methylene groups ν_s(CH$_2$) vs. temperature for compound **3** at different water contents (■: 90.9% water; □: 80% water; ●: 58% water; ▽: 40% water; ▼: <40% water heating scan; ○: <40% water cooling-scan).

The infrared spectra of the two compounds with the chiral methyl branched chains (**4** and **6**) show no symmetric stretching vibration. This result is not unexpected, due to the rigid structure of the chains with the alternating $-CH(CH_3)-$ and $-CH_2-$ groups, which considerably reduces the flexibility of the alkyl chain. However, the symmetric bending vibrational band at $1378 \, cm^{-1}$ plotted against temperature indicates for both compounds a very low phase transition <10 °C.

Analysis of the three-dimensional aggregate structures of the glycolipids maltose-1,3-oleyl (**1**), maltotriose-1-oleyl (**2**), and maltotriose-1,3-oleyl (**7**).

The glycolipid 1,3-oleyl maltoside **1** exhibits an extremely well-resolved cubic phase at 90% water con-

tent (Fig. 7a) only comparable to that found for the simple, well-characterised lipid monoolein (Fig. 7b) (Luzzati et al., 1986; Mariani et al., 1988). At 20 and 40 °C, reflections are found at $\sqrt{2}$, $\sqrt{3}$, $\sqrt{4}$, $\sqrt{6}$, $\sqrt{8}$, $\sqrt{9}$, $\sqrt{10}$, $\sqrt{12}$, and $\sqrt{14}$ of the periodicity of 11.1 and 11.7 nm, respectively, which corresponds to the cubic phase Q^{224} ($Pn3m$). At 60 and 70 °C, the cubic phase is not clearly defined and, a superposition with another cubic phase cannot be excluded. After cooling back to 20 °C the original cubic phase Q^{224} has vanished, and the main reflection at 5.49 nm can be assigned to the periodicity d_H of an inverted hexagonal phase (H_{II}) phase. For this phase also the second order at 2.78 nm and two further peaks at
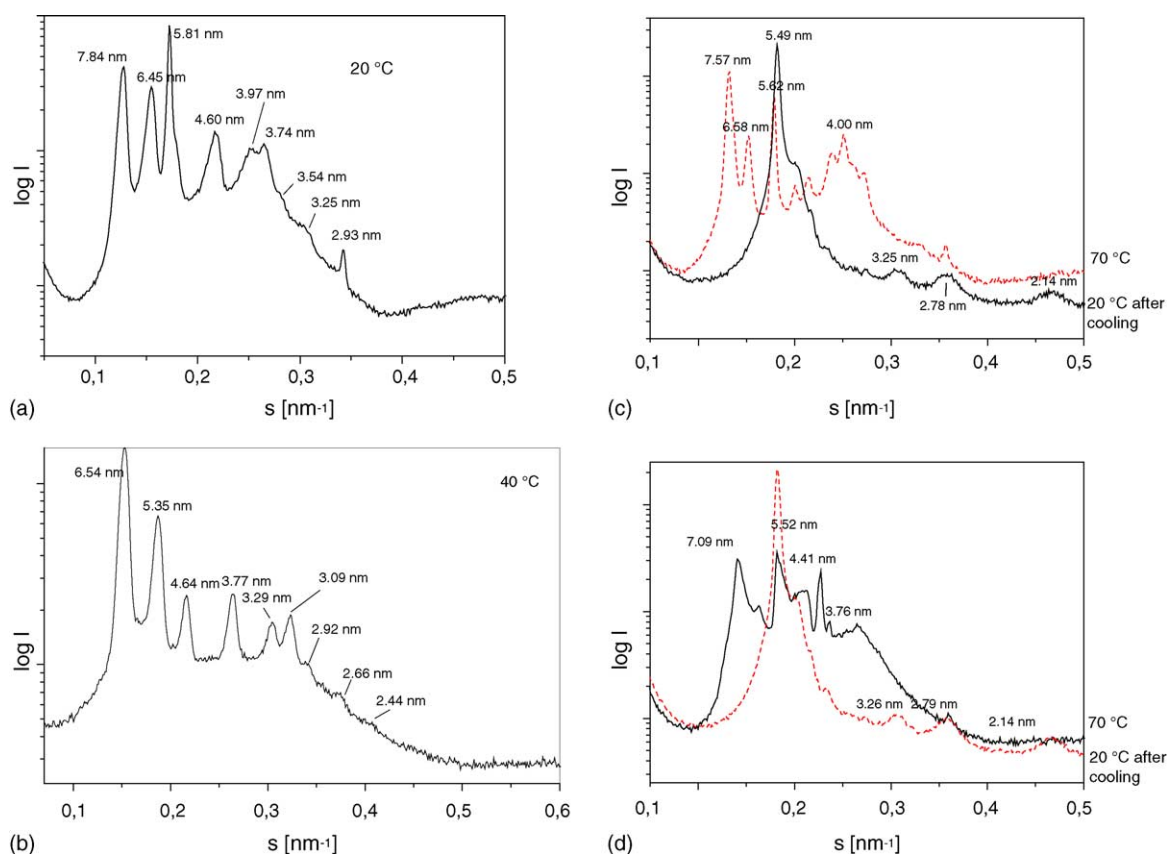
Fig. 7. (a) Small-angle X-ray diffraction patterns of maltose-1,3-oleyl (compound **1**) at 90% water content and 20 °C. The diffraction pattern is indicative for a cubic structure of space group Q^{224}. (b) Small-angle X-ray diffraction patterns of monoolein at 50% water content and 40 °C. The diffraction pattern is indicative of a cubic structure of space group Q^{224} as originally described by Luzatti et al. (1986). (c) Small-angle X-ray diffraction patterns of maltose-1,3-oleyl (compound **1**) at 90% water content at 70 °C and after cooling to 20 °C. The diffraction patterns are indicative of a cubic structure of space group Q^{224}, and of the inverted hexagonal structure H_{II}. (d) Small-angle X-ray diffraction patterns of maltose-1,3-oleyl (compound **1**) at 80% water content at 70 °C and after cooling to 20 °C. The diffraction patterns are indicative of a cubic structure of space group Q^{224}, and of the inverted hexagonal structure H_{II}.

$3.25\,nm = d_H/\sqrt{3}$ and $2.14\,nm = d_H/\sqrt{7}$ are observed (Fig. 7c). Since the sample was temperature-cycled between 10 and 65 °C in a time period of approximately 1 h prior to the measurement it can be assumed that after longer storage at 20 °C the original cubic phase should be formed again. The results of the measurements at 80% water content (Fig. 7d) can be interpreted in a similar way, except for the fact that there is a lower number of well-resolved reflections. After cooling back to 20 °C the H_{II} phase reappears.

Due to the increase of the sugar headgroup and, thus, the effective cross-section of the lipid backbone, the 1,3-oleyl maltotrioside **2** adopts only lamellar phases at 90% as well as at 80% water content (Fig. 8a and b). At 90% water content (Fig. 8a), at 60 and 70 °C a second
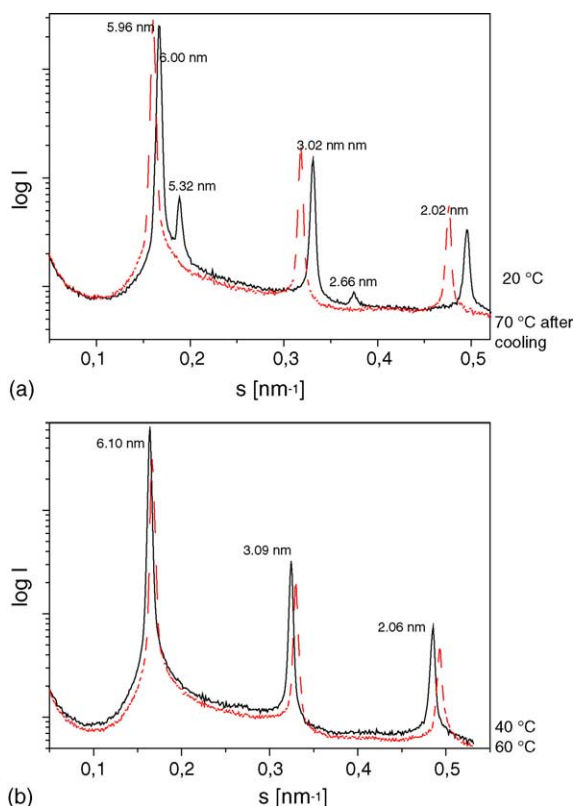
Fig. 8. Small-angle X-ray diffraction patterns of maltotriose-1,3-oleyl (compound **2**) at 90% water content and 70 °C and after recooling to 20 °C (a) and at 80% water content and 40 and 60 °C (b). The diffraction patterns are indicative of only multilamellar structures.
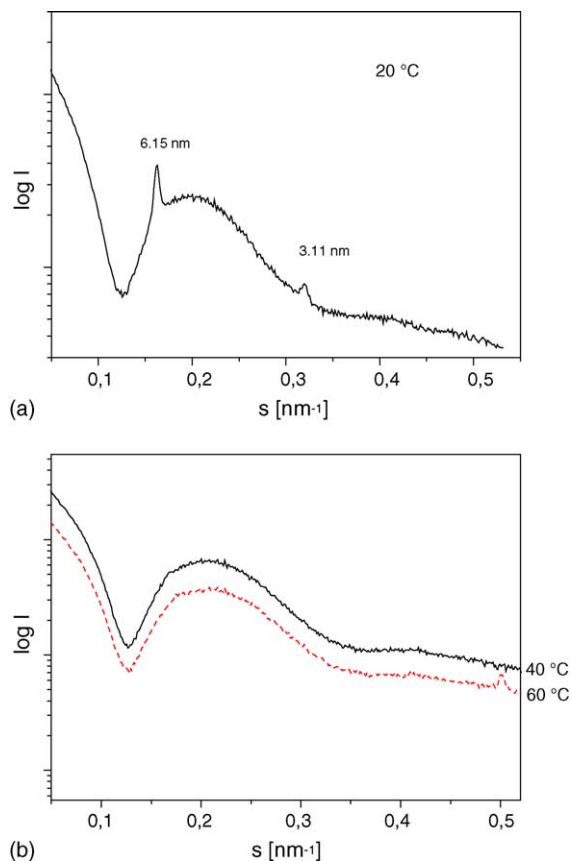
Fig. 9. Small-angle X-ray diffraction patterns of maltotriose-1-oleyl (compound **7**) at 90% water content and 40 °C (a) and at 80% water content and 40 and 60 °C (b).

lamellar periodicity at 5.43 nm is also observed, which is retained after cooling back to 20 °C. The appearance of the multilamellar structure for this compound is at the same time a proof for the assumption that the cubic phase of compound maltotriose-1,3-oleyl is of type II (inverted cubic), and not of type I (see Luzzati et al., 1986).

The compound maltotriose-1-oleyl **7** (Fig. 9a and b) exhibits under nearly all conditions, 90% and 80% water content and temperatures 20–70 °C, broad reflections in the s-range 0.13–0.35 nm^{-1}, which can be interpreted as unilamellar structures. The occurrence of sharp reflections at 20 °C for the 90% water content sample (Fig. 9a) is additionally indicative of a partial multilamellarisation (see Bouwstra et al., 1993). The existence of a cubic phase (Section 2.2.1) could not

be proved by small-angle X-ray scattering. Perhaps the existence range of this phase is too narrow or other effects like temperature dependence play an important role on the formation. Additionally SAXS experiments at water contents of 95% and higher give no reasonable results. In dilute solution (99.9% water content), however, this compound forms spherical micelles that show interaction at slightly lower water content (98%), what would be necessary for the formation of a discontinuous cubic phase (Milkereit et al., 2005). Thus the existence range of a possible discontinuous cubic phase cannot be proved or excluded, it falls between the range were the two scattering methods can be employed.

Table 1
Gel to liquid crystalline phase transition T_c determined by FT-IR, type of supramolecular aggregate structures (L: lamellar, Q: cubic, H: hexagonal), determined by wide-angle X-ray diffraction

Compound	T_c (°C)	Aggregate structures
1	15	Q/H$_{II}$
2	≤−10	L (multi)
3	45	n.m.[b]
4	no[a]	n.m.[b]
5	27	n.m.[b]
6	no[a]	n.m.[b]
7	<−20	L (uni)

[a] No stretching vibration was observed.
[b] Not measured.

3. Conclusions

The liquid crystalline properties were investigated by a combination of different methods. The thermotropic properties are strongly influenced by the chemical structure of the lipids. An unsaturation in the hydrophobic part of the molecule leads to liquid crystallinity already at ambient temperature, whereas a saturated *n*-alkyl chain results in a melting point well above that temperature. The melting point can also be lowered by using methyl branched alkyl chains, due to a disturbed packing. The influence of the chain length of the maltosides is also obvious: A chain length of more than 14 carbon atoms leads to the formation of columnar phases of the inverted type because of its wedge-shaped structure, a chain length of 10 carbon atoms on the other side lead to a Smectic A phase, due to the rod-like structure. The exchange of the α1 → 4 linked maltose headgroup (compound **3**) by an α1 → 6 linked headgroup (compound **5**) results in a rod-like shape of the molecule above the melting point that with increasing temperature becomes more wedge-shaped, as revealed by the formation of a stable cubic phase. The introduction of a third sugar moiety in the sugar head (compound **2**) stabilises the Smectic A phase over a wide temperature range. Therefore it can be concluded that the intramolecular hydrophobic–hydrophilic balance is perfect.

Another interesting observation is that in the case of the unsaturated maltoside **1** and the methyl branched maltoside **4** the phases are the same as for the corresponding 1,2-esters (Minden et al., 2002a and compound **6**). The same holds true for the transition temperatures of these compounds. They are only slightly lower for the ethers than for the esters. This could mean, that in the case of alkyl chains, which lower the melting point by packing disturbance, the effect of the ester group and the position of linkage at the glycerol moiety is less important. For saturated *n*-alkyl chains the difference between ester and ether is much larger (Kuttenreich et al., 1988; Hinz et al., 1991, 1996). Thus the unsaturated and methyl branched glyco-glycero ether lipids can serve as substitutes for the ester analogues.

The lyotropic phase behaviour of the glyco-glycero compounds is dominated by the formation of lamellar phases. Only the maltosides **1** and **3** with a chain length of 18 or 14 carbon atoms show a lyotropic polymorphism in the contact preparation with water.

The results for the phase transition measurements and the aggregate structure indicate the complexity of the structural polymorphism of glycolipids. Thus, the change from the disaccharide maltoside (compound **1**) to maltotrioside (compound **2**) leads to a dramatic decrease in the acyl chain melting temperature (Fig. 4a, Table 1) and a change from cubic inverted to a multilamellar structure. Furthermore a reduction of the number of alkyl chains – compound **2 → 7** – leads to an overall increase in alkyl chain fluidity and a change from a multi- into a unilamellar structure (Figs. 4a and 10).

Literature data on glycolipids are scarce. Thus Hinz et al. (1991) and Tenchova et al. (1996) investigated the structural polymorphism of diacyl sugars having mainly monosaccharides (glucose, galactose, mannose), but in some cases also a di- (maltose) or trisac-
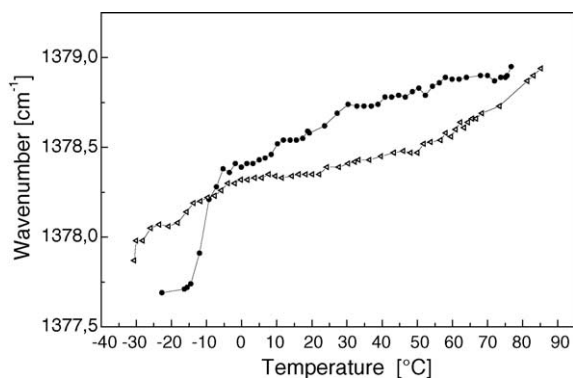
Fig. 10. Peak position of the symmetric bending vibration of the methyl groups $\delta_s(CH_3)$ vs. temperature for compounds **4** and **6** at 90% water content (**4**: △; **6**: ●).

charide (maltotriose) as backbone. As only compounds with saturated acyl chains were synthesised, the results are, however, not directly comparable. Thus, maltose- and maltotriose-containing compounds with acyl chain lengths C14 to C18 exhibited only lamellar phases and phase transition temperatures between 40 °C and approximately 70 °C depending on the acyl chain lengths (Hinz et al., 1991). However, for compounds with one sugar at higher temperatures also nonlamellar cubic and H_{II} structures were observed (Tenchova et al., 1996). Mannock et al. (1988) and Lewis et al. (1990) obtained similar results (see review by Brandenburg et al., 1998).

Glycosyl diacyl-glycerols are important components of the membranes of many plants and microorganisms. Thus, they play a role as low molecular mass antigen (Priest et al., 2003) as well as in molecular organisation (Fragata et al., 1993). The latter authors found for digalactosyl diacyl-glycerols beside the structural importance of these compounds also a role for cell recognition and adhesion (see also review by Brandenburg and Seydel).

Unfortunately, for most of the natural compounds neither the exact chemical structure nor the structural polymorphism is known. Although this should be of great importance for an understanding of its biological function.

As an example for Mal-1,3-oleyl (compound **1**) and for Mal-1,3-myristoyl (**3**) at low water concentration also a strong lyotropic behaviour, i.e., a change of the phase transition temperature, was observed (Figs. 4b and 6). So far, only very few literature data

on the lyotropism of glycolipids are available, despite the known strong water binding ability of most sugars. Only for lipopolysaccharides (LPS) and its lipid moiety, lipid A, have comprehensive investigations been published. Thus, lipid A, consisting of a diglucosamine backbone phosphorylated in positions 1 and 4′, acylated with up to seven hydrocarbon chains, as well as various rough mutant LPS differing in the length of the sugar chains (up to 11 monosaccharides), exhibited a strong lyotropic behaviour already when lowering the sugar content from 80% to 50% or below (Brandenburg et al., 1990; Seydel et al., 1993). This could be deduced from an increase in the phase transition temperature and a transition from a nonlamellar, mixed nonlamellar/unilamellar, or unilamellar into a multilamellar aggregate structure. Since LPS belong to the most important triggers of the immune system and may be present in vivo under different hydration conditions, this lyotropic behaviour should be of high biological relevance.

4. Experimental

4.1. Materials and methods

Synthesis of lipids **1**–**7** will be described elsewhere (Milkereit et al., in press).

An Olympus BH optical polarising microscope equipped with a Mettler FP 82 hot stage and a Mettler FP 80 central processor was used to identify thermal transitions and characterise anisotropic textures.

For the contact preparation a small amount of sample was placed on a microscope slide and covered with a cover glass before heating. Afterwards a small amount of solvent was placed on the slide at the edge of the cover glass. As soon as the solvent had moved under the cover glass and completely surrounded the sample with the solvent, the slide was placed again for a few seconds on the hot stage at a temperature of 100–120 °C and the phase behaviour was investigated immediately afterwards by polarizing microscopy.

4.2. Sample preparation for lyotropic phase behaviour

The glycolipid samples were dispersed in 20 mM Hepes, pH 7.0 at a defined glycolipid:water ratio. The

samples were temperature-cycled several times, i.e., heated to 60 °C, vortexed, and cooled to 10 °C.

4.3. FT-IR spectroscopy

The infrared spectroscopic measurements were performed on an IFS-55 spectrometer (Bruker, Karlsruhe, Germany). For phase transition measurements, the lipid samples were placed in a CaF_2 cuvette with a 12.5 μm Teflon spacer. Temperature-scans were performed automatically between a low initial temperature (−20 to +10 °C) and 70 °C with a heating rate of 0.6 °C/min. For measurement of hydrated lipid samples, these were spread on a ATR Ge plate, and free water was evaporated. Every 3 °C, 50 interferograms were accumulated, apodized, Fourier-transformed, and converted to absorbance spectra.

For the evaluation of the gel to liquid crystalline phase behaviour, the peak position of the symmetric stretching vibration of the methylene band $\nu_s(CH_2)$ around 2850 cm^{-1} was taken, which is a sensitive marker of lipid order (Brandenburg and Seydel, 1990). For compounds **4** and **6** with branched methyl groups the symmetric bending vibration $\delta_s(CH_3)$ around 1378 cm^{-1} was taken instead.

4.4. Small-angle X-ray scattering

X-ray diffraction experiments on the aggregate structure of the glycolipids were performed at the European Molecular Biology Laboratory (EMBL) outstation at the Hamburg synchrotron radiation facility HASYLAB using the double-focussing monochromator-mirror camera X33 (Koch and Bordas, 1983). All samples were incubated for at least 15 min at the desired temperature prior to the measurements. X-ray diffraction patterns, obtained with exposure times of 2 min using a linear gas proportional detector with delay line readout, were recorded according to previously described procedures. From the diffraction patterns, the spacing ratios can be deduced from which an assignment to defined three-dimensional aggregate structures is possible (Brandenburg et al., 1990). In the diffraction patterns presented here, the logarithm of the scattering intensity log $I(s)$ is plotted versus the scattering vector $s = 2\sin\theta/\lambda$ (2θ = scattering angle, λ = wavelength = 0.15 nm), and the d-spacings are calculated according to $s = 1/d$.

References

Blunk, D., Praefke, K., Vill, V., 1998. Amphotropic liquid crystals. In: Demus, D., Goodby, J., Gray, G.W., Spieß, H.-W., Vill, V. (Eds.), Handbook of Liquid Crystals, vol. 3. Wiley/VCH, Weinheim, pp. 305–340.

Bouligand, Y., 1998. Defects and textures. In: Demus, D., Goodby, J., Gray, G.W., Spiess, H.-W., Vill, V. (Eds.), Handbook of Liquid Crystals, vol. 1. Wiley/VCH, Weinheim, pp. 406–453.

Bouwstra, W., Gooris, G.L., Vras, W., Talsma, H., 1993. Small angle X-ray scattering: possibilities and limitations in characterization of vesicles. Chem. Phys. Lipids 64, 83–98.

Brandenburg, K., Seydel, U., 1990. Investigation into the fluidity of lipopolysaccharide and free lipid A membrane systems by Fourier-transform infrared spectroscopy and differential scanning calorimetry. Eur. J. Biochem. 191, 229–236.

Brandenburg, K., Koch, M.H.J., Seydel, U., 1990. Phase diagram of lipid A from *Salmonella minnesota* and *Escherichia coli* rough mutant lipopolysaccharide. J. Struct. Biol. 105, 11–21.

Brandenburg, K., Richter, W., Koch, M.H.J., Meyer, H.W., Seydel, U., 1998. Characterization of the nonlamellar cubic and HII structures of lipid A from *Salmonella enterica* serovar Minnesota by X-ray diffraction and freeze-fracture electron microscopy. Chem. Phys. Lipids 91, 53–69.

Fairhurst, C.E., Fuller, S., Gray, J., Holmes, M.C., Tiddy, G.J., 1998. Lyotropic surfactant liquid crystals. In: Demus, D., Goodby, J., Gray, G.W., Spieß, H.-W., Vill, V. (Eds.), Handbook of Liquid Crystals, vol. 3. Wiley/VCH, Weinheim, pp. 341–392.

Fischer, E., Helferich, B., 1911. Über neue synthetische glycoside. Liebigs Ann. Chemie 383, 68–91.

Fragata, M., Menikh, A., Robert, S., 1993. Salt-mediated effects in nonionic lipid bilayers constituted of digalactosylglycerols studied by FTIR spectroscopy and molecular modellization. J. Phys. Chem. 97, 13920–13926.

Hato, M., Minamikawa, H., Seguer, J.B., 1998. Stereochemistry-dependent self-assembly in synthetic glycolipid/water systems: the aqueous phase structure of 1,3-di-*O*-dodecyl-2-(β-maltoheptaosyl)glycerol. J. Phys. Chem. B 102, 11035–11042.

Hato, M., Minamikawa, H., 1996. The effects of oligosaccharide stereochemistry on the physical properties of aqueous synthetic glycolipids. Langmuir 12, 1658–1665.

Hato, M., 2001. Synthetic glycolipid/water systems. Curr. Opin. Colloid Interface Sci. 6, 268–276.

Heppke, G., Lötzsch, D., Morr, M., Ernst, L., 1997. New chiral side chains for ferro- and antiferro-electric liquid crystals derived from the preen-gland wax of the domestic goose. J. Mater. Chem. 7, 1993–1999.

Hinz, H.-J., Kuttenreich, H., Meyer, R., Renner, M., Fründ, R., Koynova, R., Boyanov, A.I., Tenchov, B.G., 1991. Stereochemistry and size of sugar head groups determine structure and phase behaviour of glycolipid membranes: densiometric, calorimetric and X-ray studies. Biochemistry 30, 5125–5138.

Hinz, H.-J., Tenchova, R., Tenchov, B.G., Quinn, P.J., 1996. Lamellar-non-lamellar phase transitions in synthetic glycoglycerolipids studied by time-resolved X-ray diffraction. Liq. Cryst. 20, 469–482.

Jeffrey, G.A., Wingert, L.M., 1992. Carbohydrate liquid crystals. Liq. Cryst. 12, 179–202.

Koch, M.H.J., Bordas, J., 1983. X-ray diffraction and scattering on disordered systems using synchrotron radiation. Nucl. Instrum. Meth. 208, 1303–1305.

Korchowiec, B.M., Baba, T., Minamikawa, H., Hato, M., 2001. Forces that control pH-dependent aggregation of nonionic glycolipid vesicles. Langmuir 17, 1853–1859.

Kuwahara, Y., Asami, N., Morr, M., Matsuyama, S., Suzuki, T., 1994. Chemical ecology of astigmatid mites XXXVIII. Aggregation pheromone and kairomone activity of lardolure and its analogues against *Lardoglyphus konoi* and *Carpoglyphus lactis*. Appl. Entomol. Zoo. 29, 253–257.

Kuttenreich, H., Hinz, H.-J., Inczedy-Marcsek, M., Koynova, R., Tenchov, B., Laggner, P., 1988. Polymorphism of synthetic 1, 2-*O*-dialkyl-3-*O*-β-ᴅ-galactosyl-sn-glycerols of different alkyl chain length. Chem. Phys. Lipids 47, 245–460.

Lewis, R.N.A.H., Mannock, D.A., McElhaney, R.N., 1990. Physical properties of glucosyldiacylglycerols: an infrared spectroscopic study of the gel-phase polymorphism of 1,2-di-*O*-acyl-3-*O*-(β-ᴅ-glucopyranosyl)-*sn*-glycerols. Biochemistry 29, 8933–8943.

Luzzati, V., Gulik, A., Gulik-Krzywicki, T., Tardieu, A., 1986. Lipid polymorphism revisited: Structural aspects and biological implications. In: Op den Kamp, J.A.F., Roelofsen, B., Wirtz, K.W.A. (Eds.), Lipids and Membranes: Past, Present, and Future. Elsevier, Amsterdam.

Mannock, D.A., Lewis, R.N.A.H., Sen, A., McElhaney, R.N., 1988. The physical properties of glycosyldiacylglycerols. Calorimetric studies of a homologous series of 1,2-di-*O*-acyl-3-*O*-(β-ᴅ-glucopyranosyl)-*sn*-glycerols. Biochemistry 27, 6852–6859.

Mariani, P., Luzzati, V., Delacroix, H., 1988. Cubic phases of lipid-containing systems: structure analysis and biological implications. J. Mol. Biol. 204, 165–189.

Milkereit, G., Garamus, V.M., Veermans, K., Willumeit, R., Vill, V., 2005. Structures of micelles formed by alkyl glycosides with unsaturated alkyl chains. J. Colloid Interface Sci. 284, 704–713.

Milkereit, G., Gerber, S., Brandenburg, K., Morr, M., Vill, V., in press. Synthesis and mesomorphic properties of glycosyl dialkyl- and diacyl-glycerols bearing saturated, unsaturated and methyl branched fatty acid and fatty alcohol chains. Part I: Synthesis Chem. Phys. Lipids.

Minamikawa, H., Hato, M., 1997. Phase behaviour of synthetic phytanyl-chained glycolipid/water systems. Langmuir 13, 2564–2571.

Minamikawa, H., Murakami, T., Hato, M., 1994. Synthesis of 1,3-di-*O*-alkyl-2-*O*-(b-glycosyl)glycerols bearing oligosaccharides as hydrophilic groups. Chem. Phys. Lipids 72, 111–118.

Minden, v.H.M., Brandenburg, K., Seydel, U., Koch, M.H.J., Garamus, V., Willumeit, R., Vill, V., 2000. Thermotropic and lyotropic properties of long chain alkyl glycopyranosides. Part II: disaccharide headgroups. Chem. Phys. Lipids 106, 157–179.

Minden, v.H.M., Morr, M., Milkereit, G., Heinz, E., Vill, V., 2002a. Synthesis and mesogenic properties of glycosyl diacylglycerols. Chem. Phys. Lipids 114, 55–80.

Minden, v.H.M., Milkereit, G., Vill, V., 2002b. Effects of carbohydrate headgroups on the stability of induced cubic phases in binary mixtures of glycolipids. Chem. Phys. Lipids 120, 45–56.

Morr, M., Proppe, C., Wray, V., 1995. Synthesis of asymmetrical methyl-branched chiral ketones from the corresponding homologous wax esters. A new synthesis of the insect pheromone lardolure and of 9-norlardolure. Liebigs Ann., 2001–2004.

Morr, M., Fortkamp, J., Rühe, S., 1997. Chirale methylverzweigte Tenside und Phospholipide: Synthese und Eigenschaften. Angew. Chemie 109, 2567–2569 [Angew. Chem. Int. Ed. Engl. 36, 2460–2462].

Prade, H., Miethchen, R., Vill, V., 1995. Thermotrop, flüssigkristalline Kohlenhydrat-Amphiphile. J. Prakt. Chem. 337, 427–440.

Priest, J.W., Mehlert, A., Arrowood, M.J., Riggs, M.W., Fergueson, M.A., 2003. Characterization of a low molecular weight glycolipid antigen from *Cryptosporidium parvum*. J. Biol. Chem. 278, 52212–52222.

Schultz, A., Laschat, S., Morr, M., Diele, S., Dreyer, M., Bringmann, G., 2002. Highly branched alkanoic acids from the preen-gland wax of the domestic goose as building blocks for chiral triphenylenes. Helv. Chim. Acta 85, 3909–3918.

Seydel, U., Koch, M.H.J., Brandenburg, K., 1993. Structural polymorphismus of rough mutant lipopolysaccharides Rd to Ra from *Salmonella minnesota*. J. Struct. Biol. 110, 232–243.

Tenchova, R., Tenchov, B.G., Hinz, H.J., Quinn, P.J., 1996. Lamellar-non-lamellar phase transitions in synthetic glycoglycerolipids studied by time-resolved X-ray diffraction. Liq. Cryst. 20, 469–482.

Vill, V., Minden, v.H.M., Koch, M.H.J., Seydel, U., Brandenburg, K., 2000. Thermotropic and lyotropic properties of long chain alkyl glycopyranosides. Part I: monosaccharide headgroups. Chem. Phys. Lipids 104, 75–91.

Chapter 8

How Thermotropic Properties influence the
Formation of Lyotropic Aggregates
near the Critical Micelle Concentration

HOW THERMOTROPIC PROPERTIES INFLUENCE THE FORMATION OF LYOTROPIC AGGREGATES NEAR THE CRITICAL MICELLE CONCENTRATION

V. M. Garamus[1], G. E. Milkereit[2], Regine Willumeit[1] and V. Vill[2]*

[1]GKSS Research Centre, Max-Planck-Str.1, 21502 Geesthacht, Germany
[2]Institute of Organic Chemistry, University of Hamburg, Martin-Luther-King-Platz 6, 20146 Hamburg, Germany

In this work, we investigated the lyotropic aggregation behaviour in dilute solutions of two synthetic glycolipids with same alkyl chain. The chemical structure of the carbohydrate headgroups is similar, nevertheless as reported the thermotropic phase behaviour is different. We found that the slightly tilted compound showing a complex thermotropic phase behaviour forms large aggregates with substructure already in dilute solutions and the significantly tilted compound with its simple thermotropic phase behaviour forms small spherical micelles near the CMC.

Keywords: glycolipids, lyotropic aggregation, SAXS, thermotropic phase behaviour

Introduction

In recent years, glycolipids have gained much interest in biophysics and physical chemistry. The biological interest focuses on their role in cell membranes and cell fusion processes. Simple alkyl glycosides can be found as membrane components [1], whereas more complex glycolipids are reported to serve as second messengers [2], pathogens [3–7] and some are substructures of complex endotoxins [8–10]. Especially, the type of carbohydrate headgroup plays an important role in cell recognition and membrane fusion processes [11–16].

From the industrial point of view, the surfactants from renewable sources are important ingredients for consumer health, and care products. Especially, alkyl glycosides and alkyl polyglucosides are the major group of this new natural surfactants [17–20].

Furthermore, many of the features of the self-aggregation of ionic and PEO-based surfactants are difficult or impossible to apply to alkyl glycosides in a direct and meaningful manner. More specifically, alkyl glycosides carry no charge but still have rigid carbohydrate headgroups. Therefore, they share features with PEO-based and ionic surfactants. In addition, the chirality of carbohydrate head groups has a great influence on the self-assembly in solutions [21].

Generally, the calorimetric effects of the dilute glycolipid–water systems are hardly detectable [22]. In this issue the concentrated endotoxine/phospholipid/water is described by Urban *et al*. and showed that in the case of the abundance of endotoxine the calorimetric ef-
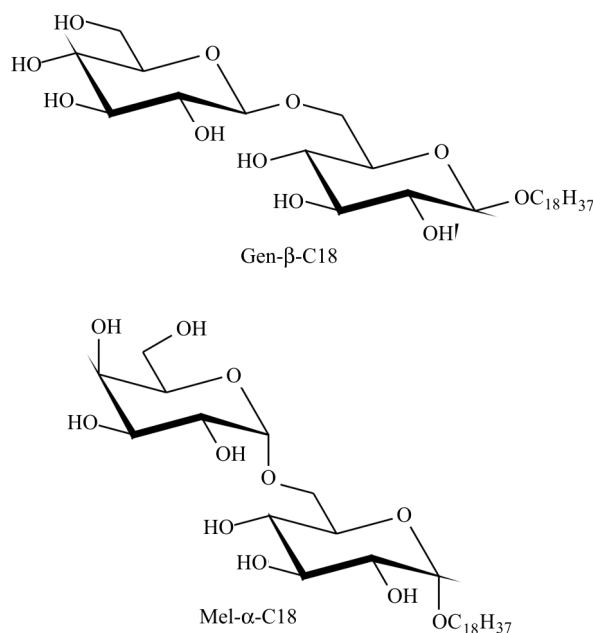
Fig. 1 Chemical structures of the investigated lipids Gen-β-C18 and Mel-α-C18

fects are vanished (the temperature range of the phase transition is extended extremely and the change in enthalpy is reduced drastically) in spite the fact that significant structural changes occur during the increasing temperature [23]. We have intend to show that the thermotropic behaviour of the dilute glycolipid system with minor thermotropic effect is accompanied with complex structural formation which are observed by using scattering technique. The thermotropic properties of

both compounds were already investigated by polarizing microscopy [24]. Mel-α-C18 shows only thermotropic Smectic A phase whereas Gen-β-C18 shows thermotropic Smectic A and cubic phases. The structure of the slightly wedge-shaped Gen-β-C18 is subject to the conflict between the hydrophilic and hydrophobic moiety, where the carbohydrate head favours the formation of columnar structures and the lipophilic tail favours the formation of lamellar structures which results in the formation of cubic phases besides the smectic phase. This structural conflict also destabilises the phase range of the liquid crystalline phase compared to the melibioside Mel-α-C18, which shows liquid crystalline phase behaviour over a temperature range of 122°C whereas the Gen-β-C18 shows a liquid crystalline phase only over a temperature interval of 98°C.

Small angle neutron scattering data were collected for solutions of Gen-β-C18 at 25°C and for Mel-α-C18 solutions at 50°C in D$_2$O. The higher temperature for second compound is applied with purpose to increase the solubility of Mel-α-C18 and to improve signal/noise ratio in scattering experiments.

In this work, we investigated the lyotropic aggregation behaviour in dilute solutions of synthetic glycolipids with different molecular shapes: slightly wedge-shaped (Gen-β-C18), and significantly tilted (Mel-α-C18). We found that a rich thermotropic phase behaviour of Gen-β-C18 is connected with formation of complex aggregates already in dilute solution, whereas a lipid Mel-α-C18 showing a simple thermotropic phase behaviour forms only small micelles in dilute solution.

Experimental

Materials and methods

Compounds

Synthesis of the compounds is described elsewhere [24]. Purity of the compounds was estimated to be >99%. Shortcuts are used to describe the compounds within the text: Mel-α-C18 for stearyl 6-O-(α-*D*-galactopyranosyl)-α-*D*-glucopyranoside, and Gen-β-C18 for stearyl 6-O-(β-*D*-glucopyranosyl)-β-*D*-glucopyranoside.

Small angle neutron scattering

Small angle neutron scattering experiments were performed with the SANS-1 instrument at the FRG1 research reactor at the GKSS Research Centre, Geesthacht, Germany [25]. Four sample-to-detector distances (from 0.7 to 9.7 m) were employed to cover the range of scattering vectors q from 0.005 to 0.25 Å^{-1}. The neutron wavelength, λ, was 8.1 Å with a wavelength resolution of 10% (full-width-at-full-maximum). The solutions were prepared in D$_2$O

(Deutero GmbH, purity 99.98 %). The samples were kept in quartz cells (Hellma) with a path length of 5 mm. The samples were placed in a thermostated holder, for isothermal conditions: T=25.0±0.5 and 50.0±0.5°C. The raw spectra were converted to an absolute scale and corrected for the backgrounds [26].

Results and discussion

Compounds

The chemical structures of the investigated compounds are shown in Fig. 1. The slightly wedge-shaped compound, Gen-β-C18, is a disaccharide with β-linkage of the alkyl chain and a glucopyranoside moiety linked $\beta1\rightarrow6$ to the first sugar ring. On the other hand, the tilted compound, Mel-α-C18, bears a galactopyranoside moiety linked $\alpha1\rightarrow6$ to the first sugar ring. In this lipid, the alkyl chain is linked via an α-glycosidic bond to the disaccharide headgroup.

Analysis of SANS data

SANS data were collected for solutions of Gen-β-C18 (c=1.0·10^{-4}, 5.0·10^{-4}, 1.0·10^{-3} g mL^{-1}) at 25°C, and Mel-α-C18 (c=6.3·10^{-4} g mL^{-1}) at 50°C in D$_2$O, these concentrations are near the CMC (CMC<1·10^{-5} g mL^{-1} for both compounds).

The obtained scattering curves are very different for the two glycosides (Fig. 2). Compound Gen-β-C18 shows a significant and rapidly decreasing scattering (d$\Sigma(q)$/d$\Omega{\sim}q^{-\alpha}$, α=1–2) at the low and intermediate intervals of the scattering vector (q<0.1 Å^{-1}). At large values of the scattering vector, q, a diffraction maximum
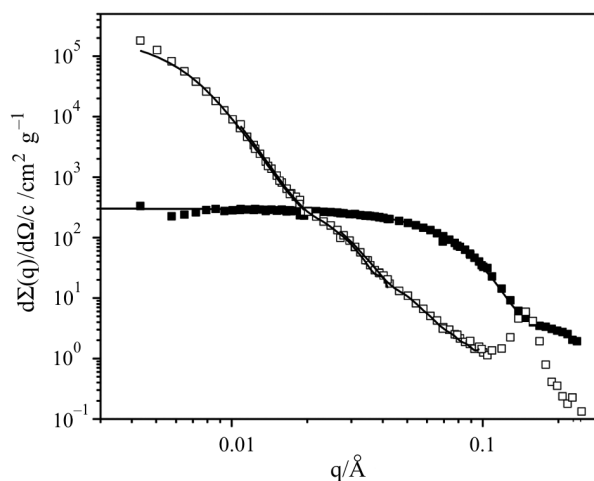
Fig. 2 Scattering curves and model fits for solutions of Gen-β-C18 ($\square$ – c=1.0·10^{-3} g mL^{-1}) and Mel-α-C18 ($\blacksquare$ – c=6.3·10^{-4} g mL^{-1}) in D$_2$O. The curves are normalized to the concentration of the surfactant in micelles. The solid lines represent fits by the IFT method

($q \approx 0.15$ Å^{-1}) can be observed. In contrast to the scattering curve of the Gen-β-C18 solution, the Mel-α-C18 scattering curve shows a small and approximately constant scattering at the low and intermediate intervals of q. It can be assumed that the two lipids form different aggregates in aqueous solution: *i*) Gen-β-C18 forms large aggregates with well-ordered plane or disc-shaped substructures; *ii*) Mel-α-C18 forms small and near spherical aggregates.

We started the analysis of the scattering data by applying the indirect Fourier transformation (IFT) method developed by Glatter [27] in the version of Pedersen [28]. This independent model approach needs only minor additional information about the possible aggregate structure: dimensions (sphere-like, rod-like or disc-like), and a maximum value of the diameter, cross section diameter or thickness, respectively. The IFT routine for spherical-like aggregates was applied to the whole q range of Mel-α-C18 scattering data. Only the low and intermediate ($q < 0.1$ Å^{-1}) q range of the scattering data of Gen-β-C18 were analysed. In the latter case, we have tried to exclude the diffraction maximum from our analysis ($q_{max} = 0.15$ Å^{-1}).

The scattering intensities ($d\Sigma(q)/d\Omega$) of the studied solutions are written via the pair distance distribution function $p(r)$. This is connected with the distribution of the scattering length density within the particles as an autocorrelation function [29]:

$$p(r) \sim \int \Delta\rho(r')\Delta\rho(r+r')dr' \qquad (1)$$

where $\Delta\rho(r)$ represents the contrast (difference between the scattering length density of aggregates at the point r, $\rho(r)$, and the averaged scattering length density of the solvent, ρ_s, $\Delta\rho(r) = \rho(r) - \rho_s$.

In the IFT approach, the pair distance distribution function is expressed as a sum of N b-splines, evenly distributed in the interval [0, D_{max}]. The values of the coefficients are calculated numerically by a least square fitting of the IFT model curve to the experimental data. In the present study, the values of D_{max} were carefully chosen to give both, good fits to the experimental data and smooth $p(r)$ functions. In the investigated q range the experimental data and the fitted curves coincide very well (Fig. 2).

The gaussian shape (Fig. 3) of the pair distribution function is characteristic for an almost spherical aggregate formed by compound Mel-α-C18. From the maximum distance of the $p(r)$ function a first estimation of the diameter (~70 Å) is possible. The shape of the $p(r)$ function of compound Gen-β-C18 on the other hand side is determined in a significant larger interval of r (~1000 Å) and suggests a slightly non-symmetrical shape of aggregates. The measured q-range is limited, therefore, it is not possible to investigate the whole size of the aggregates, the diameter of the formed aggre-
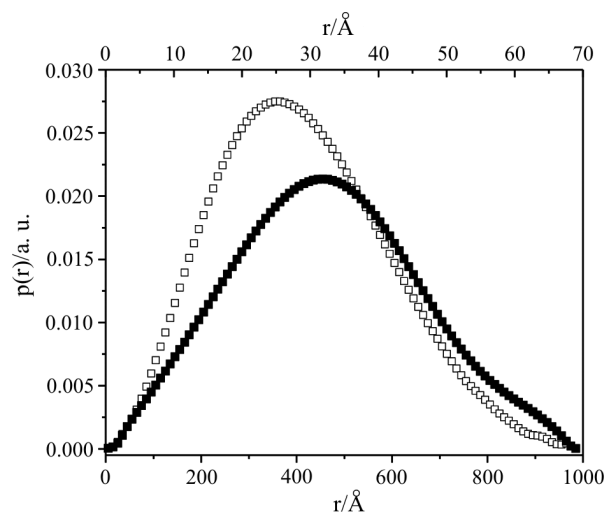
Fig. 3 Pair distance distribution functions obtained for Mel-α-C18 aggregates (■ – r-scale is in the top, D_{max}=70 Å) and for Gen-β-C18 (□ – r-scale is in the bottom, D_{max}=1000 Å)

gates is larger than 1000 Å, and the system can be polydispersed and/or non-spherical.

After determination of the pair distance distribution function, the radius of gyration of the cross section of the aggregates, R_g, can be calculated. The radius of gyration is written in the form:

$$R_g = \left[\frac{\int\limits_0^\infty r^2 p(r)dr}{2\int\limits_0^\infty p(r)dr} \right]^{1/2} \qquad (2)$$

The radii of gyration were calculated: *i*) compound Mel-α-C18 – R_g=25.0±0.8 Å (the corresponding radius of the homogeneous sphere is 32±1 Å); *ii*) Compound Gen-β-C18 – R_g=320±8 Å (the corresponding radius of the homogeneous sphere is 410±10 Å).

The analysis was continued by fitting of the Mel-α-C18 scattering data to a spherical model [29]. For the radius of the sphere a value of 31±1 Å was obtained, which agrees with the value obtained from the IFT analysis.

The diffraction maximum at a large q region points on some well-ordered substructures formed by Gen-β-C18 in the concentration range from 10^{-4} to 10^{-3} g mL^{-1}. An increase of the concentration of Gen-β-C18 by a factor of 10 does not change the shape of the scattering curve at a low and intermediate q range ($q < 0.1$ Å^{-1}) as can be seen from Fig. 4. There is no shift of the peak position of the maximum but the peak becomes sharper with increasing concentration. From the position of the peak it is possible to calculate the distance d between the layers using $q_{max}d = 2\pi$
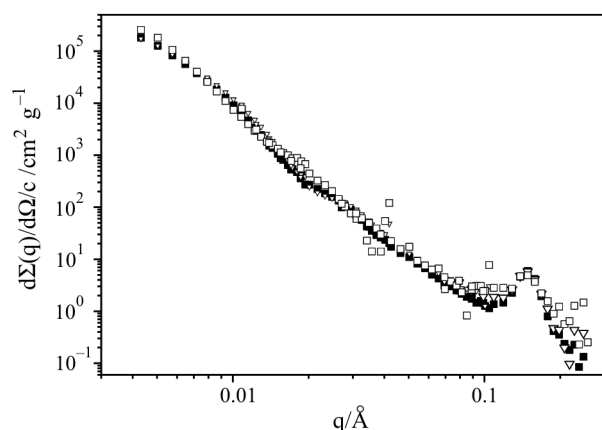
Fig. 4 Scattering curves of Gen-β-C18 solutions in D$_2$O at different concentrations of the lipid ($\blacksquare$ – c=1·10^{-3} g mL^{-1}, $\triangledown$ – c=5·10^{-4} g mL^{-1}, $\square$ – c=1·10^{-4} g mL^{-1}, T=25°C)

(d~43 Å). The length of Gen-β-C18 molecules can be calculated from the value of d. The length for one molecule in the layer (21.5 Å) points on a flexible conformation of the alkyl chain. This way of determination of molecular length can be considered only as maximum value of molecular length due to presence of hydrated water. Actually length of molecule is smaller and this supports more our conclusion on flexible conformation of alkyl chain of Gen-β-C18.

The other thermotropic properties of both compounds were already described [24]. Mel-α-C18 shows only thermotropic Smectic A phase whereas Gen-β-C18 shows thermotropic Smectic A and cubic phases. Also the lyotropic structures at a concentration of 0.1 g mL^{-1} were investigated for both compounds by small angle X-ray scattering (SAXS) [28]. At this high concentration, both compounds form lamellar structures in a broad temperature range. SANS-experiments were performed at a concentration near the CMC that is about 10^2 to 10^3 times lower than the concentrations that were used for the SAXS-measurements. At this low concentration where the interaction between aggregates can be neglected a strong influence of the molecular shape on the aggregation behaviour is observed. The significantly tilted melibioside Mel-α-C18 is packed into spherical micelles, here the imbalance between the hydrophilic and hydrophobic moiety is large, whereas in the pure state this imbalance is small, as can be seen from the thermotropic phase behaviour. On the other hand, the slightly wedge-shaped gentibioside, Gen-β-C18, is subject to the conflict between the hydrophilic and hydrophobic moiety, where the carbohydrate head favours the formation of columnar structures and the lipophilic tail favours the formation of lamellar structures. From the thermotropic properties, this can be seen in the formation of a cubic phase besides the Smectic A phase. In dilute solution, this effect decreases resulting in the formation of large disc-like aggregates, because a wedge-shaped structure would favour spherical or cylindrical structures and a rod-like structure the formation of bilayers. Hence large bilayer structures (discs) are formed as a tribute to the slightly tilted structure. With increasing concentration the interaction between the aggregates will be superior and besides other phases the lamellar phase with its bilayer structure dominates the lyotropic phases.

References

1 I. Ishizuka and T. Yamakawa, 1985. Glycolipids, In: H. Wiegandt, (Ed.), New Comprehensive Biochemistry, Elsevier, Vol. 10 (1985), p. 101.

2 S. Schutze, K. Potthoff, T. Machleidt, D. Berkovic, K. Wiegmann and M. Kronke, Cell, 71 (1992) 765.

3 F. Wagner, S. Rottem, H.-D. Held, S. Uhlig and U. Zähringer, Eur. J. Biochem., 267 (2000) 6276.

4 K. Matsuda, T. Kasama, I. Ishizuka, S. Handa, N. Yamamoto and T. Taki, J. Biol. Chem., 269 (1994) 33123.

5 K. Matsuda, I. Ishizuka, T. Kasema, S. Handa, N. Yamamoto and T. Taki, Biochim. Biophys. Acta, 1349 (1997) 1.

6 U. Zähringer, F. Wagner, E. Th. Rietschel, G. Ben-Menachem, J. Deutsch and S. Rottem, J. Biol. Chem., 272 (1997) 26262.

7 K. Matsuda, R. Harasawa, J. L. Li, T. Kasama, T. Taki, S. Handa and N. Yamamoto, Microbiol. Immunol., 39 (1995) 307.

8 U. Seydel, M. H. J. Koch and K. Brandenburg, J. Struct. Biol., 110 (1993) 232.

9 K. Brandenburg, W. Richter, M. H. J. Koch, H. W. Meyer and U. Seydel, Chem. Phys. Lipids, 91 (1998) 53.

10 K. Brandenburg, M. H. J. Koch and U. Seydel, J. Struct. Biol., 105 (1990) 11.

11 W. Curatolo, Biochim. Biophys. Acta, 906 (1987) 111.

12 V. H. M. Minden, G. Milkereit and V. Vill, Chem. Phys. Lipids, 120 (2002) 45.

13 M. Fragata, A. Menikh and S. Robert, J. Phys. Chem., 97 (1993) 13920.

14 J. L. Nivea, A. Alonso, G. Basanez, F. M. Goni, A. Gulike, R. Vargas and V. Luzatti, FEBS Lett., 368 (1995) 143.

15 M. Salman, J. Deutsch, M. Tarshis, Y. Naot and S. Rottem, FEMS Microbiol. Lett., 123 (1994) 255.

16 G. Franzoso, D. S. Dimitrov, R. Blumenthal, M. F. Barile and S. Rottem, FEBS Lett., 303 (1992) 251.

17 M. Hato, H. Minamikawa, K. Tamada, T. Baba and Y. Tanabe, Adv. Colloid Interface Sci., 80 (1999) 233.

18 C. J. Drummond and D. Wells, Colloids Surf., A, 141 (1998) 131.

19 W. von Rybinski, Curr. Opin. Colloid Interface Sci., 1 (1996) 587.

20 K. Shinoda, A. Carlsson and B. Lindman, Adv. Colloid Interface Sci., 64 (1996) 253.

21 C. E. Fairhurst, S. Fuller, J. Gray, M. C. Holmes and G. J. Tiddy, In: Handbook of Liquid Crystals: D. Demus, J. W. Goodby, G. W. Gray, H.-W. Spiess, V. Vill, Eds; Wiley-VCH, Weinheim 1998, Vol. 3, p. 341.

22 L. J. Waters, S. A. Leharne and J. C. Mitchell,
    J. Therm. Anal. Cal., 80 (2005) 43.
23 E. Urbán, A. Bóta, B. Kocsis and K. J. Lohner,
    J. Therm. Anal. Cal., (2005) in press.
24 V. H. M. Minden, K. Brandenburg, U. Seydel,
    M. H. J. Koch, V. M. Garamus, R. Willumeit and V. Vill,
    Chem. Phys. Lipids, 106 (2000) 157.
25 H. B. Stuhrmann, N. Burkhardt, G. Dietrich, R. Jünemann,
    W. Meerwinck, M. Schmitt, J. Wadzack, R. Willumeit,
    J. Zhao and K. H. Nierhaus, Nucl. Instr. Meth.,
    A356 (1995) 133.

26 G. D. Wignall and F. S. Bates, J. Appl. Crystallogr.,
    20 (1986) 28.
27 O. Glatter, J. Appl. Crystallogr., 10 (1977) 415.
28 J. S. Pedersen, Adv. Colloid Interface Sci., 70 (1997) 171.
29 L. A. Feigin and D. I. Svergun, Structure Analysis by
    Small-Angle X-Ray and Neutron Scattering, Plenum Press,
    New York 1987.

Chapter 9

Complex Effect of Ethyl Branching on the
Supramolecular Structure of a
Long Chain Neoglycolipid

Complex effect of ethyl branching on the supramolecular structure of a long chain neoglycolipid

Abstract

A new ethyl-branched neoglycolipid was synthesised from D-maltose and *N*-tetradecanoyl-(*2R*)-2-aminobutanol in three steps. The physical properties of three glycolipids (non-branched spacer, without spacer with same alkyl chain and longer alkyl chain) of similar structure were also investigated for comparison. The liquid crystalline properties were studied using polarising microscopy and the contact preparation method. Investigation of the micelle formation and structure was performed using surface tension measurements and small angle neutron scattering. The interaction between the amidic and the ethyl group leads to a better solubility of the compound with a branched ethyl spacer compared to the non-branched one and favours the formation of long cylindrical micelles. The micelle length is significantly higher than reported for n-alkyl maltosides of similar chain length, i.e., the non-polar ethyl spacer gives a better packing of the polar groups.

1. Introduction

The main problem with the investigation of the lyotropic properties of long chain n-alkyl glycosides and neoglycolipids with disaccharide headgroups is the high Krafft-eutectic temperature T_K, that makes a characterisation of the lyotropic phases difficult or often impossible [1-3]. Especially for the use in biological model systems a T_K at ambient temperature is necessary. The use of unsaturated or highly branched alkyl chains solves this problem and becomes a standard procedure in liquid crystalline chemistry [4]. Unsaturated alkyl chains on the other hand can be destroyed by β-oxidation or other effects in solution (reactants, etc.). Micelles formed by highly branched chains are different to ones formed by compounds with n-alkyl chains, due to a different packing of the chain in the micelle core as reported by Milkereit et al. [5].
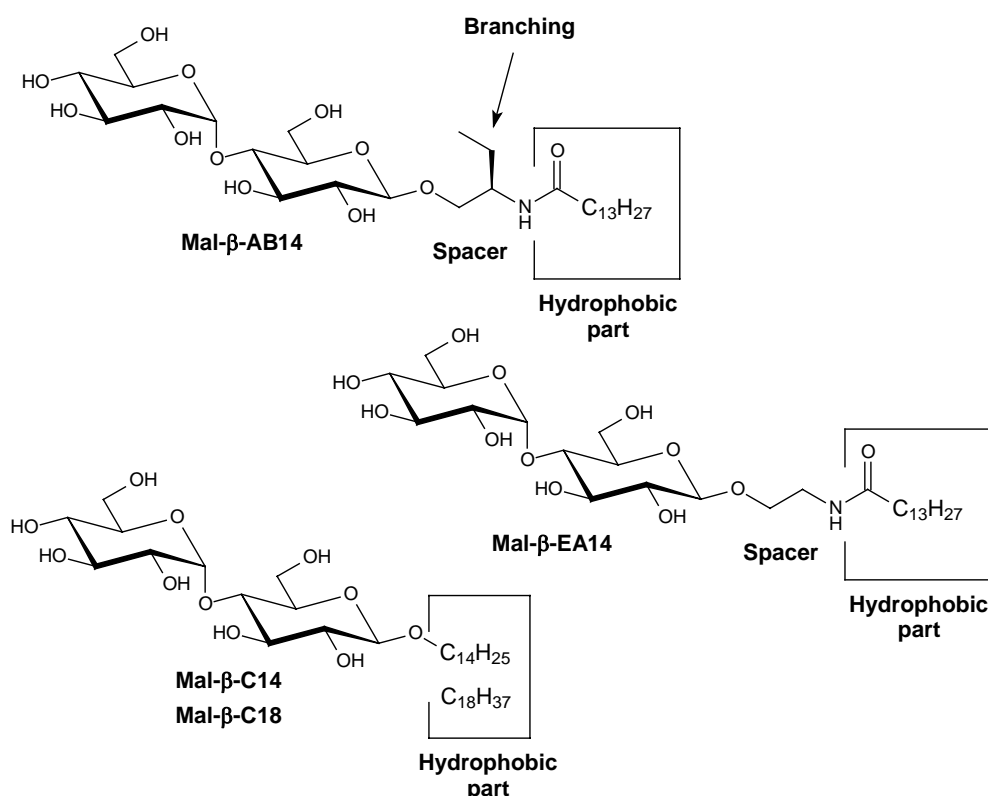
Figure 1: Molecular structures of the branched (**Mal-β-AB14**), unbranched (**Mal-β-EA14**) and the normal n-alkyl maltosides **Mal-β-C14** and **Mal-β-C18**, showing the main structural differences.

Recent reviews addressing the structure-property relationship of alkyl glycosides and their aggregation behaviour can be found in the literature [6, 7]. To date mainly short and medium chain alkyl glycosides have been widely investigated by small angle neutron scattering (SANS). The shape of the micelles varies with size of the polar group, for example the disaccharide *n*-octyl β-D-maltopyranoside forms spherical micelles in a wide concentration range but the corresponding monosaccharide *n*-octyl β-D-glucopyranoside forms rod-like micelles [8, 9]. The increasing of alkyl chain length from *n*-nonyl-*β*-D-glucoside to *n*-tetradecyl-*β*-D-maltoside favours the growth of micelles from relatively stiff cylidrical aggregates to large flexible polymer-like micelles [10, 11]. Our recent systematic studies on the effect of structure of the polar head group in the case of glycosides with unsaturated

oleyl chains (C18) shows the formation of three different types of aggregates: spherical, cylindrical and polymer-like micelles in dilute solutions when the polar group is varied i.e., trisaccharide, disaccharide with an additional amidoethoxy spacer and disaccharide [12].

In this work we present a new neoglycolipid (**Mal-β-AB14**) based on a secondary amino alcohol, that forms large micelles already in dilute solution (Figure 1). Comparison of the data with similar maltosides (tetradecyl: **Mal-β-C14**, stearyl: **Mal-β-C18** and the non-branched analogue: **Mal-β-EA14**) showed, that the micelles formed by the branched glycolipid are significantly longer.

2. Materials and Methods

Peracetylated Maltose was prepared according to the literature [13]. Thin-layer chromatography was performed on silica gel (Merck GF_{254}), and detection was effected by spraying with a solution of ethanol / sulphuric acid (9:1), followed by heating. Column chromatography was performed using silica gel (Merck, 0.063-0.200 mm, 230-400 mesh). NMR spectra were recorded on a Bruker AMX 400 or a Bruker DRX 5001 spectrometer (m_c = centred multiplet, d = doublet, t = triplet, dd = double doublet, dt = double triplet).

2.1 Polarising Microscopy

An Olympus BH optical polarising microscope equipped with a Mettler FP 82 hot stage and a Mettler FP 80 central processor was used to identify thermal transitions and characterise anisotropic textures. Contact preparation was carried out according to standard procedures [14].

2.2 Surface Tension

Surface tension was measured on a Krüss K6 Tensiometer (Krüss, Germany), using the de Noüy ring method. All measurements were carried out using bidistilled water with a surface tension of σ = 72 - 73 mN/m (20 °C). For each sample the experiment was repeated three times in order to obtain constant values. First all values were multiplied with a correction factor taken the deviation of the measured value for pure water and the literature value into account (σ_{ref} / σ). Correction for the ring geometry and the hydrostatic lifted volume of liquid were made using the method described by Harkins and Jordan or by Zuidema and Waters [15, 16].

2.3 Small angle neutron scattering

Small angle neutron scattering experiments were performed with the SANS-1 experiment at the FRG1 research reactor at the GKSS research Centre, Geesthacht, Germany [17]. Four sample-to-detector distances (from 0.7 to 9.7 m) were employed to cover the range of scattering vectors q from 0.005 to 0.25 Å^{-1}. The neutron wavelength λ was 8.1 Å with a wavelength resolution of 10 % (full-width-at-full-maximum). The solutions were prepared in D_2O (Deutero GmbH, purity 99.98 %). The samples were kept in quartz cells (Hellma) with a path length of 5 mm. The samples were placed in a thermostated holder, for isothermal conditions T = 25.0±0.5 °C and 50.0±0.5 °C. The raw spectra were corrected for the background from the solvent, sample cell and other sources, by conventional procedures [18]. The two-dimensional isotropic scattering spectra were azimuthally average, converted to an absolute scale and corrected for detector efficiency by dividing by the incoherent

scattering spectra of pure water, which was measured with a 1-mm-path-length quartz cell (Hellma). The average excess scattering length density per unit mass $\Delta\rho_m$ of the surfactant in deuterated water was determined from the known chemical composition it was equal to $\Delta\rho_m = - 4.80 \times 10^{10}$ cm/g for **Mal-β-C18** and $\Delta\rho_m = - 4.43 \times 10^{10}$ cm/g for **Mal-β-AB14**. The density of the lipids was determined using the program ChemSketch 3.50 (ACD-labs).

2.4 Synthesis

Synthesis of **Mal-β-C18, Mal-β-C14** and **Mal-β-EA14** has been described elsewhere [3,19]. The synthesis of **Mal-β-AB14** was performed in three steps (scheme 1). First the amino alcohol (*2R*)-2-aminobutane-1-ol was acylated with tetradecanoyl chloride in dichloromethane, to give the product in a good yield. The *N*-acyl alcohol was used in the glycosylation reaction with maltoseperacetate using boron trifluoride etherate as catalyst similar to the procedure described by Vill et al. [13]. However the product was only obtained in 30 % yield. One reason could be that the *N*-acyl alcohol did not dissolve completely in dichloromethane on starting the glycosylation reaction. Upon addition of the Lewis acid the precipitate dissolved immediately indicating a possible interaction of the Lewis acid with the functionalised alcohol. However addition of more Lewis acid did not increase the yield. After deprotection and recrystallisation the final product **Mal-β-AB14** was obtained in 88 % yield. Further synthetic details including NMR data can be found in the Appendix.
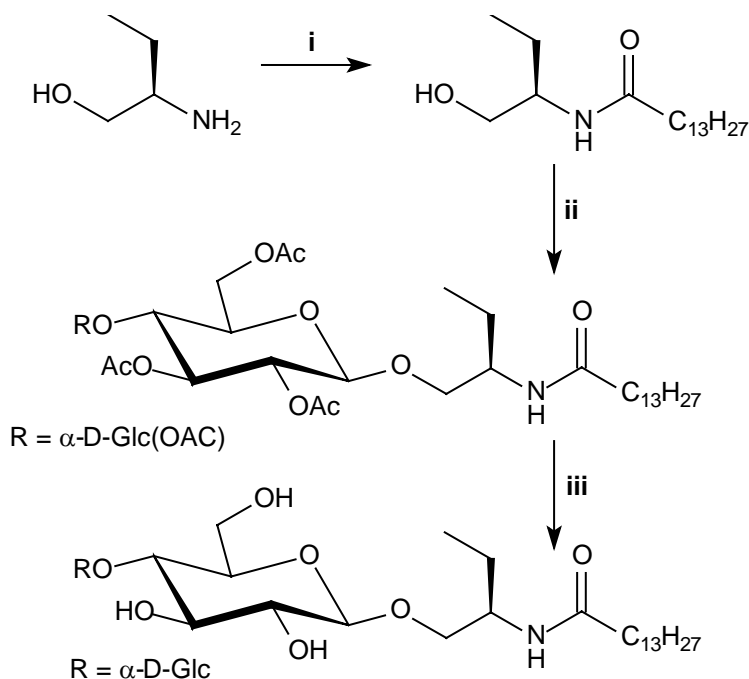
Scheme 1: Synthesis of **Mal-β-AB14**[a]

[a]Reagents: (i) Tetradecanoyl chloride, Et₃N, CH₂Cl₂ (75%); (ii) Maltoseperacetate, BF₃•Et₂O, CH₂Cl₂ (30%); (iii) NaOMe, MeOH (88%)

3. Results and Discussion

The liquid crystalline properties were investigated using polarising microscopy. The results are shown in Table 1 and in Figure 2. Compound **Mal-β-AB14** was in the glass state at room temperature. Upon heating the compound formed a lamellar Smectic A (SmA) phase. The transition temperature was estimated to be between 40 and 50 °C. The SmA phase was formed in the whole temperature range up to the clearing temperature (I) of 240 °C. On cooling from the isotropic phase the SmA phase formed and at room temperature it took several hours until the glass was formed again. The transition temperature of **Mal-β-AB14** differs from that of the other investigated maltosides with a similar chain length. The compound does not simply melt, due to the ethyl branching of the spacer that disturbs the packing of the alkyl chains, instead a glass ↔ liquid crystalline phase transition occurs. The formation of a strong hydrogen-bonding network can be seen in the small liquid crystalline phase range of **Mal-β-EA14**, where the clearing temperature is more than 100 °C lower than observed for the n-alkyl maltosides. The role of the CH_2CH_2-group in the interaction between the amide groups becomes obvious if the phase range of the liquid crystalline phases is compared. **Mal-β-EA14** forms the liquid crystalline phase only over a temperature range of 63 °C, whereas the phase range of the Smectic A phase of **Mal-β-AB14** can be estimated to be similar or even higher than that of the long chain alkyl maltoside **Mal-β-C18**.

Table 1: Thermotropic and lyotropic properties of the investigated compounds obtained by polarising microscopy and the contact preparation method (Data for **Mal-β-C14** and **Mal-β-C18** are taken from v.Minden et al. [3]; * = Myelin figures were formed in the contact preparation with water).

Thermotropic properties

Mal-β-C14	Cr	107	SmA	264	I
Mal-β-C18	Cr	106	SmA	274	I
Mal-β-EA14	Cr	102	SmA	165	I
Mal-β-AB14	g	?	SmA	240	I

Lyotropic properties

Mal-β-C14	L_α		H_1
Mal-β-C18	L_α		H_1
Mal-β-EA14	L_α^*		
Mal-β-AB14	L_α	V_1	H_1

          pure lipid   100 % water
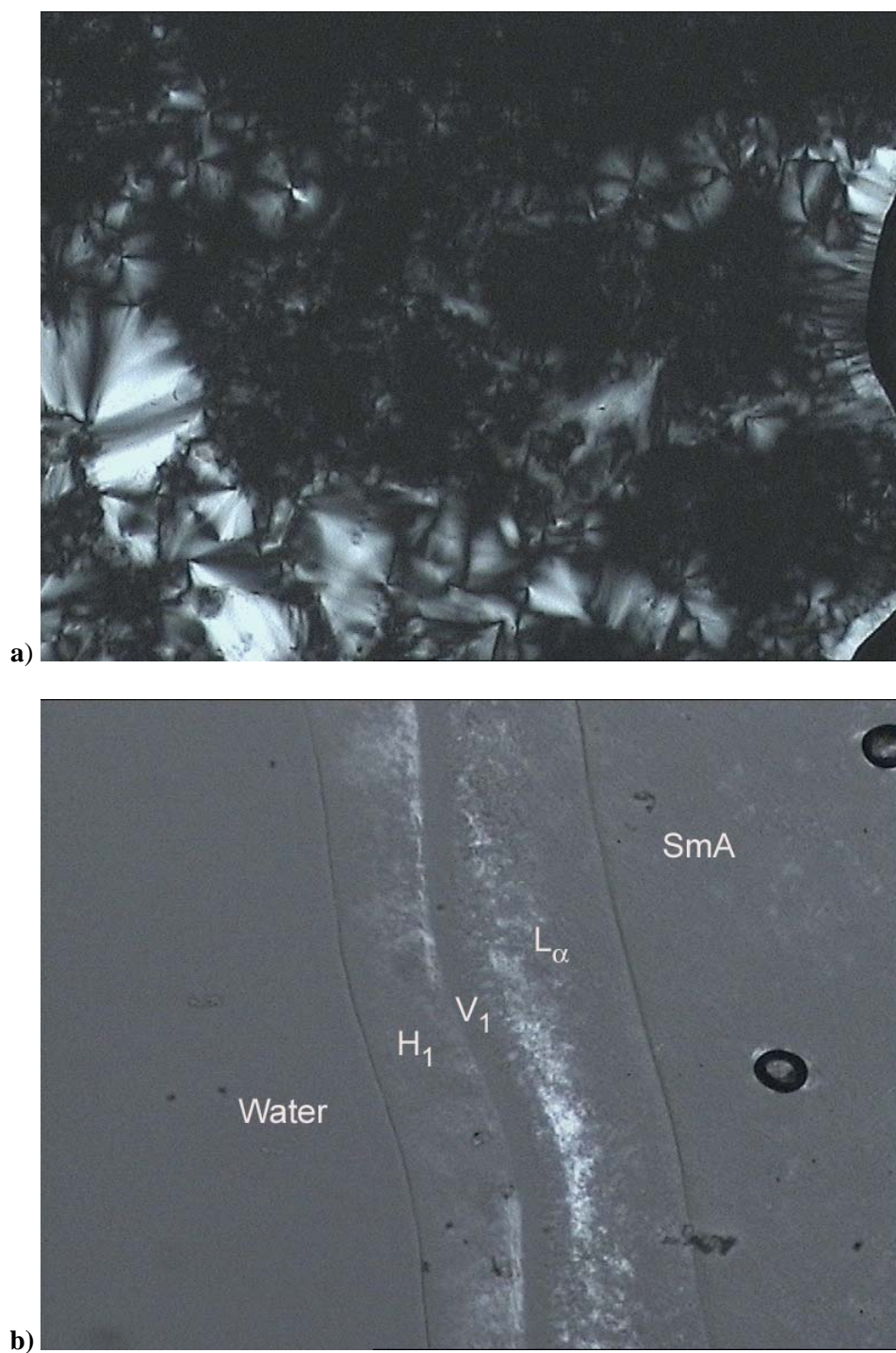
Figure 2: Polarising Microscopy - Textures of the liquid crystalline phases of **Mal-β-AB14**. a) SmA phase of the pure lipid on cooling from the isotropic solution. b) Phase sequence in the contact preparation with water (SmA - Smectic A phase of the pure lipid, L_α - Lyotropic lamellar phase, V_1 - Lyotropic cubic (type 1) phase, H_1 - Lyotropic hexagonal (type 1) phase).

The lyotropic properties of **Mal-β-AB14** also differ from those of the corresponding normal alkyl glycosides. In the contact preparation with water lamellar phases are formed on the lipid rich side. With increasing water content a cubic phase is formed followed by a hexagonal phase of type I. The alkyl glycosides **Mal-β-C18** and **Mal-β-C14** form only a lamellar and a hexagonal (type I) phase. This indicates that the amidic group also affects the lyotropic properties. The main difference in the lyotropic phase behaviour can be found between the branched and non-branched lipids. While **Mal-β-AB14** shows some lyotropic polymorphism in the contact with water, **Mal-β-EA14** only forms a lamellar phase and myelin figures as a sign of low water solubility.

Surface tension for (Figure 3) compound **Mal-β-AB14** solutions in water was measured at 25 °C. The obtained value of cmc is 0.040 ± 0.002 mM (2.5×10^{-5} g/mL). No phase separation occurred up to a concentration of 1 wt%. The value is similar to that obtained for **Mal-β-C14** (0.020 ± 0.001 mM; 1.1×10^{-5} g/mL). This means, that the influence of the spacer on the energy transfer of molecules from bulk solution to micelles is small. The non-branched **Mal-β-EA14** does not form measurable solutions between 25 °C and 70 °C, due to its bad solubility in water and/or possibly a high Krafft-temperature. For **Mal-β-C18** cmc values were not measured due to technical limitations of our tensiometer.
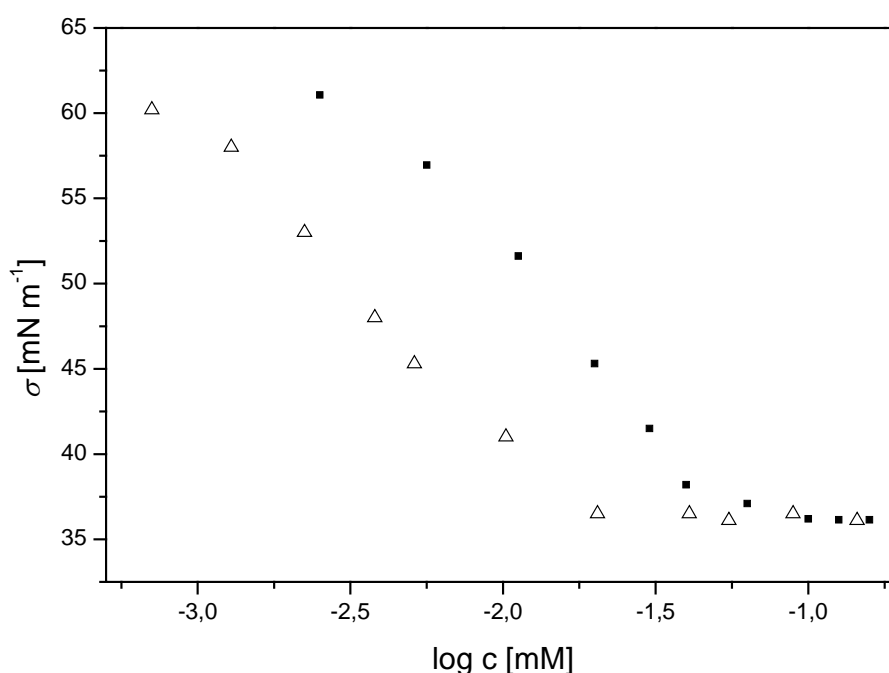
Figure 3: Surface tension plots for **Mal-β-AB14** (filled symbols) and **Mal-β-C14** (empty symbols) at 25 °C.

a)

b)

c)
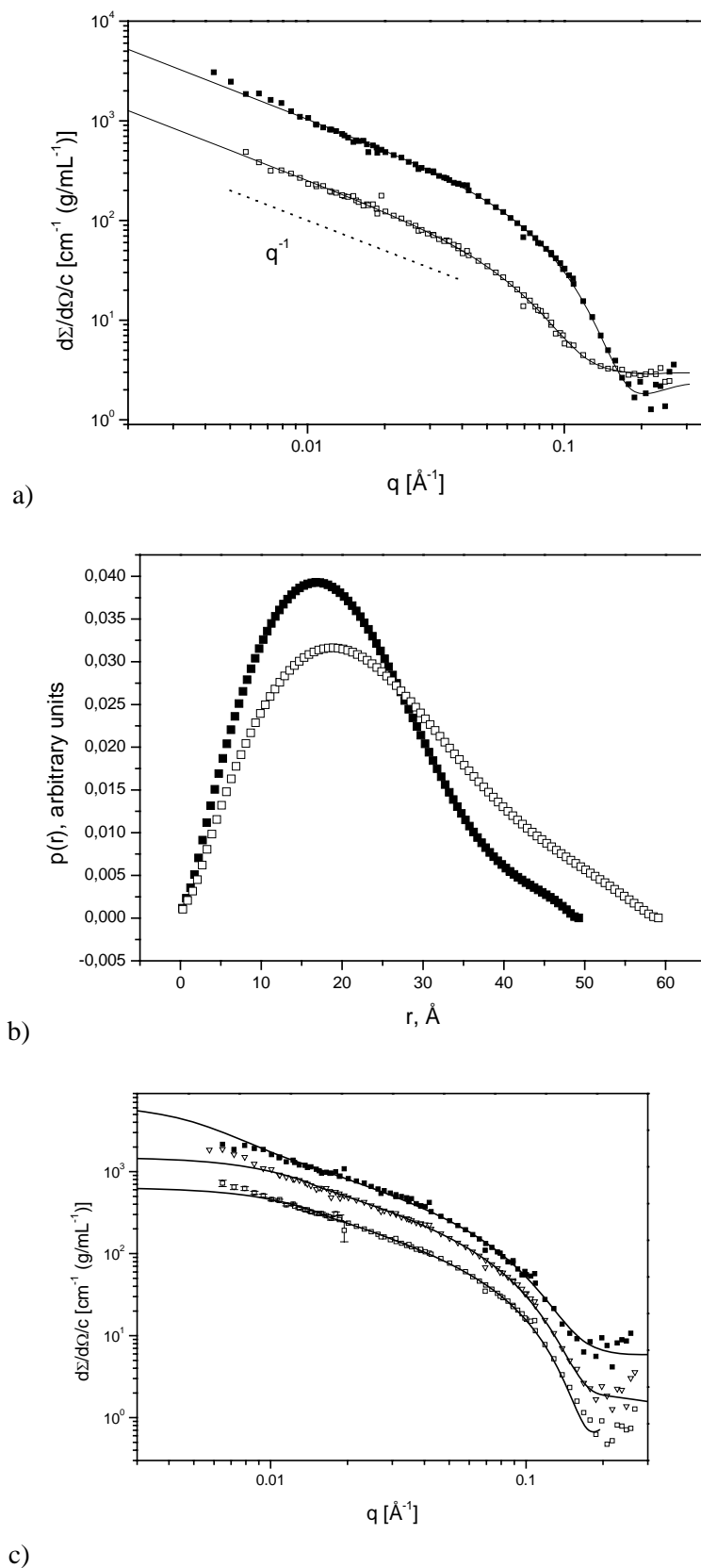
Figure 4: a) Scattering data for **Mal-β-AB14** at 25 °C (filled squares; c = 5x10^{-4} g/mL) and **Mal-β-C18** at 50 °C (empty squares; 4.3x10^{-4} g/mL) together with the model IFT fits (solid lines). The dashed line shows the dependence $d\Sigma(q)/d\Omega \sim q^{-1}$; b) pair distance distribution function p(r), for **Mal-**

β-AB14 at 25 °C (filled squares; c = 5x10^{-4} g/mL) and **Mal-β-C18** at 50 °C (empty squares; 4.3x10^{-4} g/mL); c) Scattering data for **Mal-β-AB14** (25 °C) at different concentrations: c = 1x10-4 g/mL (empty squares), c = 5x10-4 g/mL (empty triangles) and c = 1x10-3 g/mL (filled squares). Solid lines are fits (Eq. 4).

Small angle neutron scattering experiments were performed using three different concentrations of **Mal-β-AB14** in water (1x10^{-4}, 5x10^{-4} and 1x10^{-3} g/mL, at 25 °C). For comparison solutions of stearyl maltoside (**Mal-β-C18**) and the non-branched **Mal-β-EA14** were prepared. Only **Mal-β-C18** gave measurable solutions at 50 °C (see Figure 4a). The non-branched **Mal-β-EA14** does not form measurable solutions between 25 °C and 70 °C, due to its bad solubility in water and/or possibly a high Krafft-temperature. This again shows the effect of the ethyl branching in compound **Mal-β-AB14** on the solubility in water.

In case of dilute solutions the scattering intensity normalized to the concentration of the glycosides (see Figure 4c) is proportional to the mass of aggregates. The increasing of scattering with the concentration of **Mal-β-AB14** should point on micelle growth. It is a well-known behaviour for rod-like micelles.

The shape of scattering curves of **Mal-β-AB14** and **Mal-β-C18** are typical for rod-like aggregates (Figure 4a), i.e., at an intermediate q range the dependence of the differential cross section of neutron scattering is connected with $d\Sigma(q)/d\Omega \sim q^{-1}$ which reflects the scattering of the cross section of rod-like aggregates. In general the higher scattering of solutions of **Mal-β-AB14** is connected with the formation of larger rod-like aggregates (micelles) compared to **Mal-β-C18**.

Information on the local structure of the micelles can be obtained by applying the indirect Fourier transformation (IFT) to the experimental data from the high-q range (q>0.02 Å^{-1}) [20]. The asymptotic behaviour of the scattering function for $q > 1/L$, where L is the length of the cylinder, can be expressed as

$$d\Sigma(q)/d\Omega = (\frac{\pi}{q})2\pi\int_0^\infty p_{CS}(r)J_0(qr)rdr = (\frac{\pi}{q})I_{CS}(q) \qquad (1)$$

where J_0 is the zeroth-order Bessel function and $I_{CS}(q)$ is the cross-section scattering intensity. The normalized cross-section distance distribution function $p_{CS}(r)$ is given by [21]

$$p_{CS}(r) = \frac{c}{2\pi M_L}\int \Delta\rho(\mathbf{r'})\Delta\rho(\mathbf{r}+\mathbf{r'})d\mathbf{r'}, \qquad (2)$$

where the vectors $\mathbf{r}$ and $\mathbf{r'}$ lie in the cross-section plane. A first estimation of the distance distribution function $p_{CS}(r)$ is obtained by applying the IFT method (Figure 4b). Experimental data and fitted curves perfectly coincide within the range of the scattering vector q>0.02 Å^{-1}.

From $p_{CS}(r)$ the integral parameter of the micellar cross-section such as the cross-section radius of gyration $R_{CS,g}$ can be calculated according to Glatter [22]. The cross-section radius is written in the form:

$$R_{CS,g} = \left[\frac{\int_0^\infty r^2 \, p_{CS}(r)dr}{\int_0^\infty p_{CS}(r)dr} \right]^{1/2} . \tag{3}$$

The asymmetrical shape of $p_{CS}(r)$ suggests an elliptical shape of the cross section of the aggregates formed by both compounds (Figure 4b).

The model of scattering cross sections by dilute solution of rigid cylinders is given by Eq. 4 [23]:

$$d\Sigma(q)/d\Omega/(c\text{-}CMC) = M\Delta\rho_m^2 P_{cyl}(q), \tag{4}$$

where $P_{cyl}(q)$ is the form factor of a cylinder with the length L and with an elliptical cross-section with the semi axis A and B. In the case of long cylinders the scattering of the cross-section is described [23] in a decouple approximation as:

$$P_{cyl}(q) = P_{rod}(q,\,L)S_{CS}(q), \tag{5}$$

$P_{rod}(q,L)$ is the form factor of an infinitely thin rod of the length L. $S_{CS}(q)$ is the elliptical cross-section scattering function

$$S_{CS}(q) = \frac{2}{\pi} \int_0^{\pi/2} \left(\frac{2J_1(qr(A,B,\theta))}{qr(A,B,\theta)} \right)^2 d\theta, \tag{6}$$

with $r(A,B,\theta) = [A^2 \sin^2\theta + B^2 \cos^2\theta]^{1/2}$ and J_1 is the first order Bessel function.

In the final fit, five parameters were fitted: the length of cylinders L, the cross section axis A and B, a correction factor for the absolute scale and a residual background. The correction factor for the absolute scale takes small errors in concentrations into account and it is expected to be close to unity. The obtained parameters of aggregates are listed in Table 2. Literature data of the micellar structure for tetradecyl maltoside (**Mal-β-C14**) are shown in addition. It should be pointed that parameters of aggregates were calculated without taking into account interaction between them and should be considered with caution i.e., as effective ones.

Table 2: Micellar form and parameter of micellar structure of the investigated compounds and literature data for comparison (Data taken from   a - from v.Minden et al. [3] and b - from Ericsson et al. [11]).

	T [°C]	c [g/mL]	Length [Å]	R_{CS} [Å]	a-axis [Å]	b-axis [Å]	axis ratio [ε]
Mal-β-AB-14	25	1x10⁻⁴	500±200	20±1	20	21	1
Mal-β-Ab-14	25	5x10⁻⁴	1100±200	22±1	17	26	1.5
Mal-β-AB-14	25	1x10⁻³	1700±200	22±1	16	27	1.6
Mal-β-C14ᵃ	25	1x10⁻³	200	20±			
Mal-β-C14ᵇ	35	1x10⁻²	1700±200	21±1	16	26	1.6
Mal-β-C18	50	4.3x10⁻⁴	700±100	27±1	19	33	1.7

Mal-β-AB14 micelles grow with increasing concentration of glycolipid (Table 2) from 500 to 1700 Å in studied concentration range. Roughly it follows classic mean-field models for micellar growth [24] i.e., $L \sim c^{1/2}$. Micelles formed by branched glycolipid (**Mal-β-AB14**) are larger than micelles formed **Mal-β-C14** at similar concentration. It looks that growth rate is higher for **Mal-β-AB14** than **Mal-β-C14**.

The ellipticity of the cross section is similar for Mal-β-C18 ($\varepsilon = 1.7$), Mal-β-AB14 ($\varepsilon = 1.5\text{-}1.6$) and Mal-β-C14 ($\varepsilon = 1.6$). For **Mal-β-C18** the minor axis values point to an extended conformation of the alkyl chains, also for **Mal-β-AB14** and **Mal-β-C14** the minor axis values are of similar size, suggesting an extended conformation of the alkyl chains too.

Summary

Comparison of the compounds with a branched spacer **Mal-β-AB14** and a non-branched spacer **Mal-β-EA14** shows that branching significantly increases the solubility of the glycolipid in water, i.e., an existence of cmc and a rich lyotropic phase diagram.

The ethyl branched spacer also favours the growth of micelles. The micelles formed by **Mal-β-AB14** are larger than that formed by **Mal-β-C18** and significantly larger than that formed by **Mal-β-C14**. These differences cannot be explained by different experimental conditions. Solutions of **Mal-β-C18** and **Mal-β-C14** were measured at higher temperature (50 and 35 °C). The investigation of **Mal-β-C14** showed that the micellar structure increases in the interval of T from 35 to 50 °C [11]. To our knowledge, the main effect arises from the fact that the amide function builds up strong hydrogen bonding networks in the pure state and in solution that normally leads to the formation of rigid structures as reported by Masuda et al. [25] and Milkereit et al. [26]. The ethyl branching on the other hand disturbs the packing of molecules, leading to liquid crystalline phase behaviour already at room temperature, or in this case to a better dissolving at room temperature compared to **Mal-β-C18**. These two effects seem to be in equilibrium for **Mal-β-AB14**, which leads to the formation of longer aggregates than formed by the alkyl glycosides of similar length. Another interesting observation is the fact, that the spacer despite the polar amido group does not increase the polarity. Otherwise an increase of the polarity would result in the formation of shorter micelles than observed for **Mal-β-C14**.

Appendix A

Synthesis

N-Tetradecanoyl-(*2R*)-2-amino-butan-1-ol (1)

17.83 g (0.2 mol; 18.8 mL) (*R*)-(-)-2-Amino-butane-1-ol and 22.7 g (0.22 mol; 31 mL) Triethylamine were dissolved in 100 mL anhydrous dichloromethane. The solution was cooled to -10 °C and 44.43 g (48.8 mL; 0.18 mol) Tetradecanoyl chloride were added dropwise. The reaction mixture was allowed to warm to room temperature after complete addition. The precipitated solid was collected and washed with water. The product was recrystallised from light petroleum (b.p. 50-70) to give the product as a white solid.

Yield: 44.4 g (75 %).

$C_{18}H_{37}O_2N$

1-*O*-(*N*-Tetradecanoyl-(*2''R*)-2''-amino-butyl)-4-*O*-(2',3',4',6'-tetra-*O*-acetyl-α-D-glucopyranosyl)-2,3,6-tri-*O*-acetyl-ß-D-glucopyranosid (2)

1.0 g (1.5 mmol) Maltoseperacetate and 673 mg (2.25 mmol) **1** were dissolved in 60 mL of dry dichloromethane under an atmosphere of dry nitrogen. 426 mg (377 µL; 3 mmol) boron trifluoride etherate were added and the solution was stirred for five hours at room temperature until t.l.c. revealed the reaction to be complete. The reaction was quenched with 50 mL of a saturated solution of sodium hydrogen carbonate, the organic layer was separated and the aqueous layer extracted twice with dichloromethane. The combined organic phases were washed twice with water, dried over magnesium sulphate and evaporated *in vacuo*. The residue was purified by column chromatography (light petroleum b.p. 50-70 °C - ethyl acetate 2:1 → 1:1).

Yield: 450 mg (30 %) white solid.

$C_{44}H_{71}O_{19}N$

$[\alpha]_D^{20} = +30°$ (c = 0.4, CHCl$_3$)

MALDI-TOF-MS: m/z = 941.1 [M+Na]$^+$

1-*O*-(*N*-Tetradecanoyl-(*2''R*)-2''-amino-butyl)-4-*O*-(α-D-glucopyranosyl)-ß-D-glucopyranoside (Mal-β-AB14)

435 mg (0.47 mmol) **2** were dissolved in 50 mL anhydrous methanol and sodium methoxide was added (pH 8-9). The solution was stirred at room temperature until TLC revealed the reaction to be complete. It was neutralised then using DOWEX 50WX ion-exchange resin (protonated form), filtrated and evaporated *in vacuo*. The product was recrystallised from methanol.

Yield: 258 mg (88 %) white solid.

$C_{30}H_{57}NO_{12}$

$[\alpha]_D^{20} = +28°$ (c = 0.1, MeOH)

MALDI-TOF-MS: m/z = 646.9 [M+Na]$^+$

Anal.Calcd for $C_{30}H_{57}NO_{12}$:   C, 57.77; H, 9.21; N, 2.25. Found: C, 57.65; H, 9.24; N 2.17

NMR-data

***N*-Tetradecanoyl-(*2R*)-2-amino-butan-1-ol (1)**

^{1}H-NMR (400 MHz, CDCl$_3$ + TMS): δ = 5.72 (d, 1H, $J_{H-ß,NH}$ 7.1 Hz, NH), 3.78 - 3.86 (m, 1H, H-ß), 3.65 (dd, 1H, $J_{\alpha a,ß-H}$ 2.3, $J_{\alpha a,b}$ 10.7 Hz, H-αa), 3.55 (dd, 1H, $J_{\alpha b,ß-H}$ 5.9 Hz, H-αb), 2.17 (t, 2H, Alkyl-α-CH$_2$), 1.36 - 1.64 (m, 4H, γ-CH$_2$, Alkyl-ß-CH$_2$), 1.16 - 1.32 (m, 20H, Alkyl-CH$_2$), 0.93 (t, 3H, δ-CH$_3$), 0.86 (t, 3H, Alkyl-CH$_3$).

^{13}C-NMR (100 MHz, CDCl$_3$ + TMS): δ = 171.16 (C=O), 61.18 (C-α), 59.80 (C-ß), 36.71 (Alkyl-α-CH$_2$), 36.55 (Alkyl-ß-CH$_2$), 32.15, 29.36, 29.28 (Alkyl-CH$_2$), 26.78 (γ-CH$_2$), 25.75, 23.02, 21.05 (Alkyl-CH$_2$), 14.98 (δ-CH$_3$), 14.15 (Alkyl-CH$_3$).

1-*O*-(*N*-Tetradecanoyl-(*2''R*)-2''-amino-butyl)-4-*O*-(2',3',4',6'-tetra-*O*-acetyl-α-D-glucopyranosyl)-2,3,6-tri-*O*-acetyl-ß-D-glucopyranosid (2)

^{1}H-NMR (400 MHz, CDCl$_3$ + TMS): δ = 5.37 (d, 1H, NH), 5.33 (d, 1H, $J_{1',2'}$ 4.1 Hz, H-1'), 5.29 (dd, 1H, $J_{2',3'}$ 9.7, $J_{3',4'}$ 9.7 Hz, H-3'), 5.19 (dd, 1H, $J_{2,3}$ 9.2, $J_{3,4}$ 9.2 Hz, H-3), 4.98 (dd, 1H, $J_{4',5'}$ 9.7 Hz, H-4'), 4.79 (dd, 1H, H-2'), 4.74 (dd, 1H, $J_{1,2}$ 7.9 Hz, H-2), 4.43 (d, 1H, H-1), 4.39 - 4.44 (m, 1H, H-ß), 4.19 (dd, 1H, $J_{5',6a'}$ 4.1, $J_{6a',b'}$ 12.2 Hz, H-6a'), 4.16 (dd, 1H, $J_{5,6a}$ 4.5, $J_{6a,b}$ 12.0 Hz, H-6a), 3.99 (dd, 1H, $J_{5',6b'}$ 2.0 Hz, H-6b'), 3.86 - 3.95 (m,

3H, H-4, H-6b, H-5'), 3.76 (dd, 1H, H-αa), 3.61 (ddd, 1H, $J_{5,6b}$ 3.0 Hz, H-5), 3.47 (dd, 1H, H-αb), 2.06 - 2.09 (m, 2H, Alkyl-α-CH$_2$), 2.07, 2.03, 1.98, 1.96, 1.95, 1.94, 1.93 (je s, 3H, OAc), 1.37 - 1.56 (m, 4H, H-γa, H-γb, Alkyl-ß-CH$_2$), 1.14 - 1.26 (m, 20H, Alkyl-CH$_2$), 0.82 (t, 3H, δ-CH$_3$), 0.81 (t, 3H, Alkyl-CH$_3$).

^{13}C-NMR (100 MHz, CDCl$_3$ + TMS): δ = 172.9 (C=O, Amid), 170.54, 170.50, 170.27, 170.01, 169.62, 169.43 (C=O, OAc), 100.31 (C-1), 95.38 (C-1'), 75.51 (C-3), 72.84 (C-4), 72.26, 72.11 (C-2, C-5), 70.18 (C-α), 69.99 (C-2'), 69.40 (C-3'), 68.58 (C-5'), 68.07 (C-4'), 62.95 (C-6), 61.56 (C-6'), 58.75 (C-β), 36.40 (Alkyl-α-CH$_2$), 36.31 (Alkyl-ß-CH$_2$), 31.19, 29.02 (Alkyl-CH$_2$), 26.9 (γ-CH$_2$) 25.95, 24.83, 24.69, 24.17, 23.18, 22.70 (Alkyl-CH$_2$), 20.94, 20.85, 20.69, 20.62, 20.59 (-CH$_3$, OAc), 14.97 (δ-CH$_3$), 14.11 (Alkyl-CH$_3$).

1-*O*-(*N*-Tetradecanoyl-(*2''R*)-2''-amino-butyl)-4-*O*-(α-D-glucopyranosyl)-ß-D-glucopyranoside (Mal-β-AB14)

^{1}H-NMR (400 MHz, CD$_3$OD): δ = 5.17 (d, 1H, $J_{1',2'}$ 3.6 Hz, H-1'), 4.32 (d, 1H, $J_{1,2}$ 8.1 Hz, H-1), 3.99 (m$_c$, 2H, H-6a, H-β), 3.90 (dd, 1H, H-6b), 3.79 - 3.86 (m, 3H, H-4', H-6a', Alkyl-H-αa), 3.48 - 3.76 (m, 12H, H-3, H-4, H-3', H-5', H-6b', H-αa, H-αb, H-β, Alkyl-H-αb, Alkyl-β-CH$_2$), 3.45 (dd, 1H, $J_{2',3'}$ 10.1 Hz, H-2'), 3.38 (ddd, 1H, $J_{4,5}$ 9.7, $J_{5,6a}$ 2.0, $J_{5,6b}$ 4.6 Hz, H-5), 3.24 - 3.31 (m, 1H, H-2,), 1.35-1.41 (m, 2H, H-γa, H-γb), 1.11 - 1.30 (m, 20H, Alkyl-CH$_2$), 0.86 (t, 3H, $\delta-$CH$_3$), 0.84 (t, 3H, Alkyl-CH$_3$).

References

[1] R.G. Laughlin, The aqueous phase behaviour of surfactants, Academic Press, London, 1994.

[2] M. Hato and H. Minamikawa, Langmuir, 12 (1996) 1658.

[3] H.M. v.Minden, K. Brandenburg, U. Seydel, M.H.J. Koch, V.M. Garamus, R. Willumeit and V. Vill, Chem. Phys. Lipids, 106 (2000) 157.

[4] M. Hato, Curr. Opin. Coll. Interf. Sci., 6 (2001) 268.

[5] G. Milkereit, V.M. Garamus, M. Hato, M. Morr and V. Vill, J. Phys. Chem. B, 109 (2005) 1599.

[6] C. Stubenrauch, Curr. Opin. Colloid Interface Sci., 6 (2001) 160.

[7] O. Soderman, and I. Johansson, Curr. Opin. Colloid Interface Sci., 4 (2000) 391.

[8] L.-Z. He, V.M. Garamus, S.S. Funari, M. Malfois, R. Willumeit, R. and B. Niemeyer, J. Phys. Chem. B, 106 (2002) 7596.

[9] L.-Z. He, V.M. Garamus, B. Niemeyer, H. Helmholz, and R. Willumeit, J. Mol. Liq., 89 (2000) 239.

[10] C. A. Ericsson, O. Söderman, V. M. Garamus, M. Bergström, and S. Ulvenlund, Langmuir, 20 (2004) 1401.

[11] C. A. Ericsson, O. Söderman, V. M. Garamus, M. Bergström, and S. Ulvenlund, Langmuir, 21 (2005) 1507.

[12] G. Milkereit, V. M. Garamus, K. Veermans, R. Willumeit, and V. Vill, J. Colloid Interface Sci., 284 (2005) 704.

[13] V. Vill, T. Böcker, J. Thiem, and F. Fischer, Liq. Cryst., 6 (1989) 349.

[14] H.M. v.Minden, G. Milkereit and V. Vill, Chem. Phys. Lipids, 120 (2002) 45.

[15] W.D. Harkins and H.F. Jordan, J. Am. Chem. Soc., 52 (1930) 1751.

[16] H.H. Zuidema and G.W. Waters, Ind. Eng. Chem., 13 (1941) 312.

[17] H.B. Stuhrmann, N. Burkhardt, G. Dietrich, R. Jünemann, W. Meerwinck, M. Schmitt, J. Wadzack, R. Willumeit, J. Zhao and K.H. Nierhaus, Nucl. Instr. & Meth., A356 (1995) 133.

[18] G.D. Wignall and F.S. Bates, J. Appl. Cryst., 20 (1986) 28.

[19] G. Milkereit and V. Vill, to be published.

[20] O. Glatter, J. Appl. Cryst., 10 (1977) 415.

[21] J. S. Pedersen and P. Schurtenberger, J. Appl. Cryst., 29 (1996) 646.

[22] O. Glatter, in A. Wilson (Ed.), International Tables for Crystallography, Vol. C, Kluwer Academic Publishers, Dordrecht, 1992, pp. 89.

[23] J.S. Pedersen, Adv. Colloid Interface Sci., 70 (1997) 171.

[24]   M. E. Cates and S. J. Candau, J. Phys.: Condens. Matter 2 (1990) 6869.

[25] M. Masuda, V. Vill and T. Shimizu, J. Am. Chem. Soc., 122 (2000) 12327.

[26] G. Milkereit, V.M. Garamus, K. Veermans, R. Willumeit and V. Vill, Chem. Phys. Lipids, 131 (2004) 51.

Chapter 10

An Improved Synthetic Procedure for the Preparation of
N-acyl (2-aminoethyl)-β-D-glycopyranoside lipids
and characterisation of their mesogenic properties

An Improved Synthetic Procedure for the Preparation of *N*-acyl (2-Aminoethyl)-β-D-glycopyranoside Lipids and Characterisation of Their Mesogenic Properties

Abstract

A modified synthetic procedure was used for the synthesis of N-acyl (2-aminoethyl) glycosides bearing Maltose, Melibiose and Lactose carbohydrate headgroups and different acyl chains. The lipids were prepared in gram scale and investigated for their liquid crystalline properties. It was found that the polar spacer suppresses polymorphism the resulting simplified phase was found in the pure state upon heating, as well as for the lyotropic phase behaviour.

Introduction

N-acyl aminoethyl lactopyranosides have gained interest as possible substitutes for ceramides in the investiagtion of enzymatic reactions [1]. Other kinds of spacer between the carbohydrate headgroup and the lipophilic tail have also been used as substitutes for ceramides [2] or for the preparation biological active liposomes [3]. Nevertheless the synthesis of homologues series of N-acyl ethylamino disaccharides with variation of the sugar and the acyl chain has not been reported yet. Also a characterisation of its liquid crystalline properties in the pure state (thermotropic) and upon the addition of water (lyotropic) cannot be found, despite the fact that knowledge of these can explain possible biological functions of these lipids [4-7].

Liquid crystalline properties of n-alkyl glycosides on the other hand are well known for many compounds [8].

Disaccharides with alkyl chain-length of 12 to 18 carbon atoms show a complex phase behaviour, which depends on the structure of the carbohydrate headgroup [9].

1: R^1= β-D-Gal(OAc), R^2= OAc
2: R^1= α-D-Gal(OAc), R^2= OAc
3: R^1= OAc, R^2= α-D-Gal(OAc)

4: R^1= β-D-Gal(OAc), R^2= OAc
5: R^1= β-D-Gal(OAc), R^2= OAc
6: R^1= OAc, R^2= β-D-Gal(OAc)

10: R^1= β-D-Gal(OAc), R^2= OAc
11: R^1= β-D-Gal(OAc), R^2= OAc
12: R^1= OAc, R^2= β-D-Gal(OAc)

7: R^1= β-D-Gal(OAc), R^2= OAc
8: R^1= β-D-Gal(OAc), R^2= OAc
9: R^1= OAc, R^2= β-D-Gal(OAc)
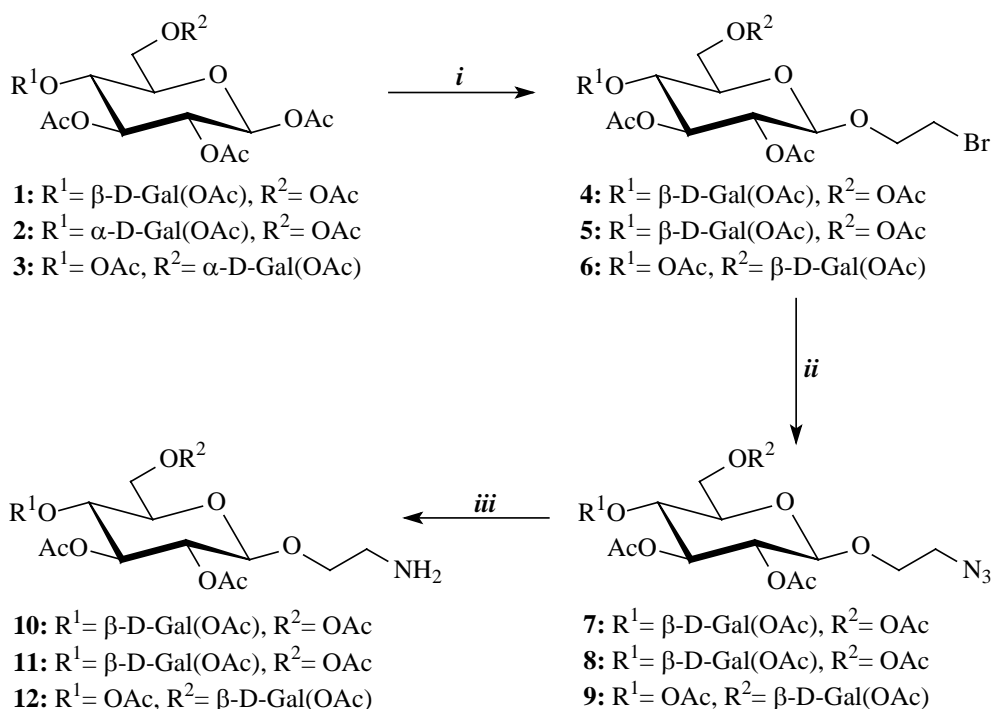
Scheme 1: Synthesis of the precursors **10**, **11** and **12**. Reagents and conditions: *i*.) HO(CH$_2$)$_2$Br, BF$_3$*Et$_2$O, CH$_2$Cl$_2$ abs., 0 °C, 2h, r.t., 18h *ii*.) NaN$_3$, DMF, r.t., 24h; *iii*.) H$_2$, Pd/C 10%, MeOH abs. or MeOH abs. / THF abs. 9:1, r.t., 1h.

Results and Discussion

Synthesis

A few *N*-acylaminoethyl β-lactosides were first synthesized by Miura et al. [10], bearing fatty acid chains with a chain length of 8, 12, 16 and 20 carbon atoms. Peracetylated lactose was condensed with Fmoc proctected ethanolamin in the route described there. After removal of the Fmoc group the aminogroup was acylated with octanoyl, dodecanoyl, hexadecanoyl and eicosanoyl chloride.

Deprotection gave the products in 22-30% overall yield. Although this yields are considerable good, they synthesized only amounts of around 300 mg. For a close physical and biological characterisation on the other hand amounts of several grams are often necessary. Therefore we used a different route for the synthesis of different *N*-acyl (2-aminoethyl) glycosides that can easily be upscaled (Scheme 1 and 2).

10, 11, 12 — *i* →

13: R^1= β-D-Gal(OAc), R^2= OAc, R^3= $C_{13}H_{27}$
14: R^1= β-D-Gal(OAc), R^2= OAc, R^3= $C_{15}H_{31}$
15: R^1= β-D-Gal(OAc), R^2= OAc, R^3=$(CH_2)_7$ C_8H_{17}
16: R^1= α-D-Gal(OAc), R^2= OAc, R^3= $C_{13}H_{27}$
17: R^1= α-D-Gal(OAc), R^2= OAc, R^3= $C_{15}H_{31}$
18: R^1= α-D-Gal(OAc), R^2= OAc, R^3=$(CH_2)_7$ C_8H_{17}
19: R^1= OAc, R^2= α-D-Gal(OAc), R^3= $C_{13}H_{27}$
20: R^1= OAc, R^2= α-D-Gal(OAc), R^3= $C_{15}H_{31}$
21: R^1= OAc, R^2= α-D-Gal(OAc), R^3=$(CH_2)_7$ C_8H_{17}

22: R^1= β-D-Gal, R^2= OH, R^3= $C_{13}H_{27}$
23: R^1= β-D-Gal, R^2= OH, R^3= $C_{15}H_{31}$
24: R^1= β-D-Gal, R^2= OH, R^3= $(CH_2)_7$ C_8H_{17}
25: R^1= α-D-Glc, R^2= OH, R^3= $C_{13}H_{27}$
26: R^1= α-D-Glc, R^2= OH, R^3= $C_{15}H_{31}$
27: R^1= α-D-Glc, R^2= OH, R^3= $(CH_2)_7$ C_8H_{17}
28: R^1= OH, R^2= α-D-Gal, R^3= $C_{13}H_{27}$
29: R^1= OH, R^2= α-D-Gal, R^3= $C_{15}H_{31}$
30: R^1= OH, R^2= α-D-Gal, R^3= $(CH_2)_7$ C_8H_{17}

Scheme 2: Synthesis of the final lipids **22-30**. Reagents and conditions: *i*.) RCOCl, DMF abs., C_5H_5N abs., 0 °C, 2h; *ii*.) NaOMe, MeOH abs., r.t., 4h.

Instead of Fmoc protected ethanolamine, we condensed the peracetylated disaccharide with bromethanol using boron trifluoride as lewis acid according to procedures described before [11]. It is noteworthy to mention that in this case glycosylation at a temperature of 0 °C gave considerable higher yields as if the reaction was stirred at room temperature. After chromatographic purification the 2-bromoethyl glycoside was obtained in yields of 50 to 60 %. Nucleophilic substitution of the bromine using sodium azide in *N,N*-dimethylformamide (DMF) afforded the corresponding azide in quantitative yields after workup. Further purification was not necessary. The 2-aminoethyl glycoside was prepared by reduction of the azide with hydrogen under catalysis of palladium on charcoal (10%). The azide was completely conversed to the amine, as could be seen in TLC (1:3 light petroleum b.p. 50-70 ethyl acetate), where the educt spot completely disappeared after 2 hours and only one single

spot that moved distinctly slower, was detected. The amine was immediately reacted with the freshly distilled acyl chloride in DMF using a catalytic amount of pyridine according to the procedure of Masuda et al. [12]. TLC (1:2 light petroleum - ethyl actete) of the reaction showed after stirring overnight only three spots, two that moved very fast (R_f 0.7 and 0.8) possibly belonging to the carbonic acid and some minor byproducts and one spot (R_f 0.3) belonging to the product. The educt spot was not detectable. After chromatographic purification the compounds were obtained in 70 to 90 % yield, depending on the acyl chain length. After deptrotection using the modified Zemplén procedure the lipids were finally obtained after recrystallization from methanol or after chromatographic purification (4:1 chloroform - methanol). Using this route nine lipids with tetradecanoyl, hexadecanoyl and oleoyl chains and lactose, maltose and melibiose carbohydrate headgroups were synthesised in good yields and in gram scale.

Liquid Crystalline Phase Behaviour

The thermotropic phase transitions were investigated using polarising microscopy. The results are shown in table 1. All compounds show liquid crystalline phase behaviour upon heating. The six compounds with n-acyl chains (**22,23,25,26,28,29**) are crystalline at ambient temperature. The lactoside **24** and the melibioside **30** with the unsaturated oleoyl chain did not crystallize, forming a glass instead. Also a defined phase transition temperature of the transition from the glassy state to the liquid crystalline phase could not be determined. It was only observed that the compound transformed into the liquid crystalline state at temperatures above 50 °C. The maltoside **27**, also carrying an oleoyl chain, was the only compound showing liquid crystalline phase behaviour already at ambient temperature. Interestingly it was observed that all compounds formed only thermotropic smectic A (bilayer) phases as liquid crystalline phase. This is surprising because their alkyl glycoside counterparts form other phases like e.g. cubic phases besides the lamellar phase [9]. An explanation for this simplified phase behaviour might be the interaction of the amidic group. The formation of a hydrogen-bonding network in the hydrophobic part of the molecule disables the formation of complex phases like cubic phases. Another deviation from the liquid crystalline phase behaviour of the corresponding alkyl glycosides can be seen in the transition temperatures. The compounds **24**-**30** show similar melting points as the n-alkyl glycosides, only for the two lactosides **22** and **23** it was found that the melting points are 15-20 °C lower. Deviation between the alkyl glycosides and the investigated compounds is found for the clearing temperatures. The clearing temperatures are lowered for all compounds by 50-75 °C compared to their n-alkyl counterparts. Three compounds showed signs of decomposition near the clearing point. Again this might be attributable to the interaction of the amidic group in the hydrophobic part that disturbs the order of the acyl chains, which then leads to a reduced stability of the liquid crystalline phase.

The lyotropic phase sequences of the investigated compounds are shown in table 2. The influence of the amino-spacer on the lyotropic phase behaviour in water is obvious at first glance. Compounds **22**, **23**, **25**, **26**, **28** and **29** bearing n-alkyl chains only form lamellar phases upon the addition of water. Due to the low water solubility of these compounds myelin figures are formed beyond the lamellar phase. The three compounds with the oleoyl chain (**24**, **27**, **30**) show lyotropic polymorphism. Beyond the lamellar phase hexagonal phases of type I can be found. In case of compound **27** with its maltose

carbohydrate headgroup a cubic phase is formed between the lamellar and the hexagonal phase. Above the cmc the maltoside **27** forms long and stiff cylindrical micelles, compared to oleyl maltoside, which forms polymer-like and flexible micelles [13].

Since mixing of glycolipids with different phase behaviour can induce new phases [14], the simplified phase behaviour of the N-acyl ethylamino glycosides can be useful to control the phase behaviour of lipid mixtures, where it might induce and/or stabilise phases that are of biological interest.

Table 1: Thermotropic phase transitions of the pure compounds (in °C; Cr = crystalline; g = glass; SmA = Smectic A phase; I = isotropic; d = decomposition)

22	Cr	147	SmA	208	d
23	Cr	148	SmA	212	d
24	g	?	SmA	180	I
25	Cr	102	SmA	164	I
26	Cr	103	SmA	191	d
27	Cr	<20	SmA	123	I
28	Cr	151	SmA	205	I
29	Cr	152	SmA	210	I
30	g	?	SmA	195	I

Table 2: Lyotropic phase sequence in the contact preparation with water (Cr = crystalline; g = glass; L_α = lamellar phase; * = Myelin figures were formed beyond the lamellar phase towards the water region; H_1 = hexagonal phase; V_1 = bicontinous cubic phase)

22	Cr	L_α*		
23	Cr	L_α*		
24	g	L_α		H_1
25	Cr	L_α*		
26	Cr	L_α*		
27	SmA	L_α	V_1	H_1
28	Cr	L_α*		
29	Cr	L_α*		
30	g	L_α		H_1
	pure compound			100 % water

Experimental

General

Thin-layer chromatography was performed on silica gel (Merck GF$_{254}$), and detection was effected by spraying with a solution of ethanol/sulphuric acid (9:1), followed by heating. Column chromatography was performed using silica gel 60 (Merck, 0.063-0.200 mm, 230-400 mesh). NMR spectra were recorded on a Bruker AMX 400 or a Bruker DRX 5001 spectrometer (m$_c$ = centred multiplet, d = doublet, t = triplet, dd = double doublet, dt = double triplet). Spectral assignments were made by the double-resonance technique COSY. An Olympus BH optical polarising microscope equipped with a Mettler FP 82 hot stage and a Mettler FP 80 central processor was used to identify thermal transitions and characterise anisotropic textures. For the contact preparation a small amount of sample was placed on a microscope slide and covered with a cover glass before heating. Afterwards a small amount of solvent was placed on the slide at the edge of the cover glass. As soon as the solvent had moved under the cover glass and completely surrounded the sample with the solvent, the slide was placed again for a few seconds on the hot stage at a temperature of 100 - 120 °C and the phase behaviour was investigated immediately afterwards by polarizing microscopy.

Synthesis

(2-Amino-ethyl) 4-*O*-(2', 3', 4', 6'-tetra-*O*-acetyl-β-D-galactopyranosyl)-2,3,6-tri-*O*-acetyl-β-glucopyranoside (10)

13.6 g (20 mmol) 4-*O*-(2', 3', 4', 6'-tetra-*O*-acetyl-β-D-galactopyranosyl)-1,2,3,6-tetra-*O*-acetyl-β-D-gluco-pyranoside and 1.85 mL (3.2 g; 26 mmol) anhydrous 2-Bromethanol were dissolved in 50 mL anhydrous dichlormethane under an atmosphere of dry nitrogen. 6.5 mL (7.4 g; 52 mmol) boron trifluoride etherate were added dropwise at 0 °C under nitrogen. Stirring was continued for 2 h at 0 °C and an additional 18 h at room temperature. The solution was poured on ice water (100 mL) and extracted twice with 50 mL dichlormethane. The combined organic phases were washed twice with 50 mL saturated sodium hydrogen carbonate solution, twice with 30 mL water, dried over magnesium sulfate and solvent removed *in vacuo*. The residue was purified by column chromatography (light petroleum b.p. 50-70 °C - ethyl acetate 1:1). Yield: 8.2 g (62 %) **4**. 7.4 g (10 mmol) **4** were dissolved in 100 mL anhydrous N,N-dimethylformamide. 6.5 g (100 mmol) sodium azide were added and the reaction mixture was stirred overnight at ambient temperature. The reaction mixture was filtered and the filtrate was poured on 100 mL water and extracted three times with 100 mL dichlormethane. The combined organic phases were washed with brine (100 mL), two times with water (100 mL) and dried over magnesium sulphate. Solvent was evaporated *in vacuo*, to give compound **7** in quantitative yield as slight yellow syrup, which was used without further purification. 7.1 g (10 mmol) **7** were dissolved in 100 mL of a 9:1 mixture of anhydrous methanol and tetrahydrofurane. 30 mg Palladium on charcoal (10%) were added and the reaction mixture was stirred under an atmosphere of hydrogen for two hours until t.l.c revealed the reaction to be complete (light petroleum b.p. 50-70 °C- ethyl acetate 1:2). The catalyst was filtered off and solvent was evaporated under reduced pressure. The residue was subjected to column chromatography (light petroleum b.p. 50-70 °C - ethyl acetate 1:3).

Yield: 6.7 g (98 %).

^{1}H-NMR (400 MHz, C$_6$D$_6$): δ = 5.54 (dd, 1H, $^{3}J_{1',2'}$ 8.1, $^{3}J_{2',3'}$ 10.4, H-2´), 5.47 (dd, 1H, $^{3}J_{3',4'}$ 3.6, $^{3}J_{4',5'}$ 1.0, H-4´), 5.41 (dd, 1H, $^{3}J_{2,3}$ 9.7, $^{3}J_{3,4}$ 9.2, H-3), 5.26 (dd, 1H, $^{3}J_{1,2}$ 8.1, H-2), 5.10 (dd, 1H, H-3´), 4.52 (dd, 1H, $^{3}J_{5,6a}$ 2.0, $^{2}J_{6a,6b}$ 12.2, H-6a), 4.31 (d, 1H, H-1´), 4.22 (d, 1H, H-1), 4.14 (dd, 1H, $^{3}J_{5,6b}$ 6.1, H-6b), 4.05-4.12 (m, 2H, H-6a´, H-6b´), 3.80-3.85 (m, 1H, OC*H$_2$*CH$_2$N), 3.70-3.74 (m, 1H, OC*H$_2$*CH$_2$N) 3.63 (dd, 1H, $^{3}J_{4,5}$ 9.2, H-4), 3.44-3.50 (m, 3H, H-5´, OCH$_2$C*H$_2$*N), 3.20 (ddd, 1H, H-5), 1.97, 1.93, 1.84, 1.73, 1.70, 1.64, 1.54 (each s, 3H, OAc). C$_{28}$H$_{41}$O$_{18}$N (679.2324)

(2-Amino-ethyl) 4-*O*-(2', 3', 4', 6'-tetra-*O*-acetyl-α-D-glucopyranosyl)-2,3,6-tri-*O*-acetyl-β-glucopyranoside (11)

13.6 g (20 mmol) 4-*O*-(2', 3', 4', 6'-tetra-*O*-acetyl-α-D-glucopyranosyl)-1,2,3,6-tetra-*O*-acetyl-β-D-glucopyranoside and 1.85 mL (3.2 g; 26 mmol) anhydrous 2-Bromethanol were reacted as described for compound **4**. Yield: 9.8 g (74 %) of compound **5**. 7.4 g (10 mmol) **5** were reacted as described for compound **7**. The product **8** was obtained in quantitative yield and used without further purification. 7.1 g (10 mmol) **8** in 100 mL anhydrous methanol were reacted as described for compound **10**.

Yield: 6.7 g (98 %).

^{1}H-NMR (400 MHz, CDCl$_3$ + TMS): δ = 6.03 (bs, 2H, NH), 5.35 (d, 1H, $^3J_{1',2'}$ 4.1, H-1'), 5.29 (dd, 1H, $^3J_{2',3'}$ 10.1, $^3J_{3',4'}$ 9.7, H-3'), 5.20 (dd, 1H, $^3J_{2,3}$ 9.2, $^3J_{3,4}$ 9.2, H-3), 4.99 (dd, 1H, $^3J_{4',5'}$ 9.9, H-4'), 4.80 (dd, 1H, H-2'), 4.77 (dd, 1H, $^3J_{1,2}$ 7.9, H-2), 4.53 (d, 1H, H-1), 4.43 (dd, 1H, $^3J_{5,6a}$ 2.8, $^2J_{6a,b}$ 12.2, H-6a), 4.19 (d, 1H, $^3J_{5',6a'}$ 2.3, $^2J_{6a',b'}$ 11.2, H-6a'), 4.16 (dd, 1H, $^3J_{5,6b}$ 4.3, H-6b), 3.98 (dd, 1H, $^3J_{5',6b'}$ 3.6, H-6b'), 3.95 (dd, 1H, $^3J_{4,5}$ 9.2, H-4), 3.84-3.93 (m, 2H, H-5', OC*H*$_2$CH$_2$N), 3.70-3.75 (m, 1H, OC*H*$_2$CH$_2$N), 3.63 (ddd, 1H, H-5), 3.49 (m$_c$, 2H, OCH$_2$C*H*$_2$N), 2.08, 2.04 (each s, 3H, OAc), 1.98 (s, 6H, OAc), 1.96, 1.94, 1.93 (each s, 3H, OAc). C$_{28}$H$_{41}$O$_{18}$N (679.2324)

(2-Amino-ethyl) 6-*O*-(2', 3', 4', 6'-tetra-*O*-acetyl-α-D-galactopyranosyl)-2,3,4-tri-*O*-acetyl-β-glucopyranoside (12)

13.6 g (20 mmol) 6-*O*-(2', 3', 4', 6'-tetra-*O*-acetyl-α-D-galactopyranosyl)-1,2,3,4-tetra-*O*-acetyl-β-D-glucopyranoside and 1.85 mL (3.2 g; 26 mmol) anhydrous 2-Bromethanol were reacted as described for compound **4**. Yield: 8.6 g (65 %) of compound **6**. 7.4 g (10 mmol) **6** were reacted as described for compound **7**. The product **9** was obtained in quantitative yield and used without further purification. 7.1 g (10 mmol) **9** in 100 mL anhydrous methanol were reacted as described for compound **10**.

Yield: 6.5 g (96 %).

^{1}H-NMR (400 MHz, CDCl$_3$ + TMS): δ = 5.45 (dd, 1H, $^3J_{3',4'}$ 3.1, $^3J_{4',5'}$ 1.0, H-4'), 5.35 (dd, 1H, $^3J_{2',3'}$ 10.7, H-3'), 5.21 (dd, 1H, $^3J_{2,3}$ 9.7, $^3J_{3,4}$ 9.7, H-3), 5.16 (d, 1H, $^3J_{1',2'}$ 3.6, H-1'), 5.11 (dd, 1H, H-2'), 5.07 (dd, 1H, $^3J_{4,5}$ 9.7, H-4), 4.93 (d, 1H, $^3J_{1,2}$ 8.1, H-2), 4.48 (d, 1H, H-1), 4.25 (ddd, 1H, $^3J_{5',6a'}$ 5.6, $^3J_{5',6b'}$ 6.6, H-5'), 4.11 (dd, 1H, $^2J_{6a',6b'}$ 11.2, H-6a'), 4.06 (dd, 1H, H-6b'), 3.90-3.98 (m, 1H, OC*H*$_2$CH$_2$N), 3.66-3.78 (m, 2H, H-6a, OC*H*$_2$CH$_2$N), 3.65 (ddd, 1H, $^3J_{5,6a}$ 5.1, $^3J_{5,6b}$ 2.5, H-5), 3.58 (dd, 1H, $^2J_{6a,6b}$ 11.2, H-6b), 3.47-3.51 (m, 2H, OCH$_2$C*H*$_2$N), 2.13, 2.12, 2.05, 2.04, 2.03, 2.00, 1.98 (each s, 3H, OAc). C$_{28}$H$_{41}$O$_{18}$N (679.2324)

(*N*-Tetradecanoyl 2-Amino-ethyl) 4-*O*-(2', 3', 4', 6'-tetra-*O*-acetyl-β-D-galactopyranosyl)-2,3,6-tri-*O*-acetyl-β-glucopyranoside (13)

3.4 g (5 mmol) **10** and 0.4 mL (396 mg, 5 mmol) anhydrous pyridine were dissolved in 80 mL anhydrous *N,N*-dimethylformamide. 1.4 mL (1.2 g; 5 mmol) freshly distilled tetradecanoyl chloride in 10 mL anhydrous *N,N*-dimethylformamide were added dropwise at 0 °C. Stirring was continued for 1 h at 0 °C and for 14 h at room temperature. The solution was poured on 60 mL ice water and extracted three times with 80 mL dichlormethane. The combined organic phases were washed two times with 80 mL saturated sodium hydrogen carbonate solution, with 50 mL water, dried over magnesium sulfate and solvent was removed *in vacuo*. The residue was purified by column chromatography (light petroleum b.p. 50-70 °C - ethyl acetate 1:1).

Yield: 3.2 g (72 %).

$[\alpha]_D^{20}$ = -15 (c = 1.0, CHCl$_3$).

^{1}H-NMR (400 MHz, CDCl$_3$ + TMS): δ = 6.04 (s, 1H, NH), 5.28 (dd, 1H, $^3J_{3',4'}$ 3.5, $^3J_{4',5'}$ 1.0, H-4'), 5.13 (dd, 1H, $^3J_{2,3}$ 9.7, $^3J_{3,4}$ 9.7, H-3), 5.04 (dd, 1H, $^3J_{1',2'}$ 8.1, $^3J_{2',3'}$ 10.1, H-2'), 4.88 (dd, 1H, H-3'), 4.83 (dd, 1H, $^3J_{1,2}$ 8.1, H-2), 4.50 (d, 1H, H-1), 4.42 (dd, 1H, $^3J_{5,6a}$ 2.0, $^3J_{6a,b}$ 12.2, H-6a), 4.41 (d, 1H, H-1'), 3.98 - 4.09 (m, 3H, H-6b, H-6a', H-6b'), 3.77-3.86 (m, 2H, H-5', OCH_2CH$_2$N), 3.72 (dd, 1H, $^3J_{4,5}$ 9.7, H-4), 3.60-3.64 (m, 1H, OCH_2CH$_2$N), 3.53 (ddd, 1H, $^3J_{5,6b}$ 6.1, H-5), 3.48-3.51 (m, 2H, OCH$_2$CH_2N), 2.20 (m$_c$, 2H, alkyl-α-CH$_2$), 2.08, 2.05, 1.99 (each s, 3H, OAc), 1.98 (s, 6H, 2x OAc), 1.97, 1.90 (each s, 3H, OAc), 1.44-1.50 (m, 2H, alkyl ß-CH$_2$), 1.14-1.28 (m, 20H, alkyl-CH$_2$), 0.81 (t, 3H, alkyl-CH$_3$).

^{13}C-NMR (100 MHz, CDCl$_3$ + TMS): δ = 172.10 (C=O, amide), 170.88, 170.67, 170.18, 170.01, 169.77 (C=O, OAC), 100.09 (C-1'), 99.67 (C-1), 71.84 (C-3), 71.63 (C-5), 70.70 (C-2), 70.62 (OCH$_2$CH$_2$N), 70.02 (C-3'), 69.70 (C-5'), 68.13 (C-2'), 65.63 (C-4'), 61.03 (C-6), 59.78 (C-6'), 47.56 (OCH$_2$CH_2N), 42.10 (alkyl-α-CH$_2$), 36.72 (alkyl-β-CH$_2$), 32.19, 30.14, 30.07, 30.04, 30.01, 29.92, 29.77, 26.50 (alkyl-CH$_2$), 21.28, 21.23, 21.11, 21.04, 20.98 (CH$_3$, OAc), 14.54 (alkyl-CH$_3$).

C$_{42}$H$_{67}$O$_{19}$N (889.4307)

(N-Hexadecanoyl 2-Amino-ethyl) 4-O-(2', 3', 4', 6'-tetra-O-acetyl-β-D-galactopyranosyl)-2,3,6-tri-O-acetyl-β-glucopyranoside (14)[10]

3.4 g (5 mmol) **10** and 1.5 mL (1.4 g; 5 mmol) freshly distilled hexadecanoyl chloride were reacted as described for compound **13**.

Yield: 3.4 g (73 %).

$[\alpha]_D^{20}$ = -16 (c = 1.1, CHCl$_3$). No optical rotation value was reported in the reference.

^{1}H-NMR (400 MHz, CDCl$_3$ + TMS): δ = 6.05 (s, 1H, NH), 5.24 (dd, 1H, $^3J_{3',4'}$ 3.5, $^3J_{4',5'}$ 1.0, H-4'), 5.14 (dd, 1H, $^3J_{2,3}$ 9.7, $^3J_{3,4}$ 9.7, H-3), 5.05 (dd, 1H, $^3J_{1',2'}$ 8.1, $^3J_{2',3'}$ 10.1, H-2'), 4.89 (dd, 1H, H-3'), 4.82 (dd, 1H, $^3J_{1,2}$ 8.1, H-2), 4.51 (d, 1H, H-1), 4.43 (dd, 1H, $^3J_{5,6a}$ 2.0, $^3J_{6a,b}$ 12.2, H-6a), 4.42 (d, 1H, H-1'), 3.97 - 4.09 (m, 3H, H-6b, H-6a', H-6b'), 3.76-3.87 (m, 2H, H-5', OCH_2CH$_2$N), 3.72 (dd, 1H, $^3J_{4,5}$ 9.7, H-4), 3.61-3.66 (m, 1H, OCH_2CH$_2$N), 3.54 (ddd, 1H, $^3J_{5,6b}$ 6.1, H-5), 3.48-3.52 (m, 2H, OCH$_2$CH_2N), 2.23 (m$_c$, 2H, alkyl-α-CH$_2$), 2.09, 2.04, 2.00 (each s, 3H, OAc), 1.98 (s, 6H, 2x OAc), 1.97, 1.92 (each s, 3H, OAc), 1.44-1.53 (m, 2H, alkyl ß-CH$_2$), 1.14-1.29 (m, 24H, alkyl-CH$_2$), 0.82 (t, 3H, alkyl-CH$_3$).

^{13}C-NMR (100 MHz, CDCl$_3$ + TMS): δ = 172.12 (C=O, amide), 170.89, 170.68, 170.19, 170.09, 169.87 (C=O, OAC), 100.07 (C-1'), 99.68 (C-1), 71.85 (C-3), 71.64 (C-5), 70.72 (C-2), 70.63 (OCH$_2$CH$_2$N), 70.08 (C-3'), 69.68 (C-5'), 68.12 (C-2'), 65.62 (C-4'), 61.05 (C-6), 59.80 (C-6'), 47.59 (OCH$_2$CH_2N), 42.08 (alkyl-α-CH$_2$), 36.70 (alkyl-β-CH$_2$), 32.18, 30.12, 30.05, 30.01, 29.92, 29.75, 29.67, 26.48 (alkyl-CH$_2$), 21.26, 21.21, 21.11, 21.05, 20.99 (CH$_3$, OAc), 14.52 (alkyl-CH$_3$).

C$_{44}$H$_{71}$O$_{19}$N (917.4620)

(N-cis-9-Octadecenoyl 2-Amino-ethyl) 4-O-(2', 3', 4', 6'-tetra-O-acetyl-β-D-galactopyranosyl)-2,3,6-tri-O-acetyl-β-glucopyranoside (15)

3.4 g (5 mmol) **10** and 1.6 mL (1.5 g; 5 mmol) freshly distilled oleoyl chloride were reacted using as described for compound **13**.

Yield: 3.1 g (65 %).

$[\alpha]_D^{20}$ = -18 (c = 1.0, CHCl$_3$).

^{1}H-NMR (400 MHz, CDCl$_3$ + TMS): δ = 6.04 (s, 1H, NH), 5.32-5.39 (m, 2H, H-olefinic.), 5.24 (dd, 1H, $^3J_{3',4'}$ 3.5, $^3J_{4',5'}$ 1.0, H-4'), 5.14 (dd, 1H, $^3J_{2,3}$ 9.7, $^3J_{3,4}$ 9.7, H-3), 5.05 (dd, 1H, $^3J_{1',2'}$ 8.1, $^3J_{2',3'}$ 10.1, H-2'), 4.89 (dd, 1H, H-3'), 4.82 (dd, 1H, $^3J_{1,2}$ 8.1, H-2), 4.51 (d, 1H, H-1), 4.43 (dd, 1H, $^3J_{5,6a}$ 2.0, $^3J_{6a,b}$ 12.2, H-6a), 4.42 (d, 1H, H-1'), 3.97-4.09 (m, 3H, H-6b, H-6a', H-6b'), 3.76-3.87 (m, 2H, H-5', OCH_2CH$_2$N), 3.72 (dd, 1H, $^3J_{4,5}$ 9.7, H-

4), 3.61-3.66 (m, 1H, OCH_2CH$_2$N), 3.54 (ddd, 1H, $^3J_{5,6b}$ 6.1, H-5), 3.48-3.52 (m, 2H, OCH$_2$CH_2N), 2.23 (m$_c$, 2H, alkyl-α-CH$_2$), 2.09, 2.04, 2.00 (each s, 3H, OAc), 1.98 (s, 6H, 2x OAc), 1.97, 1.92 (each s, 3H, OAc), 1.90-1.97 (m, 4H, allyl-CH2),1.44-1.53 (m, 2H, alkyl ß-CH$_2$), 1.14-1.29 (m, 20H, alkyl-CH$_2$), 0.82 (t, 3H, alkyl-CH$_3$).

^{13}C-NMR (100 MHz, CDCl$_3$ + TMS): δ = 172.12 (C=O, amide), 170.89, 170.68, 170.19, 170.09, 169.87 (C=O, OAC), 131.54, 131.48 (C-olefin.), 100.07 (C-1'), 99.68 (C-1), 71.85 (C-3), 71.64 (C-5), 70.72 (C-2), 70.63 (OCH_2CH$_2$N), 70.08 (C-3'), 69.68 (C-5'), 68.12 (C-2'), 65.62 (C-4'), 61.05 (C-6), 59.80 (C-6'), 47.59 (OCH$_2$CH_2N), 41.39 (alkyl-α-CH$_2$), 32.18, 30.12, 30.05, 30.01, 29.92, 29.75, 29.67, 26.48 (alkyl-CH$_2$), 21.26, 21.21, 21.11, 21.05, 20.99 (CH$_3$, OAc), 14.52 (alkyl-CH$_3$).

C$_{46}$H$_{73}$O$_{19}$N (943.4777)

(*N*-Tetradecanoyl 2-Amino-ethyl) 4-*O*-(2', 3', 4', 6'-tetra-*O*-acetyl-α-D-glucopyranosyl)-2,3,6-tri-*O*-acetyl-β-glucopyranoside (16)

3.4 g (5 mmol) **11** and 1.4 mL (1.2 g; 5 mmol) freshly distilled tetradecanoyl chloride were reacted as described for compound **13**.

Yield: 3.5 g (79 %).

$[\alpha]_D^{20}$ = +30 (c = 1.4, CHCl$_3$).

^{1}H-NMR (500 MHz, CDCl$_3$ + TMS): δ = 6.51 (s, 1H, NH), 5.41 (d, 1H, $^3J_{1',2'}$ 4.1, H-1'), 5.35 (dd, 1H, $^3J_{2',3'}$ 10.2, $^3J_{3',4'}$ 10.2, H-3'), 5.24 (dd, 1H, $^3J_{2,3}$ 9.2, $^3J_{3,4}$ 9.2, H-3), 5.04 (dd, 1H, $^3J_{4',5'}$ 10.2, H-4'), 4.85 (dd, 1H, H-2'), 4.80 (dd, 1H, $^3J_{1,2}$ 7.6, H-2), 4.50 (d, 1H, H-1), 4.46 (dd, 1H, $^3J_{5,6a}$ 2.5, $^2J_{6a,b}$ 12.2, H-6a), 4.25 (dd, 1H, $^3J_{5',6a'}$ 4.1, $^3J_{6a',b'}$ 12.2, H-6a'), 4.22 (dd, 1H, $^3J_{5,6b}$ 4.6, H-6b), 4.03 (dd, 1H, $^3J_{5',6b'}$ 2.0, H-6b'), 3.99 (dd, 1H, $^3J_{4,5}$ 9.2, H-4), 3.95 (ddd, 1H, H-5'), 3.82-3.88 (m, 1H, OCH_2CH$_2$N), 3.66 (ddd, 1H, H-5), 3.45 (m$_c$, 1H, OCH_2CH$_2$N), 3.38-3.42 (m, 2H, OCH$_2$CH_2N), 2.17-2.21 (m, 2H, alkyl-α-CH$_2$), 2.13, 2.09, 2.04, 2.02, 2.00 (each s, 3H, OAc), 1.99 (s, 6H, OAc), 1.49-1.59 (m, 2H, alkyl-ß-CH$_2$), 1.19-1.31 (m, 20H, alkyl-CH$_2$), 0.86 (t, 2H, alkyl-CH$_3$).

^{13}C-NMR (125 MHz, CDCl$_3$ + TMS): δ = 172.9 (C=O, amide), 170.54, 170.50, 170.27, 170.01, 169.62, 169.43 (C=O, OAc), 100.31 (C-1), 95.38 (C-1'), 75.51 (C-3), 72.84 (C-4), 72.26, 72.11 (C-2, C-5), 70.18 (OCH_2CH$_2$N), 69.99 (C-2'), 69.40 (C-3'), 68.58 (C-5'), 68.07 (C-4'), 62.95 (C-6), 61.56 (C-6'), 46.25 (OCH$_2$CH_2N), 42.08 (alkyl-α-CH$_2$), 36.80 (alkyl-β-CH$_2$), 32.16, 29.45, 29.30, 25.95, 24.83, 24.69, 24.17, 23.18, 22.70 (alkyl-CH$_2$), 20.94, 20.85, 20.69, 20.62, 20.59 (-CH$_3$, OAc), 14.16 (alkyl-CH$_3$).

C$_{42}$H$_{67}$O$_{19}$N (889.4307)

(*N*-Hexadecanoyl 2-Amino-ethyl) 4-*O*-(2', 3', 4', 6'-tetra-*O*-acetyl-α-D-glucopyranosyl)-2,3,6-tri-*O*-acetyl-β-glucopyranoside (17)

3.4 g (5 mmol) **11** and 1.5 mL (1.4 g; 5 mmol) freshly distilled tetradecanoyl chloride were reacted as described for compound **13**.

Yield: 3.7 g (80 %).

$[\alpha]_D^{20}$ = +30 (c = 1.2, CHCl$_3$).

^{1}H-NMR (500 MHz, CDCl$_3$ + TMS): δ = 6.02 (s, 1H, NH), 5.37 (d, 1H, $^3J_{1',2'}$ 3.8, H-1'), 5.34 (dd, 1H, $^3J_{2',3'}$ 9.8, $^3J_{3',4'}$ 9.8, H-3'), 5.20 (dd, 1H, $^3J_{2,3}$ 9.5, $^3J_{3,4}$ 9.1, H-3), 5.08 (dd, 1H, $^3J_{4',5'}$ 9.8, H-4'), 4.84 (dd, 1H, H-2'), 4.77 (dd, 1H, $^3J_{1,2}$ 8.1, H-2), 4.48 (d, 1H, H-1), 4.46 (dd, 1H, $^3J_{5,6a}$ 2.8, $^2J_{6a,b}$ 12.0, H-6a), 4.23 (dd, 1H, $^3J_{5',6a'}$ 4.1, $^2J_{6a',b'}$ 12.3, H-6a'), 4.20 (dd, 1H, $^3J_{5,6b}$ 4.4, H-6b), 4.05 (dd, 1H, $^3J_{5',6b'}$ 2.2, H-6b'), 3.96 (dd, 1H, $^3J_{4,5}$ 9.1, H-4), 3.92 (m$_c$, 1H, H-5'), 3.80-3.85 (m, 1H, OCH_2CH$_2$N), 3.64 (ddd, 1H, H-5), 3.55-3.63 (m, 1H, OCH_2CH$_2$N), 3.44-3.49 (m, 2H, OCH$_2$CH_2N), 2.20 (t, 2H, alkyl-α-CH$_2$), 2.11, 2.08, 2.01, 1.98, 1.97 (je s, 3H, OAc), 1.95 (s, 6H, OAc), 1.54-1.60 (m, 2H, alkyl-ß-CH$_2$), 1.17-1.44 (m, 24H, alkyl-CH$_2$), 0.86 (t, 3H, alkyl-CH$_3$).

^{13}C-NMR (125 MHz, CDCl$_3$ + TMS): δ = 171.02 (C=O, amide), 170.09, 170.08, 170.07, 169.78, 169.45, 169.30 (C=O, OAc), 100.12 (C-1), 95.30 (C-1'), 75.45 (C-3), 71.84 (C-4), 71.24, 71.20 (C-2, C-5), 70.09 (OCH_2CH$_2$N), 69.98 (C-2'), 69.30 (C-3'), 68.42 (C-5'), 68.01 (C-4'), 62.89 (C-6), 61.47 (C-6'), 46.18 (OCH$_2$$CH_2$N), 42.43 (alkyl-α-CH$_2$), 36.70 (alkyl-β-CH$_2$), 32.15, 29.98, 29.45, 29.35, 29.30, 25.74, 23.01, 22.92, 21.75, 21.06 (alkyl-CH$_2$), 20.90, 29.85, 20.62, 20.59, 20.55, 20.51 (CH$_3$, OAc), 14.16 (alkyl-CH$_3$).

C$_{44}$H$_{71}$O$_{19}$N (917.4620)

(*N*-*cis*-9-Octadecenoyl 2-Amino-ethyl) 4-*O*-(2', 3', 4', 6'-tetra-*O*-acetyl-α-D-glucopyranosyl)-2,3,6-tri-*O*-acetyl-β-glucopyranoside (18)

3.4 g (5 mmol) **11** and 1.6 mL (1.5 g; 5 mmol) freshly distilled oleoyl chloride were reacted as described for compound **13**.

Yield: 3.3 g (70 %).

$[\alpha]_D^{20}$ = +30 (c = 0.9, CHCl$_3$).

^{1}H-NMR (500 MHz, CDCl$_3$ + TMS): δ = 6.02 (s, 1H, NH), 5.34 - 5.41 (m, 2H, H-olefin.), 5.37 (d, 1H, $^3J_{1',2'}$ 3.8, H-1'), 5.33 (dd, 1H, $^3J_{2',3'}$ 9.8, $^3J_{3',4'}$ 9.8, H-3'), 5.21 (dd, 1H, $^3J_{2,3}$ 9.5, $^3J_{3,4}$ 9.1, H-3), 5.01 (dd, 1H, $^3J_{4',5'}$ 9.8, H-4'), 4.82 (dd, 1H, H-2'), 4.77 (dd, 1H, $^3J_{1,2}$ 8.1, H-2), 4.47 (d, 1H, H-1), 4.44 (dd, 1H, $^3J_{5,6a}$ 2.8, $^2J_{6a,b}$ 12.0, H-6a), 4.22 (dd, 1H, $^3J_{5',6a'}$ 4.1, $^2J_{6a',b'}$ 12.3, H-6a'), 4.20 (dd, 1H, $^3J_{5,6b}$ 4.4, H-6b), 4.01 (dd, 1H, $^3J_{5',6b'}$ 2.2, H-6b'), 3.97 (dd, 1H, $^3J_{4,5}$ 9.1, H-4), 3.93 (m$_c$, 1H, H-5'), 3.82 (m$_c$, 1H, OCH_2CH$_2$N), 3.64 (ddd, 1H, H-5), 3.58-3.65 (m, 1H, OCH_2CH$_2$N), 3.45 - 3.51 (m, 2H, OCH$_2$CH_2N), 2.23 (m, 2H, alkyl-α-CH$_2$), 2.11, 2.07, 2.01, 1.99, 1.98 (je s, 3H, OAc), 1.97 (s, 6H, OAc), 1.89-1.95 (m, 4H, allyl-CH$_2$), 1.49-1.55 (m, 2H, alkyl-ß-CH$_2$), 1.18-1.32 (m, 20H, alkyl-CH$_2$), 0.85 (t, 3H, alkyl-CH$_3$).

^{13}C-NMR (125 MHz, CDCl$_3$ + TMS): δ = 173.09 (C=O, Amid), 170.14, 170.10, 170.08, 169.87, 169.51, 169.34 (C=O, OAc), 131.50, 131.45 (C-olefin) 100.22 (C-1), 95.44 (C-1'), 75.41 (C-3), 71.74 (C-4), 71.17, 71.99 (C-2, C-5), 70.15 (OCH_2CH$_2$N), 69.93 (C-2'), 69.30 (C-3'), 68.41 (C-5'), 67.98 (C-4'), 62.85 (C-6), 61.45 (C-6'), 46.25 (OCH$_2$$CH_2$N), 41.37 (alkyl-α-CH$_2$), 31.84, 29.61, 29.57, 29.53, 29.31, 29.27, 29.24 (alkyl-CH$_2$), 20.84, 29.75, 20.59, 20.54, 20.52, 20.49 (CH$_3$, OAc), 14.03 (alkyl-CH$_3$).

C$_{46}$H$_{73}$O$_{19}$N (943.4777)

(*N*-Tetradecanoyl 2-Amino-ethyl) 6-*O*-(2', 3', 4', 6'-tetra-*O*-acetyl-α-D-galactopyranosyl)-2,3,4-tri-*O*-acetyl-β-glucopyranoside (19)

3.4 g (5 mmol) **12** and 1.4 mL (1.2 g; 5 mmol) freshly distilled tetradecanoyl chloride were reacted as described for compound **13**.

Yield: 3.6 g (80 %).

$[\alpha]_D^{20}$ = +48 (c = 1.1, CHCl$_3$).

^{1}H-NMR (400 MHz, CDCl$_3$ + TMS): δ = 6.07 (s, 1H, NH), 5.37 (dd, 1H, H-4'), 5.26 (dd, 1H, $^3J_{2',3'}$ 11.0, $^3J_{3',4'}$ 3.5, H-3'), 5.14 (dd, 1H, $^3J_{2,3}$ 9.7, $^3J_{3,4}$ 9.7, H-3), 5.08 (d, 1H, $^3J_{1',2'}$ 3.6, H-1'), 5.02 (dd, 1H, H-2'), 5.00 (dd, 1H, $^3J_{4,5}$ 9.7, H-4), 4.86 (dd, 1H, $^3J_{1,2}$ 8.1, H-2), 4.52 (d, 1H, H-1), 4.17 (ddd, 1H, $^3J_{4',5'}$ 1.3, $^3J_{5',6a'}$ 5.6, $^3J_{5',6b'}$ 6.6, H-5'), 4.05 (dd, 1H, $^3J_{6a',b'}$ 11.2, H-6a'), 4.02 (dd, 1H, H-6b'), 3.84 (m$_c$, 1H, OCH_2CH$_2$N), 3.68 (dd, 1H, $^3J_{5,6a}$ 5.0, $^3J_{6a,b}$ 11.1, H-6a), 3.55-3.66 (m, 4H, H-5, OCH_2CH$_2$N), 3.51 (dd, 1H, $^3J_{5,6b}$ 2.0, H-6b), 2.18 (m$_c$, alkyl-α-CH$_2$), 2.07, 2.06, 1.98, 1.97, 1.95, 1.94, 1.92 (je s, 3H, OAc), 1.42-1.50 (m, 2H, alkyl-ß-CH$_2$), 1.16-1.28 (m, 24H, alkyl-CH$_2$), 0.85 (t, 3H, alkyl-CH$_3$).

^{13}C-NMR (100 MHz, CDCl$_3$ + TMS): δ = 172.89 (C=O, amide), 170.56, 170.35, 170.21, 169.87, 169.36, 169.31 (C=O, OAc), 100.56 (C-1), 96.47 (C-1´), 72.93 (C-3), 72.66 (C-5), 71.58 (C-2), 70.02 (OCH_2CH$_2$N), 69.08 (C-

4), 68.09, 68.02 (C-4´, C-2´), 67.47 (C-3´), 66.48 (C-5´), 66.45 (C-6), 61.67 (C-6´), 47.05 (OCH$_2$CH$_2$N), 42.03 (alkyl-α-CH$_2$), 36.81 (alkyl-β-CH$_2$), 31.94, 29.72, 29.66, 29.44, 29.40, 29.37, 25.90, 22.70 (alkyl-CH$_2$), 20.80, 20.71, 20.67, 20.65 (CH$_3$, OAc), 14.13 (alkyl-CH$_3$).
C$_{44}$H$_{67}$O$_{19}$N (889.4307)

(N-Hexadecanoyl 2-Amino-ethyl) 6-O-(2', 3', 4', 6'-tetra-O-acetyl-α-D-galactopyranosyl)-2,3,4-tri-O-acetyl-β-glucopyranoside (20)

3.4 g (5 mmol) **12** and 1.5 mL (1.4 g; 5 mmol) freshly distilled hexadecanoyl chloride were reacted as described for compound **13**.

Yield: 3.6 g. (79 %)

$[\alpha]_D^{20}$ = +47 (c = 0.7, CHCl$_3$).

^{1}H-NMR (400 MHz, CDCl$_3$ + TMS): δ = 6.05 (s, 1H, NH), 5.38 (dd, 1H, $^3J_{3',4'}$ 3.5, $^3J_{4',5'}$ 1.3, H-4'), 5.27 (dd, 1H, H-3'), 5.14 (dd, 1H, $^3J_{2,3}$ 9.7, $^3J_{3,4}$ 9.7, H-3), 5.09 (d, 1H, $^3J_{1',2'}$ 3.8, H-1'), 5.03 (dd, 1H, $^3J_{2',3'}$ 11.0, H-2'), 5.00 (dd, 1H, $^3J_{4,5}$ 9.8, H-4), 4.87 (dd, 1H, $^3J_{1,2}$ 8.2, H-2), 4.53 (d, 1H, H-1), 4.17 (ddd, 1H, $^3J_{5',6a'}$ 5.6, $^3J_{5',6b'}$ 6.6, H-5'), 4.06 (dd, 1H, $^3J_{6a',b'}$ 11.2, H-6a'), 4.01 (dd, 1H, H-6b'), 3.82 (m$_c$, 1H, OCH$_2$CH$_2$N), 3.68 (dd, 1H, $^3J_{5,6a}$ 5.0, $^3J_{6a,b}$ 11.4, H-6a), 3.56-3.67 (m, 4H, H-5, OCH$_2$CH$_2$N), 3.52 (dd, 1H, $^3J_{5,6b}$ 2.0, H-6b), 2.20 (m$_c$, alkyl-α-CH$_2$), 2.07, 2.06, 1.98, 1.97, 1.96, 1.93, 1.92 (je s, 3H, OAc), 1.44-1.50 (m, 2H, alkyl-ß-CH$_2$), 1.15-1.26 (m, 24H, alkyl-CH$_2$), 0.81 (t, 3H, alkyl-CH$_3$).

^{13}C-NMR (100 MHz, CDCl$_3$ + TMS): δ = 172.88 (C=O, amide), 170.52, 170.31, 170.17, 169.83, 169.32, 169.27 (C=O, OAc), 100.52 (C-1), 96.43 (C-1'), 72.93 (C-3), 72.62 (C-5), 71.99 (OCH$_2$CH$_2$N) 71.34 (C-2), 69.04 (C-4), 68.05, 68.04 (C-4', C-2'), 67.43 (C-3'), 66.44 (C-5'), 66.41 (C-6), 61.63 (C-6'), 47.11 (OCH$_2$CH$_2$N), 42.02 (alkyl-α-CH$_2$), 36.71 (alkyl-β-CH$_2$), 32.35, 31.90, 29.68, 29.62, 29.40, 29.23, 25.86, 22.66 (alkyl-CH$_2$), 20.76, 20.67, 20.63, 20.61 (CH$_3$, OAc), 14.09 (alkyl-CH$_3$).
C$_{44}$H$_{71}$O$_{19}$N (917.4620)

(N-cis-9-Octadecenoyl 2-Amino-ethyl) 6-O-(2', 3', 4', 6'-tetra-O-acetyl-α-D-galactopyranosyl)-2,3,4-tri-O-acetyl-β-glucopyranoside (21)

3.4 g (5 mmol) **12** and 1.6 mL (1.5 g; 5 mmol) freshly distilled oleoyl chloride were reacted as described for compound **13**.

Yield: 3.4 g (73 %).

$[\alpha]_D^{20}$ = +50 (c = 1.0, CHCl$_3$).

^{1}H-NMR (400 MHz, CDCl$_3$ + TMS): δ = 6.04 (s, 1H, NH), 5.32-5.40 (m, 2H, H-olefin.), 5.40 (dd, 1H, $^3J_{3',4'}$ 3.5, $^3J_{4',5'}$ 1.3, H-4'), 5.25 (dd, 1H, $^3J_{2',3'}$ 11.0, H-3'), 5.15 (dd, 1H, $^3J_{2,3}$ 9.7, $^3J_{3,4}$ 9.7, H-3), 5.09 (d, 1H, $^3J_{1',2'}$ 3.6, H-1'), 5.03 (dd, 1H, H-2'), 5.01 (dd, 1H, $^3J_{4,5}$ 9.7, H-4), 4.87 (dd, 1H, $^3J_{1,2}$ 8.1, H-2), 4.51 (d, 1H, H-1), 4.18 (ddd, 1H, $^3J_{5',6a'}$ 5.6, $^3J_{5',6b'}$ 6.6, H-5'), 4.06 (dd, 1H, $^3J_{6a',b'}$ 11.2, H-6a'), 4.03 (dd, 1H, H-6b'), 3.85 (m$_c$, 1H, OCH$_2$CH$_2$N), 3.69 (dd, 1H, $^3J_{5,6a}$ 5.0, $^3J_{6a,b}$ 11.1, H-6a), 3.52-3.64 (m, 4H, H-5, OCH$_2$CH$_2$N), 3.52 (dd, 1H, $^3J_{5,6b}$ 2.0, H-6b), 2.17 (m$_c$, alkyl-α-CH$_2$), 2.06, 2.05, 2.00, 1.99, 1.96, 1.95, 1.92 (je s, 3H, OAc), 1.85-1.92 (m, 4H, allyl-CH$_2$), 1.43-1.50 (m, 2H, alkyl-ß-CH$_2$), 1.17-1.29 (m, 24H, alkyl-CH$_2$), 0.85 (t, 3H, alkyl-CH$_3$).

^{13}C-NMR (100 MHz, CDCl$_3$ + TMS): δ = 172.88 (C=O, amide), 170.52, 170.31, 170.17, 169.83, 169.32, 169.27 (C=O, OAc), 131.45, 131.42 (C-olefin.), 100.51 (C-1), 96.48 (C-1'), 72.91 (C-3), 72.64 (C-5), 71.97 (OCH$_2$CH$_2$N) 71.32 (C-2), 69.08 (C-4), 68.04, 68.01 (C-4', C-2'), 67.42 (C-3'), 66.46 (C-5'), 66.42 (C-6), 61.63 (C-6'), 47.09 (OCH$_2$CH$_2$N), 41.58 (alkyl-α-CH$_2$), 32.35, 31.90, 29.66, 29.64, 29.41, 29.24, 25.85, 22.66 (alkyl-CH$_2$), 20.76, 20.64, 20.63, 20.60 (CH$_3$, OAc), 14.12 (alkyl-CH$_3$).
C$_{46}$H$_{73}$O$_{19}$N (943.4777)

(N-Tetradecanoyl 2-Amino-ethyl) 4-O-(β-D-galactopyranosyl)-β-glucopyranoside (22)

3.0 g (3.4 mmol) **13** were dissolved in 50 mL anhydrous methanol and sodium methoxide was added (pH 8-9). The solution was stirred at ambient temperature until t.l.c. revealed the reaction to be complete. It was neutralised then using DOWEX 50WX ion-exchange resin (protonated form), filtrated and evaporated *in vacuo*. The product was recrystallised from methanol.

Yield: 1.6 g (80 %).

$[\alpha]_D^{20}$ = -6 (c = 0.5, DMSO).

^{1}H-NMR (400 MHz, pyridine-d$_5$): δ = 5.46 (d, 1H, $^3J_{1,2}$ 8.1, H-1'), 5.24 (d, 1H, $^3J_{1,2}$ 8.1, H-1), 4.82-5.00 (m, 5H, H-6a, H-2', H-3', H-4', H-5'), 4.59-4.70 (m, 2H, H-6a', H-6b'), 4.51-4.58 (m, 2H, H-5, H-6b), 4.40 (dd, 1H, $^3J_{3,4}$ 9.5, $^3J_{4,5}$ 9.5, H-4), 4.21-4.34 (m, 3H, H-2, H-3, OC*H*$_2$CH$_2$N), 3.81 (m$_c$, 2H, OCH$_2$C*H*$_2$N), 3.55 (m$_c$, 2H, alkyl-α-CH$_2$), 1.91-1.99 (m, 2H, alkyl-ß-CH$_2$), 1.51-1.60 (m, 20H, alkyl-CH$_2$), 1.20 (t, 3H, alkyl-CH$_3$).

C$_{28}$H$_{53}$O$_{12}$N (595.3568)

Anal. Calcd C, 56.45; H, 8.97; N, 2.35. Found C, 56.25; H, 8.93; N, 2.34

(N-Hexadecanoyl 2-Amino-ethyl) 4-O-(β-D-galactopyranosyl)-β-glucopyranoside (23)[10]

3.2 g (3.5 mmol) **14** were reacted as described for compound **22**. The product was recrystallised from methanol.

Yield: 1.8 g (82 %).

$[\alpha]_D^{20}$ = -6 (c = 0.4, DMSO). No optical rotation value was reported in the reference.

^{1}H-NMR (400 MHz, pyridine-d$_5$): δ = 5.45 (d, 1H, $^3J_{1,2}$ 8.1, H-1'), 5.22 (d, 1H, $^3J_{1,2}$ 8.1, H-1), 4.82-5.02 (m, 5H, H-6a, H-2', H-3', H-4', H-5'), 4.53-4.70 (m, 2H, H-6a', H-6b'), 4.51-4.60 (m, 2H, H-5, H-6b), 4.42 (dd, 1H, $^3J_{3,4}$ 9.5, $^3J_{4,5}$ 9.5, H-4), 4.21-4.38 (m, 3H, H-2, H-3, OC*H*$_2$CH$_2$N), 3.84 (m$_c$, 2H, OCH$_2$C*H*$_2$N), 3.57 (m$_c$, 2H, alkyl-α-CH$_2$), 1.92-2.00 (m, 2H, alkyl-ß-CH$_2$), 1.50-1.62 (m, 24H, alkyl-CH$_2$), 1.21 (t, 3H, alkyl-CH$_3$).

C$_{30}$H$_{57}$O$_{12}$N (623.3881)

Anal. Calcd C, 57.77; H, 9.21; N, 2.25. Found: C, 57.85; H, 9.24; N, 2.25

(N-cis-9-Octadecenoyl 2-Amino-ethyl) 4-O-(β-D-galactopyranosyl)-β-glucopyranoside (24)

2.9 g (3.1 mmol) **15** were reacted as described for compound **22**. The product was purified by column chromatography (chloroform - methanol 9:1).

Yield: 1.9 g (95 %).

$[\alpha]_D^{20}$ = -7 (c = 0.4, MeOH).

^{1}H-NMR (400 MHz, pyridine-d$_5$): δ = 5.30-5.44 (m, 3H, H-1', H-olefin.), 5.20 (d, 1H, $^3J_{1,2}$ 8.1, H-1), 4.82-5.01 (m, 5H, H-6a, H-2', H-3', H-4', H-5'), 4.53-4.69 (m, 2H, H-6a', H-6b'), 4.51-4.61 (m, 2H, H-5, H-6b), 4.41 (dd, 1H, $^3J_{3,4}$ 9.5, $^3J_{4,5}$ 9.5, H-4), 4.21-4.39 (m, 3H, H-2, H-3, OC*H*$_2$CH$_2$N), 3.83 (m$_c$, 2H, OCH$_2$C*H*$_2$N), 3.56 (m$_c$, 2H, alkyl-α-CH$_2$), 2.20-2.26 (m, 4H, allyl-CH$_2$), 1.92-2.01 (m, 2H, alkyl-ß-CH$_2$), 1.50-1.62 (m, 20H, alkyl-CH$_2$), 1.21 (t, 3H, alkyl-CH$_3$).

C$_{32}$H$_{59}$O$_{12}$N (649.4037)

HIRES-FAB-MS: Calc: m/z = 673.3935 [M+Na]$^+$ Found: m/z = 673.3945

(N-Tetradecanoyl 2-Amino-ethyl) 4-O-(α-D-glucopyranosyl)-β-glucopyranoside (25)

3.3 g (3.7 mmol) **16** were reacted as described for compound **22**. The product was recrystallised from methanol.

Yield: 1.8 g (81 %).

$[\alpha]_D^{20}$ = +28 (c = 0.7, MeOH).

^{1}H-NMR (400 MHz, d$_4$-Methanol): δ = 5.18 (d, 1H, $^3J_{1',2'}$ 3.5, H-1'), 4.34 (d, 1H, $^3J_{1,2}$ 8.1, H-1), 4.02 (dd, 1H, $^3J_{5,6a}$ 2.0, $^2J_{6a,b}$ 11.9, H-6a), 3.90 (dd, 1H, $^3J_{5,6b}$ 4.5, H-6b), 3.79-3.88 (m, 2H, H-4', H-6a'), 3.47-3.76 (m, 9H, H-3, H-4, H-3', H-5', H-6b', OCH_2CH$_2$N), 3.45 (dd, 1H, $^3J_{2',3'}$ 10.2, H-2'), 3.40 (ddd, 1H, $^3J_{4,5}$ 9.7, H-5), 3.15-3.34 (m, 5H, H-2, OCH$_2$CH_2N, alkyl-α-CH$_2$), 1.58 (m$_c$, 2H, alkyl-β-CH$_2$), 1.21-1.41 (m, 20H, alkyl-CH$_2$), 0.88 (t, 3H, alkyl-CH$_3$).

C$_{28}$H$_{53}$O$_{12}$N (595.3568)

Anal. Calcd C, 56.45; H, 8.97; N, 2.35. Found C, 56.65; H, 9.33; N, 2.23

(*N*-Hexadecanoyl 2-Amino-ethyl) 4-*O*-(α-D-glucopyranosyl)-β-glucopyranoside (26)

3.4 g (3.7 mmol) **17** were reacted as described for compound **22**. The product was recrystallised from methanol.

Yield: 1.8 g (79 %).

$[\alpha]_D^{20}$ = +28 (c = 0.6, MeOH).

^{1}H-NMR (400 MHz, d$_4$-Methanol): δ = 5.20 (d, 1H, $^3J_{1',2'}$ 3.6, H-1'), 4.31 (d, 1H, $^3J_{1,2}$ 8.1, H-1), 4.03 (dd, 1H, $^3J_{5,6a}$ 2.0, $^2J_{6a,b}$ 12.0, H-6a), 3.91 (dd, 1H, $^3J_{5,6b}$ 4.6, H-6b), 3.78-3.88 (m, 2H, H-4', H-6a'), 3.48-3.76 (m, 9H, H-3, H-4, H-3', H-5', H-6b', OCH_2CH$_2$N), 3.45 (dd, 1H, $^3J_{2',3'}$ 10.1, H-2'), 3.39 (ddd, 1H, $^3J_{4,5}$ 9.7, H-5), 3.15-3.30 (m, 5H, H-2, OCH$_2$CH_2N, alkyl-α-CH$_2$), 1.61-1.71 (m, 2H, alkyl-β-CH$_2$), 1.27-1.48 (m, 24H, alkyl-CH$_2$), 0.90 (t, 3H, alkyl-CH$_3$).

C$_{30}$H$_{57}$O$_{12}$N (623.3881)

Anal. Calcd C, 57.77; H, 9.21; N, 2.25. Found C, 57.80; H, 9.25; N, 2.23

(*N-cis*-9-Octadecenoyl 2-Amino-ethyl) 4-*O*-(α-D-glucopyranosyl)-β-glucopyranoside (27)

3.0 g (3.2 mmol) **18** were reacted as described for compound **22**. The product was purified by column chromatography (chloroform - methanol 9:1).

Yield: 2.0 g (94 %).

$[\alpha]_D^{20}$ = +27 (c = 0.3, MeOH).

^{1}H-NMR (500 MHz, d$_4$-Methanol): δ = 5.27-5.38 (m, 2H, H-olefin.), 5.14 (d, 1H, $^3J_{1',2'}$ 3.6, H-1'), 4.31 (d, 1H, $^3J_{1,2}$ 8.1, H-1), 3.88 (dd, 1H, $^3J_{5,6a}$ 2.1, $^2J_{6a,b}$ 12.2, H-6a), 3.79-3.87 (m, 3H, H-4', H-6b, H-6a'), 3.65-3.73 (m, 2H, H-5', H-6b'), 3.61 (m, 2H, H-3, H-3'), 3.56-3.59 (m, 2H, H-4, OCH_2CH$_2$N), 3.43-3.50 (m, H, H-2', OCH_2CH$_2$N), 3.38 (ddd, 1H, $^3J_{4,5}$ 9.3, $^3J_{5,6b}$ 5.6, H-5), 3.25-3.32 (m, 3H, H-2, OCH$_2$CH_2N), 3.16-3.21 (m, 2H, alkyl-α-CH$_2$), 1.92-2.05 (m, 4H, allyl-CH$_2$), 1.48-1.57 (m, 2H, alkyl-β-CH$_2$), 1.16-1.41 (m, 20H, alkyl-CH$_2$), 0.88 (t, 3H, alkyl-CH$_3$).

C$_{32}$H$_{59}$O$_{12}$N (649.4037)

HIRES-FAB-MS: Calc: m/z = 673.3935 [M+Na]$^+$ Found: m/z = 673.3938

(*N*-Tetradecanoyl 2-Amino-ethyl) 6-*O*-(α-D-galactopyranosyl)-β-glucopyranoside (28)

3.4 g (3.8 mmol) **19** were reacted as described for compound **22**. The product was recrystallised from methanol.

Yield: 1.8 g (81 %).

$[\alpha]_D^{20}$ = +41 (c = 1.0, MeOH).

^{1}H-NMR (400 MHz, d$_4$-MeOH): d = 4.90 (d, 1H, $^3J_{1',2'}$ 3.6, H-1´), 4.32 (d, 1H, $^3J_{1,2}$ 8.1, H-1), 4.02 (dd, 1H, $^3J_{5,6a}$ 4.1, $^2J_{6a,b}$ 11.2, H-6a), 3.91-3.96 (m, 2H, H-4´, H-5´), 3.70-3.81 (m, 6H, H-2´, H-3´, H-6a´, H-6b´, H-6b, OCH_2CH$_2$N), 3.52-3.67 (m, 3H, OCH$_2$CH_2N), 3.51 (ddd, 1H, $^3J_{4,5}$ 9.2, $^3J_{5,6b}$ 2.0, H-5), 3.44 (dd,1H, $^3J_{3,4}$ 9.2, H-4), 3.39 (dd, 1H, $^3J_{2,3}$ 9.2, H-3), 3.22 (dd, 1H, H-2), 2.20 (m$_c$, 2H, alkyl-α-CH$_2$), 1.61-1.71 (m, 2H, alkyl-β-CH$_2$), 1.28-1.46 (m, 24H, alkyl-CH$_2$), 0.94 (t, 3H, alkyl-CH$_3$).

$C_{28}H_{53}O_{12}N$ (595.3568)

Anal. Calcd C, 56.45; H, 8.97; N, 2.35. Found C, 56.28; H, 8.90; N, 2.24

(*N*-Hexadecanoyl 2-Amino-ethyl) 6-*O*-(α-D-galactopyranosyl)-β-glucopyranoside (29)

3.4 g (3.7 mmol) **20** were reacted as described for compound **22**. The product was recrystallised from methanol.

Yield: 2.0 g (85 %).

$[\alpha]_D^{20} = +43$ (c = 1.1, MeOH).

^{1}H-NMR (400 MHz, d$_4$-MeOH): d = 4.90 (d, 1H, $^3J_{1',2'}$ 3.5, H-1´), 4.31 (d, 1H, $^3J_{1,2}$ 8.1, H-1), 4.03 (dd, 1H, $^3J_{5,6a}$ 4.0, $^2J_{6a,6b}$ 11.2, H-6a), 3.90-3.96 (m, 2H, H-4´, H-5´), 3.71-3.81 (m, 6H, H-2´, H-3´, H-6a´, H-6b´, H-6b, OCH_2CH$_2$N), 3.51-3.65 (m, 3H, OCH_2CH_2N), 3.49 (ddd, 1H, $^3J_{4,5}$ 9.2, $^3J_{5,6b}$ 2.0, H-5), 3.44 (dd,1H, $^3J_{3,4}$ 9.2, H-4), 3.38 (dd, 1H, $^3J_{2,3}$ 9.2, H-3), 3.22 (dd, 1H, H-2), 2.19 (m$_c$, 2H, alkyl-α-CH$_2$), 1.61-1.70 (m, 2H, alkyl-β-CH$_2$), 1.28-1.48 (m, 28H, alkyl-CH$_2$), 0.94 (t, 3H, alkyl-CH$_3$).

$C_{30}H_{57}O_{12}N$ (623.3881)

Anal. Calcd C, 57.77; H, 9.21; N, 2.25. Found C, 57.72; H, 9.19; N, 2.23

(*N*-*cis*-9-Octadecenoyl 2-Amino-ethyl) 6-*O*-(α-D-galactopyranosyl)-β-glucopyranoside (30)

3.1 g (3.3 mmol) **21** were reacted as described for compound **22**. The product was purified by column chromatography (chloroform - methanol 9:1).

Yield: 2.0 g (93 %).

$[\alpha]_D^{20} = +40$ (c = 0.5, MeOH).

^{1}H-NMR (400 MHz, d$_4$-MeOH): d = 5.26-5.35 (m, 2H, H-olefin.), 4.91 (d, 1H, $^3J_{1',2'}$ 3.5, H-1´), 4.32 (d, 1H, $^3J_{1,2}$ 8.1, H-1), 4.03 (dd, 1H, $^3J_{5,6a}$ 4.0, $^2J_{6a,6b}$ 11.2, H-6a), 3.91-3.98 (m, 2H, H-4´, H-5´), 3.70-3.81 (m, 6H, H-2´, H-3´, H-6a´, H-6b´, H-6b, OCH_2CH$_2$N), 3.52-3.67 (m, 3H, OCH_2CH_2N), 3.51 (ddd, 1H, $^3J_{4,5}$ 9.2, $^3J_{5,6b}$ 2.0, H-5), 3.45 (dd,1H, $^3J_{3,4}$ 9.2, H-4), 3.38 (dd, 1H, $^3J_{2,3}$ 9.2, H-3), 3.22 (dd, 1H, H-2), 2.15-2.20 (m, 2H, alkyl-α-CH$_2$), 1.93-2.04 (m, 4H, allyl-CH$_2$), 1.63-1.72 (m, 2H, alkyl-β-CH$_2$), 1.30-1.48 (m, 28H, alkyl-CH$_2$), 0.94 (t, 3H, alkyl-CH$_3$).

$C_{32}H_{59}O_{12}N$ (649.4037)

HIRES-FAB-MS: Calc: m/z = 672.3935 [M+Na]$^+$ Found: m/z = 672.3941

References

[1] Miura, Y.; Arai, T.; Ohtake, A.; Ito, M.; Yamamoto, K.; Yamagata, T. Requirement for a different hydrophobic moiety and reliable chromogenic substrate for endo-type glycosylceramidases. Glycobiology **1999**, *9*, 957-960.

[2] Yoshida, H.; Ikeda, K.; Achiwa, K.; Hoshino, H. Synthesis of sulfated cerebroside analogs having mimics of ceramide and their anti-human immunodefiency virus type 1 activities. Chem. Pharm. Bull. **1995**, *43*, 594-602.

[3] Engel, A.; Chatterjee, S.W.; Al-arifi, A.; Riemann, D.; Langner, J.; Nuhn, P. Influence of spacer length on interaction of mannosylated liposomes with human phagocytic cells. Pharm. Res. **2003**, *20*, 51-57.

[4] Boullanger, P. Amphiphilic carbohydrates as tool for molecular recognition in organized systems. In *Topics in Current Chemistry*; Driguez, H., Thiem, J., Eds.; Springer-Verlag: Berlin, Heidelberg, 1998; Vol. 187, 275-312.

[5] Siegel, D. P. Inverted micellar intermediates and the transition between lamellar, cubic and inverted hexagonal lipid phases; I Mechanism of the L_a - H_{II} phase Transition. Biophys. J. **1986**, *49*, 1155-1170.

[6] Siegel, D. P. Inverted micellar intermediates and the transition between lamellar, cubic and inverted hexagonal lipid phases; II Implications for membrane-membrane interactions and membrane-fusion. Biophys. J. **1986**, *49*, 1171-11783.

[7] Siegel, D. P. Inverted micellar intermediates and the transition between lamellar, cubic and inverted hexagonal lipid phases; III Isotropic and inverted cubic state formation via intermediates in transitions between L_a.and H_{II} phases. Chem. Phys. Lipids **1986**, *42*, 279-301.

[8] Vill, V.; Hashim, R. Carbohydrate liquid crystals: structure–property relationship of thermotropic and lyotropic glycolipids. Curr. Opin. Colloid Interface Sci. **2002**, *7*, 395-409.

[9] v. Minden, H.M.; Brandenburg, K.; Seydel, U.; Koch, M.H.J; Garamus, V.M.; Willumeit, R.; Vill, V. Thermotropic and Lyotropic properties of long chain alkyl glycopyranosides. Part II: Disaccharide headgroups. Chem. Phys. Lipids **2000**, *106*, 157-179.

[10] Miura, Y.; Arai, T.; Yamagata, T. Synthesis of amphiphilic lactosides that possess a lactosylceramide-mimicking *N*-acyl structure: Alternative universal substrates for *endo*-type glycosylceramidases. Carbohydr. Res. **1996**, *289*, 193-199.

[11] Davis, B..H; Lloyd, R.C.; Jones, J.B. Controlled Site-Selective Glycosylation of Proteins by a Combined Site-Directed Mutagenesis and Chemical Modification Approach. J. Org. Chem. **1998**, *63*, 9614-9615.

[12] Masuda, M.; Vill, V.; Shimizu, T. Conformational and thermal phase behaviour of oligomethylene chains constrained by carbohydrate hydrogen-bond networks. J. Am. Chem. Soc. **2000**, *122*, 12327-12333.

[13] Milkereit, G.; Garamus, V.M.; Veermans, K.; Willumeit, R.; Vill, V. Structures of micelles formed by alkyl glycosides with unsaturated alkyl chains. J. Coll. Interf. Sci. **2005**, *284*, 704-713.

[14] v. Minden, H.M.; Milkereit, G.; Vill, V. Effects of carbohydrate headgroups on the stability of induced cubic phases in binary mixtures of glycolipids. Chem. Phys. Lipids **2002**, *120*, 45-56.

Chapter 11

General conclusions

11. General conclusions

In the preceding chapters results regarding the synthesis and different physicochemical and biophysical properties of amphiphiles were presented in detailed form. In this chapter conclusions regarding different aspects of amphiphilic compounds are given. Furthermore a few new aspects of amphiphiles are introduced.

11.1 Synthesis of amphiphilic compounds

A systematic evaluation of the amphiphilic structure and its biophysical properties requires different chemical target structures that have to be accessed easily in a few steps and in considerably good yields. The carbohydrate structure, provides a good source of different structures. In particular the three common sugars: Lactose, Maltose and Melibiose are basic structures when used for the synthesis of different amphiphilic structures. Furthermore lactose and Maltose are produced on a large industrial scale, e.g. commercial lactose is a byproduct of cheese manufacturing, which makes them low cost materials. Additionally the general structure concept introduced in Chapter One was easily realised by using these three sugars. The lactose headgroup has a rod-like molecular shape (Galactose is linked $\beta1{\rightarrow}4$ on Glucose), the Maltose headgroup is slightly wedge-shaped (Glucose is linked $\alpha1{\rightarrow}4$ on Glucose) and the Melibiose headgroup has a tilted structure (Galactose is linked $\alpha1{\rightarrow}6$ on Glucose).

These carbohydrate building blocks were easily converted into several amphiphiles as shown in figure 11.1, where the most common ones are the alkyl glycosides (I). A slight increase of the polar headgroup can be achieved by introducing a polar spacer between the carbohydrate headgroup and the lipophilic tail. In structures of type (II) the lipophilic chain is connected to the amino group of the ethanolamine spacer. In structures of type (III) the spacer is ethylene glycol. This structure is similar to that of common industrial surfactants like sodium laureth-I / II (or sodium lauryl ether sulfate) where instead of carbohydrate a sulfate headgroup can be found. Common analogues to natural lipids are the glyco glycero lipids of type (IV), (V) and (VI). Lipids of type (IV) and (VI) have similar structures in which alkyl chains are linked to the glycerol moiety via an ether group (IV) or an ester group (VI). The main difference is the position of the linkage of the chains, which is a 1,3-position of the glycerol for (IV) and a 1,2-position of the glycerol for (VI). Type (V) is also a glyco glycero structure but of an inverted type. Whereas in (IV) and (VI) two chains are connected to one sugar headgroup, the Y-shaped structure of (V) has only one chain, but two sugar residues. Furthermore the polarity is increased by replacing the ether / ester group by an amide group. Finally structures of type

(VII) have been synthesised, which can be seen as analogues of normal alkyl glycosides (I), where the *O*-glycosidic bond is replaced by an amide group.
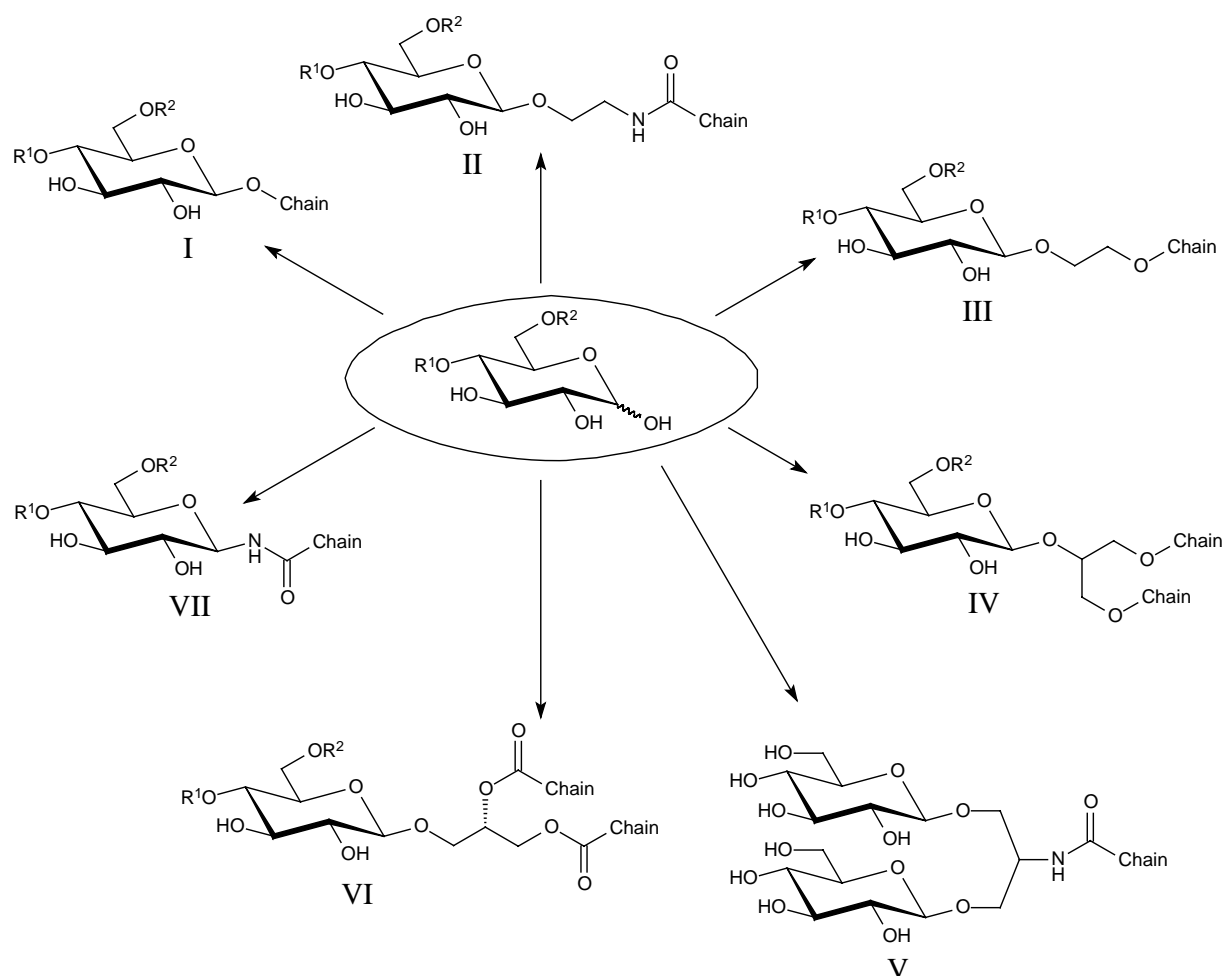

FIGURE 11.1: General types of amphiphilic structures synthesised in this thesis (R^1, R^2: position of possible sugar residues in the hydrophilic part, where *R* can be hydrogen, Glucose, Galactose or Maltose in α- or β-configuration; *Chain*: alkyl/acyl chain of the lipophilic part).

11.1.1 Alkyl glycosides

The synthesis of alkyl glycosides has been the subject of many publications. Most of the alkyl glycosides used in this thesis have been synthesised before (See for example Minden *et al.*, 2000). In principal the synthetic route starts from the protected sugar followed by replacement of the protective group on C-1 and the deprotection step (see for example Chapter 4 and 6). The desired product, with α- or β-configuration at the anomeric centre, depends on the reaction conditions and the protecting groups (Banoub and Bundle, 1979, Böcker and Thiem, 1989).

Maltri-C18:1

Gen-C18

Mel-C12 (Chain: $C_{12}H_{25}$)
Mel-C14 (Chain: $C_{14}H_{29}$)
Mel-C16 (Chain: $C_{16}H_{33}$)
Mel-C18 (Chain: $C_{18}H_{37}$)
Mel-C18:1 (Chain: $(CH_2)_8$ C_8H_{17})

Mal-C12 (Chain: $C_{12}H_{25}$)
Mal-C14 (Chain: $C_{14}H_{29}$)
Mal-C16 (Chain: $C_{16}H_{33}$)
Mal-C18 (Chain: $C_{18}H_{37}$)
Mal-C18:1 (Chain: $(CH_2)_8$ C_8H_{17})

Lac-C12 (Chain: $C_{12}H_{25}$)
Lac-C14 (Chain: $C_{14}H_{29}$)
Lac-C16 (Chain: $C_{16}H_{33}$)
Lac-C18 (Chain: $C_{18}H_{37}$)
Lac-C18:1 (Chain: $(CH_2)_8$ C_8H_{17})

Mel-α-C12 (Chain: $C_{12}H_{25}$)
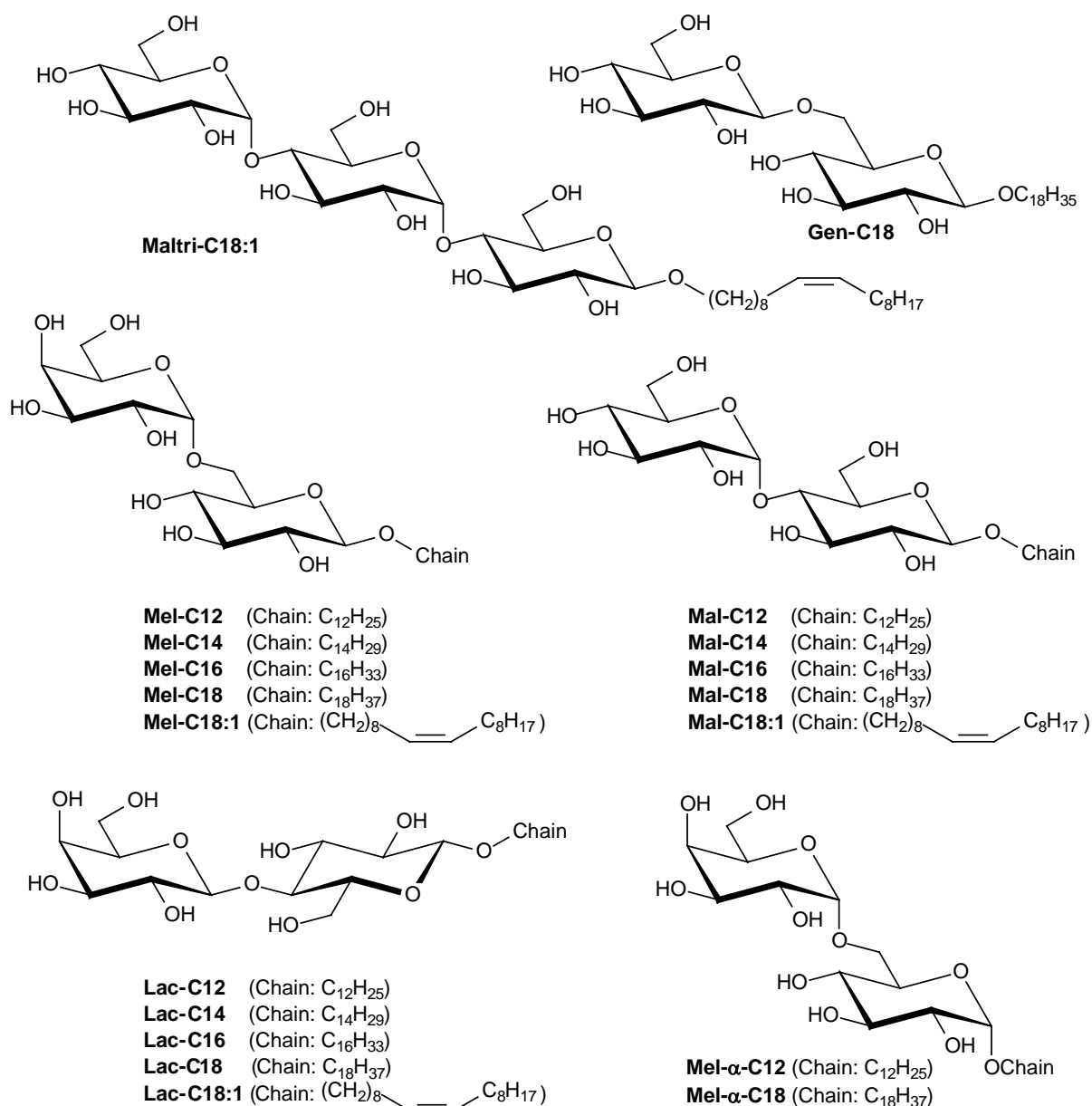**Mel-α-C18** (Chain: $C_{18}H_{37}$)

FIGURE 11.2: Alkyl glycosides synthesised and investigated in this thesis.

Upon the preparation of the desired compounds, it was found that the purification can be simplified. Normally the peracetylated β-product is purified by column chromatography directly after the glycosylation step. In this case the product was subjected to the deprotection procedure first, and afterwards purified by a simple recrystallisation from methanol, ethanol or propanol. Thus it was possible to synthesise the compounds on a larger scale (10-20 g) than described (1-2 g) by Minden *et al.* (2000). In addition to known compounds new alkyl glycosides have been synthesised, which are the lipids with an oleyl chain, **Mel-β-C18:1**, **Maltri-β-C18:1** (figure 11.2) and with methyl branched chains, **Mel-β-Phy**, **Mel-β-TMD** (figure 11.3).

The general synthetic scheme and reaction conditions are described in Chapter 4 and 6.
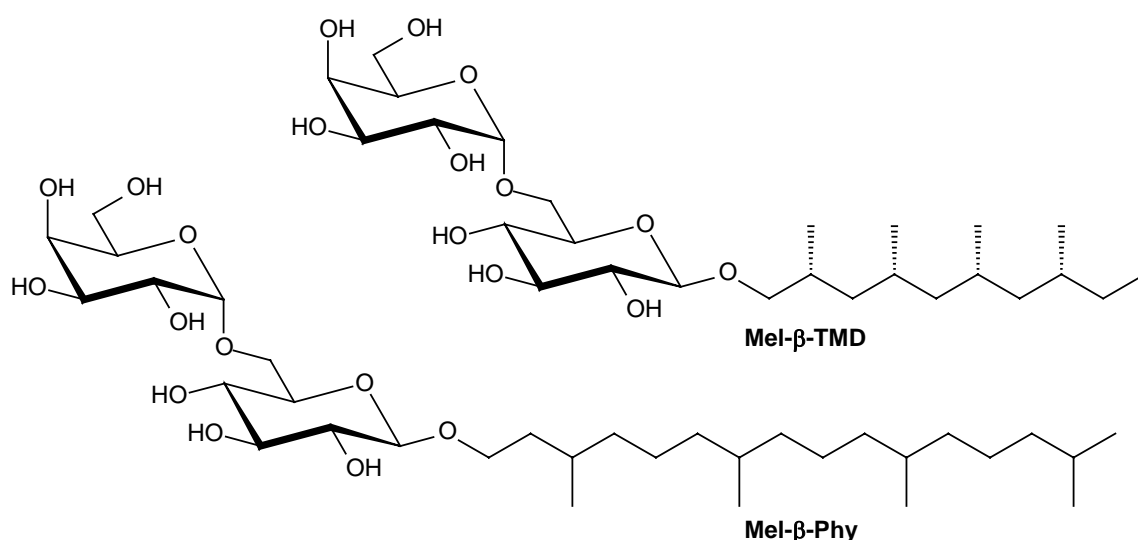
FIGURE 11.3: Alkyl glycosides bearing methyl branched alkyl chains, synthesised and investigated in this thesis.

11.1.2 *N*-Acyl glycosylamines

A convenient pathway for the preparation of bolaamphipiles based on *N*-acyl glycosylamines has been described by Masuda *et al.* (1998). This synthetic route was successfully applied to the synthesis of an *N*-oleoyl maltosyl- and melibiosylamine. As shown in scheme 11.1 the synthesis requires five steps starting from peracetylated disaccaride. After conversion into glycosyl bromide the bromine was substituted by azide, which gave the glycosylazide in quantitative yield. The reduction step had to be modified due to the bad solubility of glycosylazides in pure methanol. The compounds were therefore dissolved in a 1:1 mixture of methanol and tetrahydrofurane. As the catalyst described in the literature (platine on charcoal)

did not work properly in the solvent mixture, palladium on charcoal was used instead. This gave glycosylamines in quantitative yields. The glycosylamine was reacted with oleoyl chloride in dry dimethylformamide with pyridine as base. At the final stage the protecting groups were removed after chromatograpic purification.

A direct condensation of an unprotected glycosylamine with carbonic acid chloride as described by Kallin *et al.* (1989) and Lubineau *et al.* (1995) for monosaccharides and maltosides with short carbonic acid chains (2-12), was not successful due to the poor solubility of the glycosylamines and carbonic acid chloride in the appropriate solvents.
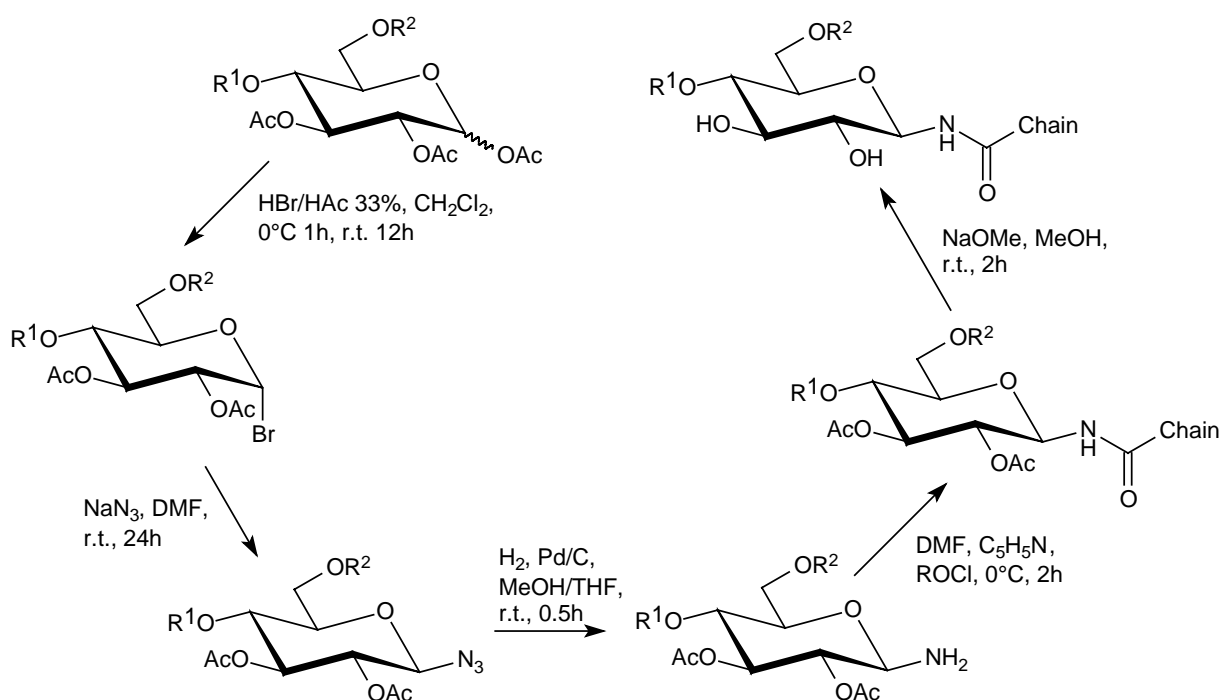
SCHEME 11.1: Synthetic route for the preparation of *N*-acyl glycosylamines with Maltose and Melibiose headgroups (Maltose: R^1=α-D-Glucose, R^2=H; Melibiose: R^1=H, R^2=α-D-Galactose; *Chain*: $C_{17}H_{33}$) .

Figure 11.4 shows the lipids that were synthesised using this synthetic route. The synthesis of these compounds has not previously been reported. A detailed description of the synthesis can be found in Appendix A.
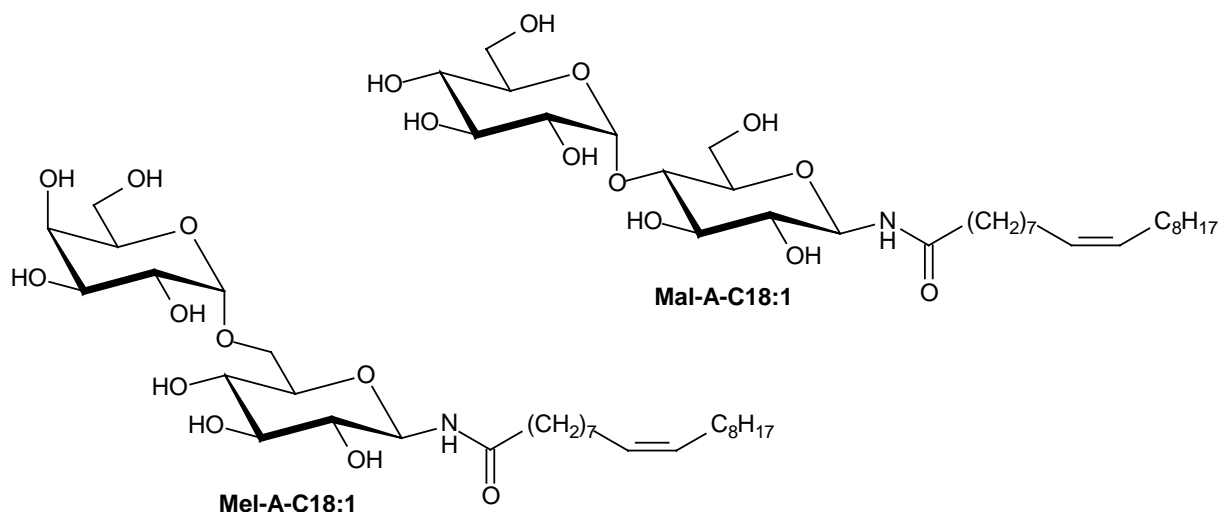
FIGURE 11.4: *N*-acyl glycosylamines synthesised and investigated in this thesis.

11.1.3 *N*-Acyl 2-aminoethyl glycosides

The synthetic route described in Chapter 10 has been found to be the most efficient way for the preparation of *N*-acyl 2-aminoethyl glycosides. It starts with the preparation of the peracetylated 2-bromoethyl glycoside followed by a nucleophilic replacement of bromine by azide and a reduction yielding 2-aminoethyl glycosides. The esterification step with the corresponding acid chloride and finally the deprotection lead to the target molecules. With this convenient route it was possible to obtain the desired compounds in high overall yields (56-65 %) and with less tedious purification steps than described in other published procedures (Miura *et al.*, 1996). Figure 11.5 shows the structures of the synthesised compounds. All compounds have been synthesised for the first time, except for compound **Lac-EA-C16**.

The lipid **Mal-AB-C14** was obtained in good yields (30 %) by direct glycosylation of *N*-tetradecanoyl-2-ethyl-2-aminoethanol with peracetylated Maltose, as described in Chapter 9.

Other synthetic routes where also employed (Scheme 11.2). Because the direct condensation of the *N*-acyl 2-ethyl-2-aminoethanol aglycon was succesful in the synthesis of **Mal-AB-C14**, an attempt was also made to use the non-branced *N*-acyl 2-aminoethanol as aglycon. Problems arose whilst dissolving the alcohol in the solvent for the glycosylation reaction, as it took large amounts of solvent to partially dissolve the alcohol. In all cases the alcohol dissolved upon the addition of the Lewis acid, boron trifluoride etherate. The yields from the direct glycosylation were also low, even for a reaction time of more than 72 hours it was not more than 0.1 to 2 %. As it was possible to obtain the glycoside of the ethyl branched

aminoalcohol where the amide group is shielded by the ethyl group, the ability of the amide group for a strong interaction and aggregation might lower the reactivity of the hydroxyl group of the alcohol in case of non-branched *N*-acyl 2-aminoethanols.

Another attempt was made by using protected 2-aminoethanol. The aminoethanol was protected using carbonylbenzyloxy chloride (Cbz) and then used in the glycosylation procedure. The glycosides were obtained in moderate yields (21 % for lactose and 30 % for Maltose and Melibiose). The Cbz-group should have been removed by hydrogenation, but this was the limiting step in this synthetic pathway as complete removal was not possible.
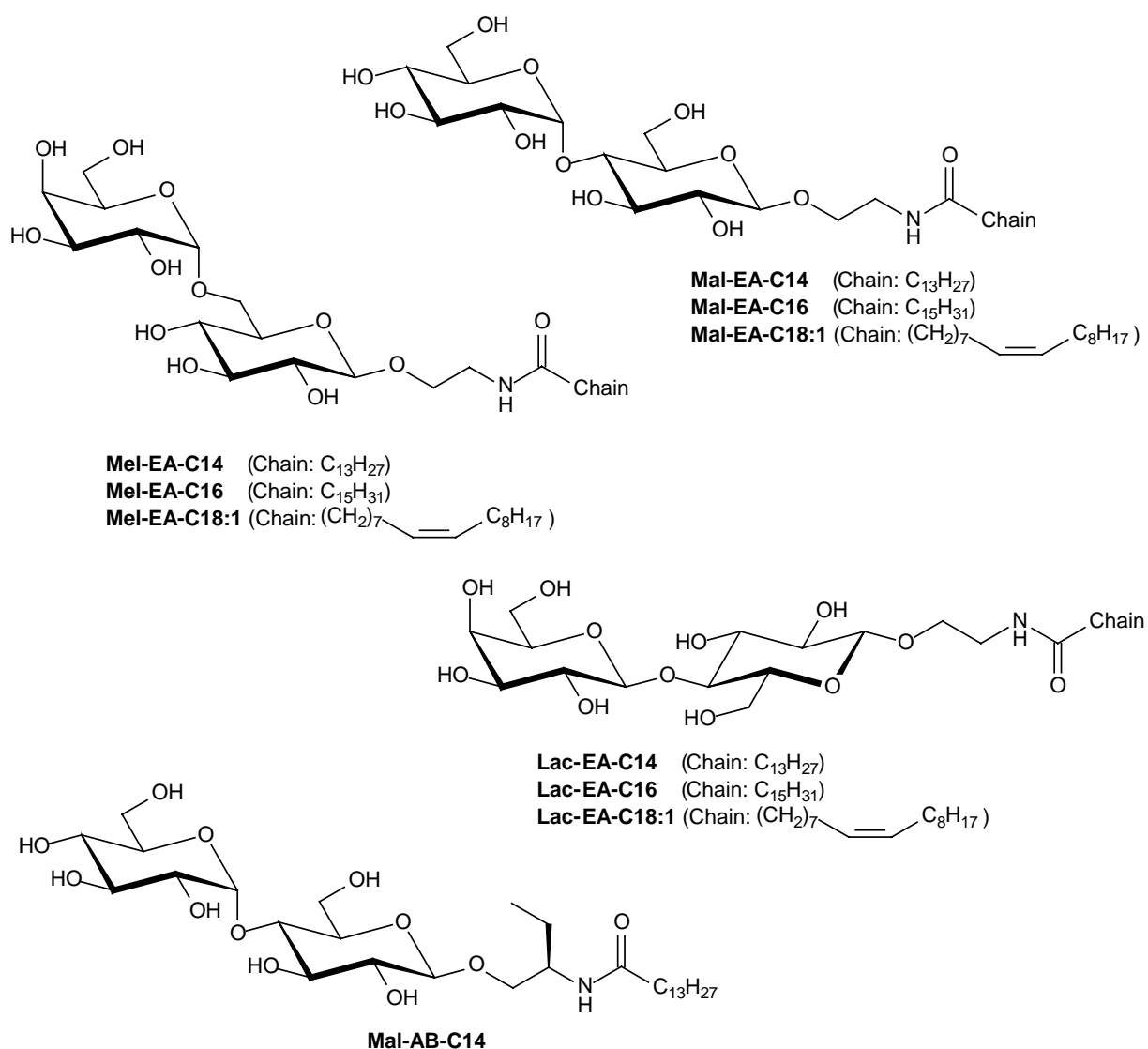

FIGURE 11.5: *N*-acyl 2-aminoethyl glycosides with (**Mal-AB-C14**) and without ethyl branching synthesised and investigated in this thesis.
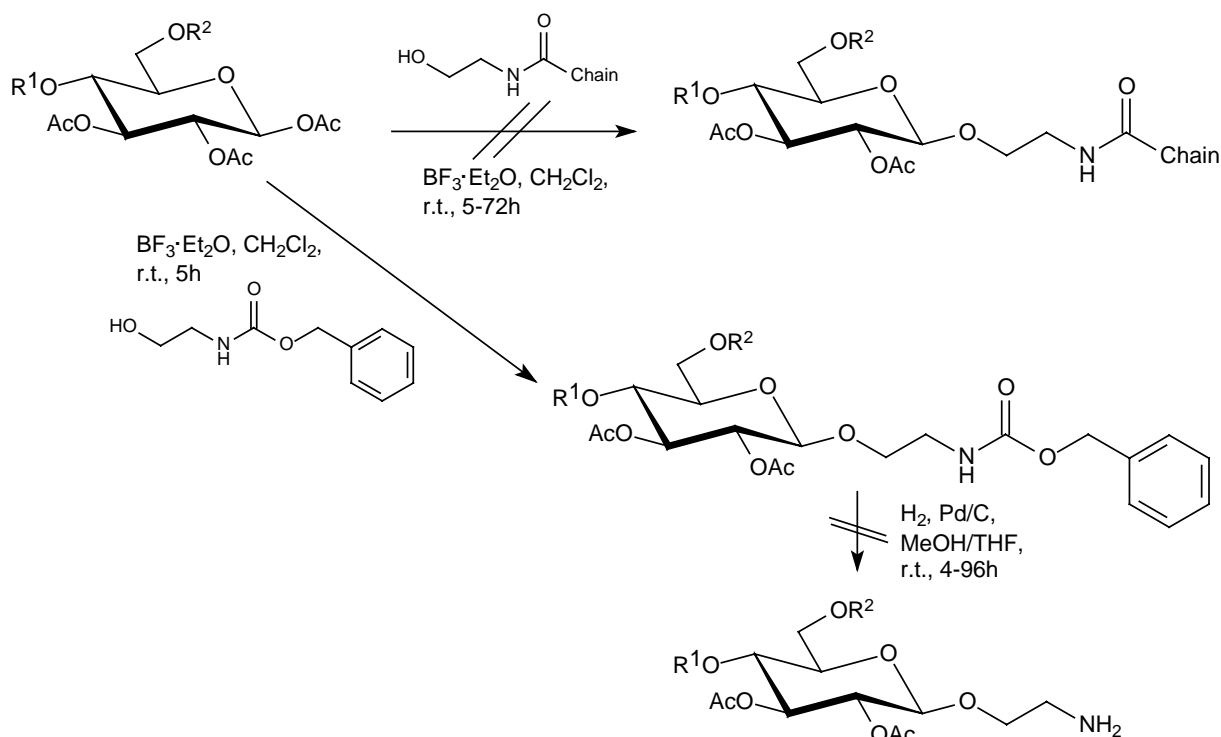
SCHEME 11.2: Attempts for the synthesis of *N*-acyl 2-aminoethyl glycosides (Lactose: R^1=β-D-Galactose, R^2=H; Maltose: R^1=α-D-Glucose, R^2=H; Melibiose: R^1=H, R^2=α-D-Galactose; *Chain*: Fatty acid chain).

11.1.4 2-Alkyloxyethyl glycosides

The synthesis of the ethylene glycol lipids was performed in three steps (scheme 11.3). First the 2-alkyl-ethanol precursors were synthesized by using a modification of the standard methods described by Wrigley *et al.* (1960). An excess of ethylene glycol was reacted with sodium. Afterwards a solution of alkylbromide in tetrahydrofurane was added. The ethylene glycol derivatives were then used as the alcohol component in the glycosylation reaction with the peracetylated disaccharide under the catalysis of boron trifluoride etherate (Vill *et al.*, 1989). The yields for the glycosylation reaction were good (30-54 %). After deprotection and recrystallisation the final products were obtained in good yields (27-53 %) in gram scale and in highest purity. The structures of the synthesized compounds are shown in figure 11.6. The synthesis of compound **Lac-EG-C12** has also been described (Yoshida *et al.*, 1995), however the authors obtained the compound only in poor yields and in milligram scale. The other lipids were synthesised for the first time in the course of this thesis. A detailed description of the synthesis can be found in appendix A.
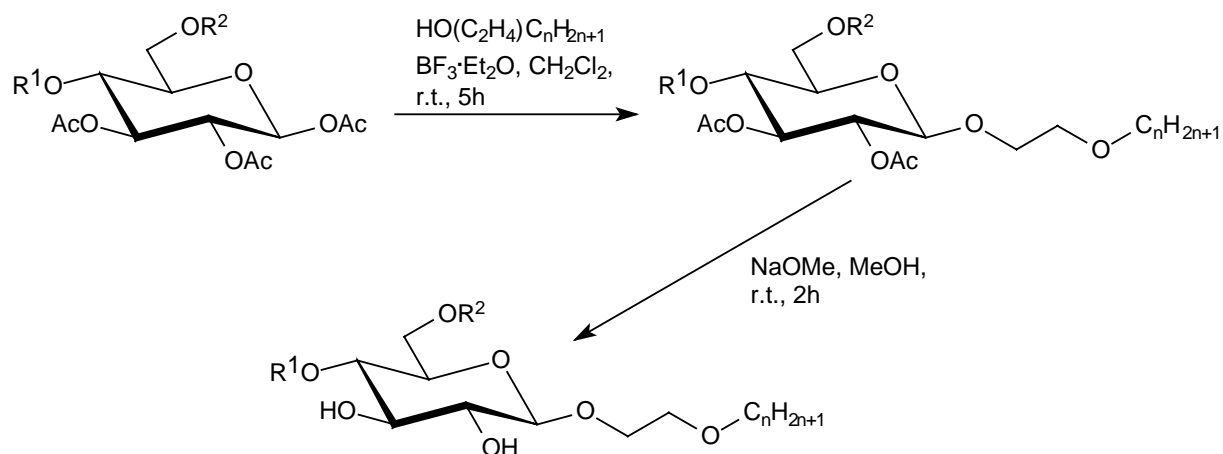
SCHEME 11.3: Synthesis of 2-alkyloxyethyl glycosides (Lactose: R^1=β-D-Galactose, R^2=H; Maltose: R^1=α-D-Glucose, R^2=H; Melibiose: R^1=H, R^2=α-D-Galactose; n=12,14,16).

Lac-EG-C12 (Chain: $C_{12}H_{25}$)
Lac-EG-C14 (Chain: $C_{14}H_{29}$)
Lac-EG-C16 (Chain: $C_{16}H_{33}$)

Mel-EG-C12 (Chain: $C_{12}H_{25}$)
Mel-EG-C14 (Chain: $C_{14}H_{29}$)
Mel-EG-C16 (Chain: $C_{16}H_{33}$)

Mal-EG-C12 (Chain: $C_{12}H_{25}$)
Mal-EG-C14 (Chain: $C_{14}H_{29}$)
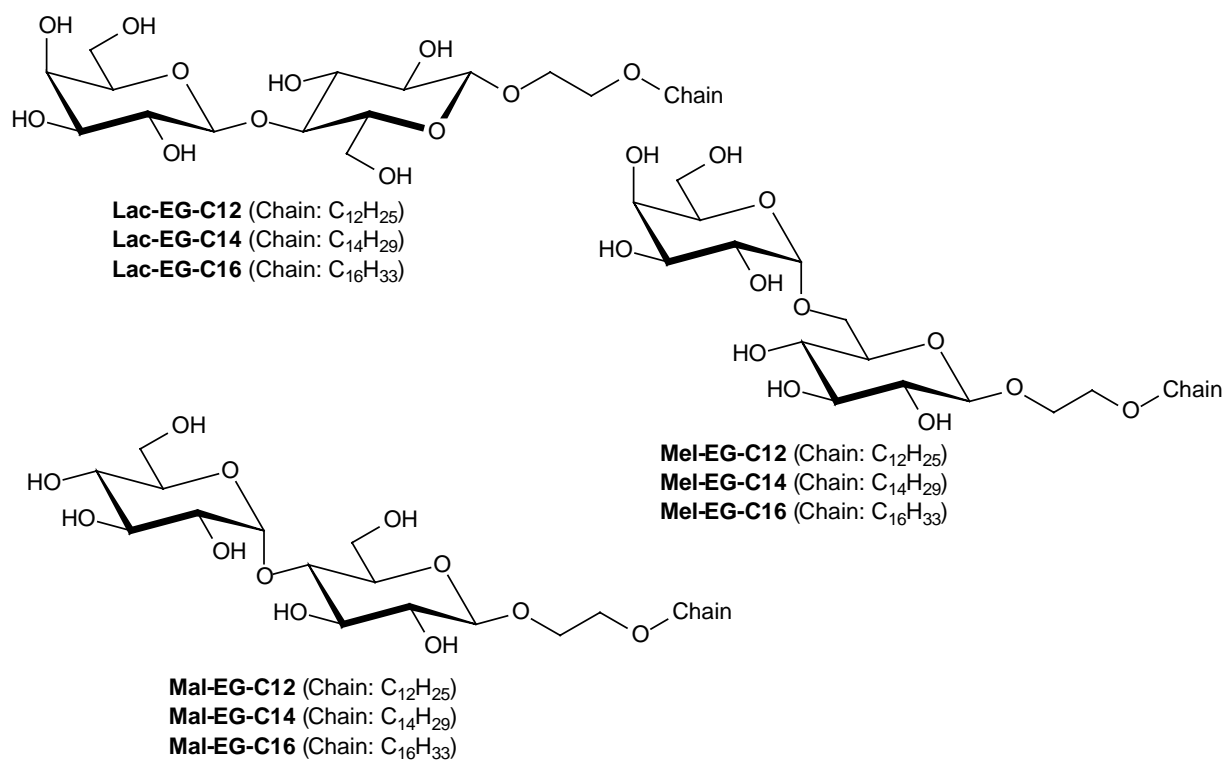**Mal-EG-C16** (Chain: $C_{16}H_{33}$)

FIGURE 11.6: 2-Alkyloxyethyl glycosides synthesised and investigated in this thesis.

11.1.5 Glyco glycero glycosides

Many novel glyco glycero lipids with different structures were synthesised during this research (Figure 11.7), seven lipids were synthesised for the first time. The compounds were synthesised by using four different routes, depending on the target structure (see Chapter 1 and 6). Glycosylation of peracetylated disaccharide and 1,3-dialkylglycerol under catalysis of boron trifluoride etherate and the following deprotection step under basic conditions has already been successful for the synthesis of the glyco glycero lipids **Mal-1,3-C14**, **Mel-1,3-C14** and **Mal-1,3-TMD** with a medium alkyl chain length. The glycosylation using a 1,3-dialkylglycerol with oleyl chains (18 carbon atoms) required a different synthetic route, as the route used for the synthesis of the medium chained lipids gave only very poor yields (10-15 %). In this case the use of the trichloracetimidate procedure (Schmidt *et al.*, 1984) with some modifications (Schmidt and Kinzy, 1994) gave the compounds **Mal-1,3-C18:1** and **Maltri-C18:1** in good overall yields (74 and 65 %). Synthesis of the glycosyl diacyl glycerol **Mal-1,2-TMD** was performed by using the well known procedure of Mannock *et al.* (1987). The synthesis of the Y-shaped lipid **Glc-Y16** required a different synthetic route. Cbz-protected serinol was used in a glycosylation reaction with peracetylated Glucose, which was also the limiting factor in this synthetic procedure due to the low yields (15 %). The yields did not increase using other glycosylation methods. After cleavage of the protective group the amine function was esterified using hexadecanoyl chloride and, finally, the acetyl groups were removed by using standard procedures.
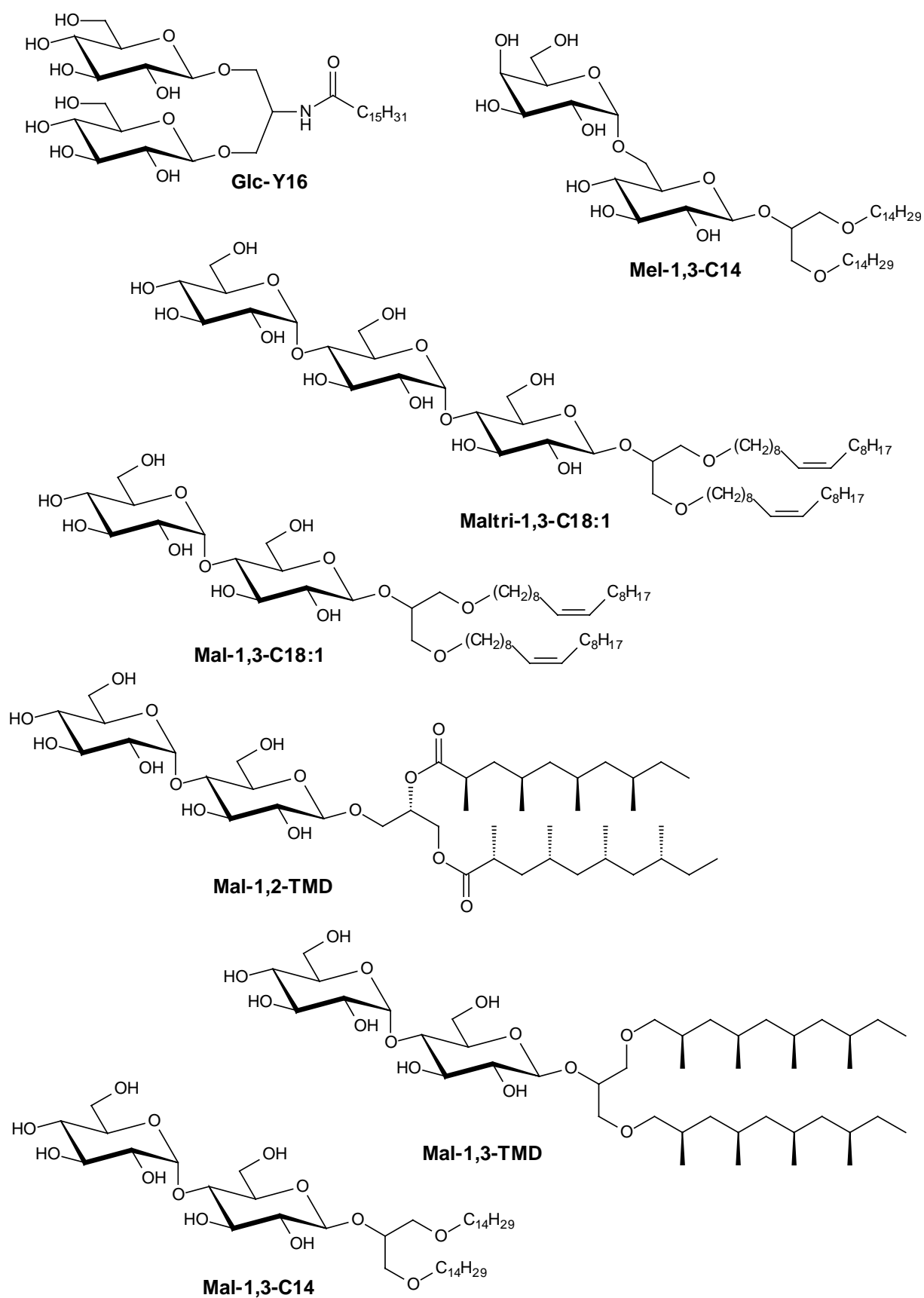
FIGURE 11.7: Glyco glycero lipids synthesised and investigated in this thesis.

11.2 Liquid Crystalline Properties

The influence of the configuration of the carbohydrate headgroup on the phase transition temperatures has been shown by Minden *et al.* (2000) and Vill *et al.* (2000). For monosaccharide headgroups differences can be seen to arise upon the configuration of single hydroxy groups, e.g. gluco (4-OH in equatorial position) vs. galacto (4-OH in axial position). In the case of disaccharide headgroups this effect can be ignored, e.g. lactose (gal-β1→4-glc) and cellobiose (glc-β1→4-glc) have similar transition temperatures. Differences arise due to variation of the position of linkage of the second sugar residue.

11.2.1 Melting point dependence on the molecular structure

Synthetic amphiphiles are useful target compounds for biological investigations even in their pure state, but the application of these is often difficult due to a high melting point, which gives the relevant liquid crystalline phase region only at temperatures well above biological temperatures. Ways to circumvent this problem include the usage of unsaturated or methyl branched compounds.

Table 11.1 shows a summary of the thermotropic phase behaviour for selected compounds with different structural elements. As can be seen alkyl glycosides with linear saturated alkyl chains are in the crystalline state at room temperature (transition temperatures are given in Appendix C). Alkyl glycosides are already in the liquid crystalline state at room temperature if the alkyl chain contains a double bond with Z-configuration or if a methyl branched chain is used. Interestingly, in the case of **Mal-A-C18:1** the compound is in the crystalline state at room temperature, whereas with compound **Mal-EA-C18:1**, where the distance between the amide group and the carbohydrate head is increased by two carbon atoms, it is in the liquid crystalline state at room temperature. This can be interpreted in the way of different interaction of the amidic groups which will be stronger in the case of **Mal-A-C18:1** where the group is part of the polar head region, while in the case of **Mal-EA-C18:1** the amide group is isolated from the carbohydrate headgroup which weakens the interaction of the amide group, as for example in a hydrogen bonding network.

In the case of the glyco glycero lipids a similar behaviour as observed for the alkyl glycosides can be found. The linear and saturated alkyl chains of the glyco glycero lipids **Mal-1,3-C14** and **Mel-1,3-C14** enables a stable packing of the chains which leads to a high melting point. The disturbed packing of the compounds with unsaturated alkyl chains (**Mal-1,3-C18:1** and **Maltri-1,3-C18:1**), as well as methyl branched chains (**Mal-1,2-TMD** and **Mal-1,3-TMD**), prevents these compounds from crystallisation.

11.2.2 Liquid crystalline phase dependence on the molecular structure

As the liquid crystalline phases can be explained in terms of a biological function, the form of these is a crucial point in the investigation of new amphiphilic lipids, and is even more important than the transition temperatures. It has already been shown that biological relevant phases like cubic phases can be induced by mixing different lipids each not forming a cubic phase (Minden *et al.*, 2002) or pathogenic lipids, like GGPL-1 that can also induce cubic phases in membrane lipid compositions (Milkereit *et al.*, to be published).

Table 11.1 shows the thermotropic liquid crystalline phases of some compounds investigated in this thesis. The phases of the remaining compounds are shown in Appendix C, as they display only lamellar smectic A phases. Table 11.1 lists all different structural elements obtained during this work.

The phase behaviour of the rod-like alkyl lactosides depends on the alkyl chain length. A chain length of 12 and 14 carbon atoms only results in the formation of smectic A phases. The elongation of the chain to 16 and 18 carbon atoms (**Lac-C16** and **Lac-C18**) disturbs the balance between the hydrophilic and hydrophobic moiety of the molecule and as a consequence cubic phases are formed. Interestingly compound **Lac-C18:1**, bearing an unsaturated alkyl chain, does not form a cubic phase, as the disturbing effect in the chain packing disables its formation.

The alkyl maltosides, with their slightly tilted carbohydrate headgroup, only show a smectic A phase for alkyl chain lengths of 12 to 18 carbon atoms and also for the unsaturated analogue **Mal-C18:1**. In this case the molecular structure enables different packing configurations of the carbohydrate headgroup, which can compensate for the influence of the hydrophobic part. Even by increasing the hydrophilic part by amidic groups (**Mal-A-C18:1**) or by using different kind of spacer (**Mal-EG-C14**, **Mal-AB-C14**, **Mal-EA-C18:1**), the formation of more phases other than a Smectic A phase, is not enabled.

The tilted molecular structure of the melibiosides results in a similar structure-phase relationship as found for the alkyl maltosides. Only the short chain compound **Mel-C12** forms a cubic phase beside the Smectic A phase. Interestingly even the voluminous branched chains of **Mel-β-TMD** and **Mel-β-Phy** cannot disturb the balance of the different molecular parts.

The introduction of a third sugar moiety results in the formation of new phases. As expected the trisaccharide **Maltri-C18:1** forms a columnar phase, due to the increased size of the hydrophilic headgroup. Nevertheless, in the case of the glyco glycero lipid **Maltri-1,3-C18:1**, with two alkyl chains, the hydrophilic and hydrophobic parts are in balance again.

In the case of disaccharide compounds a second alkyl chain enables the formation of new phases.

The maltosides with linear alkyl chains (**Mal-1,3-C14** and **Mal-1,3-C18:1**) only show columnar phases with the hydrophobic chains outside the rods, whereas the methyl branched

analogues **Mal-1,2-TMD** and **Mal-1,3-TMD** form only Smectic A phases. The melibioside **Mel-1,3-C14** shows a Smectic A and a columnar phase which shows that the tilted carbohydrate headgroup can partly compensate for the influence of a second alkyl chain.

Finally, the Y-shaped lipid **Glc-Y16** bearing two single carbohydrate headgroups and one fatty acid chain shows a columnar phase as expected owing to the broad hydrophilic headgroup. At higher temperatures a cubic phase can also be found.

TABLE 11.1: Thermotropic phases of selected compounds (left side low temperature, right side high temperature). Abbreviations: Cr, crystalline at room temperature; g, glass state at room temperature; LC, liquid crystalline at room temperature; (cub), cubic phase formed on cooling; cub, cubic phase; SmA, Smectic A phase; col, columnar phase.

Lac-C14	Cr		SmA		
Lac-C16	Cr	(cub)	SmA		
Lac-C18	Cr	(cub)	SmA		
Lac-C18:1	Cr		SmA		
Mel-C12	Cr	(cub)	SmA		
Mel-C14	Cr		SmA		
Mel-β-TMD	LC		SmA		
Mal-AB-C14	g		SmA		
Mal-EG-C14	Cr		SmA		
Mel-C18	Cr		SmA		
Mal-C18:1	g		SmA		
Mal-A-C18:1	Cr		SmA		
Mal-EA-C18:1	LC		SmA		
Mel-β-Phy	g		SmA		
Maltri-C18:1	LC		SmA	col	
Mal-1,3-C14	Cr			col	
Mal-1,3-TMD	LC		SmA		
Mal-1,2-TMD	LC		SmA		
Mal-1,3-C18:1	LC			col	
Mel-1,3-C14	Cr		SmA		cub
Maltri-1,3-C18:1	LC		SmA		
Glc-Y16	g			col	cub

11.2.3 Lyotropic phase behaviour

In contrats to the influence of the molecular structure on the thermotropic phase behaviour, the lyotropic phase behaviour is affected by small changes of the molecular structure. Table 11.2 shows the lyotropic phase behaviour of several amphiphilic compounds with Maltose and Maltotriose carbohydrate headgroups investigated in this thesis, together with some data taken from the relevant literature. The comparison of only one type of carbohydrate headgroup makes the structure-property relationship more clear. The compounds are sorted by their phase sequences, starting with the lyotropic polymorphism of inverted structures and ending with the phases of highest water content.

The first interesting fact is that, except for the lipid **Glc-Y16**, all compounds form lamellar phases. As a lamellar phase is similar to the bilayer of the biological membrane it can be assumed that all these structures have the ability to form or to be a part of membranes. The lipophilic part of the two glyco glycero lipids with alkyl chain length of 14 (**Mal-1,3-C14**) and 18 carbon atoms (**Mal-1,3-C18:1**) and a number of two chains is larger than the hydrophilic headgroup and enables the formation of inverted structures. The phase diagram is simplified to form only lamellar L_α phases for glyco glycero lipids where the hydrophilic and hydrophobic parts are in balance. This is achieved by using long alkyl chains and a larger sugar headgroup (**Maltri-1,3-C18:1**) or by a shorter alkyl chain length (**Mal-1,3-TMD** and **Mal-1,2-TMD**). Nevertheless, the polar part of the molecule cannot extend a rod-like shape of the molecule, as can be seen by the formation of myelin figures towards higher water concentration (Jeffrey and Wingert 1992; Bouligand, 1998). Next, the number of alkyl chains is reduced to one chain. As can be seen only three compounds (**Mal-EA-C14**, **Mal-EA-C16**, **Mal-A-C18:1**) exclusively form a lamellar phase. Poor water solubility, even at elevated temperatures, might be the reason why compounds **Mal-EA-C14** and **Mal-EA-C16** only form lamellar phases and myelin figures towards a higher water content. The similar compound **Mal-EA-C18:1**, which is soluble in water at room temperature, shows a lyotropic polymorphism. This could also be expected for the before-mentioned compounds **Mal-EA-C14** and **Mal-EA-C16**.

In case of the *N*-acyl maltosylamine **Mal-A-C18:1**, which is soluble in water at room temperature, only a lamellar phase is formed this may be attributable to the amide group. This is located in the polar headgroup region and can build up a strong hydrogen-bonding network that makes the formation of other phases than the lamellar phase energetically unfavourable. The *O*-glycoside analogue **Mal-C18:1**, in comparison, shows a bicontinous cubic and a hexagonal phase next to the lamellar phase.

TABLE 11.2: Lyotropic phase sequences of selected compounds. Data for compound **Mal-C12** taken from Boyd *et al.* (2000) and for **Mal-C18** and **Mal-C18:1** taken from Minden *et al.* (2000). [Abbreviations: Cr, crystalline at room temperature; g, glass state at room temperature; SmA, thermotropic smectic A phase; H_{II}, inverted hexagonal phase, V_{II}, inverted bicontinous cubic phase; L_α, lamellar phase, V_I, bicontinous cubic phase, H_I, hexagonal phase; cub, discontinous cubic phase; *, myelin figures formed beyond the lamellar phase on the water rich side].

Pure compound						*100 % water*
Mal-1,3-C14	Cr	H_{II}	V_{II}	$L_\alpha{}^*$		
Mal-1,3-C18:1	SmA	H_{II}	V_{II}	$L_\alpha{}^*$		
Mal-1,3-TMD	SmA			$L_\alpha{}^*$		
Mal-1,2-TMD	SmA			$L_\alpha{}^*$		
Maltri-1,3-C18:1	SmA			$L_\alpha{}^*$		
Mal-EA-C14	Cr			$L_\alpha{}^*$		
Mal-EA-C16	Cr			$L_\alpha{}^*$		
Mal-A-C18:1	Cr			L_α		
Mal-C14	Cr			L_α		H_I
Mal-EG-C14	Cr			L_α		H_I
Mal-C16	Cr			L_α		H_I
Mal-EG-C16	Cr			L_α		H_I
Mal-C18	Cr			L_α		H_I
Mal-EA-C18:1	SmA			L_α	V_I	H_I
Mal-C12	Cr			L_α	V_I	H_I
Mal-EG-C12	g			L_α	V_I	H_I
Mal-AB-C14	g			L_α	V_I	H_I
Mal-C18:1	g			L_α	V_I	H_I
Maltri-C18:1	SmA			L_α		cub
Glc-Y16	g				H_I	cub

The formation of hexagonal phases, with the polar headgroup curved towards the water (type I), is found for most of the single chain amphiphiles, regardless to the chain length (12-18 carbon atoms), spacer or double bonds. The formation of a bicontinous cubic phase (V_I) between the lamellar and the hexagonal phase is only found for a few compounds. As no special structural concept can be predicted from the results, it is more likely that the formation

of the V_I-phase must depend on a certain hydrophilic lipophilic balance given by the special structural order of the compound in solution.

At least the number of sugar residues of the single chain amphiphiles is increased. This was done by using a trisaccharide instead of a disaccharide headgroup (**Maltri-C18:1**) and by using a glyco glycero lipid with two carbohydrate headgroups on each end of the glycerol moiety and only one fatty acid chain (**Glc-Y16**). The effect on the phase behaviour is very different. The trisaccharide still forms a lamellar phase but the large headgroup cannot form a hexagonal one. But a discontinous cubic phase was observed using polarising microscopy. This phase, which is seldom observed, is built up by spherical micelles that are ordered in a cubic space group due to a strong interaction of the hydrophilic headgroups (Fairhurst *et al.*, 1998). This discontinous cubic phase is also found for the glyco glycero lipid **Glc-Y16**. Contrary to compound **Maltri-C18:1**, which forms a lamellar phase, **Glc-Y16** forms only a hexagonal one due to the extremely wedge shaped structure of the molecule. But both compounds form a discontinous cubic phase on the water rich side.

11.3 Hydrophilic lipophilic balance and solubility

The concept of the hydrophilic lipophilic balance (*HLB*) is a tool for the selection of a surfactant for a given application. The *HLB* is defined by Griffin (1949, 1954) as the balance of the size and strength of the hydrophilic and lipophilic moieties of the surfactant molecule and can be estimated as

$$HLB = 20 \frac{M_{hp}}{M_t} .$$
(11.1)

    with: M_{hp}: Molecular weight of the hydrophilic group

              M_t: Total molecular weight of the molecule

From these numbers typical applications of surfactants can be chosen. For instance *HLB* numbers in the range of 3-6 indicate an w/o emulsifier, while an o/w emulsifier should be indicated by a *HLB*-number range from 8-14. For surfactants that can be used for more than one application it is clear that the same *HLB*-number can belong to different applications, e.g. *HLB* 8-14 for o/w-emulsifier, 9-13 for a detergent. The *HLB*-concept is useful for room-temperature operations, however problems arise if temperature varies, as the properties of many surfactants are temperature sensitive. Some general principles can be concluded from this concept. For instance, amphiphiles classified as detergent (*HLB* 9-13) should be readily soluble in water, while w/o-emulsifiers should be soluble in less- or non-polar solvents.

Table 11.3 shows the *HLB*-values of several amphiphiles investigated in this thesis as well as their solubility in water and ethanol. Solubilities where tested at room temperature by dissolving the appropriate amount of substance in the solvent without heating the sample. It can be seen that surfactants with a high *HLB*-number are soluble in water at room temperature, despite the fact that some amphiphiles are insoluble at room temperature due to the high Krafft-temperature, which arises from the conformation of the different carbohydrate headgroups. Additionally the glyco glycero lipids **Mal-1,3-TMD**, **Mal-1,2-TMD**, **Mal-1,3-C18:1** and **Mel-1,3-C14** with *HLB* numbers of 7.44 to 8.44 have been found to be good o/w-emulsifiers (see Appendix C). In general it was found that the *HLB*-concept is also useful for the selection of carbohydrate-based amphiphiles.

TABLE 11.3: *HLB*-values according to Griffin and solubility of amphiphiles in water and ethanol (The solubility limit was tested up to a concentration of 1 w/v% lipid in water or ethanol at room temperature. Solubilities were determined in concentration intervals of 0.01, 0.1 and 1 w/v% with the result indicating up to which concentration the surfactant was finally soluble).

Compound	M_w	HLB	hydrophobic carbon atoms	solubility limit [w/v%]	
				water	ethanol
Lac-EG-C12	554.67	13.89	12	<0.01	<0.01
Mal-EG-C12	554.67	13.89	12	>1	0.1
Mel-EG-C12	554.67	13.89	12	>1	0.01
Lac-C12	510.62	13.37	12	<0.01	<0.01
Mal-C12	510.62	13.37	12	>1	0.1
Mel-C12	510.62	13.37	12	0.1	0.01
Mel-α-C12	510.62	13.37	12	>1	0.1
Maltri-C18:1	754.90	13.34	18	>1	1
Lac-EG-C14	582.73	13.23	14	0.01	0.01
Mal-EG-C14	582.73	13.23	14	0.01	0.1
Mel-EG-C14	582.73	13.23	14	0.01	0.1
Lac-EA-C14	595.73	12.90	14	<0.01	<0.01
Mal-EA-C14	595.73	12.90	14	<0.01	0.01
Mel-EA-C14	595.73	12.90	14	<0.01	0.01
Mal-C14	538.68	12.67	14	1	>1
Mel-C14	538.68	12.67	14	0.1	0.1
Mel-β-TMD	538.68	12.67	14	0.1	>1
Mal-EG-C16	610.78	12.62	16	<0.01	<0.01
Mal-EA-C16	623.78	12.32	16	<0.01	<0.01
Mel-EA-C16	623.78	12.32	16	<0.01	<0.01

Compound	M_w	HLB	hydrophobic carbon atoms	solubility limit [w/v%]	
				water	ethanol
Mal-C16	566.73	12.04	16	<0.01	<0.01
Mal-EA-C18:1	649.82	11.83	18	1	0.1
Mel-EA-C18:1	649.82	11.83	18	<0.01	0.01
Lac-C18:1	592.77	11.52	18	<0.01	0.01
Mal-C18:1	592.77	11.52	18	>1	>1
Mel-C18:1	592.77	11.52	18	>1	>1
Lac-C18	594.78	11.47	18	<0.01	<0.01
Mal-C18	594.78	11.47	18	<0.01	>1
Mel-C18	594.78	11.47	18	<0.01	<0.01
Mal-A-C18:1	605.77	11.17	17	>1	>1
Mel-A-C18:1	605.77	11.17	17	>1	0.1
Mal-AB-C14	627.83	11.00	18	1	1
Mel-β-Phy	622.83	10.96	20	<0.01	>1
Maltri-1,3-C18:1	1079.45	9.33	36	<0.01	>1
Mal-1,3-C14	809.13	8.44	28	<0.01	>1
Mal-1,3-TMD	809.13	8.44	28	<0.01	>1
Mel-1,3-C14	809.13	8.44	28	<0.01	>1
Mal-1,2-TMD	837.10	8.15	26	<0.01	>1
Mal-1,3-C18:1	917.31	7.44	36	<0.01	>1

11.4 *CMC* and Surface tension

For some surfactants the critical micelle concentration was measured by using the de Noüy ring method (see table 11.4). The *CMC* is strongly influenced by changes of the molecular structure. Surprisingly compounds with an unsaturated alkyl chain do not follow the trend observed for normal ionic surfactants, where a steady decrease of the *CMC* with increasing chain length can be observed (Holmberg *et al.*, 2003). Interestingly the Maltose-based bolaamphiphile **MDM** (see Chapter 3) also shows the tendency to form micelles. From the surface tension at the *CMC* it can be concluded that most of the amphiphiles bearing a Maltose headgroup are more surface active than amphiphiles with a Melibiose or trisaccharide headgroup. Maltose-based amphiphiles occupy a similar area per headgroup at the air-water interface. For melibiosides it can be observed that this depends on the type of alkyl chain. For a linear chain the headgroup area is large, whereas for less flexible voluminous branched chains, as well as unsaturated chains, this value becomes small.

TABLE 11.4 : *CMC* values and surface tension (γ) at the *CMC* for several surfactants.

Compound	Hydrophobic chain length	CMC [mM]	γ_{CMC} [mN m^{-1}]	T [°C]	Headgroup area a_0 [Å]
Mal-C18:1	18	0.02	38	25	47 ± 5
Lac-EG-C14	14	0.1	36	30	--
Mal-EG-C14	14	0.1	36	30	31 ± 8
Mel-EG-C14	14	0.08	39	30	50 ± 9
Mal-EA-C18:1	17	0.09	36	25	47 ± 5
Maltri-C18:1	18	0.04	43	25	128 ± 11
Mel-β-TMD	10	0.1	36	40	23.1 ± 4
Mel-β-Phy	16	0.03	36	40	37 ± 15
Mel-C14	14	0.14	41	50	60 ± 15
Mel-C18:1	18	0.003	45	25	30 ± 8
MDM (Bola)	12	0.44	--	25	--
Mal-C14	14	0.02	37	25	45 ± 4
Mal-AB-C14	14	0.04	36	25	49 ± 4

TABLE 11.5: Critical packing parameters (*CPP*) calculated from the headgroup area per molecule at the air-water interface (a_0) the carbon chain volume (v_c) and the extended chain length (l_c).

Compound	Hydrophobic carbon atoms	a_0 [Å]	v_c [Å^3]	l_c [Å]	CPP ($v_c/l_c a_0$)
Maltri-C18:1	18	128	511.6	24.27	0.16
Mel-C14	14	60	404	19.21	0.35
Mel-EG-C14	14	50	404	19.21	0.42
Mal-AB-C14	14	49	404	19.21	0.43
Mal-C18:1	18	47	511.6	24.27	0.45
Mal-EA-C18:1	17	47	484.7	23.01	0.45
Mal-C14	14	45	404	19.21	0.47
Mal-EG-C14	14	31	404	19.21	0.7
Mel-C18:1	18	30	511.6	24.27	0.7
Mel-β-Phy	20	37	565.4	21.74	0.7
Mel-β-TMD	14	23.1	404	14.15	~1

With knowledge of the headgroup area per molecule at the air-water interface, the critical packing parameter (*CPP*) was calculated. A first estimation of the aggregate structure formed above the *CMC* can then be made. Table 11.5 shows the values used for the calculation and the resulting *CPP*. Spherical aggregates should only be formed by the trisaccharide **Maltri-C18:1**, whereas planar bilayers should be formed only by the methyl branched **Mel-β-TMD**. Between these completely different structures the formation of vesicles might be possible for the ethyleneglycol derivative **Mal-EG-C14**, alkyl glycoside **Mel-C18:1** and the less dense methyl branched compound **Mel-β-Phy**. For all other compounds a cylindrical aggregate structure should be possible.

As this is only a theoretical approach, these values have to be validated by determination of the real aggregate structure in solution.

11.5 Micellar and higher aggregate structures

11.5.1 Influence of the chemical structure on the micelle shape

The determination of the aggregate structure by small-angle neutron scattering for several amphiphilic compounds has been described in detail in the preceding chapters and in Appendix B.

In this section interest is focused on a comparison of micellar / aggregate forms in dilute solution with respect to the chemical structure of the investigated molecules. As previously discussed the relationship between the liquid crystalline and other physical properties and the molecular structure can be generalised by using the structural concept introduced in Chapter One. Depending on the molecular structure, the hydratisation of the molecule can force it to assemble into a different aggregate structure, or, speaking more generally, change the molecular shape. Thus it was found that not only the liquid crystalline phases depend on the shape of the molecule but also the micellar structure is sensitive to small changes of the molecular structure.

Table 11.6 gives a summary of the micellar structure of amphiphiles investigated in this thesis as well as some literature data. The data is sorted by the micellar form, starting with spherical micelles and ending with large vesicles and bilayer structures. As previously described by He *et al*. (2000) and Heerklotz *et al*. (2004), the micellar shape of alkyl glycosides is not temperature-sensitive in a temperature range from 5 to 65 °C. Therefore the results shown in table 11.6 can be compared directly.

TABLE 11.6: Micellar structures of different glycolipids determined by SANS in this thesis together with some literature data (A: Dupuy *et al.*, 1997; B: Minden *et al.*, 2000; C: Erricsson *et al.*, 2005).

Lipid	Micellar form	Conc. [wt%]	Cross section	R_{CS} or thickness of layer [Å]	Length or radius [Å]	T [°C]
Mel-C14	sphere	0.05			21	50
Mel-C14	sphere	0.1			22	50
Mal-EG-C14	sphere	0.05			40	25
Mel-EG-C14	sphere	0.1			35	25
Glc-Y16	sphere	0.07			36	25
Glc-Y16	sphere	0.1			36	25
Mel-α-C18	sphere	0.063			31	50
Maltri-C18:1	sphere	0.01			35	25
Maltri-C18:1	sphere	0.05			35	25
Maltri-C18:1	sphere	0.1			35	25
MDM (Bola)	sphere	1			15	25
Mal-C12 (A)	ellipse	1			28	24
Lac-EG-C14	disc	0.1			12	25
Mal-C14 (B)	rod	0.1	elliptical	20	200	25
Mal-C14 (C)	rod	1	elliptical	21	1700	35
Mal-AB-C14	rod	0.01	spherical	20	500	25
Mal-AB-C14	rod	0.05	elliptical	22	1100	25
Mal-AB-C14	rod	0.1	elliptical	22	1700	25
Mal-C18	rod	0.043	elliptical	27	700	50
Mel-C18:1	rod	0.01	spherical	34	373	25
Mal-EA-C18:1	rod	0.01	spherical	24	230	25
Mal-EA-C18:1	rod	0.05	spherical	25	600	25
Mel-β-Phy	rod	0.05	elliptical	19	290	50
Mal-C18:1	polymer	0.05	spherical	25	>1200	25
Mal-C18:1	polymer	0.1	spherical	25	>1200	25
Gen-C18	disc	0.01		43 (layer)	~1000	25
Gen-C18	disc	0.05		43 (layer)	~1000	25
Gen-C18	disc	0.1		43 (layer)	~1000	25
Lac-C18:1	large aggregate	0.01			~960	50
Mel-β-TMD	bilayer/ vesicle	0.1		39 (layer)	~4000	50

The effect of the alkyl chain length on the micellar form of alkyl β-glycosides is interesting. Compounds with a slightly wedge-shaped or tilted structure (Maltose and Melibiose) no longer form small micelles but larger rod-like aggregates above a certain chain length, which is defined as "critical chain length". For maltosides this chain length was found to be 14 carbon atoms. As can be seen from table 11.6, **Mal-C12** only forms elliptical micelles with a maximum outer diameter of 28 Å, whereas two more carbon atoms in the hydrophobic chain (**Mal-C14**) lead to the formation of rod-like micelles with a length scale of more than 1700 Å. In the case of the alkyl β-melibiosides the critical chain length is about 16 or 18 carbon atoms. The tetradecyl melibioside (**Mel-C14**) still forms spherical micelles with an average radius of 22 Å, unlike the corresponding maltoside **Mal-C14**. With a chain length of 18 carbon atoms the melibioside **Mel-C18:1** also forms rod-like micelles with a length of 373 Å.

The type of anomeric linkage of the alkyl chain to the carbohydrate headgroup also influences the micellar structure. As can be seen from the two melibiosides **Mel-α-C18** and **Mel-C18:1**, the β-anomer favours the formation of rod-like micelles (L = 373 Å) whereas the α-linkage changes the molecular shape, resulting in a very wide hydrophilic part which is best packed into spherical micelles (R = 31 Å).

Data on compounds with a rod-like shape (e.g. lactosides) are difficult to obtain due to their very high Krafft-temperatures. Therefore measurable solutions of rod-like compounds were obtained for the alkyl β-lactosides with an unsaturated oleyl chain (**Lac-C18:1**) or with an ethyleneglycol spacer (**Lac-EG-C14**). This also applies to the β-gentibioside **Gen-C18** with a disaccharide headgroup consisting of two Glucose carbohydrate headgroups linked via a β1→6 glycosidic bond. Both compounds with a long alkyl chain (**Lac-C18:1** and **Gen-C18**) form large aggregates only, which can be expected for compounds with a rod-like molecular shape. The formation of large disc-like aggregates by the lipid **Gen-C18**, with a diameter of around 1000 Å but only a thickness of ~ 43 Å, is unusual. Normally the formation of spherical vesicles or similar aggregates would be expected.

If the headgroup is changed from a di- to a trisaccharide, the molecular shape becomes more cone-like, as a third sugar moiety increases the interaction and repulsive forces. As a result, **Maltri-C18:1** only forms spherical micelles, whereas the corresponding maltosides form rod- and polymerlike micelles. Also a Y-shaped structure with two carbohydrate heads and one aliphatic chain favours the formation of spherical micelles as can be seen for **Glc-Y16**. If a carbohydrate headgroup is positioned at each end of the alkyl chain, a bola-structure is obtained (compound **MDM** - for the molecular structure please refer to Chapter 3). This structure also shows the ability to form spherical micelles in a very narrow concentration range, which transforms with increasing concentration into large aggregate structures.

The type of alkyl chain has to be discussed next. Four alkyl chain types were investigated: linear without a double bond, linear with double bond, short chains with a high degree of

methyl branching, and long chains with a low degree of methyl branching. The difference between the influence of saturated and unsaturated linear chains on the micellar structure is small. When comparing the maltosides **Mal-C18** and **Mal-C18:1** it is found that in both cases rod-like micelles are formed, and only differences in the length scales are observed. On the other hand, the effect of methyl branched chains on the micellar structure is large. A long alkyl chain with a low degree of methylation retains some flexibility and leads to aggregates in a similar way to linear alkyl chains. This can be concluded from the micellar structure of the linear compound **Mel-C18:1** which forms rod-like micelles and the methyl branched compound **Mel-β-Phy**, with a chain length of 16 carbon atoms and 4 methyl groups in the branching, that also forms rod-like micelles. A difference arises only in the length scales (**Mel-C18:1**: L = 3737 Å, **Mel-β-Phy**: L = 290 Å). A short alkyl chain with a high degree of methylation on the other hand looses its flexibility (see Chapter 7), and this makes the formation of micelles difficult. Therefore compound **Mel-β-TMD** forms large bilayer structures and vesicles already in dilute solution.

The use of different spacers between the hydrophilic and the hydrophobic moiety gives the possibility of fine-tuning the micellar properties. The ethylene glycol spacer effects an increase of the hydrophilic part. In the case of the maltoside **Mal-EG-C14** this results in the formation of spherical micelles, whereas the corresponding alkyl maltoside (**Mal-C14**) already forms rod-like micelles. In the case of the melibiosides this affects the overall radius of the micelles. The micellar radius of **Mel-C14**, which forms spherical micelles, was estimated to be 17 Å, whereas for spherical micelles of **Mel-EG-C14**, a total radius of 35 Å was calculated using a core-and-shell model. Despite the fact that the large difference is probably a result of the different models, used for the calculation of the micelle radii, the difference in the pair-distance size distribution remains. A second effect is the increase of flexibility. Usually it would be expected that a compound with a rod-like molecular shape like **Lac-EG-C14**, forms large structures, but in this case the formation of small disc-like micelles has been found. These results also fit the general structural concept as the micellar shape changes from disc-like (rod-like shape of **Lac-EG-C14**) to spherical with a total radius of 40 Å (slightly wedge-shape of **Mal-EG-C14**), and to spherical with a total radius of 35 Å (tilted shape of **Mel-EG-C14**).

The hydrophilic part of the molecule is also increased by the use of an ethanolamine spacer. In this case the hydrophobic chain is linked via an amidic group to the spacer. The comparison of the lipid **Mal-EA-C18:1** and the lipid analogue without spacer **Mal-C18:1** shows that the influence is different to that found for the ethylene glycol spacer. Both compounds form rod-like micelles. Micelles of **Mal-C18:1** are polymer-like, but the micelles of **Mal-EA-C18:1** are shorter. More important is the fact that the micelles of **Mal-C18:1** have a persistence length of ~ 200 Å, whereas micelles of **Mal-EA-C18:1** show no flexibility at all.

The third type of spacer, 2-aminobutane-1-ol, which can be discussed as an ethanolamine spacer with an ethyl branching, increases the hydrophobic part of the molecule. For the glycosides **Mal-AB-C14** the formation of small micelles should be expected, if the hydrophilic part is increased by the spacer. But the opposite behaviour is observed as this compound forms long rod-like micelles. Compared to the alkyl glycoside **Mal-C14** which forms micelles with a length of 1700 Å at a concentration of 1 wt%, **Mal-AB-C14** shows this length scale at a concentration of 0.1 wt%, which is similar to the concentration behaviour of **Mal-C18:1**, where polymer-like micelles with L > 1200 Å are formed at a concentration of 0.1 wt%.

Another general observation is the fact that the spherical micelles do not change the micellar shape (e.g. sphere to rod) with increasing concentration. For rod-like micelles, on the other hand, it was observed that micelles grow in one dimension (length) with increasing concentration. The growth of micelle length can be described as

$$L \sim c^{1/2} \tag{11.2}$$

with: L : Length

c : concentration

which follows classical mean-field models for the micelle growth (Cates and Candau, 1990).

11.5.2 Micellar form and the critical packing parameter

The investigation of the aggregate structure of the amphiphiles above the *CMC* and comparison with the aggregate structures predicted by the critical packing parameter derived from the surface tension measurements is now possible. Literature values on the *CPP* and the real aggregate structure of sugar-based glycolipids are seldom reported, therefore a comparison is difficult. Some measurements of the headgroup area of decyl- and dodecyl-β-D-maltosides have been carried out by Boyd *et al.* (2000), and from this data a *CPP* of 0.50 for decyl-β-D-maltoside and 0.48 for dodecyl-β-D-maltoside has been calculated. Even within the limit of the standard deviation these values do not correlate with the micellar forms described in the literature (see also Chapter 1), which suggests a spherical and slightly elliptical shape for these two compounds.

Table 11.7 shows the micellar form determined by small-angle neutron scattering and the *CPP* calculated from the adsorption at the air-water interface. As the surface tension strongly depends on temperature this effect has also to be taken into account. Obviously nearly half the *CPP* values are not in accordance with the micellar form found in aqueous solution. Nevertheless if the deviation of the values for the headgroup area at the air-water interface is

taken into account, the *CPP* for **Mel-C14**, **Mel-C18:1** and **Mel-β-Phy**, predicts a spherical structure for **Mel-C14** and rod-like structures for **Mel-C18:1** and **Mel-β-Phy** which correlates with the micellar structure determined by SANS.

Even if the deviation is taken into account the discrepancy between the micellar form and the *CPP* remains for the two lipids with an ethyleneglycol spacer **Mal-EG-C14** and **Mel-EG-C14**.

In general the *CPP* model is only of limited use for the prediction of the aggregate structure for sugar-based amphiphiles with more complex carbohydrate headgroups.

TABLE 11.7: Micellar form estimated by SANS and critical packing parameter calculated from surface tension measurements. Deviation of the *CPP* from the micellar form is marked grey.

Compound	T_{SANS} [°C]	Micellar form	T_{CPP} [°C]	CPP
Mal-C14	35	rod	25	0.47
Mel-C14	50	sphere	50	0.35
Mel-β-TMD	50	bilayer/vesicle	40	~1
Mal-EG-C14	25	sphere	30	0.7
Mel-EG-C14	25	sphere	30	0.42
Mal-AB-C14	25	rod	30	0.43
Mal-C18:1	25	rod/polymer	25	0.45
Mel-C18:1	25	rod	25	0.7
Mal-EA-C18:1	25	rod	25	0.45
Mel-β-Phy	50	rod	40	0.7
Maltri-C18:1	25	sphere	25	0.16

11.5.3 Formation of higher ordered lyotropic aggregates

Beside the formation of micelles, the lyotropic phase diagram also shows that lyotropic aggregate structures with a higher degree of order are formed with decreasing water concentration. In this work the structure of these phases was investigated for different lipids by using SAXS and / or FTIR-spectroscopy.

The influence of the alkyl chains on the phase-behaviour of the gel-to-liquid phase transition has been found to depend on the flexibility of the alkyl chains. Whereas linear and saturated alkyl chains show a high flexibility, which results in several possible states of order, an unsaturated alkyl chain is already more rigid and the reduced packing order leads to lower

transition temperatures. Methyl branched chains show no flexibility and the phase transition also occurs at very low temperatures.

TABLE 11.8: Lyotropic aggregate structure determined by SAXS for selected compounds (Q, cubic structure; H_{II}, inverted columnar structure; L, lamellar structure).

Compound	Concentration [wt%]	Temperature [°C]	Structure	Group
Mal-1,3-C18:1	10	20-60	Q	Q^{224} (Pn3m)
	10	60-70	Q	
	20	20-70	Q	Q^{224} (Pn3m)
	10	20 (on cooling)	H_{II}	
	20	20 (on cooling)	H_{II}	
Maltri-1,3-C18:1	10	20-70	L	multi
	20	20-70	L	mulit
Maltri-C18:1	10	20-70	L	uni
	20	20-70	L	uni

The aggregate structure was then determined only for three lipids with unsaturated alkyl chains (table 11.8). The reduced flexibility results in lyotropic phases over a larger temperature range, but as the chains are more flexible than methyl branched chains, lyotropic polymorphism can be found. The results from SAXS-analysis again show the influence of the carbohydrate headgroup on the aggregate structure. The compounds with a trisaccharide headgroup (**Maltri-C18:1** and **Maltri-1,3-C18:1**) only show reflections indicative of a lamellar structure. The difference between the two chain lipid (**Maltri-1,3-C18:1**) and the single chain lipid (**Maltri-C18:1**) can be found in the ordering of the lamellar phases, a multilamellar phase formed by the two chain lipid and unilamellar structures formed by the single chain lipid. Surprisingly the disaccharide **Mal-1,3-C18:1** exhibited an extremely well-resolved cubic phase already at a higher water content and over a very broad temperature range. This cubic structure will be of interest for the investigation of a possible biological function.

11.6 Foaming

11.6.1 Foaming according to Ross-Miles

The foaming behaviour of amphiphilic compounds was investigated by a fairly simple foam test that required only a small amount of substance (see Chapter 1). The foaming behaviour was investigated for concentrations of 0.1 w/v% of amphiphile in bidistilled water at 25 °C and 50 °C. For details of the experimental set-up see Appendix C3. The results are shown in table 11.9 and table 11.10. The amphiphiles are categorised by their foaming ability into moderate, good and excellent foam forming substances. The first general observation is that the foamability is low for surfactants with low solubility and that good foamers always form clear solutions in water. Many of the investigated amphiphiles show a similar, and in part superior, foaming ability and foam stability to that observed for the ionic surfactant sodium dodecyl sulfate (**SDS**) sodium dodecylether sulfate (**SLES**) and alkylpolyglucoside (**APG**). With increasing temperature most of the amphiphiles show an increase of the foam heights. However a decrease is not observed for bad foamers, as the foam heights mainly remained unchanged. Interestingly, the foam stability is dramatically reduced for dodecyl glycosides, e.g **Mal-C12**, **Mel-C12**, **Mel-α-C12** compared to the foam stability at 25 °C. The foaming behaviour of the investigated amphiphilic compounds shows an interesting dependence on their chemical structure. Of course, this cannot be assumed for compounds that do not form clear solutions even at elevated temperature.

Short hydrophobic chains compared to the carbohydrate headgroup are necessary for amphiphiles to show good foaming ability. An additional spacer between the carbohydrate headgroup and the lipophilic chain also enhances the foaming ability.

Long chain amphiphiles are poor foaming agents due to their large hydrophobic part that reduces the interaction forces in the surface of the film in the plateau border of the foam.

Despite this an amide group instead of the glycosidic *O*-linkage results in excellent foaming properties, even for long-chain derivatives, for example **Mal-A-C18:1** and **Mel-A-C18:1**. As previously discussed, the amide group located in the polar headgroup region enhances the formation of a strong hydrogen bonding network which stabilises the film in the plateau border of the foam film.

A change of the structure of the carbohydrate headgroup (e.g. Maltose to Melibiose) has only a minor influence on the foaming properties for similar compounds.

TABLE 11.9: Foaming ability (immediately after agitation) and foam stability (remaining foam after 30 min.) at 25 °C, for selected compounds.

Compound	Foam volume immediately [mL]	Foam volume after 30 min. [mL]	Appearance of solution	Aqueous solubility [w/v%]
Moderate foamers (0-20 mL)				
SLES	20	18	clear	
Mel-EG-C14	19	15	turbid	
Mel-α-C12	16	12	turbid	
Mel-C12	15	11	clear	
Mal-EG-C14	14	13	turbid	
Mal-EA-C18:1	12	10	clear	
Mel-EA-C18:1	11	10	clear	
Maltri-C18:1	8	6	clear	
Mel-C18:1	7	6	clear	
Mal-C18:1	7	5	clear	
Lac-EA-C18:1	4	2	precipitated solid	
Mal-C16	3	2	precipitated solid	
Lac-C18:1	2	0,5	precipitated solid	
Mal-AB-C14	1	1	clear	
Mel-C14	1	0	clear	
Good foamers (20-60 mL)				
APG	60	50	clear	
Mel-A-C18:1	53	48	clear	
Mal-C14	51	47	clear	
Mel-A-C12	50	50	clear	
Mel-EG-C12	50	42	clear	
Mal-EG-C12	48	42	clear	
Mal-C12	40	35	clear	
Excellent foamers (>60 mL)				
Mal-A-C18:1	63	56	clear	
SDS	61	36	clear	

TABLE 11.10: Foaming ability (immediately after agitation) and foam stability (remaining foam after 30 min.) at 50 °C, for selected compounds.

Compound	Foam volume immediately [mL]	Foam volume after 30 min. [mL]	Appearance of solution
Moderate foamers (0-20 mL)			
Mel-C14	18	14	clear
Mal-EA-C18:1	14	12	clear
Mel-A-C16	14	12	turbid
Mel-EA-C18:1	12	10	clear
Mel-C18:1	11	10	clear
Mal-A-C16	11	10	turbid
Maltri-C18:1	10	7	clear
Lac-EG-C14	8	8	clear
Lac-EA-C18:1	8	6	turbid
Lac-C18:1	7	5	clear
Mal-C18:1	4	3	clear
Mal-C16	4	2	precipitated solid
Lac-C12	4	0	turbid
Lac-C14	3	2	precipitated solid
Lac-A-C14	2	2	precipitated solid
Mal-EA-C16	2	2	precipitated solid
Mal-EG-C16	2	2	precipitated solid
Lac-A-C16	1	1	precipitated solid
Lac-C16	1	0,5	precipitated solid
Mel-C16	1	0,5	precipitated solid
Mal-AB-C14	1	0	clear
Mel-β-Phy	10	7	clear
Mel-β-TMD	8	5	clear
Good foamers (20-60 mL)			
Mal-C12	55	25	clear
Mel-C12	54	10	clear
Mel-A-C18:1	50	49	clear
Mel-EG-C12	50	49	clear
Mal-EG-C12	50	48	clear
Mal-EG-C14	47	45	clear
SLES	30	25	clear
Mel-EG-C14	25	12	clear

Compound	Foam volume immediately [mL]	Foam volume after 30 min. [mL]	Appearance of solution
Excellent foamers (>60 mL)			
Mel-α-C12	80	35	clear
Mal-A-C18:1	68	59	clear
APG	65	55	clear
Mel-A-C12	68	35	clear
SDS	63	10	clear
Mal-C14	62	58	clear

11.6.2 Foam microscopy in the presence of hair

Having selected a foamer as a potential candidate for industrial use, it was then compared with known compounds already in use in consumer products. The foam structure of the new lipid **Mal-EG-C12** was compared with the foam structures of a commercially available alkyl polyglucoside (**APG**, Plantaren 2000UP, Cognis, Germany) and a product containing sodium laurylether sulfate (**SLES**) as the main surfactant component. The composition of the **APG** is shown in table 11.11. **Mal-EG-C12** was chosen, because it shows good water solubility and a good constant foaming behaviour at different temperatures. The tests were performed in the laboratory of the Beiersdorf AG, Hamburg. For each experiment a defined hair sample was washed with a given amount of the solution. The obtained foam was investigated by light microscopy to get information about the foam structure and furthermore, the aging of the foam was analysed. The pore size distribution was automatically calculated by using a modelling program.

TABLE 11.11: Composition of the alkyl polyglucoside Plantaren 2000UP, Cognis, Germany (Taken from the technical data sheet, Cognis, Düsseldorf, 2002).

~ 1 wt%	Hexyl α-D-glucopyranoside and Hexyl β-D-glucopyranoside
33-40 wt%	Octyl α-D-glucopyranoside and Octyl β-D-glucopyranoside
21-28 wt%	Decyl α-D-glucopyranoside and Decyl β-D-glucopyranoside
27-32 wt%	Dodecyl α-D-glucopyranoside and Dodecyl β-D-glucopyranoside
9-12 wt%	Tetradecyl α-D-glucopyranoside and Tetradecyl β-D-glucopyranoside
~ 1 wt%	Hexadecyl α-D-glucopyranoside and Hexadecyl β-D-glucopyranoside
+	Higher polymers
+	Fatty alcohol

The results are shown in figures 11.8 - 11.13. The **SLES** containing product initially formed a foam with a rhomboedric structure, whereas **APG** and **Mal-EG-C12** formed spherical foams. Upon aging, the foam structure of **APG** and **Mal-EG-C12** also changes to a rhomboedrical structure. It can also be seen that the foam of **APG** is not very stable upon aging.

The quality of the foams becomes clearer if the pore size distribution of the air bubbles inside the foam are compared. **SLES** shows a broad size distribution with similar parts of small and large air bubbles directly after foam formation. Upon aging, the maximum size distribution shifts towards larger sizes with more than 40% showing sizes larger than 100000 μm^2. Contrary to **SLES** the size distribution for **APG** and **Mal-EG-C12** shows that more than 70% of the air bubbles have initial sizes below 30000 μm^2. Upon aging the size distributions for **APG** and **Mal-EG-C12** are slightly different. Whereas for **APG** after 5 min. more than one third of the air bubbles have sizes of more than 100000 μm^2, for **Mal-EG-C12** only 25 % of the air-bubbles have sizes of more than 100000 μm^2, but still more than 40% of the bubbles are in a size range of less than 30000 μm^2.

In summary, it can be concluded that **Mal-EG-C12** is a better foaming amphiphile than the standard surfactants **SLES** and **APG**. The fact that **Mal-EG-C12** already forms a fine and stable foam as a single substance makes this compound interesting for industrial applications. The foaming properties of **SLES** are optimised in the detergent industry by mixing it with cosurfactants like cocoamphoacetates or cocamidopropylbetaines. However high concentrations of the surfactant are usually necessary. **APG** has better foaming properties at low concentrations due to the fact that **APG** is a complex mixture of different alkyl glucosides and higher adducts of Glucose with an inhomogeneous distribution of the alkyl chains length. Additionally the higher price is a disadvantage compared to **SLES**.
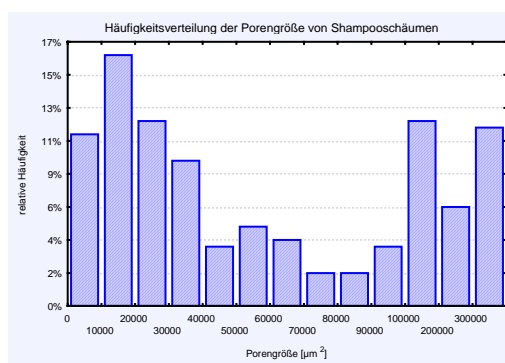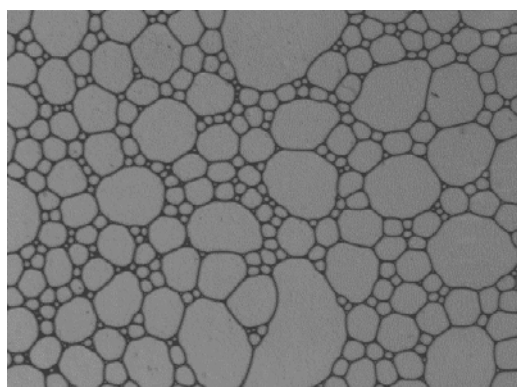

FIGURE 11.8: Left - SLES containing product foam structure (Concentration 15 wt% SLES), after 0 min; Right - Pore size distribution.
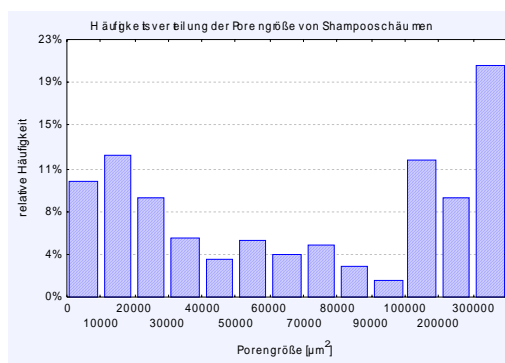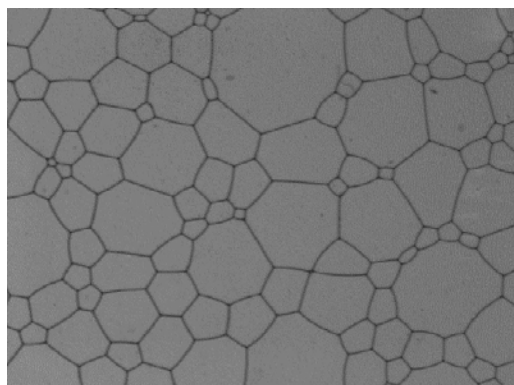
FIGURE 11.9: Left - SLES containing product foam structure (Concentration 15 wt% SLES), after 10 min; Right - Pore size distribution.
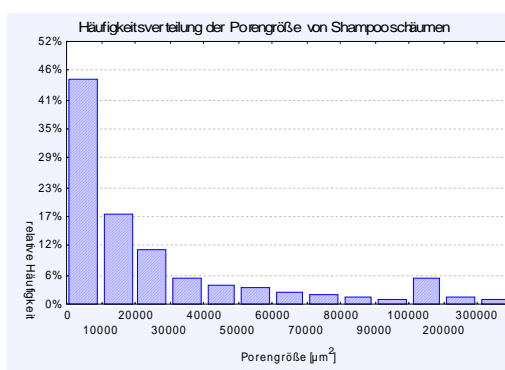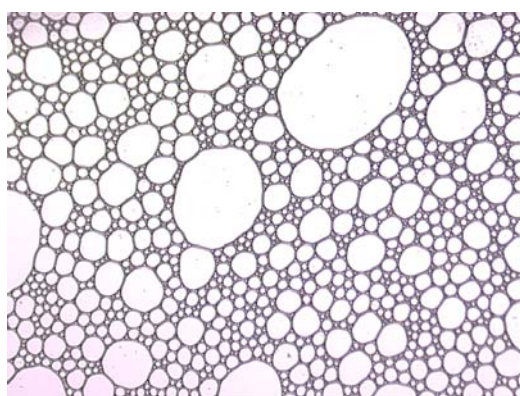
.

FIGURE 11.10: Left - APG foam structure (Concentration 0.1 wt%), after 0 min; Right - Pore size distribution.

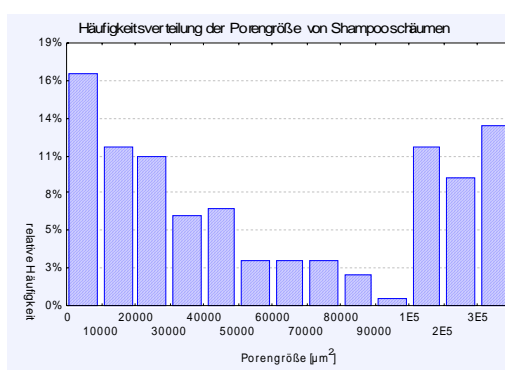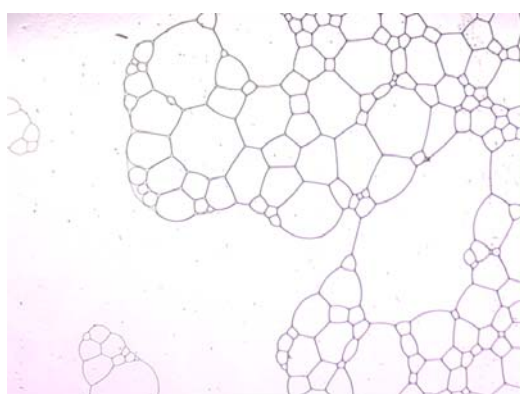**FIGURE 11.11:** Left - APG foam structure (Concentration 0.1 wt%), after 5 min; Right - Pore size distribution.
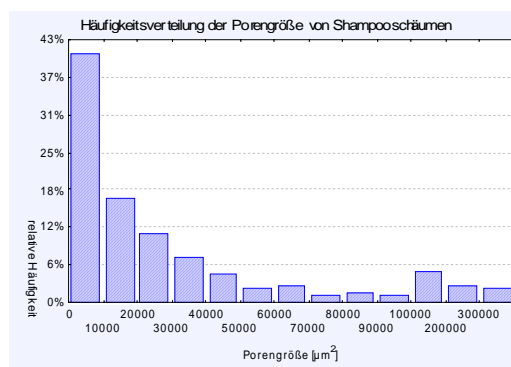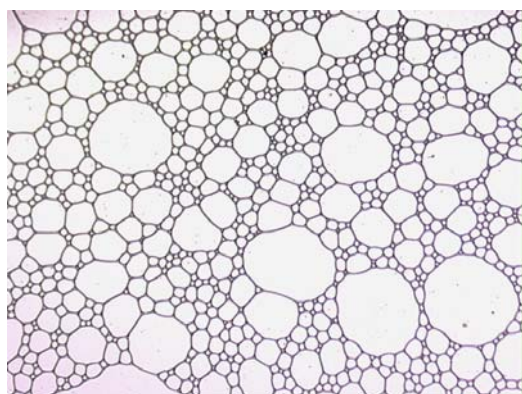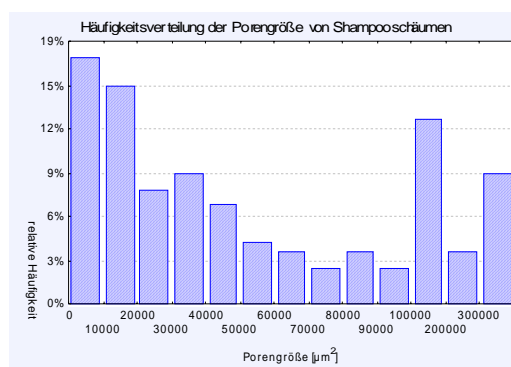
FIGURE 11.12: Left - **Mal-EG-C12** foam structure (Concentration 0.1 wt%), after 0 min; Right - Pore size distribution.
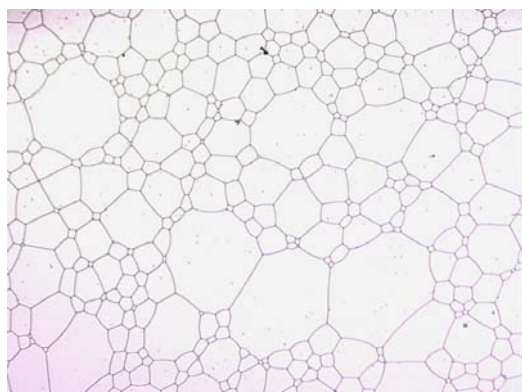

FIGURE 11.13: Left - **Mal-EG-C12** foam structure (Concentration 0.1 wt%), after 5 min; Right - Pore size distribution.

11.7 Perspectives

Based on the results of this thesis, very promising possibilities for future investigations arise. For example:

- The influence of lipids forming lyotropic cubic phases in membrane mixtures or as the major component of vesicles containing drugs or pathogens needs to be investigated.
- What and what kind is the influence of the spacer group between the polar and the non-polar part, especially the flexibility and the ability for the formation of hydrogen bonding networks, on a membrane.
- What structural changes occur if different micelle forms are mixed with proteins, and what use can be made of it?
- The investigation of formation of micelles in the presence of different salts and various salt concentrations.
- The influence of the molecular structure on the formation of mixed micelles of lipids. Design of an appreciated micelle.
- The design of micelles of defined shape allows new applications. The chirality of the carbohydrate headgroup can then be used for chiral interaction or chirality transfer.
- The investigation of the foaming behaviour in a mixture with salts and cosurfactants.
- The synthesis of amphiphiles in a technical scale and investigation of the foaming behaviour.
- The optimisation of the foaming properties by mixing different amphiphiles.
- Little is known about the micellar properties of carbohydrate-based bolaamphiphiles. Recent results show that the addition of bolaamphiphiles in micellar systems can result in different effects, for example stabilisation and growth of micelles formed by ionic surfactants upon the addition of small amounts of bolaamphiphile (Gerber *et al.*, 2005).
- The general concepts, derived from the phase behaviour of the investigated simple lipid structures can be validated in future for its use on more complex and natural structures.

11.8 References

BANOUB, J., BUNDLE, D.R., Stannic tetrachloride catalysed glycosylation of 8-ethoxycarbonyloctanol by cellobiose, lactose and maltose octaacetates; synthesis of α- and β-glycosidic linkages, *Can. J. Chem.*, 57, **1979**, 2085-2090.

BÖCKER, T., THIEM, J., Synthese und Eigenschaften von Kohlenhydrattensiden, *Tenside, Surf. Det.*, 26, **1989**, 318-324.

BOULIGAND, Y., Defects and textures. In: DEMUS, D., GOODBY, J., GRAY, G.W., SPIEß, H.-W., VILL, V. (Eds.), *Handbook of Liquid Crystals*, Vol. 3, Wiley-VCH, Weinheim, **1998**, 406-453.

BOYD, B.J., DRUMMOND, C.J., KRODKIEWSKA, I., GRIESER, F., How chain length, headgroup polymerization, and anomeric configuration govern the thermotropic and lyotropic liquid crystalline phase behaviour and the air-interfacial adsorption of glucose-based surfactants, *Langmuir*, 16, **2000**, 7359-7367.

CATES, M.E., CANDAU, S.J., Statics and dynamics of worm-like surfactant micelles, *J. Phys: Condens. Matter.*, 2, **1990**, 6869-6892.

DUPUY, C., AUVRAY, X., PEPITAS, C., RICO-LATTES, I., LATTES, A., Anomeric effects on the structure of micelles of alkyl maltosides in water, *Langmuir*, 13, **1997**, 3965-3967.

ERICSSON, C.A., SÖDERMAN, O., GARAMUS, V.M., BERGSTRÖM, M., ULVENLUND, S., Effects of temperature, salt, and deuterium oxide on the self-aggregation of alkyl glycosides in dilute solution. 2. *n*-tetradecyl-β-D-maltoside, *Langmuir*, 21, **2005**, 1507-1515.

FAIRHURST, C.E., FULLER, S., GRAY, J., HOLMES, M.C, TIDDY, G.J., Lyotropic surfactant liquid crystals. In: DEMUS, D., GOODBY, J., GRAY, G.W., SPIEß, H.-W., VILL, V. (Eds.), *Handbook of Liquid Crystals*, Vol. 3, Wiley-VCH, Weinheim, **1998**, 341-392.

GERBER, S., GARAMUS, V.M., MILKEREIT, G., VILL, V., Mixed micelles formed by SDS and a carbohydrate-based bolaamphiphile, *Langmuir*, 21 (**2005**), 6707-6711.

GRIFFIN, W.C., Calculation of HLB values of non-ionic surfactants, *J. Soc. Cosmet. Chem.*, 5, **1954**, 249-256.

GRIFFIN, W.C., Classification of surface-active agents by HLB, *J. Soc. Cosmet. Chem.*, 1, **1949**, 311-326.

HE, L.-Z., GARAMUS, V.M., FUNARI, S.S., MALFOIS, M., WILLUMEIT, R., NIEMEYER, B., Comparison of small-angle scattering methods for the structural analysis of octyl-β-D-maltopyranoside micelles, *J. Phys. Chem. B*, 106, **2002**, 7596-7604.

HEERKLOTZ, H., TSAMALOUKAS, A., KITA-TOKARCZYK, K., STRUNZ, P., GUTBERLET, T., Structural, volumetric and thermodynamic characterization of a micellar sphere-to-rod transition, *J. Am. Chem. Soc.*, 126, **2004**, 16544-16552.

HOLMBERG, K., JÖNSSON, B., KRONBERG, B., LINDMAN, B., *Surfactants and Polymers in Aqueous Solution*, 2ⁿᵈ ed., John Wiley & Sons, Chichester, **2003**, 43-46.

JEFFREY, G. A., WINGERT, L. M., Carbohydrate liquid crystals, *Liq. Cryst.*, 12, **1992**, 179-202.

KALLIN, E., LÖNN, H., NORBERG, T., ELOFSSON, M., Derivatization procedures for reducing oligosaccharides. 3. Preparation of oligosaccharide glycosylamines and their conversion into oligosaccharide-acrylamide copolymers, *J. Carbohydr. Chem.*, 8, **1989**, 597-611.

LUBINEAU, A., AUGE, J., DROUILLAT, B., Improved synthesis of glycosylamines and a straightforward preparation of *N*-acylglycosylamines as carbohydrate-based detergents, *Carbohydr. Res.*, 266, **1995**, 211-219.

MANNOCK, D.A., LEWIS, R.N.A.H., MCELHANEY, R.N., An Improved Procedure for the Preparation of 1,2-Di-*O*-acyl-3-*O*-(β-D-glucopyranosyl)-sn-glycerols, *Chem. Phys. Lipids*, 43, **1987**, 113-127.

MASUDA, M., SHIMIZU, T., Synthesis of novel a,w-type 1-glucosamide and 1-galactosamide bolaamphiphiles, *J. Carbohydr. Chem.*, 17, **1998**, 405-416.

MINDEN, v.H.M, MILKEREIT, G., VILL, V., Effects of carbohydrate headgroups on the stability of induced cubic phases in binary mixtures of glycolipids, *Chem. Phys. Lipids*, 120, **2002**, 45-56.

MINDEN, v.H.M., BRANDENBURG, K., SEYDEL, U., KOCH, M.H.J., GARAMUS, V.M., WILLUMEIT, R., VILL, V., Thermotropic and lyotropic properties of long chain alkyl glycopyranosides. Part II: disaccharide headgroups, *Chem. Phys. Lipids*, 106, **2000**, 157-179.

MIURA, Y., ARAI, T., YAMAGATA, T., Synthesis of amphiphilic lactosides that possess a lactosylceramide-mimicking *N*-acyl structure: Alternative universal substrates for *endo*-type glycosylceramidases, *Carbohydr. Res.*, 289, **1996**, 193-199.

SCHMIDT, R.R., KINZY, W., Anomeric-oxygen activation for glycoside synthesis: the trichloroacetimidate method, *Adv. Carbohydr. Chem. Biochem.*, 50, **1994**, 21-123.

SCHMIDT, R.R., MICHEL, J., ROOS, M., Direkte Synthese von *O*-α und *O*-β-Glycosyl-imidaten, *Liebigs Ann. Chem.*, **1984**, 1343-1357.

VILL, V., BÖCKER, T., THIEM, J., FISCHER, F., Studies on liquid crystalline glycosides, *Liq. Cryst.*, 6, **1989**, 349-356.

VILL, V., v.MINDEN, H.M., KOCH, M.H.J., SEYDEL, U., BRANDENBURG, K., Thermotropic and lyotropic properties of long chain alkyl glycopyranosides. Part I: Monosaccharide headgroups, *Chem. Phys. Lipids*, 104, **2000**, 75-91.

WRIGLEY, A.N., STIRTON, A.J., HOWARD, E., Higher alkyl monoethers of mono- to tetraethylene glycol, *J. Org. Chem.*, 25, **1960**, 439-444.

YOSHIDA, H., IKEDA, K., ACHIWA, K., HOSHINO, H., Synthesis of sulfated cerebroside analogs having mimicks of ceramide and their anti-human immunodefiency virus type 1 activities, *Chem. Pharm. Bull.*, 43, **1995**, 594-602.

Appendix A
Unpublished synthesis

Materials and Methods

A description of the materials and methods used for the synthesis is stated in the preceding chapters.

Synthesis

(2-Dodecyloxy-ethyl) 4-*O*-(β-D-galactopyranosyl)-β-D-glucopyranoside (Lac-EG-C12)

6.8 g (10 mmol) Lactoseperacetate and 2.4 g (11 mmol) 2-dodecyloxy-ethanol were dissolved in 100 mL of dry dichlormethane under an atmosphere of dry nitrogen. 1.99 g (1.76 mL; 14 mmol) boron trifluoride etherate were added and the solution was stirred for 5 hours at ambient temperature until t.l.c. revealed the reaction to be complete. The reaction was quenched with 50 mL of a saturated solution of sodium hydrogen carbonate, the organic layer was separated and the aqueous layer was extracted twice with dichlormethane. The combined organic phases were washed twice with water, dried over magnesium sulphate and evaporated *in vacuo*. The residue was purified by column chromatography (light petroleum b.p. 50-70 °C - ethyl acetate 1:1).

Yield: 2.51 g (30 %)

2.5 g (4.5 mmol) (2-Dodecyloxy-ethyl) 4-*O*-(2,3,4,6-tetra-*O*-acetyl-β-D-galactopyranosyl)-2,3,6-tri-*O*-acetyl-β-D-glucopyranoside were dissolved in 50 mL anhydrous methanol and sodium methoxide was added (pH 8-9). The solution was stirred at ambient temperature until t.l.c. revealed the reaction to be complete. It was neutralised then by using Amberlyst IR 120 ion-exchange resign (protonated form), filtrated and evaporated *in vacuo*. The product was purified by column chromatography (chloroform / methanol 9:1).

Yield: 1.6 g (95 %).

(2-Dodecyloxy-ethyl) 4-O-(2,3,4,6-tetra-O-acetyl-β-D-galactopyranosyl)-2,3,6-tri-O-acetyl-β-D-glucopyranoside:

^{1}H-NMR (400 MHz, CDCl$_3$ + TMS): δ = 5.28 (dd, 1H, $^3J_{4',5'}$ 1.0, H-4'), 5.13 (dd, 1H, $^3J_{3,4}$ 9.7, H-3), 5.04 (dd, 1H, $^3J_{2',3'}$ 10.1, H-2'), 4.88 (dd, 1H, $^3J_{3',4'}$ 3.5, H-3'), 4.83 (dd, 1H, $^3J_{1,2}$ 8.1, $^3J_{2,3}$ 9.7, H-2), 4.50 (d, 1H, H-1), 4.42 (dd, 1H, $^3J_{5,6a}$ 2.0, $^3J_{6a,b}$ 12.2, H-6a), 4.41 (d, 1H, $^3J_{1',2'}$ 8.1, H-1'), 3.98 - 4.09 (m, 3H, H-6b, H-6a', H-6b'), 3.77 - 3.86 (m, 2H, H-5', H-αa), 3.72 (dd, 1H, $^3J_{4,5}$ 9.7, H-4), 3.59 - 3.65 (m, 1H, H-αb), 3.53 (ddd, 1H, $^3J_{5,6b}$ 6.1, H-5), 3.46 - 3.50 (m, 2H, H-βa, H-βb), 3.35 (m$_c$, 2H, Alkyl-α-CH$_2$), 2.08, 2.05, 1.99 (each s, 3H, OAc), 1.98 (s, 6H, 2x OAc), 1.97, 1.90 (each s, 3H, OAc), 1.44 - 1.50 (m, 2H, Alkyl β-CH$_2$), 1.14 - 1.28 (m, 18H, Alkyl-CH$_2$), 0.81 (t, 3H, Alkyl-CH$_3$).

^{13}C-NMR (125 MHz, CDCl$_3$ + TMS): δ = 170.89, 170.67, 170.18, 170.02, 169.78 (C=O, OAC), 100.08 (C-1'), 99.66 (C-1), 71.85 (C-3), 71.62 (C-5), 70.67 (C-2), 70.62 (C-α), 70.01 (C-3'), 69.69 (C-5'), 68.70 (C-β), 68.14 (C-2'), 68.06 (C-α-Alkyl), 65.62 (C-4'), 61.04 (C-6), 59.79 (C-6'), 32.33, 30.15, 30.08, 30.05, 30.02, 29.93, 29.76, 26.51 (Alkyl-CH$_2$), 21.29, 21.24, 21.12, 21.05, 20.99 (CH$_3$, OAc), 14.54 (Alkyl-CH$_3$).

C$_{40}$H$_{64}$O$_{19}$ (848.4042)

$[\alpha]_D^{20}$ = +7 (c = 0.4, CHCl$_3$), Lit.: $[\alpha]_D^{20}$ = +7.0 (c = 0.27, CHCl$_3$) (Yoshida et al., 1995)

MALDI-TOF: m/z = 872.3 [M+Na]$^+$

(2-Dodecyloxy-ethyl) 4-O-(β-D-galactopyranosyl)-β-D-glucopyranoside:

^{1}H-NMR (400 MHz, pyridine-d$_5$): δ = 5.47 (d, 1H, $^3J_{1',2'}$ 8.1, H-1'), 5.24 (d, 1H, $^3J_{1,2}$ 8.1, H-1), 4.82 - 4.99 (m, 5H, H-6a, H-2', H-3', H-4', H-5'), 4.76 - 4.82 (m, 1H, H-αa), 4.59 - 4.70 (m, 3H, H-6a', H-6b', H-αb), 4.51 - 4.58 (m, 2H, H-5, H-6b), 4.40 (dd, 1H, $^3J_{4,5}$ 9.5, H-4), 4.34 (dd, 1H, $^3J_{2,3}$ 9.5, $^3J_{3,4}$ 9.5, H-3), 4.25 (dd, 1H, H-2), 4.02 (m$_c$, 2H, β-CH$_2$), 3.80 (m$_c$, 2H, Alkyl-α-CH$_2$), 1.91 - 1.99 (m, 2H, Alkyl-β-CH$_2$), 1.52 - 1.70 (m, 22H, Alkyl-CH$_2$), 1.24 (t, 3H, Alkyl-CH$_3$).

C$_{26}$H$_{50}$O$_{12}$ (554.3302)

$[\alpha]_D^{20}$ = +3 (c = 0.5, MeOH), Lit.: $[\alpha]_D^{20}$ = +2.4 (c = 0.36, MeOH) (Yoshida et al., 1995)

MALDI-TOF: m/z = 577.1 [M+Na]$^+$

Anal Calcd C, 56.30; H, 9.09. Found C, 56.35; H, 9.10

(2-Dodecyloxy-ethyl) 4-*O*-(α-D-glucopyranosyl)-β-D-glucopyranoside (Mal-EG-C12)

β-D-Maltoseoctaacetat was reacted as described for **Lac-EG-C12**.

Yield: 4.0 g (47 %).

3.8 g (4.6 mmol) (2-Dodecyloxy-ethyl) 4-*O*-(2,3,4,6-tetra-*O*-acetyl-α-D-glucopyranosyl)-2,3,6-tri-*O*-acetyl-β-D-glucopyranoside were deprotected as described for **Lac-EG-C12**. The product was recrystallised from 2-propanol.

Yield: 2.4 g (96%).

(2-Dodecyloxy-ethyl) 4-O-(2,3,4,6-tetra-O-acetyl-α-D-glucopyranosyl)-2,3,6-tri-O-acetyl-β-D-glucopyranoside:

^{1}H-NMR (400 MHz, CDCl$_3$ + TMS): δ = 5.34 (d, 1H, $^3J_{1',2'}$ 3.8, H-1'), 5.29 (dd, 1H, $^3J_{2',3'}$ 9.7, $^3J_{3',4'}$ 9.7, H-3'), 5.18 (dd, 1H, $^3J_{2,3}$ 9.2, $^3J_{3,4}$ 9.2, H-3), 4.98 (dd, 1H, $^3J_{4',5'}$ 9.7, H-4'), 4.79 (dd, 1H, H-2'), 4.76 (dd, 1H, $^3J_{1,2}$ 8.1, H-2), 4.56 (d, 1H, H-1), 4.41 (dd, 1H, $^3J_{5,6a}$ 2.8, $^3J_{6a,b}$ 12.0, H-6a), 4.13 - 4.20 (m, 2H, H-6b, H-6a'), 3.60 - 3.68 (m, 2H, H-5, H-αa), 3.45 - 3.52 (m, 2H, H-βa, H-βb), 3.35 (m$_c$, 2H, Alkyl-α-CH$_2$), 3.98 (dd, 1H, $^3J_{5',6b'}$ 2.3, $^3J_{6a',b'}$ 12.5, H-6b'), 3.93 (t, 3H, $^3J_{4,5}$ 9.2, H-4), 3.81 - 3.91 (m, 2H, H-5', H-αb), 2.07, 2.03, 1.98, 1.96, 1.95 (each s, 3H, OAc), 1.93 (s, 6H, OAc), 1.48 (m$_c$, 2H, Alkyl-β-CH$_2$), 1.12 - 1.28 (m, 18H, Alkyl-CH$_2$), 0.81 (t, 3H, Alkyl-CH$_3$).

^{13}C-NMR (100 MHz, CDCl$_3$ + TMS): δ = 170.98, 170.91, 170.66, 170.38, 170.09, 169.86 (C=O, OAC), 100.79 (C-1), 95.96 (C-1'), 75.86 (C-3), 73.17 (C-4), 72.52 (C-2), 72.06, 72.03 (C-5, α-CH$_2$), 70.41 (C-2'), 70.12 (β-CH$_2$), 69.84 (C-3'), 69.77 (Alkyl-α-CH$_2$), 69.53 (C-5'), 68.90 (C-4'), 63.28 (C-6), 61.92 (C-6'), 32.33, 30.14, 30.08, 30.05, 30.02, 29.93, 29.76, 26.51, 23.10 (Alkyl-CH$_2$), 21.36, 21.27, 21.11, 21.08, 21.04, 20.99 (CH$_3$, OAc), 14.47 (Alkyl-CH$_3$).

C$_{40}$H$_{64}$O$_{19}$ (848.9266)

$[\alpha]_D^{20}$ = +24 (c = 0.4, CHCl$_3$)

MALDI-TOF: m/z = 872.8 [M+Na]$^+$

(2-Dodecyloxy-ethyl) 4-O-(α-D-glucopyranosyl)-β-D-glucopyranoside:

^{1}H-NMR (400 MHz, d$_4$-Methanol): δ = 5.16 (d, 1H, $^3J_{1',2'}$ 3.6, H-1'), 4.33 (d, 1H, $^3J_{1,2}$ 8.1, H-1), 4.02 (dd, 1H, $^3J_{5,6a}$ 2.0, $^2J_{6a,b}$ 12.0, H-6a), 3.90 (dd, 1H, $^3J_{5,6b}$ 4.6, H-6b), 3.79 - 3.78 (m, 2H, H-4', H-6a'), 3.48 - 3.76 (m, 11H, H-3, H-4, H-3', H-5', H-6b', α-CH$_2$, β-CH$_2$), 3.45 (dd, 1H, $^3J_{2',3'}$ 10.1, H-2'), 3.39 (ddd, 1H, $^3J_{4,5}$ 9.7, H-5), 3.24 - 3.32 (m, 3H, H-2, Alkyl-α-CH$_2$), 1.59 (m$_c$, 2H, Alkyl-β-CH$_2$), 1.21 - 1.41 (m, 18H, Alkyl-CH$_2$), 0.91 (t, 3H, Alkyl-CH$_3$).

C$_{26}$H$_{50}$O$_{12}$ (554.3302)

$[\alpha]_D^{20}$ = +18 (c = 0.1, MeOH)

MALDI-TOF: m/z = 578.0 [M+Na]$^+$

Anal. Calcd C, 56.30; H, 9.09. Found C, 56.31; H, 9.11

(2-Dodecyloxy-ethyl) 6-*O*-(α-D-galactopyranosyl)-β-D-glucopyranoside (Mel-EG-C12)

β-D-Melibioseoctaacetat was reacted as described for **Lac-EG-C12**.

Yield: 3.0 g (35%).

2.9 g (1.73 mmol) (2-Dodecyloxy-ethyl) 6-*O*-(2,3,4,6-tetra-*O*-acetyl-α-D-galactopyranosyl)-2,3,4-tri-*O*-acetyl-β-D-glucopyranoside were deprotected as described for **Lac-EG-C12**. The product was recrystallised from methanol.

Ausbeute: 1.8 g (94%).

(2-Dodecyloxy-ethyl) 6-O-(2,3,4,6-tetra-O-acetyl-α-D-galactopyranosyl)-2,3,4-tri-O-acetyl-β-D-glucopyranoside:

^{1}H-NMR (400 MHz, CDCl$_3$ + TMS): δ = 5.38 (dd, 1H, $^3J_{4',5'}$ 1.3, H-4'), 5.28 (dd, 1H, $^3J_{2',3'}$ 10.5, $^3J_{3',4'}$ 3.5, H-3'), 5.14 (t, 1H, $^3J_{2,3}$ 9.7, $^3J_{3,4}$ 9.7, H-3), 5.10 (d, 1H, $^3J_{1',2'}$ 3.6, H-1'), 5.04 (dd, 1H, H-2'), 5.00 (t, 1H, $^3J_{4,5}$ 9.7, H-4), 4.87 (dd, 1H, H-2), 4.53 (d, 1H, $^3J_{1,2}$ 8.2 , H-1), 4.17 (ddd, 1H, H-5'), 4.04 (dd, 1H, $^3J_{5',6a'}$ 5.6, $^3J_{6a',b'}$ 11.2, H-6a'), 4.01 (dd, 1H, $^3J_{5',6b'}$ 6.6, H-6b'), 3.79 - 3.85 (m, 1H, H-αa), 3.68 (dd, 1H, $^3J_{5,6a}$ 5.6, $^3J_{6a,b}$ 11.4, H-6a), 3.61 - 3.66 (m, 1H, H-αb), 3.59 (ddd, 1H, $^3J_{5,6b}$ 2.0, H-5), 3.52 (dd, 1H, H-6b), 3.45 - 3.51 (m, 2H, H-βa, H-βb), 3.35 (m$_c$, 2H, Alkyl-α-CH$_2$), 2.07, 2.06, 1.98, 1.97, 1.96, 1.93, 1.91 (each s, 3H, OAc), 1.43 - 1.51 (m, 2H, Alkyl-β-CH$_2$), 1.12 - 1.30 (m, 18H, Alkyl-CH$_2$), 0.81 (t, 3H, Alkyl-CH$_3$).

^{13}C-NMR (100 MHz, CDCl$_3$ + TMS): δ = 170.53, 170.30, 170.18, 169.82, 169.33, 169.28 (C=O, OAc), 100.42 (C-1), 97.43 (C-1'), 73.93 (C-3), 73.62 (C-5), 72.01 (C-α) 71.99 (C-2), 70.71 (C-β) 70.02 (Alkyl-α-CH$_2$), 69.54 (C-4), 68.55, 68.48 (C-4', C-2'), 67.57 (C-3'), 66.42 (C-5'), 66.31 (C-6), 62.93 (C-6'), 32.33, 31.88, 29.48, 29.42, 29.38, 29.03, 25.59, 22.37 (Alkyl-CH$_2$), 20.65, 20.55, 20.50, 20.35 (-CH$_3$, OAc), 14.14 (Alkyl-CH$_3$).

C$_{40}$H$_{64}$O$_{19}$ (848.9266)

$[\alpha]_D^{20}$ = +53 (c = 0.2, CHCl$_3$)

MALDI-TOF: m/z = 872.0 [M+Na]$^+$

(2-Dodecyloxy-ethyl) 6-O-(α-D-galactopyranosyl)-β-D-glucopyranoside:

^{1}H-NMR (400 MHz, d$_4$-Methanol): δ = 4.90 (d, 1H, $^3J_{1',2'}$ 3.4, H-1'), 4.27 (d, 1H, $^3J_{1,2}$ 8.1, H-1), 3.87 - 3.94 (m, 2H, H-6a, H-αa), 3.80 - 3.87 (m, 2H, H-4', H-5'), 3.62 - 3.70 (m, 6H, H-2', H-3', H-6a', H-6b', H-6b, H-αb), 3.55 - 3.60 (m, 2H, β-CH$_2$), 3.38 - 3.46 (m, 3H, H-5, Alkyl-α-CH$_2$), 3.34 (dd, 1H, H-4), 3.30 (dd, 1H, $^3J_{2,3}$ 9.2, $^3J_{3,4}$ 9.2, H-3), 3.15 (dd, 1H, H-2), 1.47 - 1.56 (m, 2H, Alkyl-β-CH$_2$), 1.16 - 1.35 (m, 18H, Alkyl-CH$_2$), 0.84 (t, 3H, Alkyl-CH$_3$).

C$_{26}$H$_{50}$O$_{12}$ (554.3302)

$[\alpha]_D^{20}$ = +50 (c = 1.0, MeOH)

MALDI-TOF: m/z = 577.5 [M+Na]$^+$

Anal. Calcd C, 56.30; H, 9.09. Found C, 56.39; H, 9.11

(2-Tetradecyloxy-ethyl) 4-*O*-(β-D-galactopyranosyl)-β-D-glucopyranoside (Lac-EG-C14)

6.8 g (10 mmol) β-D-Lactoseoctaacetat and 2.8 g (11 mmol) 2-Tetradecyloxy-ethanol were reacted as described for **Lac-EG-C12**.

Yield: 2.9 g (34 %).

2.8 g (3.2 mmol) (2-Tetradecyloxy-ethyl) 4-O-(2,3,4,6-tetra-O-acetyl-β-D-galactopyranosyl)-2,3,6-tri-O-acetyl-β-D-glucopyranoside were deprotected as described for **Lac-EG-C12**. The product was recrystallised from methanol.

Yield: 1.8 g (92%).

(2-Tetradecyloxy-ethyl) 4-O-(2,3,4,6-tetra-O-acetyl-β-D-galactopyranosyl)-2,3,6-tri-O-acetyl-β-D-glucopyranoside:

^{1}H-NMR (400 MHz, CDCl$_3$ + TMS): δ = 5.28 (dd, 1H, $^3J_{3',4'}$ 3.5, $^3J_{4',5'}$ 1.0, H-4'), 5.12 (dd, 1H, $^3J_{3,4}$ 9.5, H-3), 5.04 (dd, 1H, $^3J_{1',2'}$ 8.1, $^3J_{2',3'}$ 10.4, H-2'), 4.88 (dd, 1H, H-3'), 4.83 (dd, 1H, $^3J_{2,3}$ 9.5, H-2), 4.49 (d, 1H, $^3J_{1,2}$ 8.1, H-1), 4.39 - 4.44 (m, 2H, H-1', H-6a), 3.98 - 4.08 (m, 3H, H-6b, H-6a', H-6b'), 3.78 - 3.84 (m, 2H, H-5', H-αa), 3.72 (dd, 1H, $^3J_{4,5}$ 9.7, H-4), 3.59 - 3.64 (m, 1H, H-αb), 3.53 (ddd, 1H, $^3J_{5,6a}$ 2.0, $^3J_{5,6b}$ 6.1, H-5), 3.46 - 3.50 (m, 2H, H-βa, H-βb), 3.34 (m$_c$, 2H, Alkyl-α-CH$_2$), 2.08, 2.05, 1.99 (each s, 3H, OAc), 1.97 (s, 6H, 2x OAc), 1.96, 1.89 (each s, 3H, OAc), 1.44 - 1.51 (m, 2H, Alkyl β-CH$_2$), 1.14 - 1.28 (m, 22H, Alkyl-CH$_2$), 0.81 (t, 3H, Alkyl-CH$_3$).

^{13}C-NMR (125 MHz, CDCl$_3$ + TMS): δ = 170.93, 170.80, 170.65, 170.12, 170.00, 169.87 (C=O, OAc), 100.08 (C-1'), 99.66 (C-1), 71.85 (C-3), 71.62 (C-5), 70.67 (C-2), 70.62 (C-α), 70.01 (C-3'), 69.69 (C-5'), 68.70 (C-β), 68.14 (C-2'), 68.06 (C-α-Alkyl), 65.62 (C-4'), 61.04 (C-6), 59.79 (C-6'), 30.91, 28.71, 28.67, 28.63, 28.59, 28.50, 28.34, 25.08, 21.67 (Alkyl-CH$_2$), 21.37, 21.09, 21.01, 20.99, 20.96, 20.94 (CH$_3$, OAc), 13.10 (Alkyl-CH$_3$).

C$_{42}$H$_{68}$O$_{19}$ (876.4355)

$[\alpha]_D^{20}$ = +15 (c = 1.1, CHCl$_3$)

MALDI-TOF: m/z = 900.1 [M+Na]$^+$

(2-Tetradecyloxy-ethyl) 4-O-(β-D-galactopyranosyl)-β-D-glucopyranoside:

^{1}H-NMR (400 MHz, Pyridin-d$_5$): δ = 5.48 (d, 1H, $^3J_{1',2'}$ 8.1, H-1'), 5.22 (d, 1H, $^3J_{1,2}$ 8.1, H-1), 4.80 - 4.95 (m, 5H, H-6a, H-2', H-3', H-4', H-5'), 4.73 - 4.79 (m, 1H, H-αa), 4.59 - 4.70 (m, 3H, H-6a', H-6b', H-αb), 4.50 - 4.56 (m, 2H, H-5, H-6b), 4.41 (dd, 1H, $^3J_{3,4}$ 9.5, $^3J_{4,5}$ 9.5, H-4), 4.32 (dd, 1H, $^3J_{2,3}$ 9.5, H-3), 4.26 (dd, 1H, H-2), 4.09 (m$_c$, 2H, β-CH$_2$), 3.83 (m$_c$, 2H, Alkyl-α-CH$_2$), 1.93 - 2.01 (m, 2H, Alkyl-β-CH$_2$), 1.56 - 1.79 (m, 22H, Alkyl-CH$_2$), 1.26 (t, 3H, Alkyl-CH$_3$).

C$_{28}$H$_{54}$O$_{12}$ (582.3615)

$[\alpha]_D^{20}$ = +2 (c = 0.2, MeOH)

MALDI-TOF: m/z = 583.4 [M+Na]$^+$

Anal. Calcd C, 57.71; H, 9.34. Found C, 57.78; H, 9.38

(2-Tetradecyloxy-ethyl) 4-O-(α-D-glucopyranosyl)-β-D-glucopyranoside (Mal-EG-C14)

β-D-Maltoseoctaacetat was reacted as described for **Lac-EG-C14**.

Yield: 4.7 g (54%).

4.6 g (5.2 mmol) (2-Tetradecyloxy-ethyl) 4-O-(2,3,4,6-tetra-O-acetyl-α-D-glucopyranosyl)-2,3,6-tri-O-acetyl-β-D-glucopyranoside were deprotected as described for **Lac-EG-C12**.

Yield: 3.1 g (98%).

(2-Tetradecyloxy-ethyl) 4-O-(2,3,4,6-tetra-O-acetyl-α-D-glucopyranosyl)-2,3,6-tri-O-acetyl-β-D-glucopyranoside:

^{1}H-NMR (400 MHz, CDCl$_3$ + TMS): δ = 5.34 (d, 1H, $^3J_{1',2'}$ 4.1, H-1'), 5.29 (dd, 1H, $^3J_{2',3'}$ 9.7, $^3J_{3',4'}$ 9.7, H-3'), 5.18 (dd, 1H, $^3J_{3,4}$ 9.2, H-3), 4.98 (dd, 1H, $^3J_{4',5'}$ 9.7, H-4'), 4.79 (dd, 1H, H-2'), 4.76 (dd, 1H, $^3J_{1,2}$ 8.1, $^3J_{2,3}$ 9.2,

H-2), 4.56 (d, 1H, H-1), 4.41 (dd, 1H, $^3J_{5,6a}$ 2.8, $^3J_{6a,b}$ 12.0, H-6a), 4.13 - 4.20 (m, 2H, H-6b, H-6a'), 3.98 (dd, 1H, $^3J_{5',6b'}$ 2.3, $^3J_{6a',b'}$ 12.5, H-6b'), 3.93 (dd, 1H, $^3J_{4,5}$ 9.4, H-4), 3.90 (m$_c$, 1H, H-5'), 3.81 - 3.87 (m, 1H, H-αa), 3.57 - 3.67 (m, 2H, H-5, H-αb), 3.46 - 3.50 (m, 2H, H-βa, H-βb), 3.32 - 3.37 (m, 2H, Alkyl-α-CH$_2$), 2.07, 2.03, 1.98, 1.95 (each s, 3H, OAc), 1.93 (s, 6H, 2x OAc), 1.43 - 1.51 (m, 2H, Alkyl-β-CH$_2$), 1.14 - 1.28 (m, 22H, Alkyl-CH$_2$), 0.81 (t, 3H, Alkyl-CH$_3$).

^{13}C-NMR (100 MHz, CDCl$_3$ + TMS): δ = 170.94, 170.87, 170.62, 170.34, 170.05, 169.82 (C=O, OAC), 100.79 (C-1), 95.97 (C-1'), 75.86 (C-3), 73.22 (C-4), 72.59 (C-2), 72.54 (C-5), 72.02 , (α-CH$_2$), 70.42 (C-2'), 70.09 (β-CH$_2$), 69.79 (C-3'), 69.51 (Alkyl-α-CH$_2$), 68.90 (C-5'), 68.48 (C-4'), 63.29 (C-6), 61.94 (C-6'), 32.32, 30.13, 30.09, 30.07, 30.05, 30.04, 30.01, 29.92, 26.50, 23.09 (Alkyl-CH$_2$), 21.32, 21.23, 21.07, 21.04, 21.00, 20.97 (CH$_3$, OAc), 14.51 (Alkyl-CH$_3$).

C$_{42}$H$_{68}$O$_{19}$ (876.4355)

$[\alpha]_D^{20}$ = +30 (c = 1.1, CHCl$_3$)

MALDI-TOF: m/z = 900.9 [M+Na]$^+$

(2-Tetradecyloxy-ethyl) 4-O-(α-D-glucopyranosyl)-β-D-glucopyranoside:

^{1}H-NMR (400 MHz, d$_4$-Methanol): δ = 5.17 (d, 1H, $^3J_{1',2'}$ 3.6, H-1'), 4.32 (d, 1H, $^3J_{1,2}$ 8.1, H-1), 4.01 (dd, 1H, $^3J_{5,6a}$ 2.0, H-6a), 3.90 (dd, 1H, $^3J_{5,6b}$ 4.6, $^2J_{6a,b}$ 12.0, H-6b), 3.79 - 3.86 (m, 2H, H-4', H-6a'), 3.48 - 3.76 (m, 11H, H-3, H-4, H-3', H-5', H-6b', α-CH$_2$, β-CH$_2$), 3.45 (dd, 1H, $^3J_{2',3'}$ 10.1, H-2'), 3.38 (ddd, 1H, $^3J_{4,5}$ 9.7, H-5), 3.24 - 3.31 (m, 3H, H-2, Alkyl-α-CH$_2$), 1.55 - 1.64 (m, 2H, Alkyl-β-CH$_2$), 1.19 - 1.42 (m, 22H, Alkyl-CH$_2$), 0.91 (t, 3H, Alkyl-CH$_3$).

C$_{28}$H$_{54}$H$_{12}$ (582.3615)

$[\alpha]_D^{20}$ = +30 (c = 0.8, MeOH)

MALDI-TOF: m/z = 583.0 [M+Na]$^+$

Anal. Calcd C, 57.71; H, 9.34. Found C, 57.80; H, 9.37

(2-Tetradecyloxy-ethyl) 6-*O*-(α-D-galactopyranosyl)-β-D-glucopyranoside (Mel-EG-C14)

β-D-Melibioseoctaacetat was reacted as described for **Lac-EG-C14**.

Yield: 2.7 g (31%).

2.6 g (3 mmol) (2-Tetradecyloxy-ethyl) 6-*O*-(2,3,4,6-tetra-*O*-acetyl-α-D-galactopyranosyl)-2,3,4-tri-*O*-acetyl-β-D-glucopyranoside were deprotected as described for **Lac-EG-C12**.

Yield: 1.8 g (99%).

(2-Tetradecyloxy-ethyl) 6-O-(2,3,4,6-tetra-O-acetyl-α-D-galactopyranosyl)-2,3,4-tri-O-acetyl-β-D-glucopyranoside:

^{1}H-NMR (400 MHz, CDCl$_3$ + TMS): δ = 5.38 (dd, 1H, $^3J_{3',4'}$ 3.5, $^3J_{4',5'}$ 1.3, H-4'), 5.27 (dd, 1H, $^3J_{2',3'}$ 11.0, H-3'), 5.14 (dd, 1H, $^3J_{3,4}$ 9.7, H-3), 5.10 (d, 1H, $^3J_{1',2'}$ 3.8, H-1'), 5.04 (dd, 1H, H-2'), 5.00 (dd, 1H, $^3J_{4,5}$ 9.8, H-4), 4.87 (dd, 1H, $^3J_{1,2}$ 8.2, $^3J_{2,3}$ 9.7, H-2), 4.53 (d, 1H, H-1), 4.17 (ddd, 1H, $^3J_{5',6a'}$ 5.6, $^3J_{5',6b'}$ 6.6, H-5'), 4.06 (dd, 1H, $^3J_{6a',b'}$ 11.2, H-6a'), 4.01 (dd, 1H, H-6b'), 3.82 (m$_c$, 1H, H-αa), 3.68 (dd, 1H, $^3J_{5,6a}$ 5.0, $^3J_{6a,b}$ 11.4, H-6a), 3.62-3.66 (m, 1H, H-αb), 3.59 (ddd, 1H, $^3J_{5,6b}$ 2.0, H-5), 3.52 (dd, 1H, H-6b), 3.46 - 3.50 (m, 2H, H-βa, H-βb), 3.34 (m$_c$, 2H, Alkyl-α-CH$_2$), 2.07, 2.06, 1.98, 1.97, 1.96, 1.93, 1.92 (each s, 3H, OAc), 1.44 - 1.50 (m, 2H, Alkyl-β-CH$_2$), 1.15 - 1.26 (m, 22H, Alkyl-CH$_2$), 0.81 (t, 3H, Alkyl-CH$_3$).

^{13}C-NMR (100 MHz, CDCl$_3$ + TMS): δ = 170.52, 170.31, 170.17, 169.83, 169.32, 169.27 (C=O, OAc), 100.52 (C-1), 96.43 (C-1'), 72.93 (C-3), 72.62 (C-5), 71.99 (C-α) 71.34 (C-2), 70.01 (C-β) 69.98 (Alkyl-α-CH$_2$), 69.04

(C-4), 68.05, 68.04 (C-4', C-2'), 67.43 (C-3'), 66.44 (C-5'), 66.41 (C-6), 61.63 (C-6'), 32.35, 31.90, 29.68, 29.62, 29.40, 29.23, 25.86, 22.66 (Alkyl-CH_2), 20.76, 20.67, 20.63, 20.61 (-CH_3, OAc), 14.09 (Alkyl-CH_3).

$C_{42}H_{68}O_{19}$ (876.4355)

$[\alpha]_D^{20} = +50$ (c = 1.1, $CHCl_3$)

MALDI-TOF: m/z = 899.8 $[M+Na]^+$

(2-Tetradecyloxy-ethyl) 6-O-(α-D-galactopyranosyl)-β-D-glucopyranoside:

^{1}H-NMR (400 MHz, d_4-Methanol): δ = 4.90 (d, 1H, $^3J_{1',2'}$ 3.4, H-1'), 4.32 (d, 1H, $^3J_{1,2}$ 8.1, H-1), 3.85 - 4.03 (m, 2H, H-6a, H-αa), 3.71 - 3.83 (m, 2H, H-4', H-5'), 3.59 - 3.68 (m, 6H, H-2', H-3', H-6a', H-6b', H-6b, H-αb), 3.53 - 3.57 (m, 2H, β-CH_2), 3.36 - 3.43 (m, 3H, H-5, Alkyl-α-CH_2), 3.31 (dd, 1H, $^3J_{3,4}$ 9.2, H-4), 3.27 (dd, 1H, $^3J_{2,3}$ 9.2, H-3), 3.14 (dd, 1H, H-2), 1.45 - 1.54 (m, 2H, Alkyl-β-CH_2), 1.11 - 1.30 (m, 22H, Alkyl-CH_2), 0.84 (t, 3H, Alkyl-CH_3).

$C_{28}H_{54}O_{12}$ (582.3615)

$[\alpha]_D^{20} = +49$ (c = 0.9, MeOH)

MALDI-TOF: m/z = 583.0 $[M+Na]^+$

Anal. Calcd C, 57.71; H, 9.34. Found C, 57.75; H, 9.36

(2-Hexadecyloxy-ethyl) 4-*O*-(β-D-galactopyranosyl)-β-D-glucopyranoside (Lac-EG-C16)

6.8 g (10 mmol) β-D-Lactoseoctaacetat and 3.2 g (11 mmol) 2-Hexadecyloxy-ethanol were reacted as described for **Lac-EG-C12**.

Yield: 2.6 g (29%).

2.5 g (2.8 mmol) (2-Hexadecyloxy-ethyl) 4-*O*-(2,3,4,6-tetra-*O*-acetyl-β-D-galactopyranosyl)-2,3,6-tri-*O*-acetyl-β-D-glucopyranoside were deprotected as described for **Lac-EG-C12**. The product was recrystallised from methanol.

Yield: 1.6 g (92%).

(2-Hexadecyloxy-ethyl) 4-O-(2,3,4,6-tetra-O-acetyl-β-D-galactopyranosyl)-2,3,6-tri-O-acetyl-β-D-glucopyranoside:

^{1}H-NMR (400 MHz, $CDCl_3$ + TMS): δ = 5.29 (dd, 1H, $^3J_{3',4'}$ 3.5, $^3J_{4',5'}$ 1.0, H-4'), 5.12 (dd, 1H, $^3J_{2,3}$ 9.7, $^3J_{3,4}$ 9.7, H-3), 5.04 (dd, 1H, $^3J_{1',2'}$ 8.1, $^3J_{2',3'}$ 10.7, H-2'), 4.88 (dd, 1H, H-3'), 4.83 (dd, 1H, $^3J_{1,2}$ 8.1, H-2), 4.49 (d, 1H, H-1), 4.38 - 4.45 (m, 2H, H-1', H-6a), 3.99 - 4.10 (m, 3H, H-6b, H-6a', H-6b'), 3.78 - 3.84 (m, 2H, H-5', H-αa), 3.72 (dd, 1H, $^3J_{4,5}$ 9.7, H-4), 3.58 - 3.62 (m, 1H, H-αb), 3.53 (ddd, 1H, $^3J_{5,6a}$ 2.0, $^3J_{5,6b}$ 6.1, H-5), 3.45 - 3.51 (m, 2H, H-βa, H-βb), 3.32 - 3.38 (m, 2H, Alkyl-α-CH_2), 2.08, 2.05, 1.99 (each s, 3H, OAc), 1.98 (s, 6H, 2x OAc), 1.96, 1.90 (each s, 3H, OAc), 1.45 - 1.52 (m, 2H, Alkyl β-CH_2), 1.12 - 1.30 (m, 26H, Alkyl-CH_2), 0.88 (t, 3H, Alkyl-CH_3).

^{13}C-NMR (100 MHz, $CDCl_3$ + TMS): δ = 170.92, 170.79, 170.64, 170.13, 170.02, 169.88 (C=O, OAc), 100.08 (C-1'), 99.69 (C-1), 71.88 (C-3), 71.63 (C-5), 70.67 (C-2), 70.62 (C-α), 70.01 (C-3'), 69.71 (C-5'), 68.72 (C-β), 68.16 (C-2'), 68.07 (C-α-Alkyl), 65.62 (C-4'), 61.05 (C-6), 59.80 (C-6'), 30.93, 28.72, 28.68, 28.60, 28.59, 28.50, 28.34, 28.01, 25.08, 21.67 (Alkyl-CH_2), 21.39, 21.10, 21.05, 20.99, 20.95, 20.94 (CH_3, OAc), 14.10 (Alkyl-CH_3).

$C_{44}H_{72}O_{19}$ (904.4668)

$[\alpha]_D^{20} = +13$ (c = 0.6, $CHCl_3$)

MALDI-TOF: m/z = 927.1 $[M+Na]^+$

(2-Hexadecyloxy-ethyl) 4-O-(β-D-galactopyranosyl)-β-D-glucopyranoside:

¹H-NMR (400 MHz, Pyridin-d_5): δ = 5.47 (d, 1H, $^3J_{1',2'}$ 8.1, H-1'), 5.22 (d, 1H, $^3J_{1,2}$ 8.1, H-1), 4.75 - 4.98 (m, 6H, H-6a, H-2', H-3', H-4', H-5', H-αa), 4.59 - 4.71 (m, 3H, H-6a', H-6b', H-αb), 4.49 - 4.55 (m, 2H, H-5, H-6b), 4.40 (dd, 1H, $^3J_{3,4}$ 9.6, $^3J_{4,5}$ 9.6, H-4), 4.33 (dd, 1H, $^3J_{2,3}$ 9.6, H-3), 4.25 (dd, 1H, H-2), 4.01 - 4.10 (m, 2H, β-CH_2), 3.80 - 3.89 (m, 2H, Alkyl-α-CH_2), 1.92 - 2.02 (m, 2H, Alkyl-β-CH_2), 1.50 - 1.81 (m, 26H, Alkyl-CH_2), 1.25 (t, 3H, Alkyl-CH_3).

$C_{30}H_{58}O_{12}$ (610.3928)

$[\alpha]_D^{20}$ = +5 (c = 1.1, MeOH)

MALDI-TOF: m/z = 633.8 [M+Na]⁺

Anal. Calcd C, 58.99; H, 9.57. Found C, 58.79; H, 9.52

(2-Hexadecyloxy-ethyl) 4-*O*-(α-D-glucopyranosyl)-β-D-glucopyranoside (Mal-EG-C16)

β-D-Maltoseoctaacetat was reacted as described for **Lac-EG-C16**.

Yield: 4.7 g (52%).

4.6 g (5 mmol) (2-Hexadecyloxy-ethyl) 4-*O*-(2,3,4,6-tetra-*O*-acetyl-α-D-glucopyranosyl)-2,3,6-tri-*O*-acetyl-β-D-glucopyranoside were deprotected as described for **Lac-EG-C12**. The product was recrystallised from methanol.

Yield: 3.1 g (95%).

(2-Hexadecyloxy-ethyl) 4-O-(2,3,4,6-tetra-O-acetyl-α-D-glucopyranosyl)-2,3,6-tri-O-acetyl-β-D-glucopyranoside:

¹H-NMR (500 MHz, $CDCl_3$ + TMS): δ = 5.40 (d, 1H, $^3J_{1',2'}$ 4.1, H-1'), 5.33 (dd, 1H, $^3J_{2',3'}$ 10.7, $^3J_{3',4'}$ 9.8, H-3'), 5.22 (dd, 1H, $^3J_{2,3}$ 9.1, $^3J_{3,4}$ 9.1, H-3), 5.03 (dd, 1H, $^3J_{4',5'}$ 9.8, H-4'), 4.83 (dd, 1H, H.2'), 4.80 (dd, 1H, $^3J_{1,2}$ 8.1, H-2), 4.59 (d, 1H, H-1), 4.45 (dd, 1H, $^3J_{5,6a}$ 2.7, $^2J_{6a,b}$ 12.0, H-6a), 4.23 (dd, 1H, $^3J_{5',6a'}$ 4.1, $^2J_{6a',b'}$ 12.3, H-6a'), 4.20 (dd, 1H, $^3J_{5,6b}$ 4.4, H-6b), 4.01 (dd, 1H, $^3J_{5',6b'}$ 2.2, H-6b'), 3.97 (dd, 1H, $^3J_{4,5}$ 9.1, H-4), 3.93 (m_c, 1H, H-5'), 3.88 (ddd, 1H, $^3J_{\alpha a,\beta a}$ 4.6, $^3J_{\alpha a,\beta b}$ 4.6, $^2J_{\alpha a,b}$ 11.0, H-αa), 3.63 - 3.70 (m, 2H, H-αb, H-βa), 3.49 - 3.56 (m, 2H, H-5, H-βb), 3.39 (t, 2H, Alkyl-α-CH_2), 2.11, 2.07, 2.01, 1.99, 1.98 (each s, 3H, OAc), 1.97 (s, 6H, OAc), 1.47 - 1.55 (m, 2H, Alkyl-β-CH_2), 1.17 - 1.32 (m, 26H, Alkyl-CH_2), 0.85 (t, 3H, Alkyl-CH_3).

¹³C-NMR (100 MHz, $CDCl_3$ + TMS): δ = 170.74, 170.67, 170.42, 170.14, 169.85, 169.62 (C=O, OAC), 100.59 (C-1), 95.77 (C-1'), 75.66 (C-3), 73.02 (C-4), 72.39 (C-2), 72.34 (C-5), 71.82 , (α-CH_2), 70.22 (C-2'), 69.89 (β-CH_2), 69.59 (C-3'), 69.30 (Alkyl-α-CH_2), 68.71 (C-5'), 68.28 (C-4'), 63.09 (C-6), 61.74 (C-6'), 32.22, 30.13, 30.09, 30.07, 30.05, 30.04, 30.01, 29.92, 29.75, 26.50, 23.09 (Alkyl-CH_2), 21.12, 21.03, 20.87, 20.84, 20.80, 20.77 (CH_3, OAc), 14.31 (Alkyl-CH_3).

$C_{44}H_{72}O_{19}$ (904.4668)

$[\alpha]_D^{20}$ = +30 (c = 1.1, $CHCl_3$)

MALDI-TOF: m/z = 927.8 [M+Na]⁺

(2-Hexadecyloxy-ethyl) 4-O-(α-D-glucopyranosyl)-β-D-glucopyranoside:

¹H-NMR (400 MHz, d_4-Methanol): δ = 5.21 (d, 1H, $^3J_{1',2'}$ 3.6, H-1'), 4.36 (d, 1H, $^3J_{1,2}$ 8.1, H-1), 4.08 (dd, 1H, $^3J_{5,6a}$ 2.0, $^2J_{6a,b}$ 12.0, H-6a), 3.91 (dd, 1H, $^3J_{5,6b}$ 4.6, H-6b), 3.80 - 3.87 (m, 2H, H-4', H-6a'), 3.50 - 3.78 (m, 11H, H-3, H-4, H-3', H-5', H-6b', α-CH_2, β-CH_2), 3.48 (dd, 1H, $^3J_{2',3'}$ 10.0, H-2'), 3.40 (ddd, 1H, $^3J_{4,5}$ 9.7, H-5), 3.26 - 3.33 (m, 3H, H-2, Alkyl-α-CH_2), 1.60 (m_c, 2H, Alkyl-β-CH_2), 1.19 - 1.46 (m, 26H, Alkyl-CH_2), 0.90 (t, 3H, Alkyl-CH_3).

$C_{30}H_{58}O_{12}$ (610.3928)

$[\alpha]_D^{20}$ = +32 (c = 1.0, MeOH)

MALDI-TOF: m/z = 634.0 [M+Na]$^+$

Anal. Calcd C, 58.99; H, 9.57. Found C, 58.85; H, 9.58

(2-Hexadecyloxy-ethyl) 6-*O*-(α-D-galactopyranosyl)-β-D-glucopyranoside (Mel-EG-C16)

β-D-Melibioseoctaacetat was reacted as described for **Lac-EG-C16**.

Yield: 2.7 g (30%).

2.6 g (2.9 mmol) (2-Hexadecyloxy-ethyl) 6-*O*-(2,3,4,6-tetra-*O*-acetyl-α-D-galactopyranosyl)-2,3,4-tri-*O*-acetyl-β-D-glucopyranoside were deprotected as described for **Lac-EG-C12**. The product was recrystallised from methanol.

Yield: 1.7 g (94%).

(2-Hexadecyloxy-ethyl) 6-O-(2,3,4,6-tetra-O-acetyl-α-D-galactopyranosyl)-2,3,4-tri-O-acetyl-β-D-glucopyranoside:

^{1}H-NMR (400 MHz, CDCl$_3$ + TMS): δ = 5.38 (dd, 1H, $^3J_{3',4'}$ 3.5, $^3J_{4',5'}$ 1.3, H-4'), 5.26 (dd, 1H, $^3J_{2',3'}$ 10.5, H-3'), 5.15 (dd, 1H, $^3J_{2,3}$ 9.7, $^3J_{3,4}$ 9.7, H-3), 5.09 (d, 1H, $^3J_{1',2'}$ 3.5, H-1'), 5.04 (dd, 1H, H-2'), 4.99 (dd, 1H, $^3J_{4,5}$ 9.7, H-4), 4.88 (dd, 1H, $^3J_{1,2}$ 8.1, H-2), 4.55 (d, 1H, H-1), 4.18 (ddd, 1H, $^3J_{5',6a'}$ 5.7, $^3J_{5',6b'}$ 6.6, H-5'), 4.05 (dd, 1H, $^3J_{6a',b'}$ 11.2, H-6a'), 4.02 (dd, 1H, H-6b'), 3.80 - 3.85 (m, 1H, H-αa), 3.70 (dd, 1H, $^3J_{5,6a}$ 5.0, $^3J_{6a,b}$ 11.7, H-6a), 3.64-3.68 (m, 1H, H-αb), 3.60 (ddd, 1H, $^3J_{5,6b}$ 2.1, H-5), 3.52 (dd, 1H, H-6b), 3.46 - 3.52 (m, 2H, H-βa, H-βb), 3.38 (m$_c$, 2H, Alkyl-α-CH$_2$), 2.07, 2.06, 1.99, 1.98, 1.96, 1.94, 1.93 (each s, 3H, OAc), 1.45 - 1.51 (m, 2H, Alkyl-β-CH$_2$), 1.12 - 1.30 (m, 26H, Alkyl-CH$_2$), 0.88 (t, 3H, Alkyl-CH$_3$).

^{13}C-NMR (100 MHz, CDCl$_3$ + TMS): δ = 170.51, 170.32, 170.18, 169.84, 169.33, 169.28 (C=O, OAc), 100.50 (C-1), 96.44 (C-1'), 72.95 (C-3), 72.61 (C-5), 72.00 (C-α) 71.38 (C-2), 70.05 (C-β) 69.90 (Alkyl-α-CH$_2$), 69.10 (C-4), 68.05, 68.02 (C-4', C-2'), 67.40 (C-3'), 66.48 (C-5'), 66.40 (C-6), 61.65 (C-6'), 32.35, 31.98, 29.68, 29.60, 29.40, 29.23, 29.05, 25.88, 22.66 (Alkyl-CH$_2$), 20.75, 20.69, 20.64, 20.62 (-CH$_3$, OAc), 14.11 (Alkyl-CH$_3$).

C$_{44}$H$_{72}$O$_{19}$ (904.4668)

$[\alpha]_D^{20} = $ +51 (c = 0.8, CHCl$_3$)

MALDI-TOF: m/z = 928.0 [M+Na]$^+$

(2-Hexadecyloxy-ethyl) 6-O-(α-D-galactopyranosyl)-β-D-glucopyranoside:

^{1}H-NMR (400 MHz, d$_4$-Methanol): δ = 4.91 (d, 1H, $^3J_{1',2'}$ 3.5, H-1'), 4.31 (d, 1H, $^3J_{1,2}$ 8.1, H-1), 3.86 - 4.05 (m, 2H, H-6a, H-αa), 3.70 - 3.84 (m, 2H, H-4', H-5'), 3.61 - 3.70 (m, 6H, H-2', H-3', H-6a', H-6b', H-6b, H-αb), 3.54 - 3.59 (m, 2H, β-CH$_2$), 3.33 - 3.43 (m, 4H, H-4, H-5, Alkyl-α-CH$_2$), 3.28 (dd, 1H, $^3J_{3,4}$ 9.7, H-3), 3.17 (dd, 1H, $^3J_{2,3}$ 9.7, H-2), 1.44 - 1.54 (m, 2H, Alkyl-β-CH$_2$), 1.10 - 1.39 (m, 26H, Alkyl-CH$_2$), 0.85 (t, 3H, Alkyl-CH$_3$).

C$_{30}$H$_{58}$O$_{12}$ (610.3928)

$[\alpha]_D^{20} = $ +51 (c = 1.0, MeOH)

MALDI-TOF: m/z = 633.9 [M+Na]$^+$

Anal. Calcd C, 58.99; H, 9.57. Found C, 59.02; H, 9.58

N-(cis-9-octadecenoyl) 4-*O*-(α-D-glucopyranosyl)-β-D-glucopyranosylamine (Mal-A-C18:1)

14 g (20 mmol) Acetobrommaltose were dissolved in 50 mL anhydrous *N,N*-dimethylformamide. 5.2 g (80 mmol) Sodium azide were added and the suspension was stirred for 24 hours in the dark at room temperature. The solvent was removed *in vacuo* and the residue was taken up in 200 mL ethyl

acetate and filtrated. The solution was washed three times with 100 mL water, dried over magnesium sulphate and solvent was removed *in vacuo*. The product was used without further purification.

3.3 g (5 mmol) 4-*O*-(2',3',4',6'-Tetra-*O*-acetyl-α-D-glucopyranosyl)-2,3,6-tri-*O*-acetyl-β-D-glucopyranosyl azide were dissolved in 50 mL of a mixture of anhydrous methanol and tetrahydrofurane (1:1 v/v) under an atmosphere of dry nitrogen. 30 mg Palladium on charcoal (10%) were added carefully and the reaction mixture was stirred for 3 hours under an atmosphere of dry hydrogen until t.l.c. revealed the reaction to be complete. The catalyst was removed by filtration and the solvent was evaporated under reduced pressure. The residue was taken up in 50 mL anhydrous *N,N*-dimethylformamide. 568 µL (7 mmol; 555 mg) Pyridine were added and the solution was cooled to 0 °C. 1.6 mL (5 mmol; 1.5 g) Oleoyl chloride were added at 0 °C. The reaction mixture was stirred overnight at room temperature and poured afterwards on 100 mL of water and extracted three times with 50 mL of dichlormethane. The combined organic phases were washed once with 100 mL saturated sodium bicarbonate solution and twice with water, dried over magnesium sulphate and solvent was removed under reduced pressure. The syrup was purified by column chromatography (light petroleum b.p. 50-70 / ethyl acetate 1:1).

Yield: 2.1 g (46%).

2.0 g (2.2 mmol) *N*-(*cis*-9-octadecenoyl) 4-*O*-(2',3',4',6'-tetra-*O*-acetyl-α-D-glucopyranosyl)-2,3,6-tri-*O*-acetyl-β-D-glucopyranosylamine were dissolved in 50 mL anhydrous methanol and sodium methoxide was added (pH 8-9). The solution was stirred at ambient temperature until t.l.c. revealed the reaction to be complete. It was then neutralised by using DOWEX 50WX ion-exchange resin (protonated form), filtrated and evaporated *in vacuo*. The product was purified by column chromatography (chloroform / methanol 9:1).

Yield: 1.3 g (97 %).

N-(cis-9-octadecenoyl) 4-O-(2',3',4',6'-tetra-O-acetyl-α-D-glucopyranosyl)-2,3,6-tri-O-acetyl-β-D-glucopyranosyl-amine:

^{1}H-NMR (500 MHz, CDCl$_3$ + TMS): δ = 6.18 (d, 1H, $^3J_{NH,1}$ 9.3, NH), 5.37 (d, 1H, $^3J_{1',2'}$ 3.8, H-1'), 5.25-5.33 (m, 3H, H-3', H-olefinic), 5.23 (dd, 1H, $^3J_{1,2}$ 9.3, H-1), 5.21 (dd, 1H, $^3J_{2,3}$ 9.7, $^3J_{3,4}$ 9.7, H-3), 5.03 (dd, 1H, H-2), 5.01 (dd, 1H, $^3J_{3',4'}$ 9.7, $^3J_{4',5'}$ 9.7, H-4'), 4.82 (dd, 1H, $^3J_{2',3'}$ 9.7, H-2'), 4.44 (dd, 1H, $^3J_{5,6a}$ 2.8, $^2J_{6a,b}$ 12.0, H-6a), 4.22 (dd, 1H, $^3J_{5',6a'}$ 4.1, $^2J_{6a',b'}$ 12.3, H-6a'), 4.20 (dd, 1H, $^3J_{5,6b}$ 4.4, H-6b), 4.01 (dd, 1H, $^3J_{5',6b'}$ 2.2, H-6b'), 3.97 (dd, 1H, $^3J_{4,5}$ 9.7, H-4), 3.90-3.95 (m, 2H, H-5', H-αa), 3.65 (dt, 1H, $^2J_{αa,b}$ 6.1, H-αb), 3.63 (ddd, 1H, H-5), 2.11, 2.07, 2.01, 1.99, 1.98 (each s, 3H, OAc), 1.97 (s, 6H, OAc), 1.62-1.76 (m, 4H, H-allylic) 1.49 - 1.55 (m, 2H, β-CH$_2$), 1.11 - 1.32 (m, 22H, Alkyl-CH$_2$), 0.85 (t, 3H, Alkyl-CH$_3$).

^{13}C-NMR (100 MHz, CDCl$_3$ + TMS): δ = 173.09 (C=O, amide), 170.14, 170.10, 170.08, 169.87, 169.51, 169.34 (C=O, OAc), 131.50, 131.45 (C-olefinic) 100.22 (C-1), 95.44 (C-1'), 75.41 (C-3), 71.74 (C-4), 71.17, 71.99 (C-2, C-5), 69.93 (C-2'), 69.30 (C-3'), 69.25 (C-α), 68.41 (C-5'), 67.98 (C-4'), 62.85 (C-6), 61.45 (C-6'), 31.84, 29.61, 29.57, 29.53, 29.31, 29.27, 29.24 (Alkyl-CH$_2$), 20.84, 29.75, 20.59, 20.54, 20.52, 20.49 (CH$_3$, OAc), 14.03 (Alkyl-CH$_3$).

C$_{44}$H$_{69}$NO$_{18}$ (899.4515)

$[\alpha]_D^{20}$ = +18 (c=0.3, CHCl$_3$)

N-(cis-9-octadecenoyl) 4-O-(α-D-glucopyranosyl)-β-D-glucopyranosylamine:

^{1}H-NMR (400 MHz, d$_4$-methanol): δ = 5.34-5.47 (m, 2H, H-olefinic), 5.04 (dd, 1H, $^3J_{1,2}$ 9.7, H-1), 5.2 (d, 1H, $^3J_{1',2'}$ 3.6, H-1'), 3.28-3.99 (m, 12H, H-3, H-3´, H-4, H-4´, H-5, H-5´, H-6a, H-6a´, H-6b, H-6b´, H-αa, H-αb),

3.48 (dd, 1H, $^3J_{2',3'}$ 9.7, H-2´), 3.26 (dd, 1H, $^3J_{2,3}$ 9.3, H-2), 1.98-2.15 (m, 4H, H-allylic), 1.61-1.71 (m, 2H, β-CH$_2$), 1.27-1.48 (m, 20H, -CH$_2$-), 0.95 (t, 3H, -CH$_3$).

C$_{30}$H$_{55}$NO$_{11}$ (605.3775)

$[\alpha]_D^{20}$ = +58 (c=0.7, C$_5$H$_5$N)

HIRES-FAB-MS: Calc: m/z = 628.3673 [M+Na]$^+$ Found: m/z = 628.3699

N-(*cis*-9-octadecenoyl) 6-*O*-(α-D-galactopyranosyl)-β-D-glucopyranosylamine (Mel-A-C18:1)

14 g (20 mmol) Acetobrommelibiose were dissolved in 50 mL anhydrous *N,N*-dimethylformamide. 5.2 g (80 mmol) Sodium azide were added and the suspension was stirred for 24 hours in the dark at room temperature. Solvent was removed *in vacuo* and the residue was taken up in 200 mL ethyl acetate and was filtrated. The solution was washed three times with 100 mL water, dried over magnesium sulphate and the solvent was removed *in vacuo*. The product was used without further purification.

3.3 g (5 mmol) 6-*O*-(2',3',4',6'-Tetra-*O*-acetyl-α-D-galactopyranosyl)-2,3,4-tri-*O*-acetyl-β-D-glucopyranosyl azide and 1.6 mL (5 mmol; 1.5 g) oleoyl chloride were reacted as described for **Mal-A-C18:1**.

Yield: 1.1 g (36 %).

N-(cis-9-octadecenoyl) 6-O-(2',3',4',6'-tetra-O-acetyl-α-D-galactopyranosyl)-2,3,4-tri-O-acetyl-β-D-gluco-pyranosylamine:

^{1}H-NMR (400 MHz, CDCl$_3$ + TMS): δ = 6.17 (d, 1H, $^3J_{NH,1}$ 9.4, NH), 5.27 (dd, 1H, $^3J_{3',4'}$ 3.1, $^3J_{4',5'}$ 1.2, H-4'), 5.24 - 5.30 (m, 3H, H-3', H-olefinic), 5.23 (d, 1H, $^3J_{1',2'}$ 3.6, H-1'), 5.22 (dd, 1H, $^3J_{1,2}$ 9.4, H-1), 5.17 (t, 1H, $^3J_{3,4}$ 9.7, H-3), 5.02 (dd, 1H, $^3J_{2,3}$ 9.7, H-2), 4.96 (dd, 1H, $^3J_{2',3'}$ 10.9, H-2'), 4.76 (t, 1H, $^3J_{4,5}$ 9.7, H-4), 4.13 (ddd, 1H, H-5'), 3.95 - 4.05 (m, 3H, H-6a', H-6b', H-αa), 3.68 (ddd, 1H, $^3J_{5,6a}$ 5.1, $^3J_{5,6b}$ 2.5, H-5), 3.65 (dd, 1H, $^3J_{6a,b}$ 11.2, H-6a), 3.61 (dt, 1H, $^3J_{αa,b}$ 6.1, H-αb), 3.58 (dd, 1H, H-6b), 2.11, 2.06, 1.98, 1.97, 1.96, 1.95, 1.92 (each s, 3H, OAc), 1.63 - 1.76 (m, 4H, H-allylic), 1.47 - 1.59 (m, 2H, β-CH$_2$), 1.11 - 1.30 (m, 22H, Alkyl-CH$_2$), 0.81 (t, 3H, Alkyl-CH$_3$).

^{13}C-NMR (125 MHz, CDCl$_3$ + TMS): δ = 173.12 (C=O, amide), 170.52, 170.31, 170.17, 169.83, 169.32, 169.27 (C=O, OAc), 131.51, 131.45 (C-olefinic), 100.52 (C-1), 96.43 (C-1'), 72.93 (C-3), 72.62 (C-5), 71.34 (C-2), 69.98 (C-α), 69.04 (C-4), 68.05, 68.04 (C-4', C-2'), 67.43 (C-3'), 66.44 (C-5'), 66.41 (C-6), 61.63 (C-6'), 31.90, 29.68, 29.62, 29.40, 29.23, 25.86, 22.66 (Alkyl-CH$_2$), 20.76, 20.67, 20.63, 20.61 (-CH$_3$, OAc), 14.09 (Alkyl-CH$_3$).

C$_{44}$H$_{69}$NO$_{18}$ (899.4515)

$[\alpha]_D^{20}$ = +30 (c=0.5, CHCl$_3$)

N-(cis-9-octadecenoyl) 6-O-(α-D-galactopyranosyl)-β-D-glucopyranosylamine:

^{1}H-NMR (400 MHz, d$_4$-methanol): δ = 5.33-5.40 (m, 2H, H-olefinic), 5.02 (dd, 1H, $^3J_{1,2}$ 9.5, H-1), 4.89 (d, 1H, $^3J_{1',2'}$ 4.1, H-1'), 4.01 (dd, 1H, $^3J_{5,6a}$ 4.1, $^2J_{6a,b}$ 11.2, H-6a), 3.85 - 3.95 (m, 3H, H-4', H-5', H-αa), 3.69 - 3.80 (m, 4H, H-2', H-3', H-6a', H-6b, H-6b', H-αb), 3.50 (ddd, 1H, $^3J_{4,5}$ 9.2, $^3J_{5,6b}$ 2.0, H-5), 3.43 (dd, 1H, H-4), 3.38 (dd, 1H, $^3J_{2,3}$ 9.2, $^3J_{3,4}$ 9.2, H-3), 3.21 (dd, 1H, H-2), 1.98-2.14 (m, 4H, H-allylic), 1.60 - 1.70 (m, 2H, β-CH2), 1.27 - 1.49 (m, 20H, Alkyl-CH2), 0.93 (t, 3H, Alkyl-CH3).

C$_{30}$H$_{55}$NO$_{11}$ (605.3775)

$[\alpha]_D^{20}$ = +60 (c=0.8, C$_5$H$_5$N)

HIRES-FAB-MS: Calc: m/z = 628.3673 [M+Na]$^+$ Found: m/z = 628.3694

Reference

YOSHIDA, H., IKEDA, K., ACHIWA, K., HOSHINO, H., Synthesis of sulfated cerebroside analogs having mimicks of ceramide and their anti-human immunodefiency virus type 1 activities, *Chem. Pharm. Bull.*, 43, **1995**, 594-602.

Appendix B
Unpublished SANS- and surface tension results

Materials and methods
SANS-experiments, Surface tension experiments and data treatment were carried out as described in chapters 2, 3, 4, 5, 8 and 9.

Compounds: Lac-EG-C14, Mal-EG-C14, Mel-EG-C14

1.) Surface Tension:

TABLE B1: Adsorption at the air-water interface and data calculated from the pre *CMC*-slope (T = 30 ± 4 °C)

	Lac-EG-C14	*Mal-EG-C14*	*Mel-EG-C14*
CMC [mM L^{-1}]	0.1 ± 0.09	0.1 ± 0.08	0.08 ± 0.02
CMC [g mL^{-1}]	5.8x10^{-5}	5.8x10^{-5}	4.6x10^{-5}
γ_{CMC} [mN m^{-1}]	36	36	39
γ_{min} [mN m^{-1}]	35	36	38
Carbon chain volume υ_c [Å^3]	404	404	404
Extended chain length l_c [Å]	19.21	19.21	19.21
Head group area a_0 [Å^2]	--	31 ± 8	50 ± 9
Packing parameter $\upsilon_c / (l_c a_0)$	--	0.7	0.42
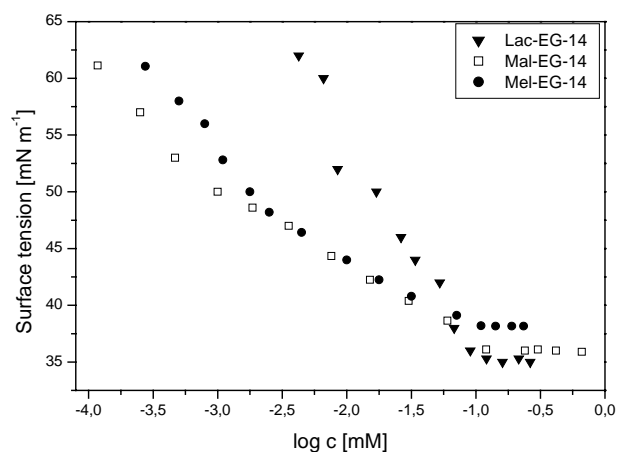
FIGURE B1: Surface tension plot for **Mal-EG-C14**, **Mel-EG-C14** and **Lac-EG-C14** at T = 55 °C.

Appendix

2.) SANS

Lac-EG-C14
Data-treatment: Freeform using the IFT-routine with a thickness pair-distribution function

Results:

TABLE B2: Results of SANS data analysis by the model independent approach (IFT).

Compound	Concentration [g mL^{-1}]	T [°C]	Micellar shape	Dmax [Å]	R_g [Å]
Lac-EG-C14	1x10^{-3}	25	disc-like	100	12 ± 2, $\mathbf{R_{T,g}}$
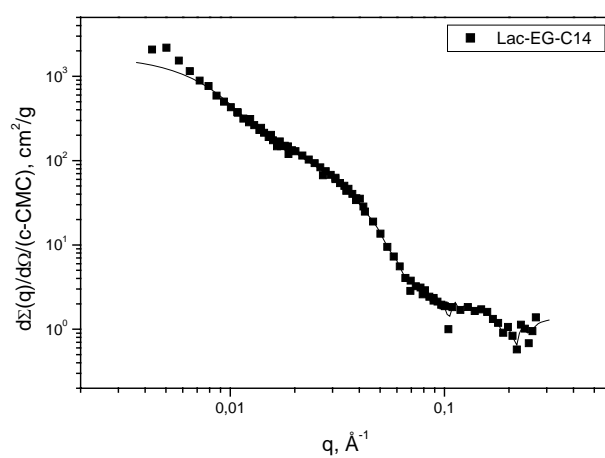
FIGURE B2: Scattering data for **Lac-EG-C14** (filled squares) together with the model fit (solid line).

Mal-EG-C14, Mel-EG-C14
Data-treatment: IFT-routine, Core-and-shell model

Results:

TABLE B3: Results of SANS data analysis by the model independent approach (IFT).

Compound	Concentration [g mL^{-1}]	T [°C]	Micellar shape	Dmax [Å]	R_g [Å]
Mal-EG-C14	1x10^{-4}	25	spherical	90	27.6 ± 0.3
Mel-EG-C14	1x10^{-3}	25	spherical	75	23.4 ± 0.3

TABLE B4: Results of SANS data analysis by the fitting of the two-shell spherical micelle model: R_c is the radius of core, R_t is the total radius of micelle and Δ is the ratio of the contrast between shell and core.

Compound	Concentration [g mL^{-1}]	T [°C]	R_c [Å]	R_t [Å]	Δ
Mal-EG-C14	1x10^{-4}	25	22 ± 1	40 ± 1	0.22 ± 0.01
Mel-EG-C14	1x10^{-3}	25	22 ± 1	35 ± 1	0.22 ± 0.01
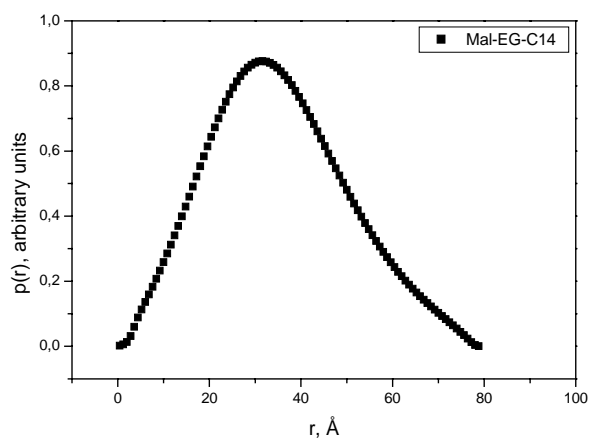
Figure B3: Pair distance distribution functions, p(r) for **Mal-EG-C14**.
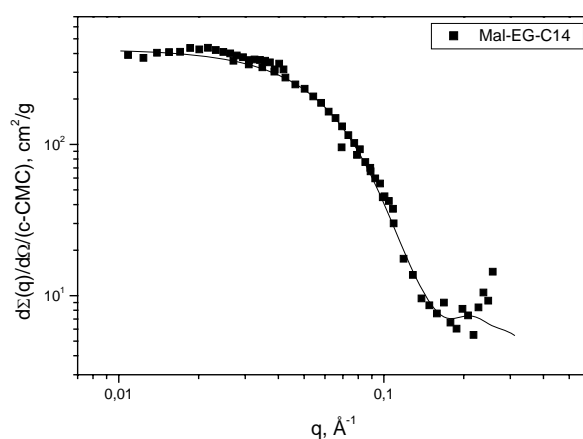
Figure B4: Scattering data for **Mal-EG-C14** (filled squares) together with the model fit (solid line).
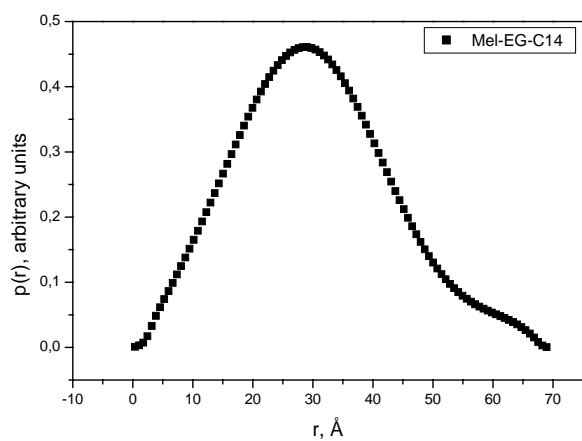
Figure B5: Pair distance distribution function, p(r) for **Mel-EG-C14**.
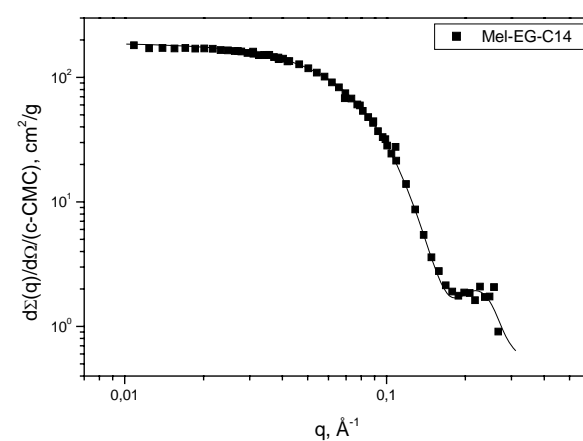
Figure B6: Scattering data for **Mel-EG-C14** (filled squares) together with the model fit (solid line).

Compound: Mel-C14, Mel-C18:1, Lac-C18:1

1.) Surface tension

TABLE B5: Adsorption at the air-water interface and data calculated from the pre CMC-slope (T = 50 ± 8 °C for **Mel-C14** and T = 25 ± 1 °C for **Mel-C18:1**)

	Mel-C14	*Mel-C18:1*
CMC [mM L^{-1}]	0.14 ± 0.02	0.003 ± 2x10^{-4}
CMC [g mL^{-1}]	7.5x10^{-5}	1.8x10^{-6}
γ_{CMC} [mN m^{-1}]	41	45
γ_{min} [mN m^{-1}]	41	40
Carbon chain volume υ_c [Å^3]	404	511.6
extended chain length l_c [Å]	19.21	24.27
Head group area a_0 [Å^2]	60 ± 15	30 ± 8
packing parameter $\upsilon_c / (l_c a_0)$	0.35	0.7
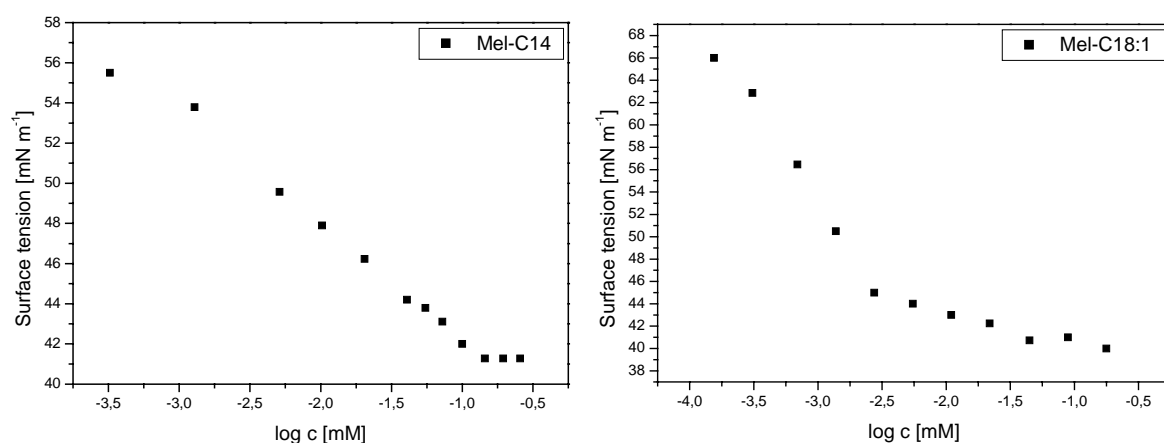
FIGURE B7: Surface tension plots for **Mel-C14** (T = 50±8 °C) and **Mel-C18:1** (T = 25 ± 1 °C).

Appendix

2.) SANS
Data treatment:
        Lac-C18:1:
        Calculation of the Porod-parameter ($d\Sigma(q)/d\Omega \sim Aq^{-4}$) according to chapter 4.
   Mel-C14: IFT-routine, spherical-model
        Mel-C18:1: IFT-routine, cylindrical model

Results:

TABLE B6: Results of SANS data analysis by the model independent approach (IFT) and model fitting.

Compound	*Concentration [g mL^{-1}]*	*T [°C]*	*Micellar shape*	*Dmax [Å]*	*Length or radius [Å]*	*R_g [Å]*
Mel-C14	5×10^{-4}	50	spherical	60	21 ± 0.2	--
Mel-C14	1×10^{-3}	50	spherical	60	22 ± 0.2	--
Lac-C18:1	1×10^{-4}	50	large aggregate	--	~ 960	--
Mel-C18:1	1×10^{-4}	25	cylindrical	60	373 ± 8	34 ± 1
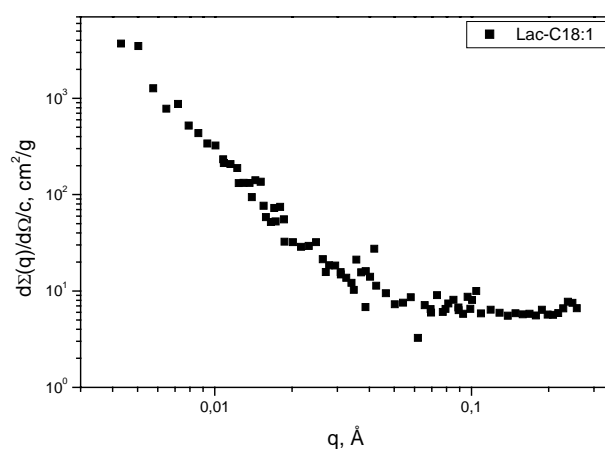
FIGURE B8: Scattering data for **Lac-C18:1**.
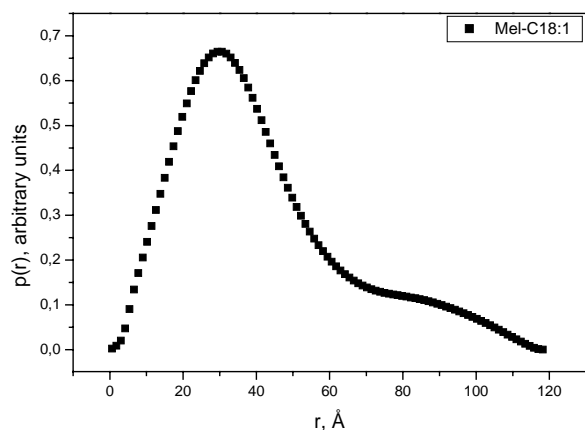
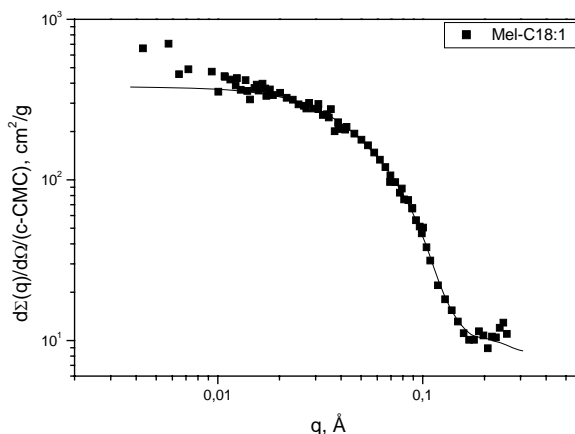**Figure B9:** Pair distance distribution function, p(r) for **Mel-C18:1**.

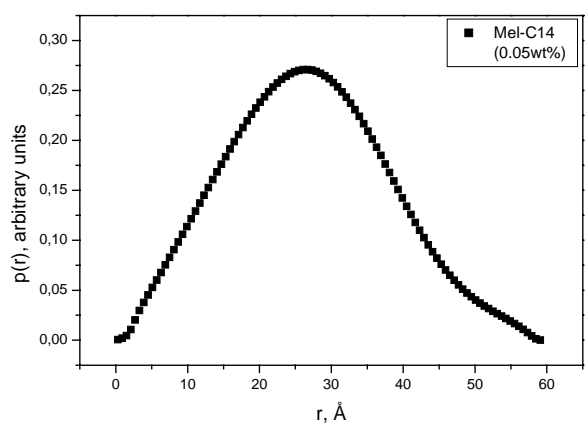**Figure B10:** Scattering data for **Mel-C18:1** (filled squares) together with the model fit (solid line).

Figure B11: Pair distance distribution function, p(r) for **Mel-C14**, c = 5×10^{-4} g/mL.
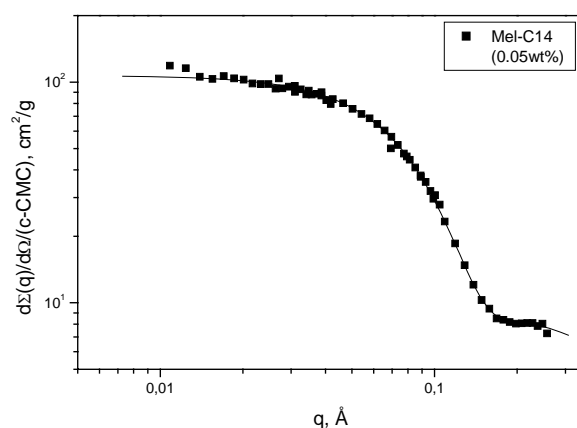

Figure B12: Scattering data for **Mel-C14** (filled squares) together with the model fit (solid line), c = 5×10^{-4} g/mL.
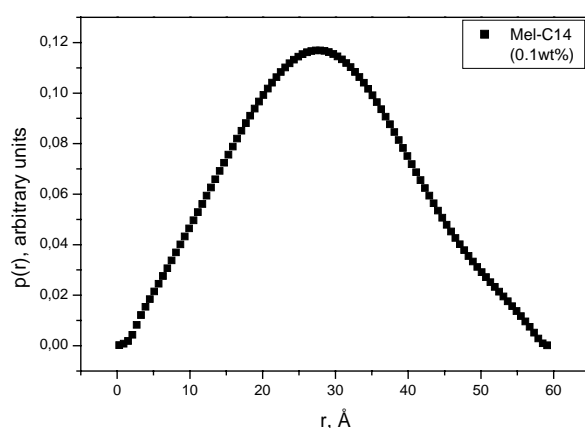

Figure B13: Pair distance distribution function, p(r) for **Mel-C14**, c = 1×10^{-3} g/mL.
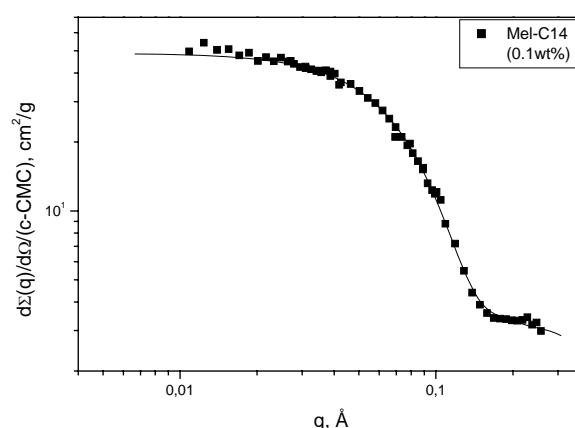

Figure B14: Scattering data for **Mel-C14** (filled squares) together with the model fit (sold line), c = 1×10^{-3} g/mL.

Appendix C

C.1 Thermotropic phase sequences

Lac-C12	Cr	SmA	I	
Mal-C12	Cr	SmA	I	taken from: Boyd *et al.* (2000)
Mal-C14	Cr	SmA	I	taken from: Minden *et al.* (2000)
Mal-C16	Cr	SmA	I	
Mal-C18	Cr	SmA	I	taken from: Minden *et al.* (2000)
Mel-C16	Cr	SmA	I	
Lac-EG-C12	Cr	SmA	I	
Lac-EG-C14	Cr	SmA	I	
Lac-EG-C16	Cr	SmA	I	
Mal-EG-C12	g	SmA	I	
Mal-EG-C16	Cr	SmA	I	
Mel-A-C18:1	Cr	SmA	d	
Mel-EG-C12	g	SmA	I	
Mel-EG-C14	Cr	SmA	d	
Mel-EG-C16	Cr	SmA	I	

C.2 Emulsification

Method

A defined amount of amphiphile was suspended in octyldodecanol at 60-70 °C in a test tube. 60 v/v% water and 0.7 w/v% magnesium sulfate were added, the tube was sealed and emulsification was achieved by shaking the test tube for two minutes. The degree of emulsification was determined after 20 seconds, 5 min. and 60 min.

Results

Emulsification behaviour of different glyco glycero lipids at different concentrations of lipid.

Compound	Conc. [w/v%]	Emulsification [%]		
		20 sec.	5 min.	60 min.
Mal-1,3-TMD	1	100	90	90
	0.1	80	80	70
Mal-1,2-TMD	1	100	85	85
	0.1	80	80	80
Mel-1,3-C14	1	90	60	20
	0.1	70	30	10
Mal-1,3-C18:1	1	100	100	100
	0.1	80	80	80

C.3 Foaming

Measurements were performed by using 100 mL or 25 mL measuring cylinders. Before usage the cylinders were filled with concentrated nitric acid for 24 h, and after rinsing with bidistilled water, filled with bidistilled water for another 24 h. The solutions were prepared by weighing the surfactant / lipid and adding bidistilled water up to a weight of 10 g (approx. 10 mL). The solutions were equilibrated at 25 °C or 50 °C prior to use. Foaming was achieved by turning the closed cylinder around at a rate of 20 times during 30 seconds. The experiment was repeated until deviation was no larger than 5 %. Foam volumes were determined immediately (foaming ability) and after 30 minutes (foam stability).

References

BOYD, B.J., DRUMMOND, C.J., KRODKIEWSKA, I., GRIESER, F., How chain length, headgroup polymerization, and anomeric configuration govern the thermotropic and lyotropic liquid crystalline phae behaviour and the air-interfacial adsorption of glucose-based surfactants, *Langmuir*, 16, **2000**, 7359-7367.

MINDEN, V.H.M., BRANDENBURG, K., SEYDEL, U., KOCH, M.H.J., GARAMUS, V.M., WILLUMEIT, R., VILL, V., Thermotropic and lyotropic properties of long chain alkyl glycopyranosides. Part II: disaccharide headgroups, *Chem. Phys. Lipids*, 106, **2000**, 157-179.

Appendix D

Safety information

In the table below all relevant chemicals used in this work are listed with information about the classification (hazard sign, dangerous properties in form of R-phrases) and secure handling (S-phrases).

Name	Hazard sign	R	S
(R)-2-Aminobutan-1-ol	C	34	26-36/37/39-45
2-Amino-1,3-propandiol	C	34	26-36/37/39-45
2-Bromethanol	T+	10-26/27/28-36/37/38-68	16-26-28A-36/37/39-45
2-Propanol	F, Xi	11-36-37	7-16-24/25-26
4-(1-Pyrrolidinyl)pyridine	T	25-35	26-36/37/39-45
Acetobrommaltose	--	23/24/25-36/37/38	45-26-36/37/39
Acetone	F, Xi	11-36-66-67	9-16-26
Benzyl chloroformate	F, C, N	11-20-34-50/53	16-26-36/37/39-45-61
Boron trifluoride etherate	F, T	15-34-48/23	6.3-26-36/37/39-45
Celite	Xn	48/20	22
Chloroform	Xn	22-38-40-48/20/22	36/37
Dichloromethane	Xn	40	23.2-24/25-36/37
Dodecanol	N	50	61
Dodecanoylchloride	C	34	26-36/37/39-45
Epichlorhydrine	T	45-10-E23/24/25-34-43	53-45
Ethanol	F	11	7-16
Ethyl acetate	F, Xi	11-36-66-67	16-26-33
Penta-*O*-acetyl-β-D-glucose	--	--	22-24/25
Hexadecanoyl chloride	C	14-34-37	26-36/37/39-45
Hydrazine hydrate	T, N	45-E23/24/25-34-43-50/53	53-26-36/37/39-45-60-61
Ion-exchange resin	Xi	36	26
Light petroleum b.p. 50-70	F, Xn, N	11-38-48/20-51/53-62-65-67	16-23.2-24-33-36/37-61-62
Methanol	F, T	11-23/24/25-39/23/24/25	7-16-36/37-45
N,N'-Dicyclohexylcarbodiimide	T	22-24-41-43	24-26-37/39-45
N,N-Dimethylformamide	T	61-E20/21-36	53-45
n-Hexane	F, Xn, N	11-38-48/20-51/53-62-65-67	9-16-29-33-36/37-61-62
Oleoyl chloride	C	34	26-36/37/39-45
Palladium on Charcoal (10%)	F	11	15
Platin on Charcoal (10%)	F	11	15
Potassium carbonate	Xi	36/37/38	22-26
Pyridine	F, Xn	11-20/21/22	26-28.1
Silica gel	--	--	22
Sodium	F, C	14/15-34	5.3-8-43.7-45
Sodium azide	T+, N	28-32-50/53	28.1-45-60-61
Sodium hydrogen carbonate	--	--	22-24/25
Tetradecanoyl chloride	C	34	26-36/37/39-45
Tetrahydrofurane	F, Xi	11-19-36/37	16-29-33
Tetramethylsilan	F+	12	9-16-29-43.3
Tin (IV) chloride	C	34-52/53	7/8-26-45-61
Toluene	F, Xn	11-38-48/20-63-65-67	36/37-46-62
Trichloracetonitrile	T, N	23/24/25-51/53	45-61
Triethylamine	F,C	11-20/21/22-35	3-16-26-29-36/37/39-45
Trimethylsilyl trifluormethansulfonate	C	10-14-34-37	26-36/37/39-45

Acknowledgements

Ein Dank Allen die mich während der Zeit dieser Arbeit ertragen und sowohl moralisch als auch tatkräftig unterstützt haben und Allen mit denen ich erfolgreich zusammenarbeiten durfte:

Meiner Familie: Als da wären meine Eltern, die mir das Studium ermöglicht haben, Meine Schwester nebst Mann und Kindern, und last but not least Sabine, die meine Launen und Hobbies ausgehalten hat, besonders wenn es statt Abendbrot mal wieder Feuerlöschen in Bramfeld gab.

Meinen Freunden und Bekannten, ohne die das Leben äußerst fade wäre: Andi („zum Lachen reichts immer"), Niels, Peter, Kai, Martin, Koen, Anja und Frank, Ossi („jeder sollte einen haben") und Roxana, Holger, Ratzi, Marcus und Nessi, Matze, Stephan, Sven und Agnes.

Meinen Kollegen der AG Vill, Matze „Ich wars nicht" Wulf, Sven „Chaoskönig" Gerber, Nicole „Götz es brennt!!!" Heine, Gaja „wir schreiben dann mal eben ein Programm" Peters, Naho „die wahre Säulenchromtographiekönigin" Fujimoto.

Lars und Nico, den letzten „echten Thiems".

Meinen nicht-flüssigkristallinen Korrekturlesern für unzählige Publikationen und diese Arbeit: Patricia and Ron Bascombe, Maja und Fin Lorenzen, Alexandra Fliegel und Thomas Radszuweit.

Prof. Dr. Joachim Thiem und Prof. Dr. Volkmar für die Überlassung des Themas und den großzügigen wissenschaftlichen Freiraum bei der Bearbeitung des Themas.

Regine Willumeit für die Möglichkeit einen großen Teil meiner Forschungsarbeit am GKSS durchzuführen.

Vasyl Haramus für eine hervorragende Betreuung am GKSS und eine tolle Zeit dort.

List of Publications

Patent
DE, submitted

Accepted Publications

Minden, v.H.M., Morr, M., Milkereit, G., Heinz, E., Vill, V., Synthesis and mesogenic properties of glycosyl diacylglycerols, *Chemistry and Physics of Lipids*, 114, **2002**, 55-80.

Minden, v.H.M., Milkereit, G., Vill, V., Effects of carbohydrate headgroups on the stability of induced cubic phases in binary mixtures of glycolipids, *Chemistry and Physics of Lipids*, 120, **2002**, 45-56.

Milkereit, G., Morr, M., Thiem, J., Vill, V., Thermotropic and lyotropic properties of long chain alkyl glycopyranosides Part III: pH-sensitive headgroups, *Chemistry and Physics of Lipids*, 127, **2004**, 47-63.

Abeygunaratne, S., Jákli, A., Milkereit, G., Sawade, H., Vill, V., Antiferroelectric ordering of amphiphilic glycolipids in bent-core liquid crystals, *Physical Review E*, 69, **2004**, 021703-1-6.

Milkereit, G., Garamus, V.M., Veermans, K., Willumeit, R., Vill, V., Synthesis and mesogenic properties of a Y-shaped glyco glycero lipid, *Chemistry and Physics of Lipids*, 131, **2004**, 51-61.

Garamus, V.M., Milkereit, G., Gerber, S., Vill, V., Micellar structure of a sugar-based bolaamphiphile in pure solutions and destabilizing effectes in mixtures of glycolipids, *Chemical Physics Letters*, 392, **2004**, 105-109.

Milkereit, G., Garamus, V.M., Yamashita, J., Hato, M., Morr, M., Vill, V., Comparison of the supramolecular structures of two glycolipids with chiral and non-chiral methyl branched alkyl chains from natural sources, *The Journal of Physical Chemistry B*, 109, **2005**, 1599-1608.

Milkereit, G., Garamus, V.M., Veermans, K., Willumeit, R., Vill, V., Structure of micelles formed by alkyl glycosides with unsaturated alkyl chains, *Journal of Colloid and Interface Science*, 284, **2005**, 704-713.

Milkereit, G., Gerber, S., Brandenburg, K., Morr, M., Vill, V., Synthesis and mesomorphic properties of glycosyl dialkyl- and diacylglycerols bearing saturated, unsaturated and methyl branched fatty acid and fatty alcohol chains. Part I: Synthesis, *Chemistry and Physics of Lipids*, 135, **2005**, 1-14.

Milkereit, G., Brandenburg, K., Gerber, S., Koch, M.H.J., Andrä, J., Morr, M., Seydel, U., Vill, V., Synthesis and mesomorphic properties of glycosyl dialkyl- and diacylglycerols bearing saturated, unsaturated and methyl branched fatty acid and fatty alcohol chains. Part I: Mesomorphic properties, *Chemistry and Physics of Lipids*, 135, **2005**, 15-26.

Gerber, S., Garamus, V.M., Milkereit, G.,Vill, V., Mixed micelles formed by SDS and a bolaamphiphile with carbohydrate headgroups, *Langmuir*, 21, **2005**, 6707-6711.

Vill, V., Milkereit, G., Gerber, S., Jankowski, K., Terjung, A., Schmidt, R.R., From Y- to Siamese-Twin shaped glycolipids - Influence on the thermotropic phase behaviour, *Journal of Thermal Analysis & Calorimetry*, 82, **2005**, 471- 475.

Garamus, V.M., Milkereit, G., Willumeit, R., Vill, V., How thermotropic properties influence the formation of lyotropic aggregates near the critical micelle concentration, *Journal of Thermal Analysis & Calorimetry*, 82, **2005**, 477-481.

Poster presentations

Minden, v.H.M., Milkereit, G., Morr, M., Vill, V., 20th International Carbohydrate Symposium, 27.08. - 01.09.2000, Hamburg, *Synthesis and mesogenic properties of glycosyl diacylglycerols*.

Milkereit, G., Minden, v.H.M., Vill, V., 4th Workshop on functional materials: Synthesis and Characterisation of mesoscalic systems, 06. - 07.04.2001, GKSS Forschungszentrum, Geesthacht, *Synthesis and mesogenic properties of glyco glycero conjugates*.

Milkereit, G., Veermans, K., Vill, V., Symposium des Sonderforschungsbereiches 470: Glycostructures in Biological Systems VII, 10. - 11.12.2001, Universität Hamburg, *The Chirality of glycolipids as control and monitor of biophysical properties*.

Garamus, V.M., Milkereit, G., Veermans, K., Willumeit, R., Vill, V., Deutsche Neutronentagung, 01. - 02.09.2004, Dresden, *Structures of micelles formed by alkyl glycosides with unsaturated alkyl chains*.

Milkereit, G., Gerber, S., Vill, V., Garamus, V.M., Hato, M., Shingu, Y., Symposium des Sonderforschungsbereiches 470: Glycostructures in Biological Systems XIII, 01. - 03.12.2004, Universität Hamburg, *Natural and synthetic carbohydrate-based lipids: Influence of the molecular structure on the formation of supramolecular aggregates.*

Oral presentation

Wissenschaftliches Kolloqium des Sonderforschungsbereiches 470, 27.04.2001, Universität Hamburg, *Synthese steuerbarer Glycolipide.*

Curriculum vitae

<u>Götz</u> Eckart Milkereit

Geboren 30.08.1973 in Lübeck

Schulausbildung

1980 - 1984	Grundschule, Nahe
1984 - 1993	Gymnasium im Schulzentrum Süd, Norderstedt
1993	Zeugnis der Allgemeinen Hochschulreife

Studium

1993	Immatrikulation im Fach Chemie (Diplom) an der Universität Hamburg
1993 - 1996	Grundstudium
1996	Vordiplom
1996 - 2000	Hauptstudium
2000	Diplomarbeit bei Prof. Dr. J. Thiem (Arbeitsgruppe Dr. V. Vill): „Synthese und Untersuchung der mesogenen Eigenschaften von neutralen und ionischen Alkylglycosiden"
2000	Abschluß und Verleihung des akademischen Grades Diplom-Chemiker

Promotion

ab 03/2001	Promotion an der Universität Hamburg und am GKSS Forschungszentrum, Geesthacht unter Betreuung von Prof. Dr. J. Thiem und Prof. Dr. V. Vill: „Investigation of colloidal, biophysical and liquid crystalline properties of synthetic alkyl glycosides and glycolipids"

Beruflicher Werdegang

03/2000 - 08/2000	Studentische Hilfskraft am Institut für Organische Chemie
03/2001 - 06/2003	Wissenschaftlicher Mitarbeiter im Sonderforschungsbereich 470 „Glycostrukturen in Biosystemen"
07/2003 - 06/2005	Stipendiat im Graduiertenkolleg 464 „Glycokonjugate: Darstellung, Analyse und Funktion"
08/2004 - 05/2005	Mitarbeit in einem Projekt der Firma Beiersdorf AG, Hamburg